

**Kinetic Resolution of Chiral α -Olefins Using
Enantiopure Ziegler-Natta Polymerization Catalysts**

Thesis by
Endy Yeo-Jung Min

In Partial Fulfillment of the
Requirements for the Degree of
Doctor of Philosophy

Division of Chemistry and Chemical Engineering
California Institute of Technology
Pasadena, CA

2006

(Defended October 18, 2005)

© 2006

Endy Yeo-Jung Min

All Rights Reserved

DEDICATION

To the Three Wise Men

who improved my relationship with chemistry:

Paul Wagenknecht, Ed Chichester, and Clair Cheer

ACKNOWLEDGEMENTS

First and foremost, I would like to thank my advisor John Bercaw. He gave me the opportunity to learn his approach to science and the value of pursuing important questions, not just interesting ones. Watching him set high standards and drive toward that goal with methodical rigor and unwavering integrity has been inspirational. He also provided me with kind and encouraging words when I experienced the “research blues.” But most of all, I respect him for his humbleness despite all his accomplishments.

I would also like to thank my committee members Bob Grubbs, Brian Stoltz, and Julia Kornfield for their time and research suggestions.

Many former and present Bercaw group members have helped me during my time at Caltech. Chris Levy was the first to train me how to use the high-vacuum line and the swivel frit, essential tools to doing chemistry the Bercaw way. He was the first to break ground on the kinetic resolution project, providing me with a springboard for my research. Cliff Baar and Jeff Byers also worked on this project with me. I thank them for useful scientific discussions and for being good teammates to commiserate with.

There also have been many post-docs who just knew a lot of chemistry. Being able to consult them was invaluable to me. I want to thank John Scollard, Alex Muci, Christoph Balzarek, Reto Dorta, Alan Heyduk, Joseph Sadighi, Parisa Mehrkhodavandi, Tom Driver, Travis Williams, and Xin Wei Li.

Former graduate students in the group helped me through many times I was stuck in my research. In particular, I would like to thank Antek Wong Foy, Susan Schofer, and John Owens who were always approachable and eager to help. Then there are others who

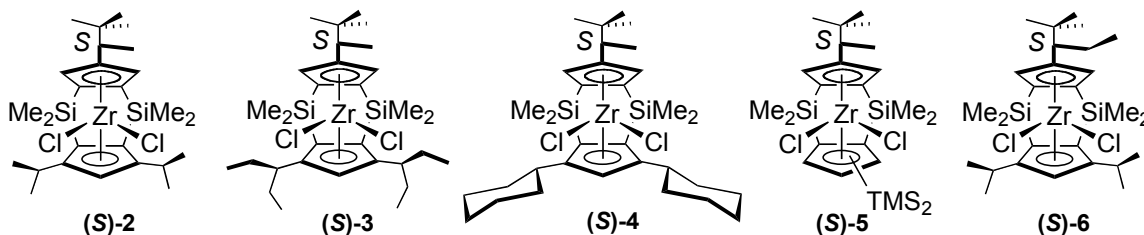
just made the Bercaw group a fun place to work. Dave Weinberg, Theo Agapie, Paul Elowe, Steve Baldwin, and George Chen were people who always made me feel like I was in summer camp. Other past members I would like to thank for their scientific discussions and suggestions are: Chris Brandow, Lily Ackerman, Sara Klamo, Annita Zhong, Deanna Zubris, Vsevolod Rostovstev, Jeff Yoder, and Paul Chirik.

Thank you to Mike Day and Larry Henling for X-ray crystallography data, to Rick Gerhart for his glass blowing skills and conversations about far away places. Thank you also to Theo Strinopoulos for generating the error amplification plots.

Finally, I would like to thank all my friends and family outside of the chemistry world, who have helped me to maintain a balanced outlook during my time at Caltech. Without them, I probably still would have gotten a Ph.D., but I do not think I would have kept my sanity.

ABSTRACT

Towards the goal of kinetic resolution of chiral olefins, a series of enantiopure C_1 -symmetric metallocenes has been synthesized for use in the polymerization of chiral olefins. The new precatalysts were based on the parent precatalyst $\{(\text{SiMe}_2)_2[\eta^5\text{-C}_5\text{H}(\text{CHMe}_2)_2][\eta^5\text{-C}_5\text{H}_2((S)\text{-CHMeCMe}_3)]\}\text{ZrCl}_2$, (*S*)-**2**, which has a doubly, silylene-linked ligand framework. The new precatalysts include $\{(\text{SiMe}_2)_2[\eta^5\text{-C}_5\text{H}(\text{CHEt}_2)_2][\eta^5\text{-C}_5\text{H}_2((S)\text{-CHMeCMe}_3)]\}\text{ZrCl}_2$, (*S*)-**3**, $\{(\text{SiMe}_2)_2[\eta^5\text{-C}_5\text{H}(\text{CHCy}_2)_2][\eta^5\text{-C}_5\text{H}_2((S)\text{-CHMeCMe}_3)]\}\text{ZrCl}_2$, (*S*)-**4** (Cy = cyclohexyl), $\{(\text{SiMe}_2)_2[\eta^5\text{-C}_5\text{H}(\text{CHTMS}_2)_2][\eta^5\text{-C}_5\text{H}_2((S)\text{-CHMeCMe}_3)]\}\text{ZrCl}_2$, (*S*)-**5** (TMS = trimethylsilyl), and $\{(\text{SiMe}_2)_2[\eta^5\text{-C}_5\text{H}(\text{CHMe}_2)_2][\eta^5\text{-C}_5\text{H}_2((S)\text{-CHEtCMe}_3)]\}\text{ZrCl}_2$, (*S*)-**6**.



The zirconocene dichlorides (*S*)-**2**, (*S*)-**3**, (*S*)-**4**, and (*S*)-**5** have an enantiopure 3,3-dimethyl-2-butyl (“methylnepentyl”) substituent on the “upper” cyclopentadienyl ligand. The zirconocene dichloride (*S*)-**6** has an enantiopure 2,2-dimethyl-3-pentyl (“ethylnepentyl”) substituent on the “upper” cyclopentadienyl ligand.

When activated with methylaluminoxane (MAO), these metallocenes show unprecedented activity for the polymerization of racemic monomers bearing substitution

at the 3- and/or 4-positions. In addition, due to the optically pure nature of these single site catalysts, polymerization of racemic monomers serves as a transition metal-mediated kinetic resolution strategy. The polymeric product is enriched with the faster reacting enantiomer, while the recovered monomer is enriched with the slower reacting enantiomer. The two components are easily separated, thus affecting the resolution. A modest kinetic resolution was achieved ($s = k_{faster}/k_{slower} = \text{ca. } 2$) with most olefins surveyed. In the case of 3,4-dimethyl-1-pentene and 3,4,4-trimethyl-1-pentene, high levels of separation were obtained ($s > 12$). X-ray crystal structure determinations for (*S*)-**2**, (*S*)-**3**, and (*S*)-**4** have been used to examine the prevailing steric interactions expected in the diastereomeric transition states for propagation during polymerization. In comparison to (*S*)-**2**, slight improvements in the selectivity of 3-methyl-1-hexene and 3,5,5-trimethyl-1-hexene were observed with polymerizations using (*S*)-**3**. Likewise, the polymerizations of 3-methyl-1-pentene and 3,5,5-trimethyl-1-hexene using (*S*)-**6** showed a modest increase in selectivity, relative to (*S*)-**2**. The kinetic resolution of chiral olefins containing a polar functionality also has been attempted with (*S*)-**2**. Although the selectivity of these polymerization experiments is yet to be determined, preliminary work indicates that NMR can be used to analyze the (*S*)-Mosher esters of the olefins to obtain the enantiomeric excess.

TABLE OF CONTENTS

DEDICATION	iii
ACKNOWLEDGEMENTS	iv
ABSTRACT	vi
TABLE OF CONTENTS	viii
LIST OF FIGURES	x
LIST OF SCHEMES	xi
LIST OF TABLES	xii
INTRODUCTION	1
1 CHAPTER ONE	1-4
LIGAND STERIC EFFECTS ON THE KINETIC RESOLUTION OF CHIRAL α -OLEFINS USING C_1 -SYMMETRIC ZIRCONOCENE POLYMERIZATION CATALYSTS	
1.1 ABSTRACT	1-4
1.2 INTRODUCTION	1-6
1.3 RESULTS AND DISCUSSION	1-14
1.3.1 Synthesis of (S)-Methylneopentyl-ThpZrCl ₂	1-14
1.3.2 Polymerization of Chiral Olefins Using (S)-2	1-15
1.3.3 Evaluating Selectivity Factor Values	1-16
1.3.4 Assignment of Absolute Configuration of Recovered Monomer	1-21
1.3.5 Authenticity of the Absolute Chirality of 34DM1P	1-21
1.3.6 Proposed Mechanism of the Diastereoselectivity	1-22
1.3.7 Synthesis of (S)-3 and (S)-4	1-25
1.3.8 New Polymerization Method	1-29
1.3.9 Preparation of (S)-3-Methyl-1-Pentene	1-30
1.3.10 Polymerization Results Using (S)-2, (S)-3, (S)-4	1-31
1.3.11 Crystal Structure	1-33
1.3.12 Preparation of (S)-5	1-37
1.3.13 Crystal structure of (S)-5	1-40
1.3.14 Activity of Catalysts	1-43
1.3.15 Affect of MAO on Activity	1-45
1.3.16 Preparation of 3,4,4-Trimethyl-1-Pentene	1-48
1.4 CONCLUSIONS	1-49
1.5 EXPERIMENTAL SECTION	1-51
2 CHAPTER TWO	2-1
EFFECTS OF SITE EPIMERIZATION ON THE KINETIC RESOLUTION OF CHIRAL α -OLEFINS USING C_1 -SYMMETRIC ZIRCONOCENE POLYMERIZATION CATALYSTS	
2.1 ABSTRACT	2-1
2.2 INTRODUCTION	2-3
2.3 RESULTS AND DISCUSSION	2-7
2.3.1 Preparation and Optimization of (S)-MNCpH	2-7
2.3.2 Preparation of (R)-Ethylneopentyl Alcohol (ENOH)	2-12
2.3.3 Optimization of (S)-ENCpH	2-14

2.3.4	Ferrocene of (S)-LiENCp.....	2-16
2.3.5	Enzymatic Kinetic Resolution of (S)-MNOH and (S)-ENOH.....	2-17
2.3.6	Preparation of (S)-6 and Polymerizations of Chiral Olefins Using (S)-6.....	2-18
2.4	EXPERIMENTAL SECTION	2-21
3	CHAPTER THREE	3-1
	PROGRESS TOWARD THE KINETIC RESOLUTION OF CHIRAL POLAR OLEFINS USING C_1 -SYMMETRIC ZIRCONOCENE POLYMERIZATION CATALYST	
3.1	ABSTRACT	3-1
3.2	INTRODUCTION.....	3-2
3.3	RESULTS AND DISCUSSION	3-4
3.3.1	Protection and Polymerization of Olefinic Alcohols with Trialkyl Silyl Groups	3-4
3.3.2	Degradation of Polar Monomers by MAO	3-6
3.3.3	Polymerization of N, N'-Bis(Trimethyl Silyl) Allyl Amine.....	3-7
3.3.4	Enantioassay of Polar Monomers.....	3-8
3.4	CONCLUSIONS	3-11
3.5	EXPERIMENTAL SECTION	3-12
A.	Appendix A.....	1
	X-RAY CRYSTALLOGRAPHIC DATA FOR (S)-3	
B.	Appendix B.....	20
	X-RAY CRYSTALLOGRAPHIC DATA FOR (S)-4	
C.	Appendix C.....	47
	X-RAY CRYSTALLOGRAPHIC DATA FOR (S)-5	
D.	Appendix D.....	72
	POLYMERIZATION DATA FOR (S)-3, (S)-4, AND (S)-5	

LIST OF FIGURES

CHAPTER 1

Figure 1.1. Plots of ee vs. conversion as a function of selectivity factors.....	1-8
Figure 1.2. Kinetic resolution of (<i>rac</i>)-4M1H using (<i>S</i> , <i>S</i>)-(EBTHI)ZrCl ₂ /MAO.....	1-12
Figure 1.3. Enantiomeric transition states.	1-13
Figure 1.4. Plots of ee of recovered substrate vs. conversion.....	1-17
Figure 1.5. Plots of ee of recovered substrate vs. conversion.....	1-18
Figure 1.6. Diastereomeric transition states.	1-25
Figure 1.7. Front ORTEP views of (<i>S</i>)- 2 , (<i>S</i>)- 3 , and (<i>S</i>)- 4	1-34
Figure 1.8. Side ORTEP views of (<i>S</i>)- 2 , (<i>S</i>)- 3 , and (<i>S</i>)- 4	1-35
Figure 1.9. Newman projection of (<i>S</i>)- 2	1-36
Figure 1.10. Target (<i>S</i>)-MNThp _{TMS} ZrCl ₂	1-40
Figure 1.11. Crystal structures of (<i>S</i>)- 5b and (<i>S</i>)- 5c	1-41
Figure 1.12. Brintzinger's doubly bridged metallocenes.	1-42
Figure 1.13. Turnover frequencies (TOF) of (<i>S</i>)- 4 and (<i>S</i>)- 3	1-43
Figure 1.14. TOF of (<i>S</i>)- 3 in various solvents.	1-44
Figure 1.15. TOF of (<i>S</i>)- 4 in benzene vs. toluene.....	1-45
Figure 1.16. ¹ H NMR(C ₆ D ₆) spectra of three different batches (a, b, c) of MAO.	1-47

CHAPTER 2

Figure 2.1. NMR Scale Reaction of LiCp + (<i>S</i>)-MNOMs + TMEDA in THF.	2-10
Figure 2.2. NMR Scale Reaction of KCp + (<i>S</i>)-MNOMs + TMEDA in THF.	2-11
Figure 2.3. ¹³ C NMR of [(<i>rac</i>)-ENCp] ₂ Fe and [(<i>S</i>)-ENCp] ₂ Fe.....	2-17

CHAPTER 3

Figure 3.1. Possible coordination of oxygen atom to transition metal center.	3-4
Figure 3.2. ¹ H NMR of Mosher esters: 3-buten-2-ol (CDCl ₃), 4-penten-2-ol (C ₆ D ₆).....	3-9
Figure 3.3. ¹⁹ F NMR (500 MHz) of Mosher esters of 3-buten-2-ol and 4-penten-2-ol. .3-9	

APPENDIX A

Figure A.1. ORTEP view of (<i>S</i>)- 3	6
Figure A.2. Unit cell of X-ray structure of (<i>S</i>)- 3	7

APPENDIX B

Figure B.1. ORTEP view of (<i>S</i>)- 4	25
Figure B.2. ORTEP view for (<i>S</i>)- 4	26
Figure B.3. Unit cell of X-ray structure of (<i>S</i>)- 4	27

APPENDIX C

Figure C.1. ORTEP view of (<i>S</i>)- 5b	52
Figure C.2. ORTEP view of (<i>S</i>)- 5c	53
Figure C.3. Unit cell of X-ray structure of (<i>S</i>)- 5b and (<i>S</i>)- 5c	54

LIST OF SCHEMES

CHAPTER 1

Scheme 1.1. Kinetic resolution: one enantiomer is preferentially converted to product.	1-6
Scheme 1.2. Kinetic resolution of enantiomers A/B.	1-7
Scheme 1.3. Versatility of olefin as chiral synthon.	1-9
Scheme 1.4. Potential kinetic resolution of naproxen, an anti-inflammatory drug.	1-9
Scheme 1.5. Kinetic resolution of alkenes by asymmetric dihydroxylation.	1-10
Scheme 1.6. Kinetic resolution through selective polymerization.	1-11
Scheme 1.7. Stereospecific polymerization using a heterogeneous catalyst.	1-11
Scheme 1.8. Synthesis of (<i>S</i>)-MNThpZrCl ₂ .	1-14
Scheme 1.9. Synthesis of dithiolate of (<i>S</i>)- 2 .	1-15
Scheme 1.10. Site epimerization and insertion mechanism.	1-23
Scheme 1.11. Synthesis of 1,3-dialkylcyclopentadiene.	1-26
Scheme 1.12. Synthesis of (<i>S</i>)-MNThp ligand with various alkyl substituents.	1-27
Scheme 1.13. Synthesis of (<i>S</i>)-MNThp _R ZrCl ₂ .	1-28
Scheme 1.14. Synthesis of (<i>S</i>)-3-methyl-1-pentene.	1-30
Scheme 1.15. Synthesis of TMS substituted cyclopentadiene.	1-38
Scheme 1.16. Synthesis of doubly bridged ligand for (<i>S</i>)- 5 .	1-39
Scheme 1.17. Synthesis of 3,4,4-trimethyl-1-pentene.	1-49
Scheme 1.18. Many stereocenters in the vicinity of the active site.	1-50

CHAPTER 2

Scheme 2.1. Site epimerization mechanism.	2-4
Scheme 2.2. Synthesis of (<i>S</i>)-LiMNCp.	2-8
Scheme 2.3. Synthesis of ferrocene of (<i>S</i>)-LiMNCp.	2-9
Scheme 2.4. Synthesis of (<i>S</i>)-ethylneopentyl alcohol.	2-13
Scheme 2.5. Enzymatic kinetic resolution of methylneopentyl alcohol.	2-17
Scheme 2.6. Preparation of (<i>S</i>)- 6 .	2-18

CHAPTER 3

Scheme 3.1. Protection of 3-buten-2-ol with TESCl and TBSCl.	3-5
Scheme 3.2. Derivatization of polar monomer for enantioassay.	3-8
Scheme 3.3. Work-up of polymerization and derivatization attempt.	3-10

LIST OF TABLES

CHAPTER 1

Table 1.1. Kinetic resolution of chiral α -olefins using (S)- 2	1-16
Table 1.2. Theoretical conversion, ee, and <i>s</i> values.....	1-20
Table 1.3. Optimization of (S)-1-iodo-3-methyl pentane.....	1-31
Table 1.4. Kinetic resolution chiral olefins using (S)- 2 , (S)- 3 , (S)- 4	1-32

CHAPTER 2

Table 2.1. Temperature affect on the polymerization of 344TM1P using (S)- 2	2-5
Table 2.2. Dependence of reaction conversion on solvent.....	2-12
Table 2.3. Composition of products and starting materials in various solvents.....	2-15
Table 2.4. Kinetic resolution of chiral 3-methyl substituted olefins using (S)- 6	2-20

CHAPTER 3

Table 3.1. Polymerization of Trialkyl Silyl Protected Alcohols.....	3-6
---	-----

APPENDIX A

Table A.1. Crystal data and structure refinement for (S)- 3	2
Table A.2. Atomic coordinates and U_{eq} for (S)- 3	8
Table A.3. Selected bond lengths [\AA] and angles [$^{\circ}$] for (S)- 3	10
Table A.4. Bond lengths [\AA] and angles [$^{\circ}$] for (S)- 3	11
Table A.5. Anisotropic displacement parameters ($\text{\AA}^2 \times 10^4$) for (S)- 3	18

APPENDIX B

Table B.1. Crystal data and structure refinement for (S)- 4	21
Table B.2. Atomic coordinates and U_{eq} for (S)- 4	28
Table B.3. Selected bond lengths [\AA] and angles [$^{\circ}$] for (S)- 4	32
Table B.4. Bond lengths [\AA] and angles [$^{\circ}$] for (S)- 4	33
Table B.5. Anisotropic displacement parameters ($\text{\AA}^2 \times 10^4$) for (S)- 4	43

APPENDIX C

Table C.1. Crystal data and structure refinement for (S)- 5b and (S)- 5c	48
Table C.2. Atomic coordinates and U_{eq} for (S)- 5b and (S)- 5c	55
Table C.3. Selected bond lengths [\AA] and angles [$^{\circ}$] for (S)- 5b and (S)- 5c	58
Table C.4. Bond lengths [\AA] and angles [$^{\circ}$] for (S)- 5b and (S)- 5c	59
Table C.5. Anisotropic displacement parameters ($\text{\AA}^2 \times 10^4$) for (S)- 5b and (S)- 5c	68

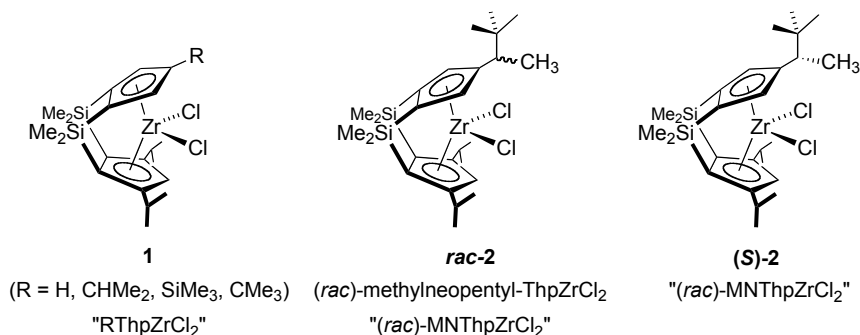
APPENDIX D

Table D.1. Kinetic resolution of chiral olefins using (S)- 2	73
Table D.2. Kinetic resolution of chiral olefins using (S)- 3	74
Table D.3. Kinetic resolution of chiral olefins using (S)- 4	74

INTRODUCTION

Enantiopure, simple (without functional groups) olefins are highly versatile synthons for asymmetric synthesis and are monomers for the development of new polymers with novel optical and/or physical properties. For these reasons, facile and practical routes to enantiopure olefins are highly desired. Despite the great progress in the kinetic resolution of many and varied classes of substrates, the practical kinetic resolution of simple chiral olefins remains a formidable challenge. The absence of functional groups poses a great challenge for the establishment of diastereomeric transition states with sufficient energy difference, which is necessary for an effective kinetic resolution.

In an effort to address this difficulty, we have explored olefin polymerization catalysis as a possible approach to obtain enantiopure olefins. It was previously reported in the group that doubly bridged zirconocene catalysts, **1** and (*rac*)-**2**, activated with methylaluminoxane (MAO) polymerized propylene with good syndiospecificity and activity. The modification of (*rac*)-**2** with an enantiopure 3,3-dimethyl-2-butyl (“methylneopentyl”) substituent has been accomplished to explore its kinetic resolution capabilities, [(*S*)-**2**].



In chapter 1, the results from the polymerization of 3- and 4-methyl olefins using (*S*)-**2** are discussed. New precatalysts based on the parent metallocene were prepared by replacing the isopropyl groups on the lower cyclopentadienyl ring with larger substituents. The synthesis and the polymerization results of these new precatalysts are discussed in chapter one. A working model of the polymerization mechanism involved in the olefin enantiomer selection is also proposed.

Whereas chapter 1 discusses the effect of changing steric bulk on the bottom cyclopentadienyl ring of (*S*)-**2**, chapter 2 discusses the effect of increasing steric bulk on the top ring. Based on the mechanism proposed in chapter 1, it is suggested that increasing the bulk of the top ring may increase the rate of site epimerization and enhance enantiomer selectivity. Hence, the methylneopentyl group was replaced with a 2,2-dimethyl-3-pentyl (“ethylneopentyl”) group. The synthesis and the polymerization results are reported in chapter 2.

The selective polymerization approach to kinetic resolution of chiral olefins was extended to chiral olefins containing polar functionalities. The preparation of functionalized monomers and the optimization of polymerization conditions are reported in chapter 3. The recovery and enantioassay of unreacted monomer require further investigation.

Dr. Chris Levy undertook the groundbreaking work of the kinetic resolution project. The works contributed by him are reported in chapter 1 and are as follows: the synthesis and characterization of (*S*)-**2**, the first set of polymerization data using (*S*)-**2**, and the assignment of absolute configuration of 3,4,4-trimethyl-1-pentene and 3,5,5-trimethyl-1-hexene. Dr. Cliff Baar obtained the second set of polymerization data using

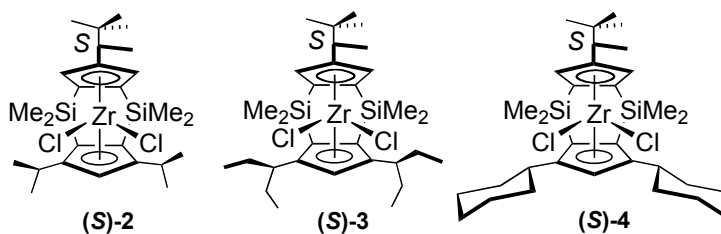
(S)-2. Theo Strinopoulos generated the error amplification plots, Figure 1.4 and Figure 1.5. Mike Day and Larry Henling provided all X-ray crystallographic data. The author contributed all other work reported herein.

1 CHAPTER ONE

LIGAND STERIC EFFECTS ON THE KINETIC RESOLUTION OF CHIRAL α -OLEFINS USING C_1 -SYMMETRIC ZIRCONOCENE POLYMERIZATION CATALYSTS

1.1 ABSTRACT

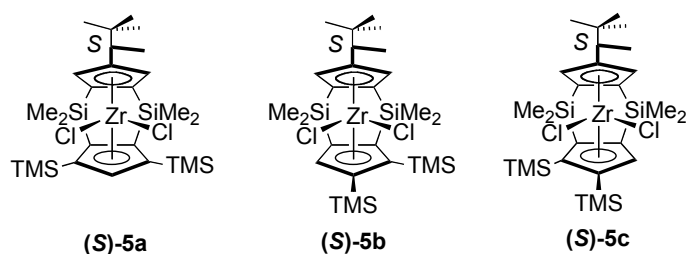
Towards the goal of kinetic resolution of chiral α -olefins through selective polymerization, enantiopure C_1 -symmetric metallocenes based on the parent precatalyst, (*S*)-**2**, have been synthesized. To investigate how larger substituents on the bottom cyclopentadienyl ring affect the selectivity of the catalyst, new precatalysts (*S*)-**3** and (*S*)-**4** were prepared.



When activated with methylaluminoxane (MAO), these metallocenes show unprecedented activity for the polymerization of racemic monomers bearing substitution at the 3- and/or 4-positions. A modest kinetic resolution was achieved ($s = k_{faster}/k_{slower} =$ ca. 2) with most olefins surveyed. In the case of 3,4-dimethyl-1-pentene and 3,4,4-trimethyl-1-pentene, high levels of separation were obtained ($s > 12$). X-ray crystal

structure determinations for (*S*)-**2**, (*S*)-**3**, and (*S*)-**4** have been used to examine the prevailing steric interactions expected in the diastereomeric transition states for propagation during polymerization.

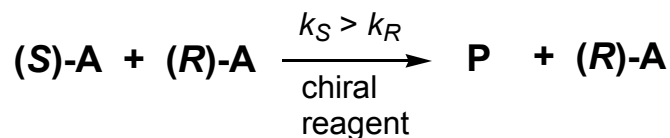
The preparation of (*S*)-**5a** was attempted, but rather than the desired product, (*S*)-**5b** and (*S*)-**5c** were obtained. It is unclear whether (*S*)-**5** was present or not from NMR data. Some selectivity ($s = 1.5$) was observed for polymerization of 3-methyl-1-pentene using this precatalyst mixture.



1.2 INTRODUCTION

The development of methods that will produce molecules of high optical purity is an important pursuit in chemical synthesis. As of date, three general ways to achieve this goal exist.¹ One approach involves asymmetric synthesis, which converts achiral substrates to chiral molecules.² The second method exploits the chiral pool of enantiopure starting materials that nature provides. The final route is resolution, which involves the separation of enantiomers by physical or chemical methods.³

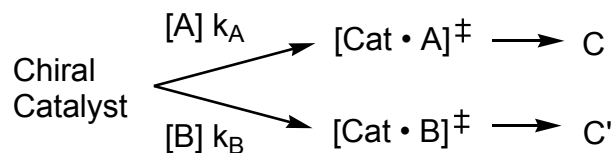
The three general methods for resolution are classical resolution, chiral chromatography, and kinetic resolution.⁴ In classical resolution, a stoichiometric amount of chiral resolving agent binds to the substrate to form diastereomers that are separated.⁵ Subsequently, the substrate is released from the resolving agent by chemical means. Chiral chromatography uses a chiral stationary phase to resolve enantiomers in a mobile phase. Finally, kinetic resolution is a chemical process that selectively transforms one of the enantiomers of a racemic mixture into product and leaves the other enantiomer unmodified (Scheme 1.1).^{3,4}



Scheme 1.1. Kinetic resolution: one enantiomer is preferentially converted to product.

Kinetic resolution requires the formation of diastereomeric transition states that result from the interaction between an enantiopure chiral catalyst and enantiomeric

substrates (Scheme 1.2).¹ The disparate energy levels of the transition states cause one enantiomer to convert to product at a faster rate than its counterpart. The goal of any kinetic resolution process is rendering a large enough difference in the transition states such that one enantiomer is transformed while its counterpart remains unchanged.



Scheme 1.2. Kinetic resolution of enantiomers A/B.³

In kinetic resolution, the yield of optically pure compound is limited to 50%, whereas a 100% transformation via asymmetric synthesis is possible. Nonetheless, this disadvantage is compensated by the fact that small increases in conversion can yield significant improvements in the percentage of enantiomeric excess, especially if the selectivity factor (*s*) is high.³

The selectivity factor is defined as the ratio of the reaction rates of the two enantiomers and is related to both the reaction conversion (*c*) and enantiomeric excess (*ee*) (eq. 1.1 and Figure 1.1).¹

$$s = \frac{k_{fast}}{k_{slow}} = \frac{\ln [(1 - c)(1 - ee)]}{\ln [(1 - c)(1 + ee)]} \quad (\text{Eq. 1.1})$$

s = selectivity factor
 c = % conversion/100
 ee = % enantiomeric excess/100

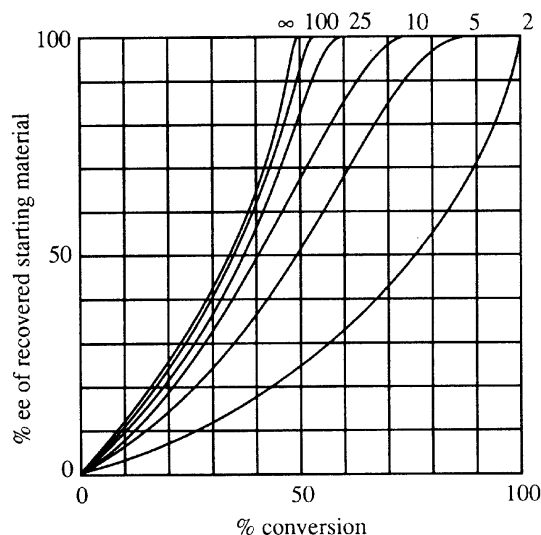
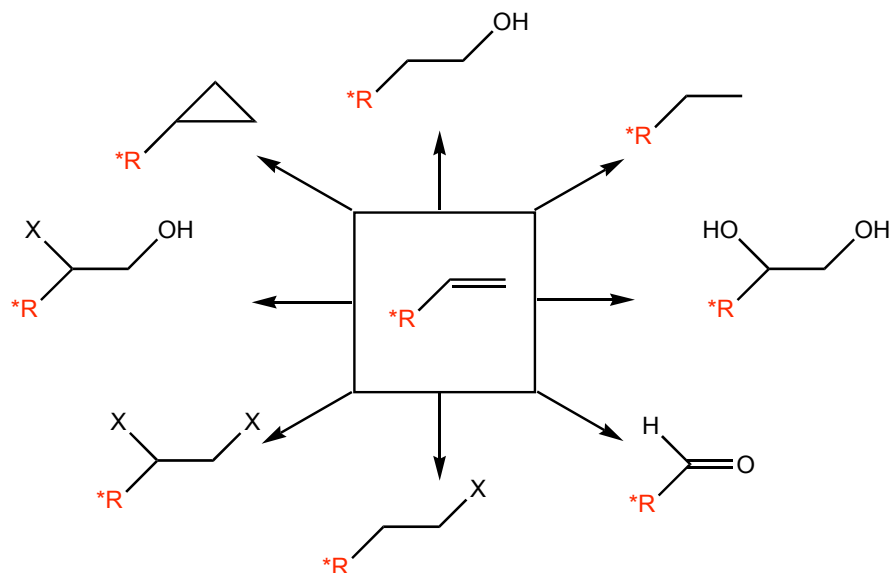
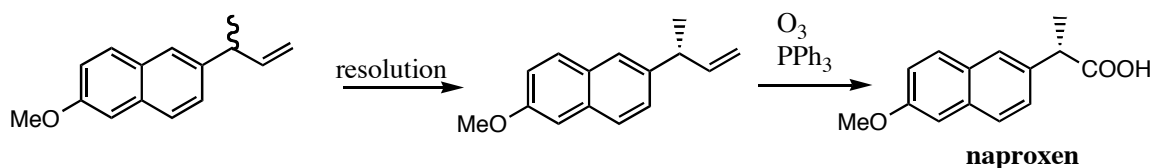


Figure 1.1. Plots of ee vs. conversion as a function of selectivity factors. The curves represent the selectivity factors.³

A facile and effective method to kinetically resolve chiral, simple (those without heteroatom substituents) olefins is desirable because enantiopure olefins can be easily functionalized to a wide variety of enantiopure molecules via established organic reactions (Scheme 1.3). Moreover, important chiral molecules or precursors containing vinyl groups can be directly resolved and isolated (Scheme 1.4). Enantiopure olefins can also function as chiral monomers to make new polymers with novel physical and/or optical properties. These new materials may be used as chiral supports for the separation of enantiomers, chiral supports for metal catalysts, or as optically active polymer for optical devices.



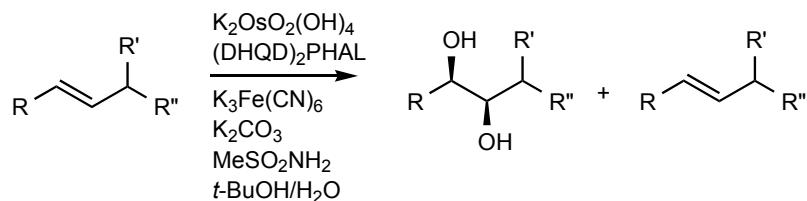
Scheme 1.3. Versatility of olefin as chiral synthon.



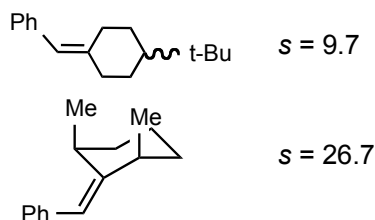
Scheme 1.4. Potential kinetic resolution of naproxen⁶, an anti-inflammatory drug.

The most successful kinetic resolutions of olefins have involved allylic alcohols,⁷ allylic ethers,⁸ and dienes.⁹ The kinetic resolution of simple racemic alkenes has been less successful.⁴ The alkene's lack of functionality poses a great difficulty in producing diastereomeric transition states with sufficient energy differences.

A few examples of kinetic resolution of simple alkenes via oxidative transformations can be found. For example, the osmium tetroxide-cinchona alkaloid system developed by Sharpless mediates the dihydroxylation of axially disymmetric internal olefins with modest efficiency.¹⁰ In a related report, asymmetric dihydroxylation was used to resolve 2,6-dimethylbenzylidenecyclohexane (Scheme 1.5).¹¹



(DHQD)₂PHAL = 1,4-bis(9-O-dihydroquinidine)phthalazine

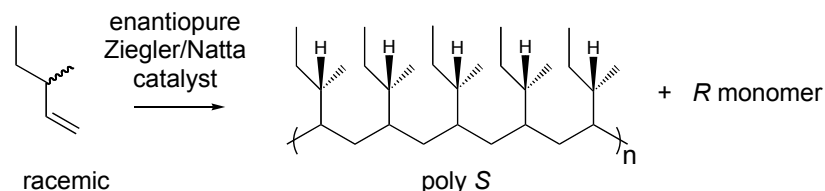


Scheme 1.5. Kinetic resolution of alkenes by asymmetric dihydroxylation.⁴

In contrast, reductive kinetic resolution strategies have not been reported for unfunctionalized olefins.¹² In addition to the limitations discussed above, reductive strategies for simple chiral alkenes suffer from the added difficulty of separating unreacted alkene from product alkane fractions. In an attempt to address limitations in the application of kinetic resolution to unfunctionalized olefins, we have explored olefin polymerization catalysis as a possible alternative.

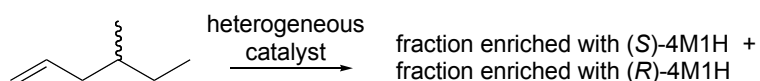
Ziegler-Natta and metallocene catalysts have demonstrated very high levels of enantiofacial selectivity in the polymerization of prochiral olefins and have produce polymer with a well-defined microstructure or tacticity.¹³ These catalysts also are extremely active, producing in many cases $>10^3$ kilograms of polymer/g of metal·h.¹⁴ Based on these observations, using enantiopure Ziegler-Natta or metallocene catalysts to affect kinetic resolution of chiral alkenes by preferentially polymerizing one enantiomer and leaving the less reactive enantiomer behind appeared particularly attractive (Scheme

1.6). The enantioenriched olefin should be recoverable by simple filtration. Moreover, an optically active polymer by virtue of enantiopure substituents in the polymer side chain, may likewise be isolated.



Scheme 1.6. Kinetic resolution through selective polymerization.

Several studies lend support to this strategy for the kinetic resolution of chiral olefins. Proposing that heterogeneous Ziegler-Natta catalysts contain chiral active sites that are responsible for stereospecific polymerization, Natta used a heterogeneous catalyst to obtain highly crystalline, optically active fractions of poly-(4-methyl-1-hexene) (Scheme 1.7).¹⁵



Scheme 1.7. Stereospecific polymerization using a heterogeneous catalyst.

Moreover, Ciardelli demonstrated that a modest kinetic resolution of chiral monomers can be achieved with enantiopure homogeneous metallocene catalysts (Figure 1.2).¹⁶ Using (*S,S*)-ethylene bis(tetrahydroindenyl) zirconium dichloride (EBTHI)ZrCl₂/MAO system, the *S* enantiomer of racemic 4-methyl-1-hexene was preferentially incorporated into the polymer (*s* = 1.4).¹⁷ Although the same catalyst

system failed to polymerize 3-methyl-1-pentene, the monomer has since been polymerized by other homogeneous metallocene catalysts.¹⁸ C_s - or racemic C_2 -symmetric precatalysts, however, were employed, precluding any possible kinetic resolution.

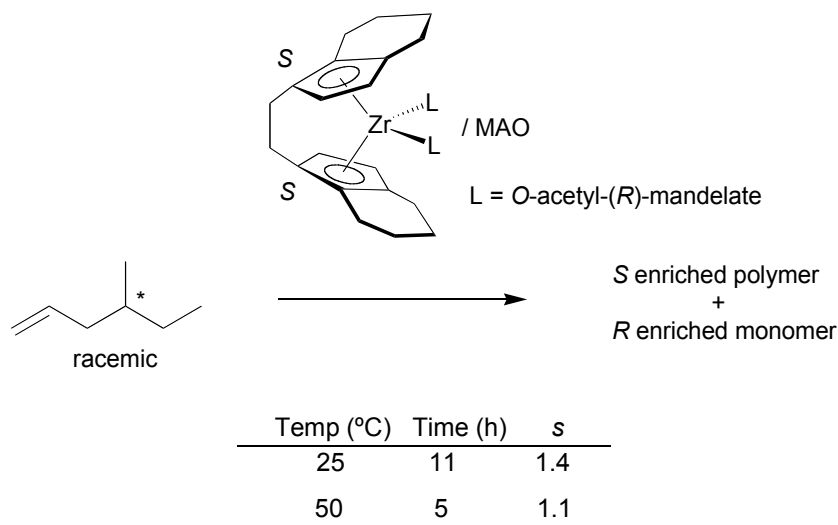


Figure 1.2. Kinetic resolution of (*rac*)-4M1H using (*S,S*)-(EBTHI)ZrCl₂/MAO.

C_s -symmetric precatalysts generate enantiomeric transition states (Figure 1.3); thus, both olefinic enantiomers are incorporated with equal preference. Racemic C_2 -symmetric catalysts, similarly, produce enantiomeric transition states. The abovementioned precedents clearly indicate the necessity for enantiopure precatalysts that produce diastereomeric transition states, leading to preferential enchainment of one enantiomer.

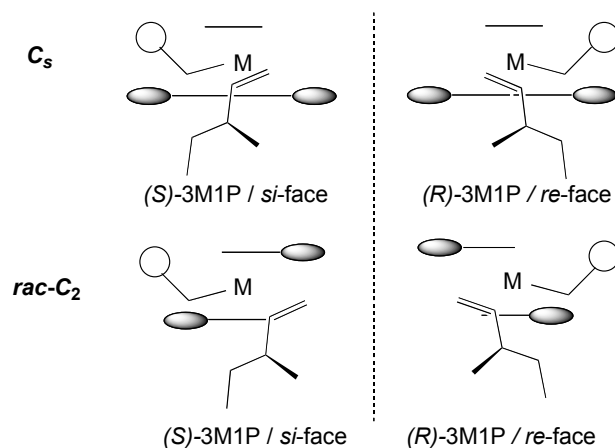
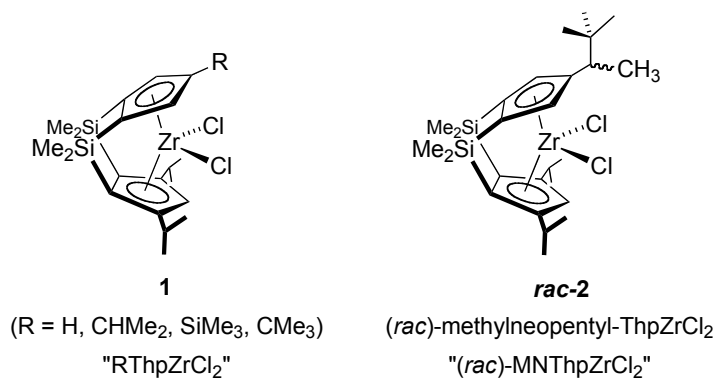


Figure 1.3. Enantiomeric transition states.
3-methyl-1-pentene (3M1P) coordinated to C_s and racemic C_2 -symmetric catalysts.

Tim Herzog previously reported that doubly bridged zirconocene catalysts (**1**) activated with MAO, polymerized propylene with very high syndiospecificities and with extremely high activities.¹⁹ Modification of this catalyst system with a racemic 3,3-dimethyl-2-butyl ("methylnepentyl") substituent was also accomplished (**2**).²⁰



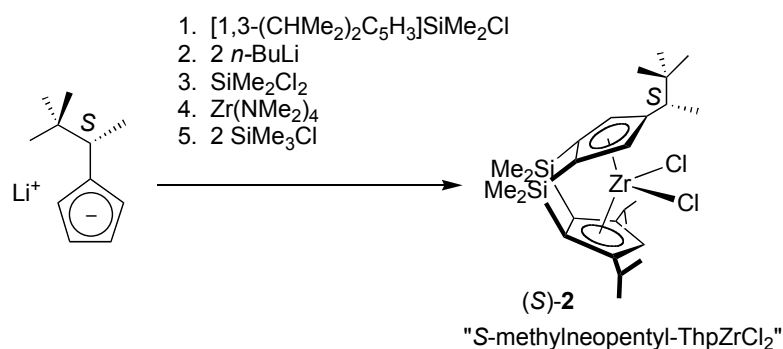
Reported herein, with an enantiopure methylnepentyl (MN) substituent, partial kinetic resolution of simple racemic α -olefins has been carried out. For 3,4-dimethyl-1-pentene and 3,4,4-trimethyl-1-pentene, synthetically useful degrees of

separation can be achieved ($s > 12$). These substrates represent some of the simplest organic molecules to be kinetically resolved to date.

1.3 RESULTS AND DISCUSSION

1.3.1 Synthesis of (*S*)-Methylnepentyl-ThpZrCl₂

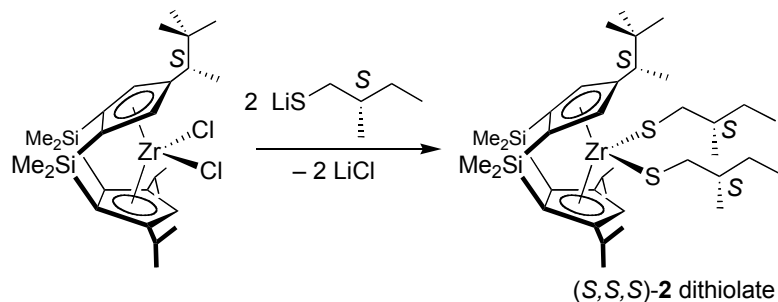
The precatalyst (*S*)-methylnepentylThpZrCl₂, (*S*)-**2**, was first prepared by Chris Levy following the established procedures for (*rac*)-MNThpZrCl₂ (Scheme 1.8).^{19,20} An enantiopure (*S*)-methylnepentyl was installed on the top cyclopentadienyl (Cp) ring to produce a C₁-symmetric precatalyst. The preparation of (*S*)-methylnepentyl cyclopentadiene, (*S*)-MNCpH, will be discussed in chapter 2.



Scheme 1.8. Synthesis of (*S*)-MNThpZrCl₂.

The optical purity of the precatalyst was assayed by reaction of (*S*)-**2** with 2 equivalents of lithium (*S*)-3-methyl-1-butanethiolate (Scheme 1.9).²¹ The ¹H NMR and ¹³C NMR spectra of (*S,S,S*)-**2** dithiolate were compared to the NMR spectra of

diastereomers resulting from the reaction of (*rac*)-**2** with the lithio thiolate. Resonances corresponding to the (*R,S,S*) diastereomer were not observed, suggesting >98% optical purity.



Scheme 1.9. Synthesis of dithiolate of (*S*)-**2**.

1.3.2 Polymerization of Chiral Olefins Using (*S*)-**2**

The first polymerization data using (*S*)-**2** was obtained by Chris Levy. When activated with MAO, (*S*)-**2** polymerized 4-methyl-1-hexene (4M1H) and all 3-methyl olefins surveyed. In general, a polymerization experiment involved adding MAO, tetradecane, olefin, and catalyst solution into a 10-mL round bottom flask equipped with a Teflon needle valve joint. Tetradecane acts as both a solvent and an internal standard for GC monitoring of reaction conversion. Also, the conversion was determined by mass difference of olefin added and olefin recovered after polymerization. The ee of the recovered olefins was analyzed by polarimetry on neat olefin or by conversion to carboxylic acids then to diastereomeric mandelic esters, which were analyzed by ^1H and ^{13}C NMR.²²

As Table 1.1 shows, the MAO-activated (*S*)-**2** demonstrated modest kinetic resolution of all olefins with the best selectivity ($s = 12$) for 3,4,4-trimethyl-1-pentene (344TM1P; entry 3). The worst kinetic resolution was observed with 4-methyl-1-hexene ($s = 1.1$; entry 5).

Table 1.1. Kinetic resolution of chiral α -olefins using (*S*)-2****

entry	olefin	abbreviation	t (h)	TOF (h ⁻¹)	% c	% ee	$s = \frac{k_S}{k_R}$
1		3M1P	26.2	360	41.8	14.5	1.7
2		34DM1P	70	55	55	27.9	2
3		344TM1P	48	8.6	21.5	22.2	12
4		355TM1H	21.1	150	41.9	18.4	2
5		4M1H	20.5	97	51.3	2.39	1.1

MAO = methylaluminoxane

TOF = Turnover frequency =
[(moles olefin reacted)/(moles Zr)] / t

% c = percent conversion

% ee = percent enantiomeric excess

s = selectivity factor

1.3.3 Evaluating Selectivity Factor Values

Since s values are calculated based on experimentally measured ee and c values, it is important to see how relative errors in ee and c will propagate to relative errors in s . First we will examine separately how relative errors in ee and c affect the relative error in s . When the relative error in c is zero, the relative error in s is equal to the amplification

factor A_{ee} multiplied by the relative error in ee (eq. 1.2). This relationship is illustrated in Figure 1.4.²³ Figure 1.5 and eq. 1.3 describe how the relative error in c affects the relative error in s when the relative error in ee is zero. The colored curves are lines of constant A_{ee} . The black lines show the enantiomeric excess versus conversion for selected s values.

$$\frac{\Delta s}{s} = A_{ee}(c, ee) \frac{\Delta ee}{ee} \quad (\text{Eq. 1.2})$$

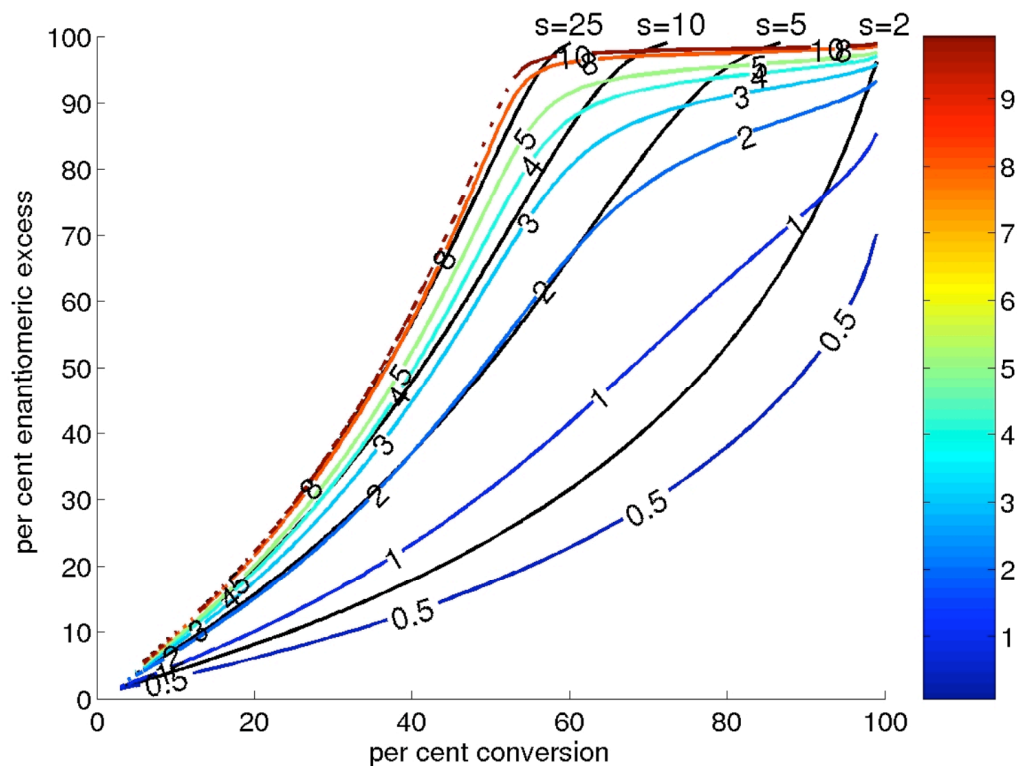


Figure 1.4. Plots of ee of recovered substrate vs. conversion.

Contours of constant error amplification factor, $A_{ee}(c, ee)$, where c denotes conversion and ee denotes enantiomeric excess. The value of A_{ee} is calculated for the case of zero relative error in c . The black curves show the ee as a function of conversion for the cases of $s = 2, 5, 10$, and 25 .

$$\frac{\Delta s}{s} = A_c(c, ee) \frac{\Delta c}{c} \quad (\text{Eq. 1.3})$$

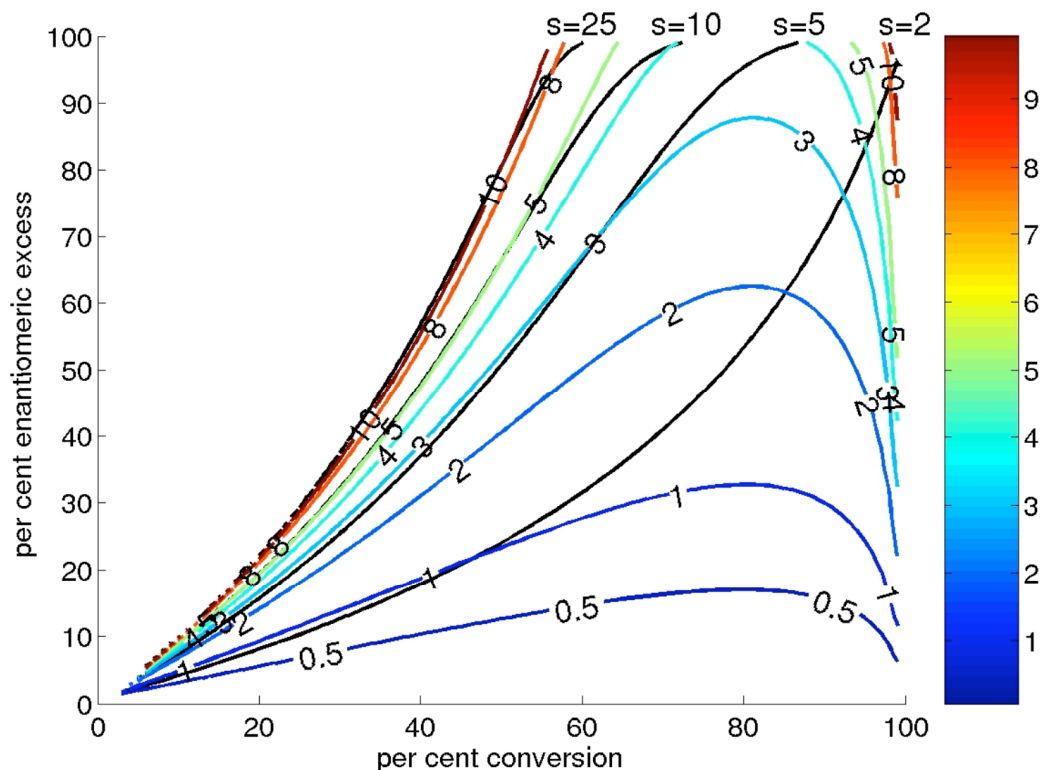


Figure 1.5. Plots of ee of recovered substrate vs. conversion.

Contours of constant error amplification factor, $A_c(c, ee)$, where c denotes conversion and ee denotes enantiomeric excess. The value of A_c is calculated for the case of zero relative error in ee . The black curves show the ee as a function of conversion for the cases of $s = 2, 5, 10$, and 25 .

A_{ee} and A_c are large in the region with red and green contour lines and small in the blue region. Therefore, even small relative errors in conversion and ee will lead to large errors in s in the red region but not in the blue region. Note that the high selectivities are in the red and green regions, and the low selectivities are in the blue region. This means that high selectivity will have high A_{ee} and A_c , and thus large uncertainty in selectivity. In other words, the greater the selectivity, the greater the difficulty in determining the precise value of s .

For example, if s is near $s = 5$, the uncertainty Δee in the measurement of ee propagates to a greater uncertainty Δs , but only by a factor of 2 over most of the course of the reaction (up to ~60% conversion). The situation is much worse if s is greater than 10; uncertainty in ee is amplified by a factor of 5 or more.

Comparing Figure 1.4 and Figure 1.5, one can see that below 80% ee , the relative error in conversion has a greater effect on the s value than the relative error in ee . This is important to note because experimental error in conversion measurement is greater than in ee measurement.

We determined which region to run our experiments with the above discussion in mind. When very little of the monomer has been converted, the uncertainty in determining s is relatively large. In general, the trajectory for any particular s moves to the lowest error amplification values along its path as conversion increases to roughly 30%. The second constraint was to stop the reaction at 60% conversion, in order to have enough unreacted monomer to enantioassay (0.5 mL–1 mL). Experimentally, we maintained a conversion range between 30% and 60%.

To give a more quantitative understanding of Figure 1.4 and Figure 1.5, Table 1.2 has been generated, which shows calculated values for the propagation of uncertainty in the two selectivity regions where most of our experiments lie. The first region of high selectivity is near the point with $ee = 75$ and $c = 50$ and has $s = 15$. The second region of low selectivity is near the point with $ee = 25$ and $c = 50$ and has $s = 2$. For the high selectivity points in rows A and B, we varied either conversion or ee by $\pm 2\%$ and the resulting change in s was approximately 14% and 10%, respectively. In contrast, a $\pm 2\%$

uncertainty in ee or conversion in the low selectivity region (rows C and D) results in roughly $\pm 2\%$ uncertainty in s , that is the uncertainty is not amplified there.

Table 1.2. Theoretical conversion, ee, and s values

	conversion	ee	s
A	0.51	0.75	13.7
	0.5	0.75	15.6
	0.49	0.75	18.1
B	0.5	0.765	17.1
	0.5	0.750	15.6
	0.5	0.735	14.2
C	0.51	0.25	2.04
	0.5	0.25	2.08
	0.49	0.25	2.13
D	0.5	0.255	2.12
	0.5	0.250	2.08
	0.5	0.245	2.06

In reality, both relative errors in ee and c are simultaneously affecting the relative error in s . The total relative error in s is given by eq. 1.4, which is the addition of equation 1.2 and equation 1.3. It is important to consider this error discussion when evaluating s values generated from polymerization experiments, such as those in Table 1.1. The relative errors in s for polymerization data reported in the following sections are shown in appendix D.

$$\frac{\Delta s}{s} = A_c(c, ee) \frac{\Delta c}{c} + A_{ee}(c, ee) \frac{\Delta ee}{ee} \quad \text{Eq. 1.4}$$

1.3.4 Assignment of Absolute Configuration of Recovered Monomer²⁴

Using (*S*)-2/MAO (Table 1.1), the *S* monomer of the olefin was preferentially enchain in all cases of olefins surveyed. The prevailing absolute configuration in the recovered monomer was determined by comparison of their optical rotations with literature reports.²⁵ For 3,5,5-trimethyl-1-hexene and 3,4,4-trimethyl-1-pentene, the rotations of enriched material had never been reported. The (*S*)-Mandelic ester derivatives of enriched 3-methyl-1-pentene (3M1P), 3,4-dimethyl-1-pentene (34DM1P), 3,4,4-trimethyl-1-pentene (344TM1P), and 3,5,5-trimethyl-1-hexene (355TM1H) were prepared and analyzed by NMR. All products showed less intensity for the ¹H NMR upfield signal of the diastereotopic methyl groups (α to the methyl Mandelic ester moiety), which argues for a common absolute configuration in these olefins. Since all the recovered olefins rotated in the direction of (*R*)-3M1P and (*R*)-34DM1P, it was assumed that the recovered 355TM1H and 344TM1P were enriched in *R* monomer. With these assignments in hand, the relative retention times for olefin derivatives as obtained from chiral GC were used to assign enantiomer selectivity with other catalyst systems.

1.3.5 Authenticity of the Absolute Chirality of 34DM1P

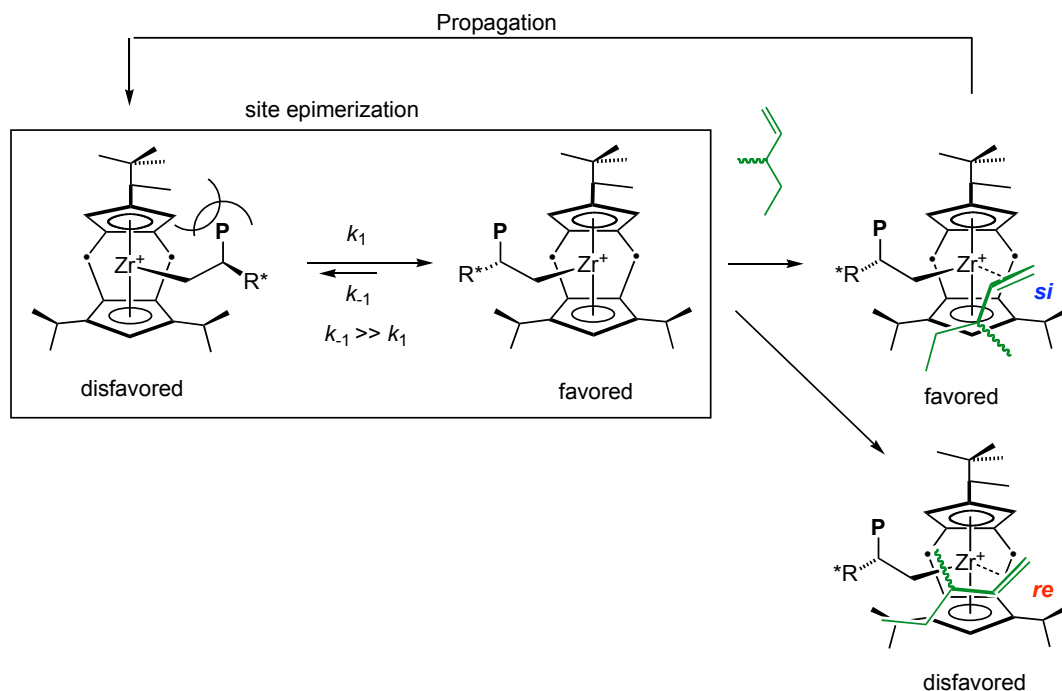
During our analysis of the relevant literature, we found a discrepancy in the assignment of the absolute configuration and the optical rotation for enantiomers of 3,4-dimethyl-1-pentene. For the (+) specific rotation, one series of papers assigned the enantiomer (*S*)-34DM1P.²⁶ However, another series of articles has correlated the (+) specific rotation to the opposite enantiomer (*R*)-3,4-DM1P.²⁷ Due to this conflict in the literature, it was necessary to unambiguously assign each enantiomer its proper optical

rotation. The literature is in agreement regarding the absolute configuration of structurally related (-)(*R*)-2,3-dimethylbutyric acid. The absolute configuration of this acid has been established by comparison to well-established steroid natural products.²⁸ Since this acid is the product of 34DM1P oxidation with NaIO₄ and RuCl₃ and since the stereocenter is retained during the oxidation process, determination of the absolute configuration of 34DM1P follows directly. Hence, the 34DM1P monomer recovered following polymerization with (*S*)-**2** was converted to 2,3-dimethylbutyric acid, and the optical rotation was measured: $[\alpha]_{\text{D}}^{26} -18.1156^{\circ}$ (*c* 0.9860, ethanol). The specific rotation is consistent with (-)(*R*)-2,3-dimethylbutyric acid, identifying the recovered olefin as (-)(*R*)-3,4-dimethyl-1-pentene.

1.3.6 Proposed Mechanism of the Diastereoselectivity

¹³C NMR of poly-(3M1P) obtained from polymerization with (*S*)-**2**/MAO was compared to literature reports of the NMR spectra of poly-(3M1P).²⁹ The comparison suggested that the polymer was isotactic. Furthermore, the polymer does not melt, but rather decomposes at 350 °C, which further suggests high isotacticity.

An analysis of steric interactions in the active metal site of (*S*)-**2** in conjunction with current understanding of polymerization mechanism may provide a working model for the polymerization of 3M1P by (*S*)-**2**/MAO and an explanation for how an isotactic polymer enriched in the *S* monomer is obtained (Scheme 1.10).



Scheme 1.10. Site epimerization and insertion mechanism.

Previously, it had been demonstrated that α -olefin coordinates to the metal center anti to the growing polymer chain,³⁰ orienting the methyl substituent down away from the polymer chain and into the pocket between the isopropyl groups of the lower Cp ring. After the 1,2-insertion of the olefin, the polymer chain swings to the other side of the catalyst and is ready for another olefin coordination. Site epimerization is this process of polymer chain swinging to the opposite side of the metallocene wedge after each migratory insertion of monomer. To minimize steric interactions, the growing polymer chain swings to the more open (left) side of the catalyst to avoid steric interaction with the methyl group of the chiral substituent on the top ring.³¹

Tim Herzog reported that in the case of concentrated propylene conditions, syndiotactic polymer forms. This result suggests that olefin insertion rate is faster than the rate of site epimerization, leading to propylene insertion on both sides of the catalyst.

Under dilute conditions, the rate of insertion is slower than the rate of epimerization. Hence, the chain has a chance to swing away from the methyl side before an insertion can occur. Insertions occur mostly on the right side, leading to an isotactic polymer.

To explain the isotacticity of poly-(3M1P), we propose that the greater size of 3M1P compared to propylene render the site epimerization rate to be greater than the propagation rate of 3M1P. Hence, the incoming olefins will encounter the same chiral side of the catalyst during each enchainment, leading to a highly isotactic poly-(3M1P).

The position of the polymer chain directs the enantiofacial selection (*re* versus *si*) of the olefin. The enantiofacial selection in turn influences which enantiomer (*S* or *R*) of the olefin is inserted. Although the energy difference in the diastereomeric transition states is no doubt small, one can rationalize the diastereomeric preferences on relative steric interactions (Figure 1.6). The incoming olefin coordinates to the metal in such a fashion to minimize steric interaction. Such coordination places the larger 3-position substituent (*R* = Et, isopropyl, *t*-Bu, neopentyl versus Me) in the more open region between the lower Cp isopropyl groups. For both the *R* and the *S* monomers, the hydrogen on the 3-position would point into the pocket towards the Cp 4-position hydrogen. For the *R* monomer, the olefin *R* substituent is directed toward the lower right isopropyl arm of the Cp ligand. In contrast, the *R* substituent of the *S* monomer resides in the more open region between the lower Cp arm groups.

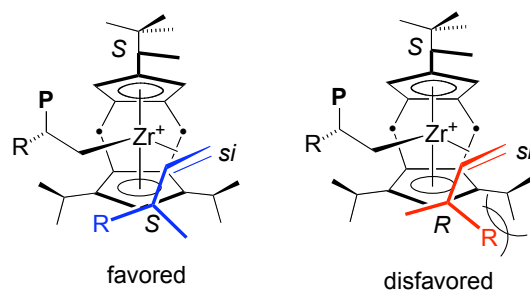


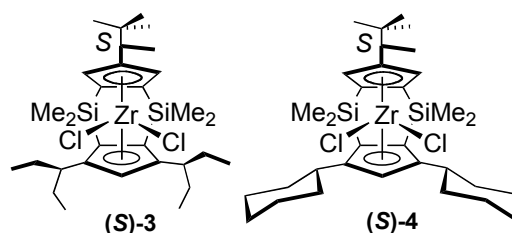
Figure 1.6. Diastereomeric transition states.

The selection for the *S* or the *R* monomer is an indirect relay of chirality. The (*S*)-methylneopentyl group of the upper Cp ring directs the preferred side of the catalyst for the polymer chain to reside. The placement of the chain directs the incoming olefin to one side of the metallocene wedge, where one enantioface is preferred. Enantiofacial selectivity then influences the selection for *S* or *R* monomer. Hence, it is the steric interaction of the olefin substituent with the chiral pocket provided by the lower Cp, and not the chiral methylneopentyl group, that directs the selection of *S* or *R* monomer.

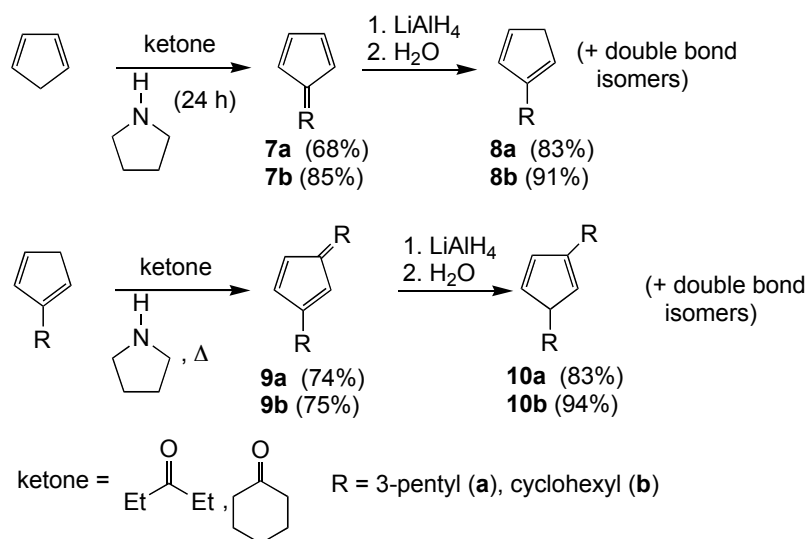
1.3.7 Synthesis of (*S*)-3 and (*S*)-4

Because the main steric interaction for differentiating the diastereotopic transition states was between the bottom Cp substituents and the large R group on carbon 3 of the incoming olefin, it was reasoned that larger substituents on the bottom Cp may afford a greater interaction and thereby better diastereotopic differentiation.

In order to explore the effect of changing the nature of the 3,5-substituents on the lower Cp of the zirconocene catalysts, (*S*)-**3** and (*S*)-**4** were prepared.



The incorporation of various alkyl groups involves the pyrrolidine-catalyzed condensation of cyclopentadiene with the appropriate ketone to produce the fulvene (**7**, Scheme 1.11).³² The fulvene is then reduced with LAH. After another cycle of condensation and reduction, the 1,3-dialkylcyclopentadienes (**10**, R_2CpH) is obtained. The 1,3 disubstituted cyclopentadiene can be obtained exclusively, and none of the 1,2 disubstituted, using the following fulvene route.

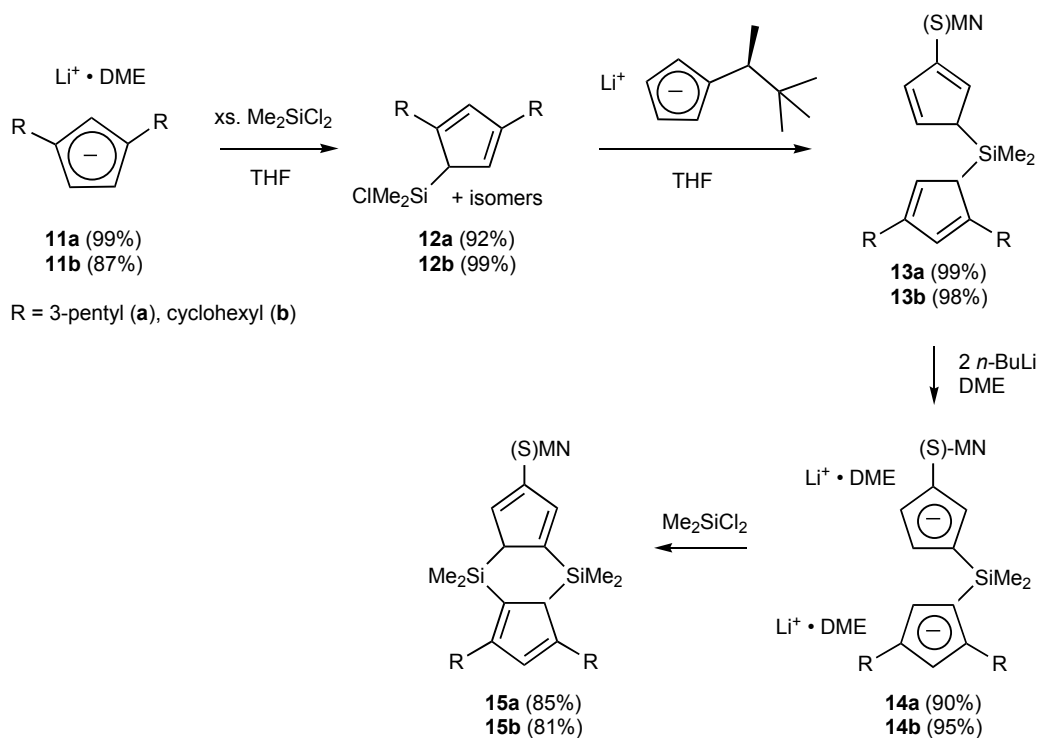


Scheme 1.11. Synthesis of 1,3-dialkylcyclopentadiene.

The construction of the final ligand using **10** follows the general synthetic approach similar to that developed by Bulls and Brintzinger where a singly bridged

dianionic ligand is treated with SiMe_2Cl_2 to form the doubly bridged protonated ligand.³³

The basic approach is shown in the following Scheme 1.12.

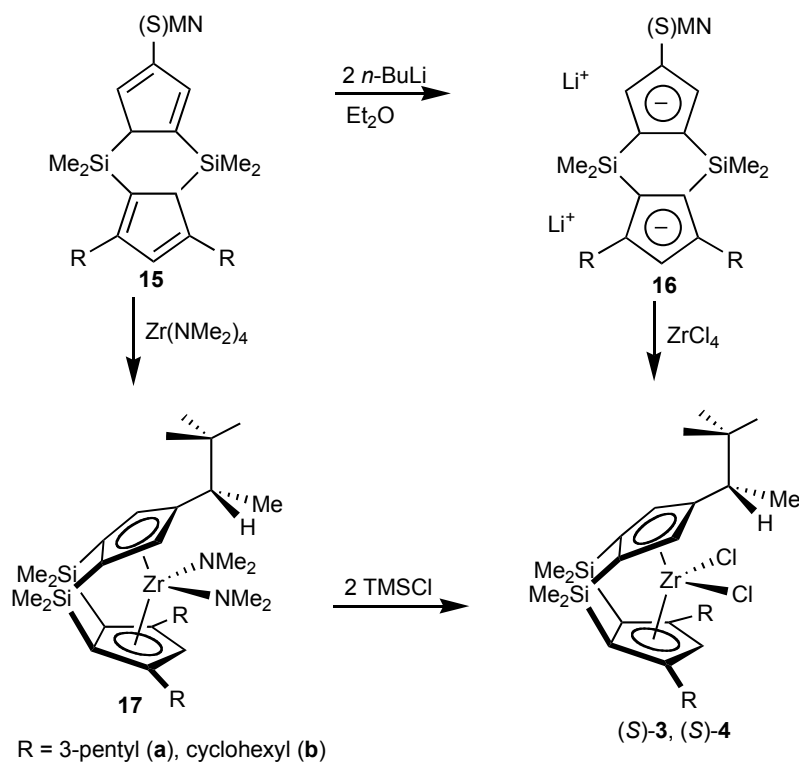


Scheme 1.12. Synthesis of (S)-MNThp ligand with various alkyl substituents.

10 is deprotonated with $n\text{-BuLi}$ to give lithium(1,3-dialkylcyclopentadienylide) (**11**) in high yields. **11** is reacted with excess SiMe_2Cl_2 to give **12** as a yellow oil in the case where $\text{R} = 3\text{-pentyl}$ and a yellow solid for $\text{R} = \text{Cy}$. To obtain the singly bridged ligand, **12** is reacted with (S)-LiMNCp to yield **13** as a thick yellow oil. Deprotonation of **13** with $n\text{-BuLi}$ gives the singly bridged dianions **14** as a fine white solid. To obtain the final ligand, the dianion is reacted with SiMe_2Cl_2 to yield the doubly bridged ligand, **15**.

These ligands can be deprotonated with $n\text{-BuLi}$ to yield the dianionic ligands (**16**) and reacted with ZrCl_4 to obtain the corresponding catalyst (Scheme 1.13). The

metallation can also be carried out by using an amine elimination route.³⁴ **15** is treated with $\text{Zr}(\text{NMe}_2)_4$ in refluxing xylenes under a strong Ar purge. The strong Ar purge is necessary to drive away the dimethylamine by-product and drive the reaction to completion. In all cases ($\text{R} = 3\text{-pentyl, Cy}$), the (1,2,3,5)-isomer of **17** is produced. The diamide is treated with an excess amount of trimethylsilyl chloride (TMSCl) in toluene to produce the dichloride precatalysts. By either methods, the (1,2,3,5)-isomer of the dichloride is produced. Generally, the amide route produces higher yields of the final product.



Scheme 1.13. Synthesis of $(\text{S})\text{-MNThp}_\text{R}\text{ZrCl}_2$.

1.3.8 New Polymerization Method

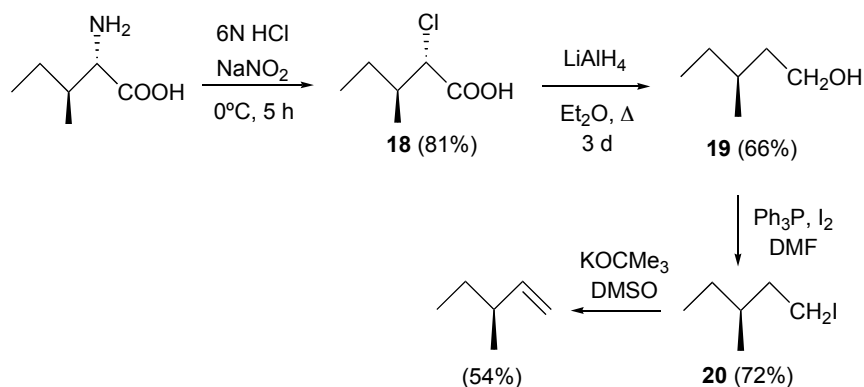
The data in Table 1.1 was obtained using an old polymerization method, which led to inconsistent data due to olefin loss during aliquot sampling. Also, conversion was determined by mass difference of olefin added and olefin recovered. Such method of conversion determination proved to be inaccurate because it was difficult to vacuum transfer all the olefin. Either experimental error would have led to an overestimation of conversion, leading to underestimation of *s*. Procedural changes were implemented to diminish the experimental errors.

First, a polymerization apparatus was developed to minimize olefin loss during solution sampling for reaction monitoring. Rather than determine conversion by mass of olefin, it was determined by gas chromatography (GC). Once the reaction reached 30–60% conversion, all volatiles were vacuum transferred from the reaction solution for enantioassay. The recovered olefin solution was oxidized to a carboxylic acid by Ru-catalyzed NaIO_4 oxidation.²² The acid is next converted to the methyl ester by treating it with a BF_3/MeOH solution. Previously, the acid was converted to the Mandelic ester and analyzed by NMR to obtain the ee, which was a lengthier and more involved procedure than the BF_3 treatment. By the new method, the enantiomeric excess is determined by separation on enantioselective gas chromatography, which is generally considered a more accurate method than NMR. These procedural changes helped to minimize experimental errors and to provide consistent results.

1.3.9 Preparation of (S)-3-Methyl-1-Pentene

The possibility of racemization during either step of enantioassay derivatization was a concern. In order to perform a control experiment, enantiopure (S)-3-methyl-1-pentene was prepared and subjected to the derivatization process (Scheme 1.14).

L-Isoleucine was a convenient starting point for the synthesis because it already contained the desired stereoconfiguration. L-Isoleucine was converted to the chloroacid (**18**) by reaction with excess NaNO_2 in 6 M HCl .³⁵ Next, the chloroacid was reduced to the alcohol by reaction with LAH in ether for 3 d.



Scheme 1.14. Synthesis of (S)-3-methyl-1-pentene.

The distilled alcohol was then converted to the iodide (**20**).³⁶ The literature preparation of **20** involved adding 3 equiv each of triphenyl phosphine, imidazole, and iodine successively to an ether:acetonitrile (3:1) solution of the alcohol.³⁷ Following this procedure, a 40% yield of the iodide was obtained. After testing different solvents and bases in order to optimize the yield (Table 1.3), the addition of I_2 to a DMF solution of triphenyl phosphine and alcohol was determined to give the best yield.

Table 1.3. Optimization of (*S*)-1-iodo-3-methyl pentane

Reagents	Base	Solvent	Yield %
PPh ₃ + ROH + I ₂	Imidazole	3 Et ₂ O : 1 CH ₃ CN	40
	Pyridine	CH ₂ Cl ₂	< 40
	Pyridine	CH ₃ CN	< 40
	None	CH ₂ Cl ₂	< 40
	None	CH ₃ CN	46
	None	DMF	76

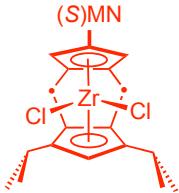
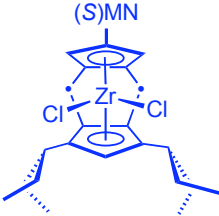
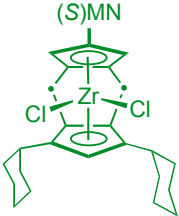
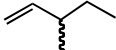
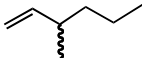
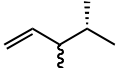
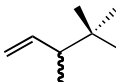
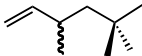
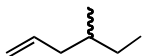
Finally, elimination by potassium *tert*-butoxide in DMSO resulted in (*S*)-3-methyl-1-pentene. The olefin was distilled away from the high boiling solvent to yield 100 g of product. The iodide rather than the tosylate was chosen for this elimination step because the tosylate favors the addition reaction and forms the ether product along with the elimination alkene product.³⁸ The iodide, however, favors the elimination product.

With (*S*)-3-methyl-1-pentene in hand, the enantiopure olefin was treated to the same derivatization procedure, oxidation with NaIO₄/RuCl₃ and methyl esterification with BF₃/MeOH. The GC trace confirmed the absence of racemization (*ee_s* > 98%), demonstrating that the enantioassay procedure is valid for 3-methyl-1-pentene.

1.3.10 Polymerization Results Using (*S*)-2, (*S*)-3, (*S*)-4

MAO-activated (*S*)-**3** and (*S*)-**4** were used to polymerize the same array of chiral olefins as in Table 1.1. Also, polymerization experiments were repeated with (*S*)-**2** by Cliff Baar, with the exception of 344TM1P. The results are shown in table 1.4. Comparing data for (*S*)-**2** in Table 1.1 and table 1.4, one can clearly see the difference in *s* values of 3M1P and 34DM1P obtained from polymerizations using the old procedure versus the new procedure.

Table 1.4. Kinetic resolution chiral olefins using (S)-2, (S)-3, (S)-4

							
		TOF (h ⁻¹)	<i>s</i>	TOF (h ⁻¹)	<i>s</i>	TOF (h ⁻¹)	<i>s</i>
1		47	2.4	314 (88)	2.3 (0.25)	967 (86)	2.6 (0.26)
2		551	1.8	285 (21)	3 (0.16)	1888 (158)	1.9 (0.03)
3		34	15.9	83 (29)	12.6 (0.55)	346 (61)	13.9 (2.8)
4		7.3	12.1	6 (2)	2.9 (0.6)	103 (44)	13
5		37	2.1	24 (7)	6.4 (0.8)	507 (60)	1.5 (0.23)
6		73.7	1.1	90 (25)	1.2 (0.11)	4222 (1483)	1.2 (0.04)

a) Values in parentheses are standard deviations.

b) More detailed tables are provided in Appendix D.

Small but significant *s* values have been demonstrated. Even for the smallest chiral α -olefin, 3-methyl-1-pentene, there is a modest kinetic resolution (*s* = 2.3–2.6; entry 1). The most significant kinetic resolution was observed with 3,4-dimethyl-1-pentene, which contains methyl substitution on both the 3- and the 4-positions (*s* = 12.6–15.9; entry 3). Very poor kinetic resolution was observed with 4-methyl-1-hexene, where the stereogenic center is separated from the double bond by a methylene unit (*s* = 1.1–1.2; entry 6). Since the metal center interacts most directly with the carbons 1 and 2 of the olefin, moving the olefin chiral center one position farther from the metal center would likely hamper chiral discrimination. For all listed olefins, the *S* enantiomer of the racemic olefins was preferentially polymerized.

Compared to (*S*)-**2**, the *s* values obtained from polymerizations using (*S*)-**3** and (*S*)-**4** show virtually no changes (table 1.4). One exception is the kinetic resolution of 3,5,5-trimethyl-1-hexene by (*S*)-**3** (entry 5). Compared to (*S*)-**2**, a 3-fold increase in selectivity was observed, and compared to (*S*)-**4**, a 4-fold increase. This increase in *s* value suggests a fine-tuning of the catalyst pocket environment for the interaction with 355TM1H. Furthermore, a 1.6-fold increase in *s* value for 3M1H was observed with (*S*)-**3** (*s* = 3), compared to (*S*)-**2** (*s* = 1.8) and (*S*)-**4** (*s* = 1.9) (entry 2). Notably, the catalysts demonstrated a greater variation in selectivity with the hexenes, 355TM1H and 3M1H, than with the pentenes. For the pentenes, there was virtually no change in *s* values across the three catalysts, with the exception of 344TM1P.

The polymerization of 344TM1P with (*S*)-**3** was exceptionally slow. Although the catalyst loading was six times as much as the usual, after multiple polymerization experiments, the highest conversion obtained was 20% after 24 h. After 91 h, the conversion was still 20%, indicating decomposition of the catalyst. Perhaps the low activity of (*S*)-**3** in polymerizing 344TM1P indicates that the active site pocket is more sterically congested than that of (*S*)-**2** and (*S*)-**4**.

1.3.11 Crystal Structure

Single crystals of (*S*)-**2** and (*S*)-**3** were obtained by recrystallization from concentrated toluene solution (Figure 1.7 and Figure 1.8). (*S*)-**4** was recrystallized from methylene chloride.

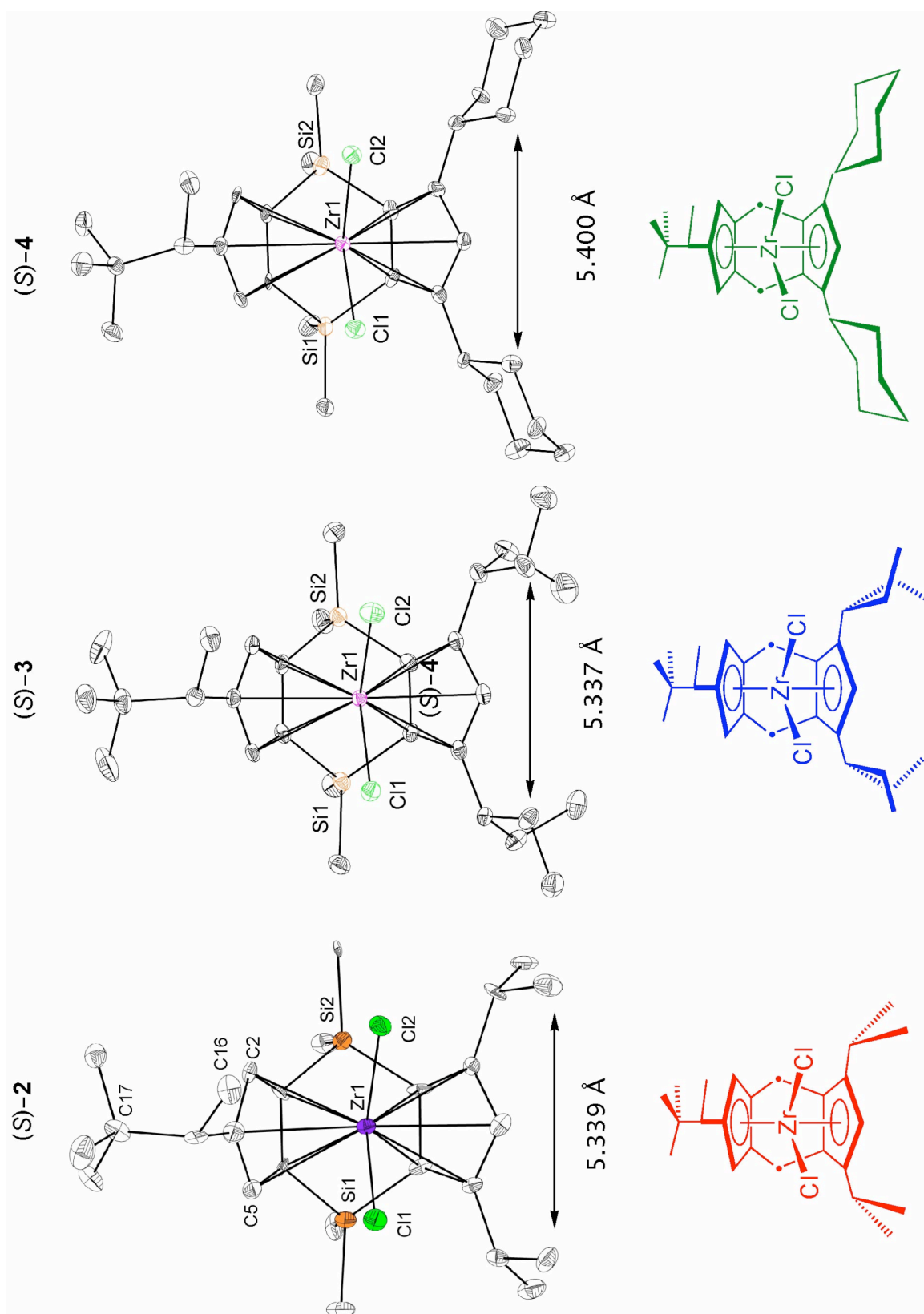


Figure 1.7. Front ORTEP views of (S)-2, (S)-3, and (S)-4.

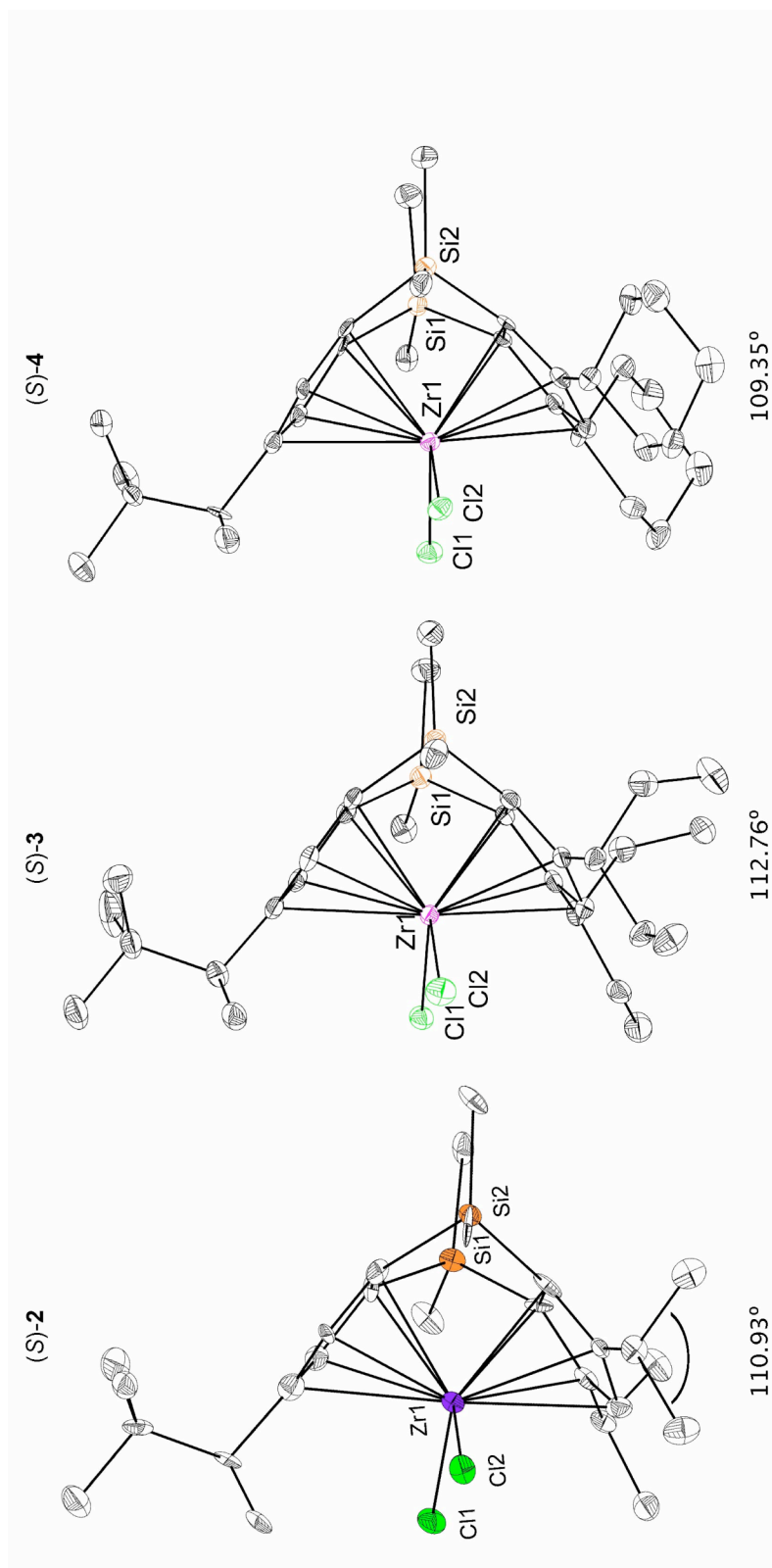


Figure 1.8. Side ORTEP views of (S)-2, (S)-3, and (S)-4. The angle of the isopropyl substituent of (S)-2 is 110.93°. The analogous angles for (S)-3 and (S)-4 are also listed.

A Newman projection down the C15-C1 bond of (*S*)-**2** indicates that the *tert*-butyl group of methylnepentyl substituent lies above the plane of the upper Cp ligand, nearly perpendicular to the Cp plane (Figure 1.9). The orientation of the *tert*-butyl group forces the methyl group to point down and right toward the wedge of the metallocene. The occupation of the methyl group in the right upper quadrant of the metallocene effectively differentiates the left and right sides of the molecule.

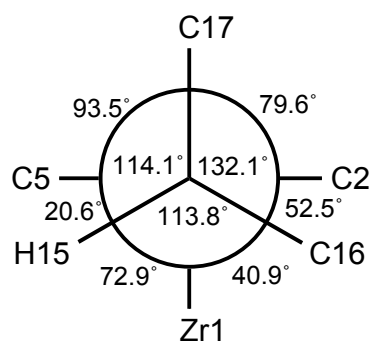


Figure 1.9. Newman projection of (*S*)-**2**.

As the crystal structures illustrate, the methylnepentyl substituents of (*S*)-**3** and (*S*)-**4** are oriented in a similar manner to (*S*)-**2**. For all three structures, the substituents of the bottom Cp assume a conformation such that the methine protons are directed up and back towards the SiMe₂ groups. One arm of the substituent is periplanar to the bottom Cp, and the other arm is nearly perpendicular to the bottom Cp. The 3-pentyl substituents of (*S*)-**3** adopt a staggered conformation so that the pocket between the 3- and 5-substituents is not much different than the pocket of (*S*)-**2**. Similarly, the cyclohexyl groups of (*S*)-**4** adopt an eclipsed chair conformation that points away from the pocket. There is an even smaller change in steric bulk relative to the (*S*)-**2**. Hence, the overall

steric environment of the open pockets of (*S*)-**2**, (*S*)-**3**, and (*S*)-**4** are rather similar, which may explain the similar *s* values across all 3 precatalysts.

Dividing the pocket into two regions, inner and outer, the inner pockets of the three precatalysts are more similar than the outer pockets. Perhaps the 3- and 4-positions of the olefins interact closely with this region. However, beyond this inner pocket, the substituents on the bottom ring render the outer region of the pocket very different. Maybe the 5-position of the olefins interacts with this outer pocket region, and therefore, we see a difference in *s* value for the hexenes, 3M1H and 355TM1H. The methyls of the 3-pentyl substituents of (*S*)-**3** have more freedom of motion than the methylene units of (*S*)-**4**, which are tied back into a cyclohexyl group. Hence, the outer pocket regions of (*S*)-**2** and (*S*)-**4** are similar to each other, and the outer pocket of (*S*)-**3** is distinct from (*S*)-**2** and (*S*)-**4**. A polymerization experiment with 3-methyl-1-heptene or longer olefin would provide some insight into this conjecture.

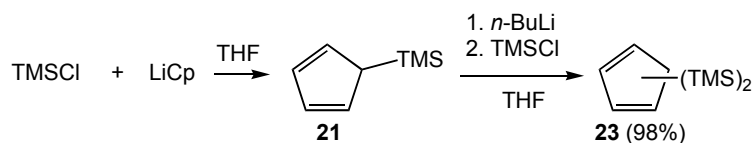
1.3.12 Preparation of (*S*)-**5**

Motivated by the prospects that a more sterically crowded pocket may exert greater diastereoselectivity, a catalyst containing tertiary substituents on the bottom Cp was desired. Tim Herzog previously reported that a singly bridged ligand containing two *tert*-butyl groups could be prepared, but the second bridge could not be linked successfully.³¹ According to a molecular modeling analysis, the *tert*-butyl groups were too bulky to allow for the second bridge.³¹ Hence, a catalyst containing trimethyl silyl (TMS) groups was targeted. The TMS groups lie farther out from the Cp ring and allow

the double linking to proceed. An achiral doubly bridged metallocene containing two TMS groups on one of the Cp rings had been previously prepared by Shige Miyake.³⁹

Bis(TMS)cyclopentadiene (**23**, TMS₂CpH) could not be prepared following the fulvene route used to prepare dialkylcyclopentadienes for (*S*)-**2**, (*S*)-**3**, and (*S*)-**4**. **23** was initially prepared following the procedure developed by Desurmont.⁴⁰ The procedure involved adding TMSCl to a solution of NaCp at 0 °C to obtain a mixture of **21**, **23**, and CpH dimer. The product mixture was separated by distillation to obtain a low yield of 17%. It was suspected that the low yield was due to dimerization of the product during distillation. The separation of Cp dimer and **23** by distillation was also difficult.

Rather than preparing **23** in one step and obtaining poor yields, the strategy was changed to obtain **23** stepwise from **21**.⁴¹ Although this procedure involved three steps, this method with some modifications produced better yields, and no distillation was required (Scheme 1.15).

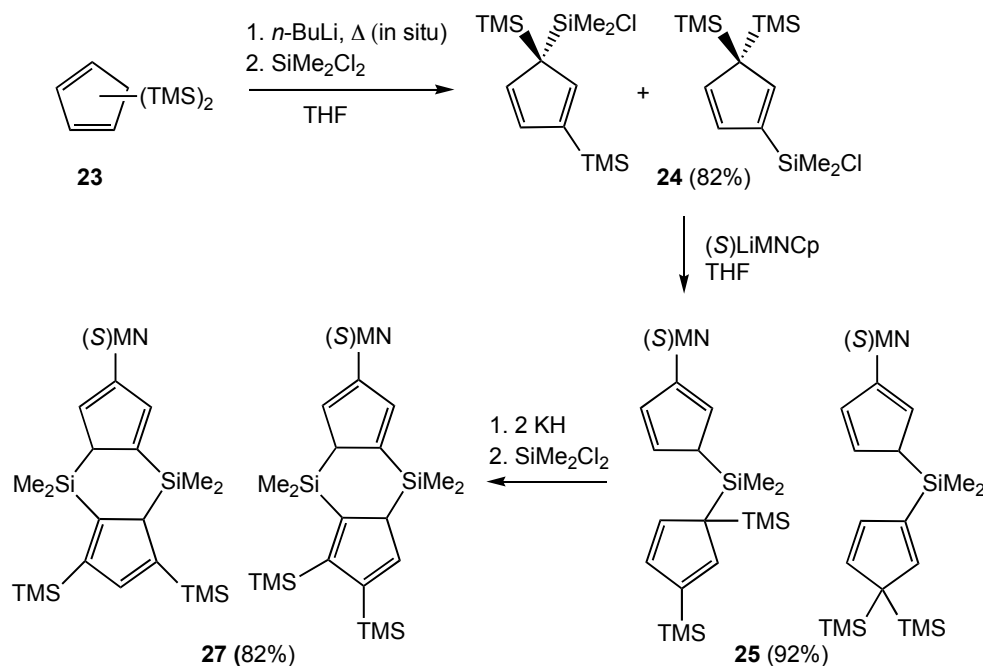


Scheme 1.15. Synthesis of TMS substituted cyclopentadiene.

According to the literature procedure, LiCp/THF solution is treated with 1.5 equiv of TMSCl.⁴¹ All volatiles are then vacuum transferred, to which 1.05 equiv of *n*-BuLi is added. LiTMSCp is isolated and treated with TMSCl to obtain the product **23**. A couple of modifications to this procedure were made. In the first step, the amount of TMSCl added was reduced from 1.5 equiv to 1.05 equiv because during the vacuum transfer of

21 after the reaction, the excess TMSCl vacuum transfers over also and reacts with *n*-BuLi used in the subsequent step. Also, the precedent synthesis involved adding TMSCl to LiCp/THF at room temperature slowly. Concerned that slow addition at room temperature may promote formation of **23**, TMSCl was vacuum transferred onto LiCp/THF solution at $-78\text{ }^{\circ}\text{C}$ and was allowed to stir in $-78\text{ }^{\circ}\text{C}$ bath overnight. By this method, only **21** was obtained.

After deprotonation of **21** and treatment with TMSCl, only **23** was produced cleanly and in high yield. **23** was carried onto prepare the doubly bridged ligand **27** (Scheme 1.16). It was initially believed that deprotonation of the ligand isomers would produce only the desired (1,2,3,5)-isomer and subsequent metallation would yield the desired catalyst, (*S*)-**5a** (Figure 1.10). The dilithio ligand (**26**) was metallated with ZrCl_4 in methylene chloride.³⁹



Scheme 1.16. Synthesis of doubly bridged ligand for (*S*)-**5**.

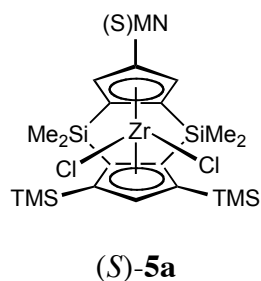


Figure 1.10. Target (S)-MNThp_{TMS}ZrCl₂.

1.3.13 Crystal structure of (S)-5

After trying many different solvents (methylene chloride, toluene, TMS₂O), crystals were finally obtained from cold pentane. Rather than the structure of the desired (S)-**5a** precatalyst, the X-ray crystallography showed that two (1,2,3,4)-isomers had co-crystallized in the same space group (Figure 1.11). One isomer places a TMS group on the same side of the metallocene wedge as the methyl group of MN substituent on the top ring, (S)-**5b**. The other isomer places a TMS group on the opposite side of the methyl group, (S)-**5c**.

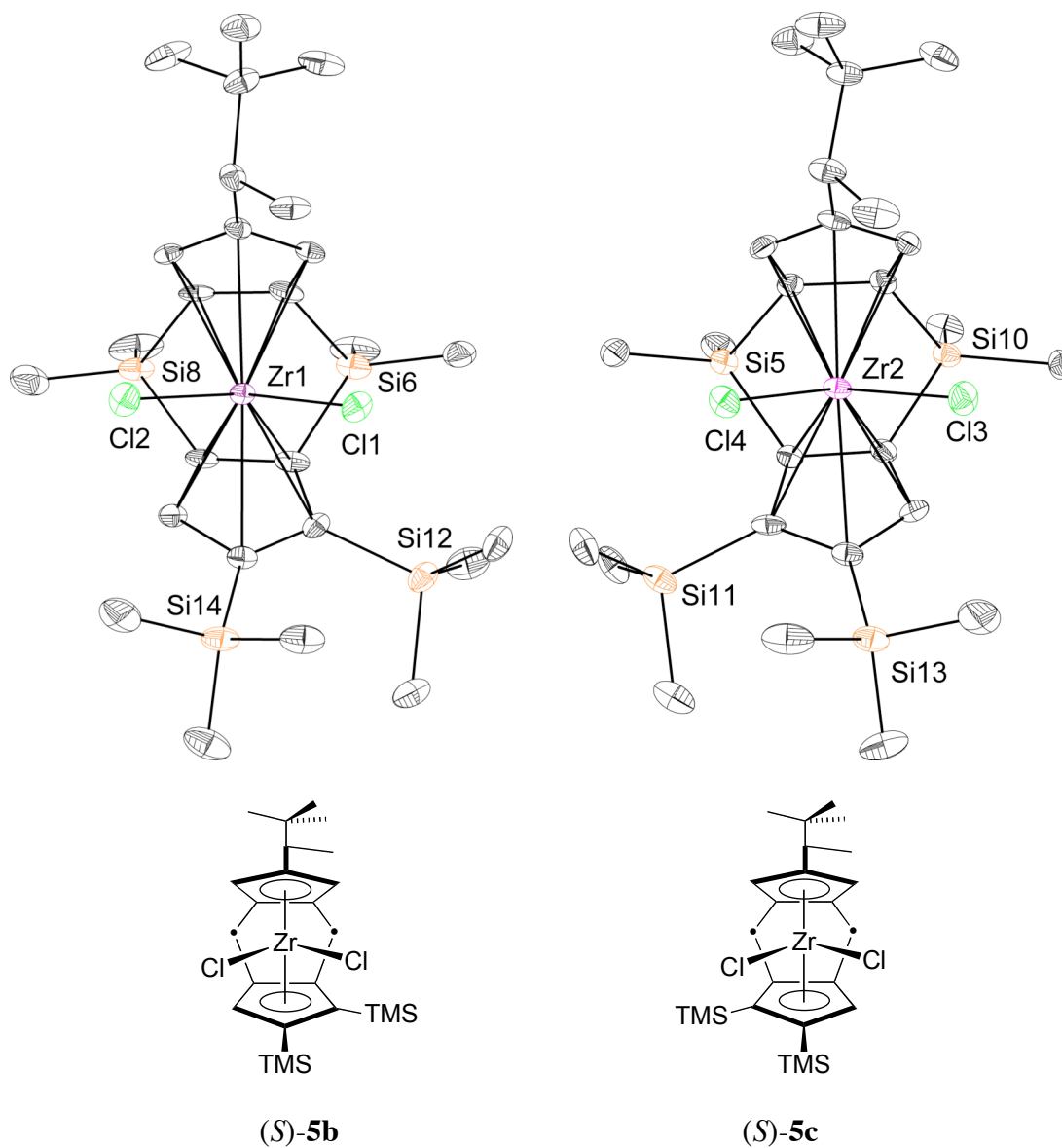


Figure 1.11. Crystal structures of (S)-5b and (S)-5c.

Polymerization of 3M1P was attempted with the MAO-activated crude sample of this precatalyst mixture. Surprisingly, the catalyst(s) polymerized 3M1P with high activity. Also, some kinetic resolution was achieved ($s = 1.5$), with the *S* monomer preferentially enchainned. The high activity of this catalyst mixture was a surprise considering Brintzinger's report on two doubly bridged catalysts (Figure 1.12).^{33a} Both

of these catalysts are active catalysts for the polymerization of ethylene, but both are extremely sluggish for propylene polymerization. Brintzinger attributes this to poor steric interaction between the methyl group of propylene and the substituents on carbon 4 of the Cp rings. Based on these findings, it was believed that a pocket is required for propylene insertion. Hence, it was somewhat surprising that (*S*)-**5b** and (*S*)-**5c**, neither isomer containing a pocket, were able to polymerize 3M1P with good activity.

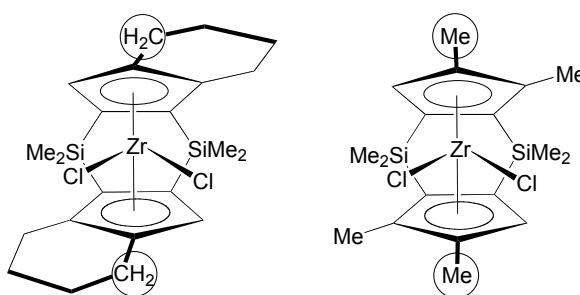


Figure 1.12. Brintzinger's doubly bridged metallocenes.

The difference in activity between Brintzinger's catalysts and (*S*)-**5b** and (*S*)-**5c** may be due to the fact that the TMS groups are extended farther away from the Cp ring than a methyl group. The Si-Cp bond length is 1.90 Å, whereas C-Cp bond length is typically about 1.50 Å. The greater arm length may allow just enough space for the α -substituent of the olefin to reside. Although a good turnover rate for the polymerization of 3M1P has been observed, low molecular weight chains are produced, as indicated by GC traces showing a strong dimer peak and a small trimer peak.

1.3.14 Activity of Catalysts

Generally, the catalysts become inactive over time in solution. (*S*)-**2** proved to be the sturdiest precatalyst. (*S*)-**2** could be stored in the drybox at room temperature for months without much decomposition. Also, the solution of (*S*)-**2** can be stored in the drybox at $-35\text{ }^{\circ}\text{C}$ for up to two weeks without a significant decrease in activity. (*S*)-**3** can be stored in solid form in the drybox, at room temperature for up to 3 months. (*S*)-**4** will decompose to a green solid within one month at room temperature in the drybox. Solutions of (*S*)-**3** and (*S*)-**4** show reduced or no activity after being stored in the drybox at $-35\text{ }^{\circ}\text{C}$ for one day. All the catalysts were stored in the drybox at $-35\text{ }^{\circ}\text{C}$ in solid form. With all polymerizations, the turnover rate decreased over time because olefin concentration decreased over time and because the catalyst was decomposing in solution (Figure 1.13). To compensate for catalyst decomposition, enough catalyst was used for each polymerization so that 30–60% conversion could be reached within the first 2 d. Preparing a fresh catalyst solution just before injecting it into the polymerization reaction also ensured reliable polymerization results.

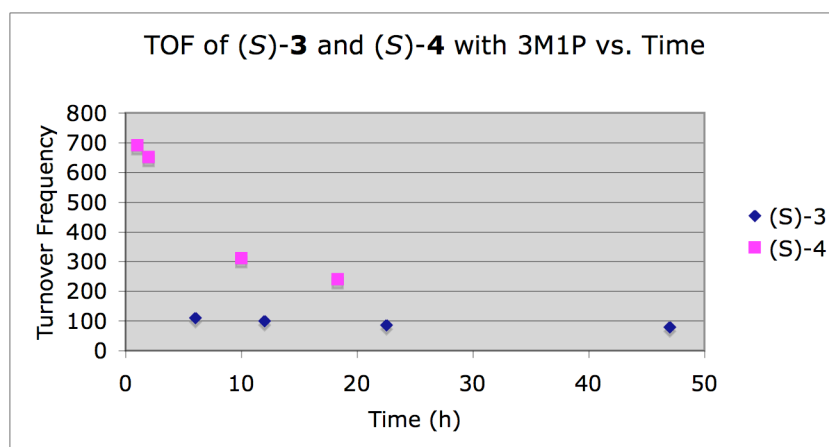


Figure 1.13. Turnover frequencies (TOF) of (*S*)-**4** and (*S*)-**3**.

(*S*)-**4**/MAO was generally much more active than (*S*)-**3**/MAO (Figure 1.14, Figure 1.15). The greater activity of (*S*)-**4**/MAO may be due to greater solubility. Polymerizations have been run with catalysts dissolved in tetradecane, toluene, and benzene. In most cases, turnover frequency (TOF) was highest when the precatalysts were dissolved in toluene, then benzene, and then tetradecane. This trend was more consistent with (*S*)-**4** and not as consistent with (*S*)-**3** (Figure 1.14, Figure 1.15).

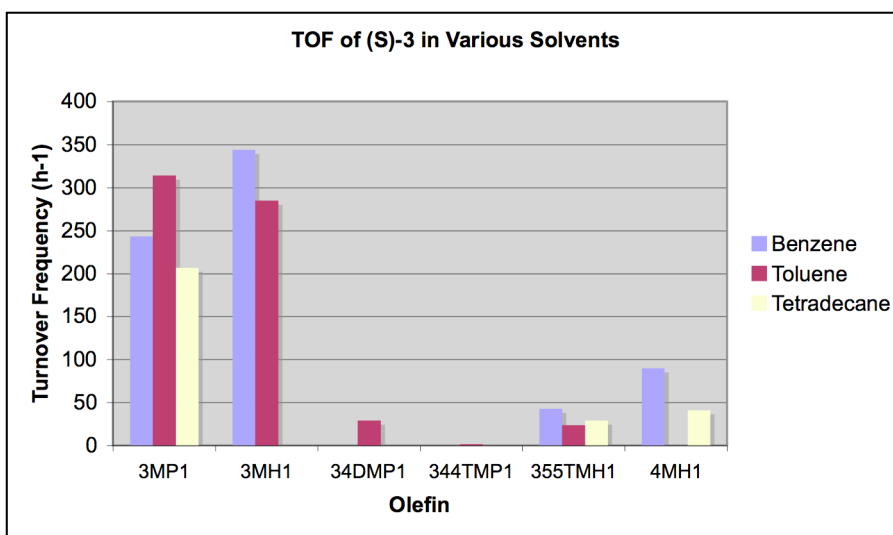


Figure 1.14. TOF of (*S*)-**3** in various solvents.

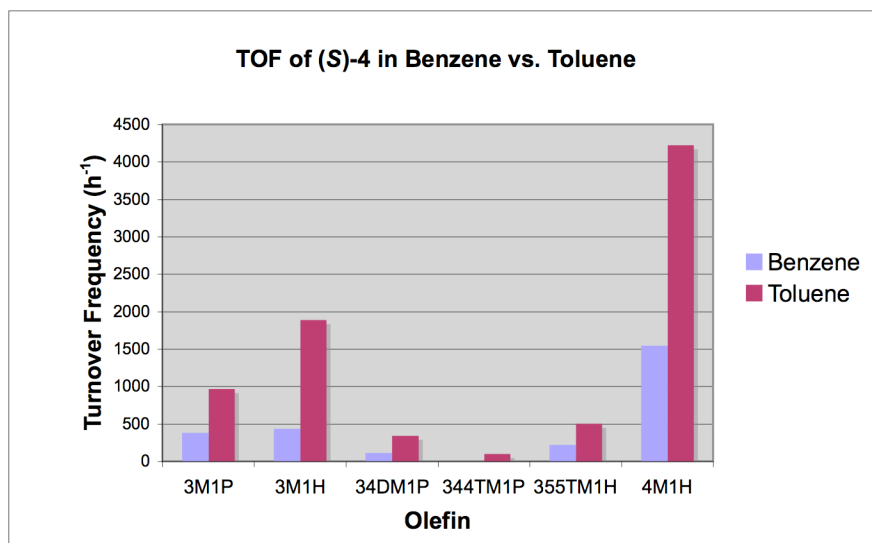


Figure 1.15. TOF of (*S*)-4 in benzene vs. toluene.

For (*S*)-4, 4M1H has a higher TOF than any of the 3-methyl olefins. It could be argued that the double bond of 4M1H is less sterically congested compared to 3-methyl olefins, and hence, inserts at a faster rate. Among the 3-methyl olefins, 3M1P and 3M1H have the faster TOF compared to 34DM1P and 355TM1H. This observation may be explained by the smaller size of 3M1P and 3M1H. This trend is observed for (*S*)-3 but not as clearly for (*S*)-4.

1.3.15 Affect of MAO on Activity

Methylaluminoxane (MAO) is a cocatalyst that activates the metal dichloride precatalyst. Its structure and mechanism are not clearly defined and understood. It is generally believed that MAO activates the precatalyst by converting the metal-chloride bond into a metal-alkyl bond that is labile to olefin insertion.⁴² For these polymerizations, MAO was purchased from Albemarle as a 10% or 30% toluene solution. Left standing at

room temperature, the clear MAO solution becomes cloudy as gel formation occurs over time. A 10% MAO solution will remain clear for up to 6 months. The 30% MAO solution will stay clear for 6 d.⁴³ Because gel formation hampers the activation capability of MAO, toluene was removed from the solution of MAO, and MAO was stored in dry form. The toluene solution of MAO was transferred to a 24/40 500-mL round bottom flask, equipped with a large stir bar and a needle valve joint. While stirring vigorously and heating the flask in a 150 °C oil bath, all volatiles, including toluene and trimethyl aluminum, were removed *in vacuo*. The remaining white powder was stirred and heated in a 150 °C bath overnight to completely remove traces of solvent and trimethyl aluminum.

It was observed that different batches of MAO produced different polymerization rates, and in some cases, polymerization was completely hampered. ¹H NMR of the different batches of MAO was taken in C₆D₆.

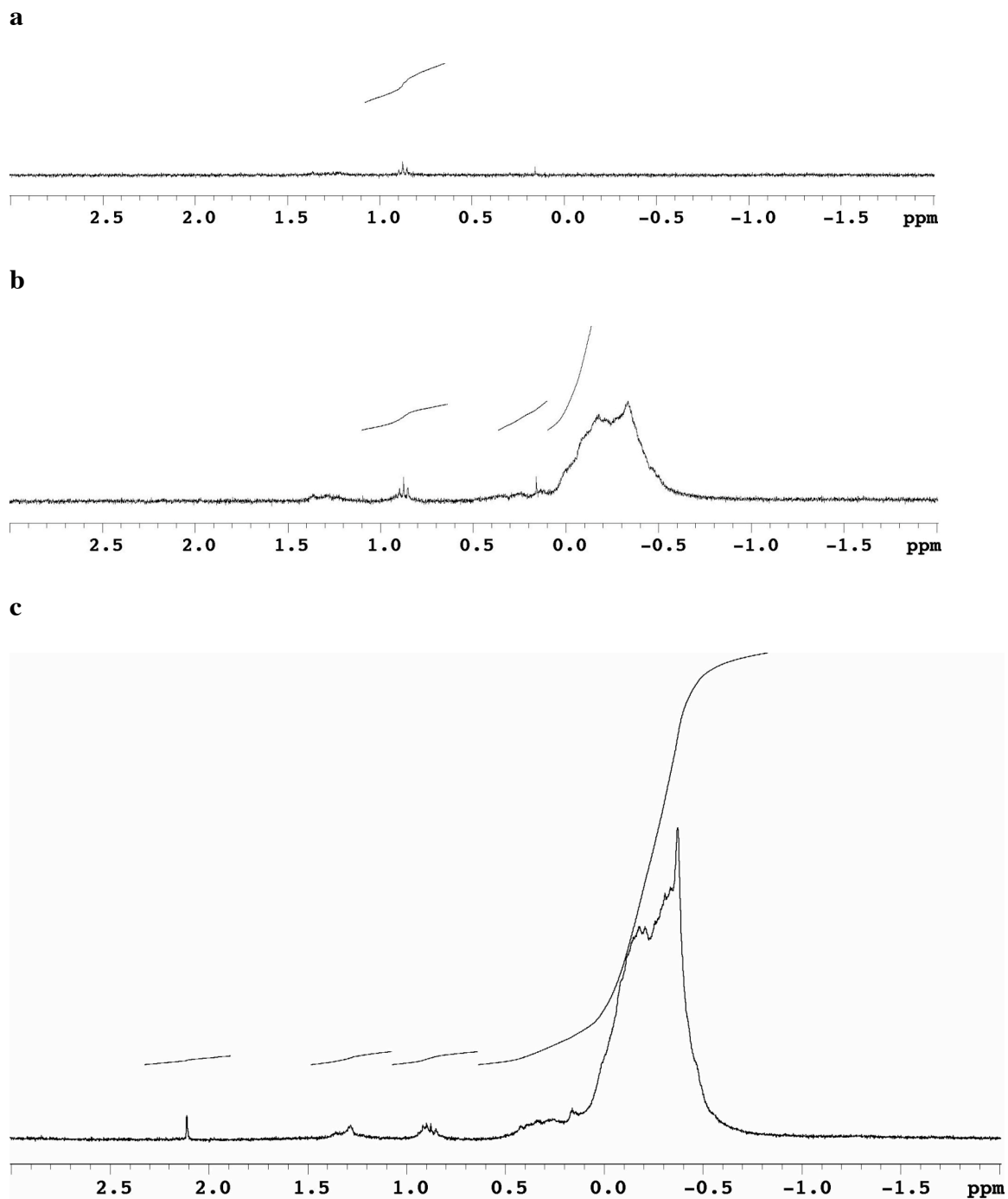


Figure 1.16. ^1H NMR(C_6D_6) spectra of three different batches (a, b, c) of MAO.

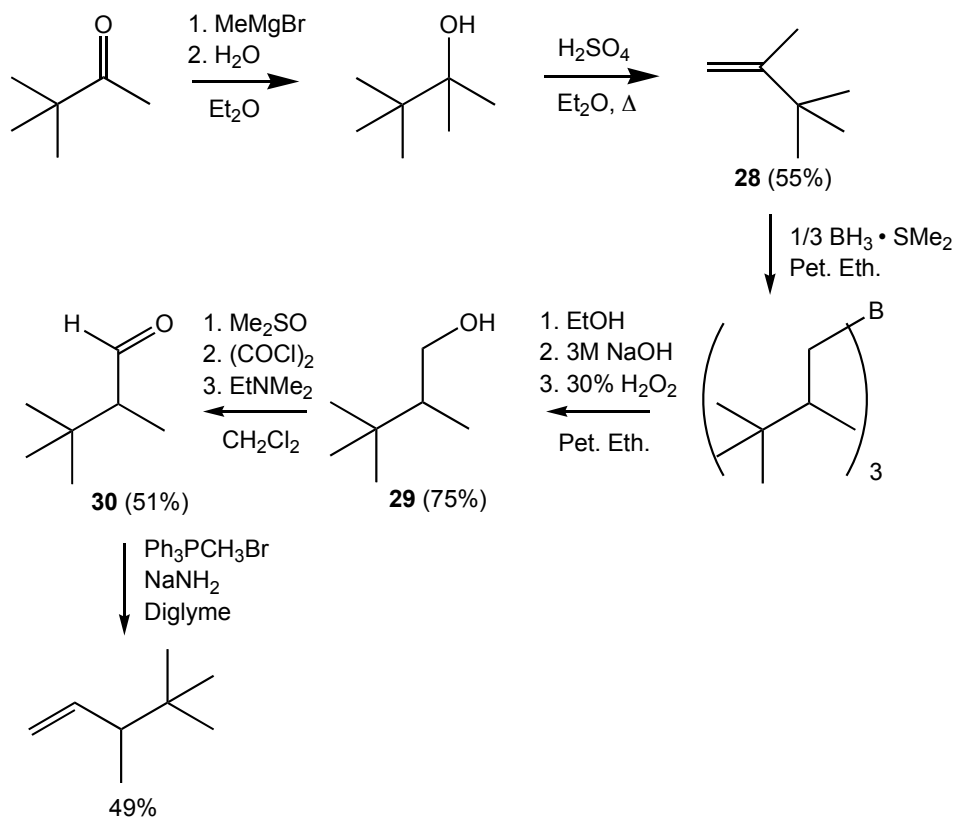
The MAO batches that led to extremely low or no activity did not show no signals in the ^1H NMR (Figure 1.16a). The MAO batches that led to good activity showed a

broad and large signal from -0.6 ppm to 0.2 ppm (Figure 1.16b). The MAO that led to the fastest activity showed the broad signal and a sharp singlet at -0.4 ppm (Figure 1.16c). This singlet belongs to trimethyl aluminum. These spectra suggested that the drying process greatly affected the physical and chemical form of the MAO. If the MAO is not stirred vigorously and heated long enough, granular forms of MAO precipitated. These granules, providing less surface area, are less soluble in the polymerization solution and result in low activity. Vigorous stirring and sufficient heating temperature and time will result in fine powder that produces good activity. However, too much heating time can lead to gel formation and no activity. Hence, it is necessary to have vigorous stirring to produce fine powder, and the right amount of heating to remove all trimethyl aluminum and toluene, but not so much as to produce gel formation.

1.3.16 Preparation of 3,4,4-Trimethyl-1-Pentene

Most of the olefins surveyed were commercially available with the exception of 3,4,4 trimethyl-1-pentene, which was synthesized in several steps (Scheme 1.17). The initial step involves the methylation of pinacolone with a methyl Grignard reagent, followed by an aqueous work-up to produce the tertiary alcohol. In situ, the alcohol is dehydrated by the addition of sulfuric acid.⁴⁴ After isolating and drying the alkene (**28**), it undergoes hydroboration to yield exclusively the primary alcohol (**29**).⁴⁵ The corresponding aldehyde (**30**) is obtained by Swern oxidation of **29**.⁴⁶ The desired olefin is prepared via the Wittig reaction from **30**.⁴⁷ The Wittig reaction was initially performed in THF, but it proved difficult to distill THF away from the olefin. Hence, a high boiling

solvent, such as diglyme, was used so that the low boiling olefin (104 °C) could be vacuum transferred away from diglyme.



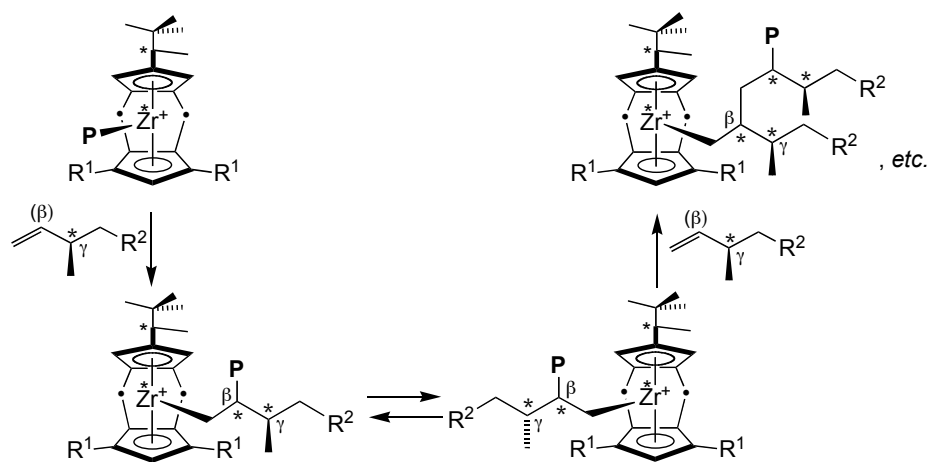
Scheme 1.17. Synthesis of 3,4,4-trimethyl-1-pentene.

1.4 CONCLUSIONS

Enantiopure C_1 -symmetric metallocene catalysts that polymerize relatively bulky, racemic 3-methyl substituted olefins with unprecedented activities have been developed. The different insertion rates of the olefin enantiomers allow for the partial kinetic resolution of simple racemic alkenes. For 3,4-dimethyl-1-pentene, $s > 15$ has been

achieved. In some cases, $s > 12$ was obtained for the polymerization of 3,4,4-trimethyl-1-pentene. These examples provide the first practically useful kinetic resolution of such simple unfunctionalized monomers. A general mechanism to explain both the isotacticity of the resulting polymers as well as the preferred enantiomer selectivity for catalysts (*S*)-**2**, (*S*)-**3**, and (*S*)-**4** has been proposed. This proposed mechanism is simplified in that it is based only on enantiomorphic site control, which uses a steric interaction argument to explain the preferred diastereomeric selection.

The situation, however, may be significantly more complicated by chain-end control. Under chain-end control, the chirality of the last inserted monomer influences which enantiomer is enchain next. Considering the number of stereocenters in the vicinity of the active site, it is likely that both chain-end control and site control are influencing diastereomeric selection (Scheme 1.18).



Scheme 1.18. Many stereocenters in the vicinity of the active site.

The importance of chain-end control in determining the relative rates of enantiomer polymerization was recently demonstrated using (*rac*)- C_2 and C_S -symmetric metallocene

catalysts.⁴⁸ More relevantly, co-polymerizations of ethylene and propylene with chiral olefins using (*S*)-**2** have demonstrated that diastereomeric selection is a function of both the site control and the polymer chain end chirality (largely at β and γ positions).⁴⁹

1.5 EXPERIMENTAL SECTION

General Procedures

All air and/or moisture sensitive materials were handled using high-vacuum line, swivel frit assembly, glovebox, Schlenk, and cannula techniques under a nitrogen or argon atmosphere.⁵⁰ Argon was purified by passage through MnO on vermiculite and activated 4 Å molecular sieves. All glassware was oven dried before use. Solvents were dried and degassed over sodium benzophenone ketyl or over titanocene.⁵¹ 1,2-Dimethoxyethane (DME) was dried and degassed over sodium benzophenone ketyl. Methylene chloride, triethylamine, Me₂SiCl₂, and Me₃SiCl were stored over and distilled from CaH₂ immediately before use. The hexane solution of *n*-BuLi was stored under Ar at 10 °C.

Unless otherwise mentioned, all starting materials were purchased from Aldrich and used as received. Pinacolone, dimethylsulfoxide (DMSO), diglyme were dried over sieves for at least two d before use. MeMgBr (3 M/Et₂O), mesyl chloride, and BH₃SMe₂ (10–10.2 M) were used from freshly opened bottles, and oxalyl chloride was used from a freshly opened ampule. ZrCl₄, Ph₃PCH₃Br, and NaNH₂ were dried on the vacuum line overnight and handled in the drybox. Potassium hexamethyldisilazide [KN(TMS)₂] and

Zr(NMe₂)₄ were sublimed before handling in the drybox. (*S*)-2-methylbutane-1-thiol was synthesized according to literature methods.⁵² The preparation of (*S*)-LiMNCp is described in chapter 2. (*S*)-**2** was synthesized by the route previously reported for the racemic counterpart, except that (*S*)-LiMNCp was used in place of the racemate.²⁰ (*S*)-Ethylthiooctanoate was made according to the literature procedure.⁵³ Dicyclopentadiene was thermally cracked, and the distilled cyclopentadiene was stored at -80 °C. For the large-scale synthesis of (*S*)-3-methyl-1-pentene and its precursors, all reagents and solvents were used immediately from freshly opened bottles and were not further purified prior to use.

All olefins surveyed, with the exception of 3,4,4-trimethyl-1-pentene, were purchased from Chemsampco. They were dried and degassed over LAH for 2 d, vacuum transferred, and stored in Schlenk flasks over CaH₂. In some cases, olefins stored over LAH formed into an unusable gel. Methylaluminoxane (MAO) was purchased from Albemarle as 10% or 30% toluene solution. All volatiles were removed *in vacuo* to give a white powder. The white MAO solid was dried at 150 °C for 12 h at high vacuum. Tetradecane was stirred over pieces of Na metal for 24 h at room temperature. Tetradecane was vacuum distilled using a Vigoreaux column into a dry Schlenk flask and stored in the drybox. Toluene used for polymerization was vacuum transferred into a small Schlenk flask from sodium benzophenone ketyl and stored over sieves in the drybox.

Instrumentation. NMR spectra were recorded on the Varian Mercury VX300 (¹H, 300 MHz, ¹³C, 75.5 MHz) spectrometer. Gas chromatographs were obtained on an Agilent 6890 Series gas chromatography using a 30 m x 0.25 mm, γ-cyclodextrin

trifluoroacetyl “ChiralDEX-TA” column from Advanced Separations Technology. Optical rotations were measured on a Jasco P1030 polarimeter at ambient temperature. A 1-mL cell with a 1-dm path length was used. Optical rotations were also measured on a Jasco P1010 polarimeter at ambient temperature using a 1-mL cell. ($\lambda = 589$ nm, path length 50.00 mm)

6,6-Diethylfulvene, 7a. The following procedure was performed under ambient atmosphere. 3-Pentanone (65 g, 751 mmol) was added to a solution of cyclopentadiene (50 g, 751 mmol) dissolved in 250 mL of methanol. Pyrrolidine (8.01 g, 113 mmol) was syringed into the solution. The bright yellow solution was capped and allowed to stir overnight at room temperature. The reaction mixture was neutralized with 50% (v/v) acetic acid and transferred to a separatory funnel containing 100 mL of water. After the layers were separated, the aqueous layer was extracted with diethyl ether (3 x 100 mL). The combined organic layer was washed with water (2 x 100 mL), saturated NaHCO_3 (1 x 100 mL), and brine (1 x 100 mL). The organic layer was dried over MgSO_4 , filtered, concentrated, and Kugelrohr distilled (25 °C, $<10^{-3}$ mmHg) to yield 68.14 g (68%) of bright yellow oil. ^1H NMR (300 MHz, C_6D_6 , δ): 6.5 (s, 4H, C_5H_4), 2.3 (quint, 4H, CH_2), 0.9 (t, 6H, CH_3).

3-Pentylcyclopentadiene isomers, 8a. **7a** (30 g, 223 mmol), dissolved in 100 mL of diethyl ether, was added over 1 h to an ether solution (330 mL) of LAH (8.55 g, 226 mmol) under Ar. The solvent refluxed very gently during the addition. The reaction was stirred at room temperature for 4 h and was quenched with 9 g of water, 9 g of 15%

NaOH, and 27 g of water. The solution was filtered, concentrated, and Kugelrohr distilled (30 °C, $<10^{-3}$ mmHg) to give 31 g (83%) of pale, yellow oil. ^1H NMR (300 MHz, C_6D_6 , δ): 5.93–6.50 (m's, 5H, C_5H_5), 2.10–2.26 (m, 1H, CH), 1.09–2.19 (m, 4H, CH_2), 0.76–0.90 (m, 6H, CH_3).

3-(3-Pentyl)-6,6-diethylfulvene, 9a. The target was prepared analogously to **7a** by combining **8a** (15.52 g, 114 mmol), 3-pentanone (10.79 g, 126 mmol), and pyrrolidine (10.54 g, 148 mmol) in 100 mL of methanol. The reaction was stirred in ambient atmosphere at room temperature for 20 d. The work-up was also analogous to **7a**. 17.22 g (74%) of bright orange oil was obtained via Kugelrohr distillation (80 °C, $<10^{-3}$ mmHg). ^1H NMR (300 MHz, C_6D_6 , δ): 6.57 (dd, $J = 5.4, 1.8$ Hz, 1H, C_5H_3), 6.46 (dd, $J = 5.4, 1.8$ Hz, 1H, C_5H_3), 6.24 (t, $J = 2.4$ Hz, 1H, C_5H_3), 2.3 (m, 4H, $(\text{CH}_2)_2\text{C}$), 2.25 (m, 2H, $(\text{CH}_2)_2\text{CH}$), 1.46–1.62 (m, 4H, $(\text{CH}_2)_2\text{CH}$), 0.93 (q, $J = 7.8$ Hz, 12H, CH_3).

1,3-Bis(3-pentyl)cyclopentadiene isomers, 10a. In an analogous manner to **8a**, **9a** (12.54 g, 61.04 mmol) was dissolved in ether (80 mL) and added to LAH (3.48 g, 91.7 mmol), suspended in 150 mL of ether. The reaction was quenched with 3.5 g of water, 3.5 g of 15% NaOH, and 10.5 g of water. The crude product was Kugelrohr distilled (90 °C, $<10^{-3}$ mmHg) and yielded 10.47 g (83%) of pale yellow oil. ^1H NMR (300 MHz, C_6D_6 , δ): 2.3, 3.0, 5.87, 6.09, 6.12 (5 s's, 4H, C_5H_4), 2.12–2.22 (m, 2H, CH), 1.27–1.57 (m, 8H, CH_2), 0.90 (t, $J = 7.4$ Hz, 6H, CH_3), 0.82 (t, $J = 7.1$ Hz, 6H, CH_3).

Lithium 1,3-bis(3-pentyl)cyclopentadienide•DME, 11a. Pentane (125 mL) is vacuum transferred onto **10a** (20.5 g, 98.7 mmol) in a swivel frit assembly. *n*-BuLi (67.9 mL, 1.6 M in hexane, 108.6 mmol) is added via syringe over 5 min at $-78\text{ }^{\circ}\text{C}$. The solution was allowed to warm slowly to room temperature and to stir for 6 h. DME (11.3 mL, 108.6 mmol) was vacuum transferred onto the reaction mixture. After 2 h of stirring at room temperature, the solution was cooled with an ice bath, and the resulting white solid was filtered and washed with pentane (3 x 75 mL). The white solid was dried *in vacuo* resulting in a fine white powder (21.9 g, 99%).⁵⁴ ^1H NMR (300 MHz, $\text{THF-}d_8$, δ): 5.36–5.39 (m, 3H, C_5H_3), 3.43 (s, 4H, DME CH_2), 3.27 (s, 6H, DME CH_3), 2.19 (m, 2H, CH), 1.35–1.61 (m, 8H, CH_2), 0.81 (t, $J = 7.5\text{ Hz}$, 12H, CH_3).

$[\text{C}_5\text{H}_3(\text{CHEt}_2)_2]\text{SiMe}_2\text{Cl}$ isomers, 12a. THF (150 mL) was vacuum transferred onto **11a** (10.0 g, 43.0 mmol) in a swivel frit assembly.⁵⁵ While the solution was cooled to $-78\text{ }^{\circ}\text{C}$, dichlorodimethylsilane (9.0 mL, 74.2 mmol) was vacuum transferred, and the reaction mixture was allowed to warm to room temperature in a dry ice/acetone bath overnight. The reaction was stirred at $25\text{ }^{\circ}\text{C}$ for another 24 h. The solvent was removed *in vacuo* leaving a white paste, and the product was extracted away from LiCl salts with petroleum ether (3 x 100 mL). After solvent removal *in vacuo*, a yellow oil was obtained which was used in the next step without further purification (11.69 g, 92%).

$(\text{SiMe}_2)[\text{C}_5\text{H}_3(\text{CHEt}_2)_2][\text{C}_5\text{H}_4((S)\text{-CHMeCMe}_3)]$, 13a. THF (100 mL) was vacuum transferred onto (*S*)-LiMNCp (6.17 g, 39.5 mmol) in a swivel frit assembly. THF (25 mL) was vacuum transferred onto **12a** in a 50-mL round bottom flask. The

solution of **12a** was cannula transferred onto the (*S*)-LiMNCp solution at 0 °C, and the mixture was stirred at room temperature overnight. The solvent was removed *in vacuo*, and the product was extracted from the LiCl with petroleum ether (3 x 100 mL). After the solvent was removed *in vacuo*, the resulting orange oil was Kugelrohr distilled (110 °C, <10⁻³ mmHg) to give 16.10 g (99%) of product. ¹H NMR (300 MHz, C₆D₆, δ): 6.01–6.61, 2.96–3.6 (m, 7H, Cp H), 2.12–2.58 (m, 3H, CH), 1.30–1.64 (m, 8H, CH₂), 1.22 (d, *J* = 7.2 Hz, 3H, MN CH₃), 0.98 (s, 9H, *t*-Bu), 0.72–0.95 (m, 12H, CH₂CH₃), –0.14, –0.04 (br s, 6H, Si(CH₃)₂).

Li₂{(SiMe₂)[C₅H₂(CH₂Et)₂][C₅H₃((*S*)-CHMeCMe₃)]}•DME, 14a. 150 mL of ether was vacuum transferred onto **13a** (16.1 g, 39.2 mmol) in a swivel frit assembly. *n*-BuLi (54.0 mL, 1.6 M in hexane, 86.4 mmol) was syringed onto the solution while the reaction was cooled to –78 °C. The clear solution was stirred at room temperature overnight. Solvent was removed *in vacuo* from the slightly cloudy solution, and petroleum ether (125 mL) was vacuum transferred resulting in a cloudier solution. DME (9.0 mL, 86.4 mmol) was vacuum transferred, producing copious amounts of precipitate. After cooling in an ice bath, the solution was filtered, and the white solid was collected. The solid was dried *in vacuo* resulting in a fine white powder (32.5 g, 90%). ¹H NMR (300 MHz, THF-*d*₈, δ): 5.86 (m, 1H, C₅H₃), 5.81 (m, 1H, C₅H₃), 5.71 (d, *J* = 2.7 Hz, 1H, C₅H₂), 5.67 (t, *J* = 2.7 Hz, 1H, C₅H₃), 5.55 (d, *J* = 3.0 Hz, 1H, C₅H₂), 3.43 (s, 4H, DME CH₂), 3.27 (s, 6H, DME CH₃), 2.67 (quint, *J* = 6.9 Hz, 1H, CH₂Et), 2.47 (q, *J* = 6.9 Hz, 1H, MN CH), 2.21 (quint, *J* = 6.9 Hz, 1H, CH₂Et), 1.36–1.64 (m, 8H, CH₂), 1.21 (d, *J* =

7.2 Hz, 3H, MN CH₃), 0.85 (s, 9H, *t*-Bu), 0.81 (t, *J* = 7.5 Hz, 12H, CH₂CH₃), 0.29, 0.30 (s, 6H, Si(CH₃)₂).

(SiMe₂)₂[C₅H₂(CH₂Et)₂][C₅H₃((*S*)-CHMeCMe₃)], **15a**. THF (150 mL) was vacuum transferred onto the dilithio salt **14a** (10.0 g, 19.5 mmol). At -78 °C, SiMe₂Cl₂ (1 equiv) was vacuum transferred, and the solution was allowed to warm to room temperature overnight. All volatiles were removed *in vacuo*. The ligand was extracted away from LiCl with petroleum ether. After drying the ligand under vacuum, it was Kugelrohr distilled (130 °C, <10⁻³ mmHg) to give a pale yellow oil (85%).

{(SiMe₂)₂[η⁵-C₅H(CH₂Et)₂][η⁵-C₅H₂((*S*)-CHMeCMe₃)]}ZrCl₂, (*S*)-**3**. In a swivel frit apparatus, the **15a** (0.95 g, 2.0 mmol) was dissolved in 50 mL of ether. *n*-BuLi (2.78 mL, 4.45 mmol) was syringed into the flask. The solution was allowed to stir for 24 h at room temperature under Ar. In another round bottom flask, ZrCl₄ (541 mg, 2.3 mmol) was dissolved in ether. The solution was cannula transferred to the ligand solution, and the solution became cloudy after 10 min. This mixture was allowed to stir at room temperature under Ar for 24 h. The solution was filtered to remove LiCl. The solvent was removed *in vacuo*, and hexamethyldisiloxane was added. Upon stirring, white solid precipitated out of solution. This white powder was collected on the swivel frit and dried. In the drybox, the white powder was recrystallized from cold toluene. After about 5 h, colorless crystals began to form. ¹H NMR (300 MHz, benzene-*d*₆, δ): 0.52, 0.54, 0.59, 0.62 (s, 4H, Si(CH₃)₂), 0.58 (td, *J* = 1.7, 7.2 Hz, 6H, CH₂CH₃), 0.81 (s, 9H, C(CH₃)₃), 1.02 (m, 6H, CH₂CH₃), 1.37 (m, 2H, CH₂), 1.56 (m, 2H, CH₂), 1.64 (d, *J* =

7.2 Hz, MN CH₃), 1.69 (m, 2H, CH₂), 2.38 (m, 2H, CH₂), 2.68 (m, 2H, CHEt₂), 2.90 (q, J = 7.2 Hz, 1H, MN CH), 6.45 (s, 1H, C₅H₁), 6.67 (d, J = 1.8 Hz, 1H, C₅H₂), 6.79 (d, J = 1.8 Hz, 1H, C₅H₂). Anal. Calcd for C₃₀H₅₀Si₂ZrCl₂: C, 57.28; H, 8.01. Found: C, 56.57; H, 8.40.

6-Cyclohexylfulvene, 7b. Into a 500-mL round bottom flask, cyclopentadiene (43.77 g, 0.622 mol), 200 mL of MeOH, and cyclohexanone (64.99 g, 0.662 mol) were added. Upon adding pyrrolidine (7.06 g, 0.099 mol), the solution became slightly warm and yellow in color. After 30 min, the solution became a cloudy, brown solution, which was allowed to stir overnight at room temperature. The reaction mixture was worked up in the same manner as **7a**. A clear, bright reddish brown liquid was obtained (92.0 g, 85%). ¹H NMR (300 MHz, C₆D₆, δ): 1.30 (m, 2H, CH₂); 1.41 (m, 4H, CH₂); 2.34 (m, 4H, C(CH₂)₂); 6.62 (m, 4H, C₅H₄).

Cyclohexylcyclopentadiene isomers, 8b. An oven-dried 1-L round bottom flask was charged with LiAlH₄ (14.28 g, 0.376 mol). The flask was equipped with a dry ice condenser and an addition funnel. After flushing with Ar, dry Et₂O (400 mL) was cannula transferred onto LAH. **7b** was added drop wise at a rate appropriate for gentle refluxing (~1 h). The solution was stirred at room temperature overnight. The reaction was quenched by slowly dripping H₂O (14 mL), 15% NaOH (42 mL), and H₂O (14 mL), in that order. After filtering away the white precipitate, the remaining yellow solution was dried over MgSO₄ and filtered. The solvent was removed by rotary evaporation. A viscous, bright yellow oil was obtained (45.98 g, 91%). ¹H NMR (300 MHz, C₆D₆, δ):

1.1–2.3 (m's, 11H, Cy H), 2.74, 2.80 (m's, 1H, C₅H₅), 5.95, 6.18, 6.24, 6.35, 6.49, 6.54 (m's, 4H, C₅H₅).

Dicyclohexylfulvene, 9b. Into a 250-mL round bottom flask, **8b** (19.9 g, 134 mmol), MeOH (68 mL), and cyclohexanone (14.04 g, 143 mmol) were added. Pyrrolidine (1.43 g, 20 mmol) was syringe added over 2 min to yield a yellow solution. The reaction mixture was refluxed overnight to yield a bright orange solution. The solution was neutralized with 50% acetic acid and worked up in the same manner as **7a**. The crude brown oil was Kugelrohr distilled (<10⁻³ mmHg, 130 °C) to obtain a bright yellow oil, which crystallizes upon standing at room temperature (22.94 g, 75%). ¹H NMR (300 MHz, C₆D₆, δ): 1.34, 1.46, 1.74, 2.01, 2.40 (m's, 21H, Cy H), 6.33 (dd, *J* = 5.4 Hz, 1.8 Hz, 1H, C₅H₃), 6.59 (dd, 5.4 Hz, 1.8 Hz, 1H, C₅H₃), 6.67 (dd, 5.4 Hz, 1.8 Hz, 1H, C₅H₃).

1,3-Dicyclohexylcyclopentadiene isomers, 10b. An oven-dried 500-mL round bottom flask was equipped with an addition funnel and a dry ice condenser. LiAlH₄ (4.01 g, 106 mmol) and dry Et₂O (200 mL) were added. **9b** (22.94 g, 101 mmol) was dissolved in 100 mL of Et₂O and drop added over 30 min. The solution was allowed to stir at room temperature overnight. The reaction was quenched by adding H₂O (6 g), 15% NaOH (18 g), and H₂O (6 g). After filtering the solution, it was dried over MgSO₄ and filtered. The solvent was removed by rotary evaporator to obtain a bright yellow oil (21.90 g, 94.2%). ¹H NMR (300 MHz, C₆D₆, δ): 1.24, 1.70, 1.85, 1.98, 2.24 (m's, 22H, Cy H), 2.74, 2.80 (m's, 1H, C₅H₄), 5.87 (m, 1H, C₅H₄), 6.13 (m, 1H, C₅H₄), 6.21 (m, 1H, C₅H₄).

Li[(C₅H₃Cy₂)], **11b.** A medium swivel frit apparatus was assembled. Into a 250-mL round bottom flask, **10b** (8.99 g, 39.0 mmol) was weighed. 200 mL of Et₂O was vacuum transferred. While cooling in –78 °C bath, *n*-BuLi (27.3 mL, 1.6 M, 42.9 mmol) was syringe added. The solution was allowed to warm to room temperature and stirred for 4 h. The mixture was filtered and washed with ether (3 x 50 mL). The solvent was removed *in vacuo*, and the solid was dried overnight (8.0 g, 87%). ¹H NMR (300 MHz, THF-*d*₈, δ): 1.2–1.4, 1.6–1.75, 1.85 (m's, 20H, Cy CH₂), 2.35 (m, 2H, Cy CH), 5.35, 5.38 (m, 3H, C₅H₃).

(C₅H₃Cy₂)SiMe₂Cl, **12b.** **11b** (7.90 g, 33.4 mmol) was weighed into a 250-mL round bottom flask and attached to a swivel frit assembly in the drybox. Dry THF (~150 mL) and dry Me₂SiCl₂ (5.0 mL, 41.2 mmol) were vacuum transferred onto **11b**. The reaction mixture was allowed to stir at –78 °C and warm to room temperature gradually overnight. All volatiles were removed *in vacuo*. Pentane (~50 mL) was vacuum transferred. The clear yellow solution was filtered and washed 3 times to remove LiCl. The solvent was removed *in vacuo*, leaving a white fluffy powder (10.4 g, 99%). ¹H NMR (300 MHz, C₆D₆, δ): 0.10, 0.25 (br s, 6H, SiMe₂), 1.25, 1.65, 1.90 (m's, 20H, Cy CH₂), 2.27, 2.50 (m's, 2H, Cy CH), 3.45 (br s, 1H, C₅H₃), 5.87 (br s, 1H, C₅H₃), 6.28 (s, 1H, C₅H₃).

SiMe₂(C₅H₃Cy₂)[C₅H₄((*S*)-CHMeCMe₃)], **13b.** In the drybox, **12b** (2.35 g, 7.27 mmol) and (*S*)-LiMNCp (1.14 g, 7.27 mmol) were added into a 100-mL round bottom flask. The flask was connected to a swivel frit. 50 mL of dry THF was vacuum

transferred. The mixture was stirred at room temperature overnight. The solvent was removed *in vacuo*, and pentane (~40 mL) was vacuum transferred. The white precipitate was filtered. The solvent was removed *in vacuo*, leaving an orange oil. The oil was dried overnight (3.11 g, 98%).

$\text{Li}_2\{\text{SiMe}_2(\text{C}_5\text{H}_2\text{Cy}_2)[\text{C}_5\text{H}_3((S)\text{-CHMeCMe}_3)]\}\cdot\text{DME}$, 14b. 50 mL of dry pentane was vacuum transferred onto the singly linked ligand (3.11 g, 7.12 mmol) in a 100 mL round bottom flask of a swivel frit assembly. At 0 °C, *n*-BuLi (9.35 mL, 1.6 M, 14.96 mmol) was syringe added. After stirring for 30 min, dry DME (1.56 mL, 14.96 mmol) was vacuum transferred onto the solution. After stirring overnight, white precipitate formed. The mixture was cooled to 0 °C, filtered, and washed 3 times. The white solid was dried for 3 h (3.0 g, 95%). ^1H NMR (300 MHz, $\text{THF-}d_8$, δ): 0.28 (s, 6H, $\text{Si}(\text{CH}_3)_2$), 0.84 (s, 9H, $\text{C}(\text{CH}_3)_3$), 1.18 (d, 3H, MN CH_3), 1.32 (m, 10H, Cy CH_2), 1.70 (m, 6H, Cy CH_2), 1.88 (m, 4H, Cy CH_2), 2.36 (m, 1H, Cy CH), 2.46 (qt, 1H, MN CH), 2.78 (m, 1H, Cy CH), 3.27 (s, 6H, DME CH_3), 3.42 (s, 4H, DME CH_2), 5.63 (m, 3H, C_5H_3), 5.82 (m, 2H, C_5H_2).

$(\text{SiMe}_2)_2(\text{C}_5\text{H}_2\text{Cy}_2)[\text{C}_5\text{H}_3((S)\text{-CHMeCMe}_3)]$, 15b. Dilithio salt (4.32 g, 8.5 mmol) was weighed into a 250-mL round bottom flask of a swivel frit assembly. Dry THF (100 mL) and Me_2SiCl_2 (1.1 mL, 9.13 mmol) were vacuum transferred. After stirring the pale yellow solution at room temperature overnight, the volatiles were removed *in vacuo*. Petroleum ether was vacuum transferred (~50 mL), and white precipitate formed. The solution was filtered, and the solvent was removed *in vacuo*,

leaving a bubbly white solid, which was dried for 3 h (3.32 g, 81%). ^1H NMR (300 MHz, C_6D_6 , δ): -0.25 (m, 6H, $\text{Si}(\text{CH}_3)_2$); 0.55, 0.62 (m, 6H, $\text{Si}(\text{CH}_3)_2$), 1.03 (s, 9H, $\text{C}(\text{CH}_3)_3$), 1.28 (d, 3H, MN CH_3), 1.28–2.8 (m, 20H, Cy CH_2), 2.32 (tt, 1H, Cy CH), 2.56 (m, 1H, MN CH), 2.82 (tt, 1H, Cy CH), 3.5 (m, 2H, Cp H), 6.46 (m, 2H, Cp H), 7.02 (m, 1H, Cp H).

$\text{Li}_2\{(\text{SiMe}_2)_2(\text{C}_5\text{H}_2\text{Cy}_2)[\text{C}_5\text{H}_3((S)\text{-CHMeCMe}_3)]\}\cdot\text{DME}$, **16b.** The product was prepared in the same manner as **16a** by treating **15b** (0.50 g, 1.01 mmol) with *n*-BuLi (1.4 mL, 1.6 M, 2.22 mmol) and DME (1 mL, 9.6 mmol). White powder was obtained (0.6 g, 93.6%). ^1H NMR (300 MHz, $\text{THF-}d_8$, δ): 0.2 (br s, 12H, $\text{Si}(\text{CH}_3)_2$); 0.82 (s, 9H, $\text{C}(\text{CH}_3)_3$), 1.22 (d, 3H, MN CH_3), 1.2–1.8 (m's, 20H, Cy CH_2), 2.52 (d, 3H, MN CH_3), 2.68 (m, 6H, Cy CH_2), 3.25 (s, 6H, DME CH_3), 3.4 (s, 4H, DME CH_2), 5.35, 5.85 (s, 2H, C_5H_2), 6.0 (br s, 1H, C_5H_1).

$\{(\text{SiMe}_2)_2(\eta^5\text{-C}_5\text{H}_1\text{Cy}_2)[\eta^5\text{-C}_5\text{H}_2((S)\text{-CHMeCMe}_3)]\text{Zr}(\text{NMe}_2)_2$, **17b.** Into a 50-mL flask, **15b** (0.93 g, 1.9 mmol), $\text{Zr}(\text{NMe}_2)_4$ (0.51 g, 1.9 mmol), and dry xylenes (25 mL) were placed. The flask was equipped with a condenser and a 180° needle valve joint. Under an Ar purge, the Teflon stopcock was replaced with a septum. A long needle was passed through the septum and halfway down the condenser. The yellow solution was refluxed under a strong Ar purge to drive away HNMe_2 . The reaction was monitored by placing a wet pH paper at the outlet end of the long needle. When the pH paper gave a neutral reading, all volatiles were removed *in vacuo*. A brown, crusty residue was obtained and used in the next step without further purification. ^1H NMR

(300 MHz, C_6D_6 , δ): 0.6, 0.9 (m's, 12H, $Si(CH_3)_2$), 1.25 (d, 3H, MN CH_3), 1.2–2.0 (m's, 20H, Cy CH_2), 2.6 (m's, 2H, Cy CH), 2.68 (q, 1H, MN CH), 2.75, 2.92 (s, 12H, NMe_2), 6.3 (s, 1H, C_5H_1), 6.4, 6.45 (d's, 2H, C_5H_2)

$\{(SiMe_2)_2(\eta^5-C_5H_1Cy_2)[\eta^5-C_5H_2((S)-CHMeCMe_3)]ZrCl_2$, (S)-4. *Via diamide:*

The flask containing the crude **17b** was switched to a swivel frit assembly in the drybox. Toluene (25 mL) and $TMSCl$ (10 equiv) were vacuum transferred. The solution was stirred overnight at room temperature. The volatiles were removed. The white powder was filtered from $(TMS)_2O$ and dried (61%). Single crystals were obtained from cold CH_2Cl_2 . *Via dilithio:* Into a 50-mL round bottom flask, **16b** (0.54 g, 0.85 mol) and $ZrCl_4$ (0.20 g, 0.85 mol) were weighed in a drybox. The flask was connected to a condenser and a 180° needle valve joint. Toluene was vacuum transferred (~30 mL). The solution was refluxed for 12 h. The solution was orange and contained white precipitate. The condenser was replaced with a swivel frit assembly. Half of the solvent was removed *in vacuo*. The resulting white precipitate was filtered, washed 3 times, and dried. 1H NMR (300 MHz, C_6D_6 , δ): 0.48 (s, 3H, $Si(CH_3)_2$), 0.50 (s, 3H, $Si(CH_3)_2$), 0.54 (s, 3H, $Si(CH_3)_2$), 0.58 (s, 3H, $Si(CH_3)_2$), 0.78 (s, 9H, $C(CH_3)_3$), 1.0–1.4 (m, 10H, Cy CH_2), 1.61 (d, 3H, MN CH_3), 1.6 (m, 6H, Cy CH_2), 1.73 (m, 4H, Cy CH_2), 2.5–2.7 (m, 2H, Cy CH), 2.87 (q, 1H, MN CH), 6.42 (s, 1H, Cp H), 6.64 (s, 1H, Cp H), 6.75 (s, 1H, Cp H).

(S,S)-2-Chloro-3-methyl pentanoic acid, 18. Into a 12-L round bottom flask equipped with a mechanical stirrer, L-isoleucine (500 g, 3.81 mol) was dissolved with 6 M HCl (7.5 L). The solution was cooled to $<5^\circ C$. A precooled ($<5^\circ C$) solution of

NaNO₂ (631 g, 9.1 mol) dissolved in 750 mL of H₂O was added dropwise with vigorous stirring and efficient cooling so that the temperature was maintained <10 °C. Emission of brown gas was observed. After 5 h, additional NaNO₂ (100 g, 1.5 mol) dissolved in 100 mL of water was added. The brown reaction mixture was stirred overnight and allowed to warm to room temperature. The next day, the solution was clear, bright green, to which urea (637 g, 10.6 mol) and Na₂CO₃ (375 g, 2.86 mol) were added. 2-L portions of the reaction solution were extracted with ethyl acetate (3 x 700 mL). The combined organic phase was dried over MgSO₄, filtered, concentrated on a rotary evaporator, and distilled (94 °C–95 °C, ~1 mmHg) to yield 464.6 g (81%) of product. ¹H NMR (300 MHz, C₆D₆, δ): 10.54 (br s, 1H, COOH), 3.98 (d, *J* = 6.6 Hz, 1H, CHCl), 1.86–2.00, (m, 1H, CHCH₃), 1.44–1.58 (m, 1H, CH₂), 1.03–1.07 (m, 1H, CH₂), 0.80 (d, *J* = 6.6 Hz, 3H, CHCH₃), 0.66 (t, *J* = 7.3 Hz, 3H, CH₂CH₃).

(S)-3-Methyl-1-pentanol, 19. A 12-L round bottom flask, equipped with a condenser and a magnetic stir bar, was charged with anhydrous ether (7 L) and LAH (250 g, 6.58 mol). The gray slurry was cooled to 5 °C. **18** (464.6 g, 3.08 mol), dissolved in 500 mL of ether, was added drop-wise over 4 h, maintaining temperature below 15 °C. The solution was refluxed gently for 72 h. Equipped with a dry ice condenser, the reaction was quenched very slowly with water (250 mL), 15% NaOH (250 mL), and water (750 mL) via a syringe pump.⁵⁶ The solution was filtered, concentrated, and vacuum distilled from crushed CaCO₃ (48 °C, 18 torr) to obtain 208.3 g (66%) of alcohol. ¹H NMR (300 MHz, C₆D₆, δ): 3.5 (m, 2H, CH₂OH), 2.6 (br, 1H, OH), 1.0–1.6 (m's, 5H, CH₂ and CH), 0.88 (t's, 6H, CH₃).

(S)-1-Iodo-3-methylpentane, 20.³⁶ **19** (150 g, 1.47 mol) and Ph₃P (439 g, 1.67 mol) were dissolved in 1 L of DMF. Via a solid addition funnel, I₂ (374 g, 1.48 mol) was added over 1.5 h while the round bottom flask was cooled in an ice bath. The orange reaction mixture was stirred at room temperature for 4 h. All volatile material was distilled at 1 mmHg into a receiving flask cooled in a dry ice bath. The distillate was transferred to a separatory funnel containing 3 L of ice-cold water. After the iodide settled to the bottom, it was separated and washed with sat. Na₂S₂O₃. The crude iodide was vacuum distilled from CaSO₄ (26.5 °C–27.5 °C, ~1 mmHg) using a Vigreux column to give 223 g (72%) of product, which was stored in an aluminum foil wrapped bottle at –80 °C. ¹H NMR (300 MHz, C₆D₆): δ 2.69–2.85 (m, 2H, CH₂I), 1.51–1.63, 1.17–1.35 (m, 2H, CH₂CH₂I), 0.81–0.95, 1.00–1.1 (m, 2H, CH₂CH₃), 0.70 (t, *J* = 7.5 Hz, 3H, CH₂CH₃), 0.59 (d, *J* = 6.6 Hz, 3H, CHCH₃).

(S)-3-Methyl-1-pentene. Potassium *tert*-butoxide (283 g, 2.53 mol) was dissolved in DMSO (2.5 L) in a 3-neck 5-L round bottom flask equipped with an addition funnel, a distillation apparatus, and a stopcock. **20** was placed in the addition funnel. The system was connected to a mercury bubbler via the side-arm above the distillation receiving flask. The pressure of the system was reduced to 220 mmHg, and the iodide was added dropwise to the reaction flask. As the product formed, it distilled. About 100 mL of crude material was collected. The crude product was purified by fractional distillation (54 °C, 760 mmHg) to yield 114 g (54%) of olefin. ¹H NMR (300 MHz, C₆D₆, δ): 5.6 (m, 1H, HC=), 4.9–5.0 (m, 2H, H₂C=), (hept, 1H, CH), 1.2 (quint, 2H, CH₂), 0.9 (d, 3H, CH₃CH), 0.8 (t, 3H, CH₂CH₃).

TMSCpH isomers, 21. LiCp (3.5 g, 48.6 mmol) was weighed into a 250-mL round bottom flask and capped with a 180° needle valve joint. While cooling in a –78 °C bath, THF (125 mL) and TMSCl (5.8 g, 53.4 mmol) were vacuum transferred. The solution was allowed to stir at –78 °C and gradually warm to room temperature overnight. All volatiles were vacuum transferred away from LiCl into a 250-mL round bottom flask. The clear and colorless distillate was used in the next step without further purification. The GC indicated that only TMSCpH and TMSCl were present, and no TMS₂CpH.

LiTMSCp, 22. The round bottom flask containing **21**/THF solution was attached to a swivel frit assembly. While cooling at –78 °C, *n*-BuLi (33 mL, 1.6 M, 53.5 mmol) was syringed quickly. The solution was allowed to stir in –78 °C and gradually warm to room temperature overnight. The solvent was removed *in vacuo*. Petroleum ether (125 mL) was vacuum transferred. The white slurry was filtered, and the solid was washed three times. The solvent was removed *in vacuo*, and the solid was dried overnight to obtain a bright white powder (7.11 g, 100%). ¹H NMR (300 MHz, C₆D₆, δ): 0.11 (s, 9H, Si(CH₃)₃), 5.82, 5.88 (m, 4H, C₅H₅).

(TMS)₂CpH, 23. In the drybox, **22** was weighed into a 250-mL round bottom flask, which was connected to a swivel frit. THF (125 mL) was vacuum transferred, followed by TMSCl (–78 °C). The solution was allowed to stir in –78 °C and gradually warm to room temperature overnight. All volatiles were vacuum transferred out of the flask. Petroleum ether (100 mL) was vacuum transferred onto the white paste. The solution was filtered and washed three times to remove LiCl. The solvent was removed

by rotary evaporator to yield a yellow oil (10.2 g, 98%). ^1H NMR (300 MHz, C_6D_6 , δ): -0.031 (s, 18H, $\text{Si}(\text{CH}_3)_3$), 6.45, 6.74 (m, 4H, C_5H_4).

(TMS) $_2$ CpSiMe $_2$ Cl isomers, 24. **23** (10.38 g, 49.3 mmol) was weighed into a 250-mL round bottom flask. The flask was equipped with a swivel frit assembly. Petroleum ether was vacuum transferred (100 mL). While cooling at -78°C , *n*-BuLi (33.9 mL, 1.6 M, 54.2 mmol) was syringed onto the solution. The solution was stirred in a -78°C bath and was allowed to warm to room temperature gradually overnight. All volatiles were removed *in vacuo*. THF (125 mL) was vacuum transferred. The cloudy, yellow solution was refluxed for 3 h under vacuum. SiMe_2Cl_2 (7.18 mL, 59.2 mmol) was vacuum transferred onto the $\text{Li}(\text{TMS})_2\text{Cp}$ solution while vigorously stirring at -78°C . The solution was allowed to stir in -78°C bath and warm to room temperature. All volatiles were removed *in vacuo*. The reaction flask was connected to a swivel frit assembly, and petroleum ether (100 mL) was vacuum transferred. The solution was filtered, and all volatiles were removed *in vacuo*. The dark yellow oil was Kugelrohr distilled at $60\text{--}90^\circ\text{C}$ to collect a pale yellow oil (12.25 g, 82%). ^1H NMR (300 MHz, C_6D_6 , δ): -0.06 (s, 18H, $\text{Si}(\text{CH}_3)_3$), 0.04 (s, 9H, $\text{Si}(\text{CH}_3)_3$), 0.12, 0.16 (s, 6H, $\text{Si}(\text{CH}_3)_2\text{Cl}$), 0.22 (s, 9H, $\text{Si}(\text{CH}_3)_3$), 0.52 (s, 6H, $\text{Si}(\text{CH}_3)_2\text{Cl}$), 6.48, 6.82, 6.86, 6.92, 6.96 (m's, 6H, Cp H).

$\text{SiMe}_2(\text{C}_5\text{H}_3\text{TMS}_2)[\text{C}_5\text{H}_4((S)\text{-CHMeCMe}_3)]$, 25. A 100-mL round bottom flask was charged with (*S*)-LiMNCp (1.01 g, 6.5 mmol) in the drybox. In another 100-mL round bottom flask, **24** (1.96 g, 6.5 mmol) was weighed. The flask containing **24** was

connected to the filtrate side of a swivel frit, and the flask containing (*S*)-LiMNCp was connected to the other side of the swivel frit. With the swivel frit parallel to the vacuum line, THF (25 mL) was vacuum transferred into both round bottom flasks. After stirring to dissolve, the solution of **24** was allowed to pass through the frit onto the (*S*)-LiMNCp solution while cooling in a $-78\text{ }^{\circ}\text{C}$ bath. The round bottom flask was rinsed 3 times. The clear, slightly yellow solution was allowed to stir and warm to room temperature overnight. All volatiles were removed *in vacuo*. Petroleum ether (40 mL) was vacuum transferred onto the white paste. The cloudy solution was filtered and washed three times. All volatiles were removed *in vacuo* and dried overnight. The oil was Kugelrohr distilled at $120\text{ }^{\circ}\text{C}$ at 10^{-3} mmHg. A pale yellow oil was collected (2.46 g, 92%).

$\text{K}_2\{\text{SiMe}_2(\text{C}_5\text{H}_2\text{TMS}_2)[\text{C}_5\text{H}_3((\text{S})\text{-CHMeCMe}_3)]\}$, **26.** **25** (2.46 g, 5.93 mmol) was weighed into a 100-mL round bottom flask. Into another 100-mL round bottom flask, $\text{KN}(\text{TMS})_2$ (2.36 g, 11.9 mmol) was weighed. The flask containing $\text{KN}(\text{TMS})_2$ was connected to the filtrate side of a swivel frit and the flask containing **25** to the other end. THF (25 mL) was vacuum transferred into both flasks. After stirring to dissolve, the $\text{KN}(\text{TMS})_2$ solution was allowed to pass through the frit onto the solution of **25** while cooling in a $-78\text{ }^{\circ}\text{C}$ bath. The dark yellow solution was allowed to stir in the bath overnight. All volatiles were removed from the cloudy solution. Petroleum ether was vacuum transferred, filtered, and washed. The solvent was removed *in vacuo* and the tan-colored powder was dried. In the drybox, the tan-colored powder was transferred to a new round bottom flask and equipped with a swivel frit assembly. THF (25 mL) was vacuum transferred. The brown solution was cooled in a $0\text{ }^{\circ}\text{C}$ bath and filtered. The

solid collected was washed with cold THF to yield a bright white powder. The solvent was removed *in vacuo*, and the solid was dried overnight (1.98 g, 68%). ^1H NMR (300 MHz, THF- d_8 , δ): 0.10 (s, 18H, Si(CH₃)₃), 0.44 (s, 12H, Si(CH₃)₂), 0.75 (s, 9H, *t*-Bu), 1.1 (d, 3H, MN CH₃), 2.35 (q, 1H, MN CH), 5.50, 5.62, 5.65 (m, 3H, C₅H₃), 6.35 (s, 2H, C₅H₂).

(SiMe₂)₂(C₅H₂TMS₂)[C₅H₃((*S*)-CHMeCMe₃)], **27**. **26** (1.47 g, 2.98 mmol) was weighed in a 100-mL round bottom flask and connected to a swivel frit assembly. THF (75 mL) and SiMe₂Cl₂ (0.4 mL, 3.3 mmol) were vacuum transferred while the flask was cooled in a -78 °C bath. The solution was stirred in a -78 °C bath and allowed to warm to room temperature overnight. All volatiles were removed *in vacuo*. Petroleum ether was vacuum transferred, and the solution was filtered and washed. All volatiles were removed, and the oil was dried overnight (1.15 g, 82%).

Li₂{(SiMe₂)₂(C₅H₁TMS₂)[C₅H₂((*S*)-CHMeCMe₃)]}, **28**. A round bottom flask containing **27** (2.82 g, 5.96 mmol) was connected to a swivel frit assembly. THF (75 mL) was vacuum transferred. While cooling in a -78 °C bath, *n*-BuLi (7.8 mL, 12.5 mmol) was syringed onto the solution. The solution was allowed to stir overnight in a -78 °C bath. All volatiles were removed *in vacuo* from the brown, clear solution. Petroleum ether was vacuum transferred. The solution was filtered, washed, and the solvent was removed *in vacuo*. The off-white solid was dried overnight (1.78 g, 62%). ^1H NMR (300 MHz, THF- d_8 , δ): 0.20, 0.25, 0.36, 0.40 (s, 12H, Si(CH₃)₂), 0.26, 0.32 (s,

18H, Si(CH₃)₃), 0.85 (s, 9H, *t*-Bu), 1.2 (d, 3H, MN CH₃), 2.50 (q, 1H, MN CH), 6.0 (br s, 2H, C₅H₂), 6.68 (s, 1H, C₅H₁).

{{(SiMe₂)₂(η⁵-C₅H₁TMS₂)[η⁵-C₅H₂((*S*)-CHMeCMe₃)]}ZrCl₂, (*S*)-5. Into a 50-mL round bottom flask, **28** (557 mg, 1 mmol) and ZrCl₄ (233 mg, 1 mmol) were weighed. The flasks were connected to a swivel frit assembly. CH₂Cl₂ (20 mL) was vacuum transferred. The tan slurry was stirred in -78 °C bath for 3 h, and then at room temperature for 3 h more. All volatiles were removed *in vacuo*. Petroleum ether (30 mL) was vacuum transferred, and the slurry was filtered and washed three times. All volatiles were removed *in vacuo* to yield a glassy, pale yellow solid. The product was recrystallized from pentane. ¹H NMR (300 MHz, C₆D₆, δ): 0.35, 0.4, 0.57, 0.6 (s, 12H, Si(CH₃)₂), 0.41, 0.62 (s, 18H, Si(CH₃)₃), 0.77 (s, 9H, *t*-Bu), 1.6 (d, 3H, MN CH₃), 0.82 (q, 1H, MN CH), 6.5, 6.8, 7.15 (m, 3H, Cp H).

2,3,3-Trimethyl-1-butene, 28. Pinacolone was dried over sieves before use. A 3-necked, 5-L round bottom flask was equipped with a dry ice condenser, 500-mL addition funnel, and a septum. The apparatus was flushed with argon. Pinacolone (237.9 g, 2.38 mol) and ethyl ether (500 mL) were cannula transferred into the flask. The solution was cooled in an ice bath. After cannula transferring MeMgBr (800 mL, 3.0 M in Et₂O, 2.4 mol) into the addition funnel, MeMgBr was added over 2 h while cooling the flask in an ice bath. The mixture was further stirred at room temperature for 2 h more. Water (500 mL) was added very slowly at a rate of gentle refluxing, about 2 h. The mixture was stirred at room temperature overnight. The organic layer was decanted away

from the white, amorphous solid. About half of the solvent was removed under reduced pressure, leaving the alcohol product, which was a colorless needle. The alcohol/ether solution and water (250 mL) were transferred to a 3-necked, round bottom flask equipped with a dry ice condenser and 500-mL addition funnel. Via addition funnel, a mixture of concentrated sulfuric acid (300 mL) and water (250 mL) was added at room temperature over 1 h. The orange solution was stirred at room temperature overnight. At ambient pressure, the product was distilled using a Vigoreux column (78–80 °C) to yield 127.58 g of clear, colorless liquid (55%). ^1H NMR (300 MHz, C_6D_6 , δ): 1.02 (s, 9H, *t*-Bu), 1.68 (s, 3H, CH_3), 4.75 (m, 1H, =CH), 4.83 (m, 1H, =CH).

2,3,3-Trimethyl-1-butanol, 29. A 2-necked, 2-L round bottom flask was equipped with a dry ice condenser and a 100-mL addition funnel. The apparatus was connected to an oil bubbler and flushed with argon. Petroleum ether (500 mL) and **28** (dried over LAH and vacuum transferred over before use) (127.58 g, 1.3 mol) were cannula transferred. Via the addition funnel, BH_3SMe_2 (45 mL, 10 M, 0.43 mol) was added over 50 min. The solution was stirred at room temperature for 4 h. Ethanol (400 mL) was added very slowly (4 h). The solution was stirred at room temperature overnight. 3 M NaOH (160 mL) was added, followed by a slow addition of 30% H_2O_2 (160 mL). The solution was extracted with ethyl ether (3 x 250 mL). The combined organic layer was washed with brine (200 mL), dried over MgSO_4 , and filtered. The solvent was removed by rotary evaporator. The product was vacuum distilled (20 mmHg, 68–70 °C) to obtain a clear, colorless liquid (113.4 g, 75%). ^1H NMR (300 MHz, C_6D_6 , δ): 0.81 (s, 9H, *t*-Bu), 0.93 (d, $J = 6.9$ Hz, 3H, CH_3), 1.30 (m, 1H, CH), 1.44 (m,

1H, OH) (chemical shift will change depending on concentration), 3.15 (dd, $J = 9.9$ Hz, 8.4 Hz, 1H, CH₂), 3.61 (dd, $J = 10.2$ Hz, 3.9 Hz, 1H, CH₂).

2,3,3-Trimethyl-1-butanaldehyde, 30. An oven-dried 3-necked, 2-L round bottom flask was equipped with a 125-mL addition funnel, 250-mL addition funnel, and a septum with a low-temperature thermometer through the center. The assembly was flushed with argon. Methylene chloride (500 mL) was cannula transferred and cooled to -50 °C. Via addition funnel, oxalyl chloride (82.7 g, 0.65 mol) was added over 5 min. DMSO (101.7 g, 1.3 mol) (previously dried over sieves) was added at a rate to maintain solution temperature between -60 °C and -50 °C (**Caution: DMSO and oxalyl chloride reacts violently at room temperature**). **29** (68.78 g, 0.59 mol) (dried over sieves) was then drop added, keeping temperature below -50 °C. The round bottom flask containing **29** was rinsed with 250 mL of methylene chloride. The rinse was added to the reaction mixture. The solution was stirred at -50 °C for 30 min. EtNMe₂ (216.5 g, 2.7 mol) was drop added at a rate to maintain temperature between -30 °C and -60 °C. The white slurry was stirred at room temperature overnight. Water (300 mL) was added, resulting in an orange solution. The layers were separated, and the organic layer was washed with water (300 mL), brine (300 mL), dried over MgSO₄, and filtered. The solvent was removed by rotary evaporator while cooling the flask in ice water. The product was vacuum distilled (15 mmHg, 63 °C) to obtain a clear and colorless liquid (34.8 g, 51%). ¹H NMR (300 MHz, C₆D₆, δ): 0.73 (s, 9H, *t*-Bu), 0.77 (d, $J = 7.2$ Hz, 3H, CH₃), 1.76 (qd, $J = 7.2, 1.8$ Hz, 1H, CH), 9.54 (d, $J = 3$ Hz, 1H, COH).

3,4,4-Trimethyl-1-pentene. Into a one-necked, 1-L round bottom flask, $\text{Ph}_3\text{PCH}_3\text{Br}$ (119.8 g, 0.34 mol) and NaNH_2 (15.7 g, 0.40 mol) were weighed in the drybox. Diglyme (dried over sieves for 3 d) (500 mL) was cannula transferred while stirring at $-78\text{ }^\circ\text{C}$. The slurry was allowed to warm to room temperature and stirred for 1 h. Under a strong argon purge, **30** (dried over sieves) was cannula transferred onto the yellow slurry while cooling in a $-78\text{ }^\circ\text{C}$ bath. The slurry became white, and the mixture was allowed to warm slowly to room temperature overnight. The solution was vacuum distilled via a simple column (1 mmHg, oil bath $45\text{ }^\circ\text{C}$) to separate the low boiling products and desired product away from diglyme and solids. The crude product was further fractionally distilled ($102\text{--}104\text{ }^\circ\text{C}$) at ambient pressure to yield a clear and colorless liquid (16.4 g, 49%). ^1H NMR (300 MHz, C_6D_6 , δ): 0.84 (s, 9H, *t*-Bu), 0.91 (d, $J = 6.9\text{ Hz}$, 3H, CH_3), 1.82 (m, 1H, CH), 4.94 (ddd, $J = 7.2, 2.1, 0.3\text{ Hz}$, 1H, =CH), 4.98 (m, 1H, =CH), 5.73 (m, 1H, CH).

Polymerization Procedures. A long-necked 10-mL round bottom Schlenk flask was made. The side arm was enlarged to fit a septum that was tightened with a copper wire.⁵⁷ MAO (250 mg) and tetradecane (1.5 mL, distilled from Na) are weighed into the flask in the drybox, under an atmosphere of nitrogen. A Teflon needle valve is fitted to the Schlenk flask, and the flask is degassed on the high-vacuum line. Olefin (1.8 mL) is vacuum transferred from LiAlH_4 or CaH_2 into a measuring cylinder and then into the flask containing the MAO/tetradecane mixture. The olefin is stirred in the MAO suspension for 1 h to ensure the removal of all traces of moisture. Prior to catalyst injection an aliquot is taken via the side arm of the Schlenk flask (fitted with a septum)

and is immediately quenched with *n*-butanol. The catalyst solution, prepared in the drybox immediately before use, is taken up with a gas tight syringe. Before taking the catalyst syringe out of the drybox, the syringe needle is sealed by piercing it into a 24/40 rubber septum. The flask is placed under an atmosphere of argon, and the catalyst solution is injected via the side arm of the Schlenk flask (0.50 mL of a 3.5×10^{-3} M solution in toluene is typical). The solution usually changes from colorless to light yellow or pink upon catalyst addition. When the desired conversion is reached, a final aliquot is taken, and the contents of the flask are immediately frozen at 77 K and degassed under high vacuum. The unreacted olefin and toluene is vacuum transferred into a receiving flask. The aliquots are used for the GC determination of conversion, with tetradecane serving as the internal standard for integration. The polymer can be isolated by first quenching the residue with methanol (10 mL) followed by a 1 M solution of HCl in methanol (10 mL). The methanol is removed *in vacuo*, and the tetradecane is then removed by Kugelrohr distillation. The polymer is suspended in methanol, filtered, washed, and dried *in vacuo*. In order to more easily isolate the polymer, the polymerization can be carried out in toluene. The solvent is easily removed, precluding the need for the Kugelrohr distillation.

Enantioassay of Recovered Olefins. Optical purity was determined by enantioassay of the methyl ester derivative on a chiral GC column. A typical procedure for the derivatization is as follows. Olefin/toluene solution (200 mg) is added to a 20-mL vial containing CCl_4 (4 mL), CH_3CN (4 mL), H_2O (6 mL), and NaIO_4 (4 equiv). $\text{RuCl}_3 \cdot 3\text{H}_2\text{O}$ (10 mg) is added and the biphasic reaction mixture is stirred vigorously for

24 h at room temperature, after which time H_2O (5 mL) and CH_2Cl_2 (5 mL) are added.⁵⁸

The organic layer is separated and washed with $\text{Na}_2\text{S}_2\text{O}_3(\text{aq})$ (to reduce any I_2 and I_3^- present) and then brine. The solution is dried over MgSO_4 , filtered, and the solvent is removed *in vacuo* to give a light yellow oil, which often is malodorous. The sweet-smelling methyl esters are prepared by boiling a BF_3/MeOH (15%) solution (5 mL) of the carboxylic acid (~100 mg) for 5–10 min in a capped 20-mL vial. For 3,4,4-trimethyl-1-pentene enantioassay, 10–15 mL of BF_3/MeOH solution is necessary. The methyl ester was extracted into petroleum ether (15 mL), which was dried prior to injection on the chiral GC column.

REFERENCES AND NOTES

- ¹ Eliel, E. L.; Wilen, S. H.; Mander, L. N. *Stereochemistry of Organic Compounds*, New York: Wiley, 1994.
- ² (a) *Asymmetric Synthesis*; Morrison, I. D., ed.; Academic Press: Orlando, 1983-1985, Vol. 1-5. (b) *Comprehensive Asymmetric Catalysis*; Jacobsen, E. N., Pfaltz, A., Yamamoto, A., eds.; Springer: New York, 1999, Vol. 1-3.
- ³ Hoveyda, A. H.; Didiuk, M. T. *Curr. Org. Chem.* **1998**, *2*, 489-526.
- ⁴ Keith, J. M.; Larrow, J. F.; Jacobsen, E. N. *Adv. Synth. Catal.* **2001**, *343*, 5.
- ⁵ Jacques, J.; Collet, A.; Wilen, S. H. *Enantiomers, Racemates, and Resolutions*, Malabar: Krieger, Florida, 1991.
- ⁶ *New trends in synthetic medicinal chemistry*; Gualtieri, F., ed.; Wiley-VCH: Weinheim, New York, 2000.
- ⁷ (a) Gao, Y.; Hanson, R. M.; Klunder, J. M.; Ko, S. Y.; Masamune, H.; Sharpless, K. B. *J. Am. Chem. Soc.* **1987**, *109*, 5765. (b) Martin, V. S.; Woodard, S. S.; Katsuki, T.; Yamada, Y.; Ikeda, M.; Sharpless, K. B. *J. Am. Chem. Soc.* **1981**, *103*, 6237. (c) Kitamura, M.; Kasahara, I.; Manbe, K.; Noyori, R.; Takaya, H. *J. Org. Chem.* **1988**, *53*, 708.
- ⁸ (a) Adams, J. A.; Ford, J. G.; Stamatos, P. J.; Hoveyda, A. H. *J. Org. Chem.* **1999**, *64*, 9690. (b) Morken, J. P.; Didiuk, M. T.; Visser, M. S.; Hoveyda, A. H. *J. Am. Chem. Soc.* **1994**, *116*, 3123.
- ⁹ La, D. S.; Alexander, J. B.; Cefalo, D. R.; Graf, D. D.; Hoveyda, A. H.; Schrock, R. R. *J. Am. Chem. Soc.* **1998**, *120*, 9720.
- ¹⁰ (a) VanNieuwenhze, M. S.; Sharpless, K. B. *J. Am. Chem. Soc.* **1993**, *115*, 7864. (b) Hamon, D. P. G.; Tuck, K. L.; Christie, H. S. *Tetrahedron* **2001**, *57*, 9499. (c) Christie, H. S.; Hamon, D. P. G.; Tuck, K. L. *Chem. Commun.* **1999**, 1989. (d) Corey, E. J.; Noe, M. C. *J. Am. Chem. Soc.* **1996**, *118*, 11038. (e) Corey, E. J.; Noe, M. C.; Guzman-Perez, A. *J. Am. Chem. Soc.* **1995**, *117*, 10817.
- ¹¹ Gardiner, J. M.; Norret, M.; Sadler, I. H. *Chem. Commun.* **1996**, 2709.

-
- ¹² Reductive strategies have been successfully employed for the resolution of allylic alcohols: (a) Kitamura, M.; Kashara, I.; Manabe, K.; Noyori, R.; Takaya, H. *J. Org. Chem.* **1988**, *53*, 710.
- ¹³ (a) Brintzinger, H. H.; Fischer, D.; Mülhaupt, R.; Rieger, B.; Waymouth, R. M. *Angew. Chem. Int. Ed. Engl.* **1995**, *34*, 1143. (b) Britovsek, G. J. P.; Gibson, V. C.; Wass, D. F. *Angew. Chem. Intl. Ed. Engl.* **1999**, *38*, 428. (c) Coates G. W. *Chem. Rev.* **2000**, *100*, 1223. (d) Resconi, L.; Cavallo, L.; Fait, A.; Piemontesi, F. *Chem. Rev.* **2000**, *100*, 1253.
- ¹⁴ Facts and figures for the chemical industry. *Chemical and Engineering News*, June 25, 2001, 79, 42.
- ¹⁵ Natta, G.; Pino, P.; Mazzanti, P.; Corradini, P.; Giannini, U. *Rend. Acc. Naz. Lincei VIII*, **1955**, *19*, 397-403.
- ¹⁶ Ciardelli, F.; Carlini, C.; Altomare, A. *Ziegler Catalysis*; Springer-Verlag: Berlin, 1995, 454-467.
- ¹⁷ MAO is methylaluminumoxane, (MeAlO)_n.
- ¹⁸ (a) Sacchi, M. C.; Barsties, E.; Tritto, I.; Locatelli, P.; Brintzinger, H. H.; Stehling, U. *Macromolecules* **1997**, *30*, 1267. (b) Oliva, L.; Longo, P.; Zambelli, A. *Macromolecules* **1996**, *29*, 6383.
- ¹⁹ Herzog, T. A.; Zubris, D. L.; Bercaw, J. E. *J. Am. Chem. Soc.* **1996**, *118*, 11988.
- ²⁰ Veghini, D.; Henling, L. M.; Burkhardt, T. J.; Bercaw, J. E. *J. Am. Chem. Soc.*, **1999**, *121*, 564.
- ²¹ Baar, C. R.; Levy, C. J.; Min, E. Y.; Henling, L. M.; Day, M. W.; Bercaw, J. E. *J. Am. Chem. Soc.* **2004**, *126*, 8216.
- ²² (a) Carlsen, P. H. J.; Katsuki, T.; Martin, V. S.; Sharpless, K. B. *J. Org. Chem.* **1981**, *46*, 3936. (b) Parker, D. *J. Chem. Soc., Perkin Trans. II* **1983**, 83. (c) Chataigner, I.; Lebreton, J.; Durand, D.; Guingant, A.; Villiéras, J. *Tet. Lett.* **1998**, *39*, 1759.
- ²³ Thank you to Theo Strinopoulos for generating these Matlab plots.
- ²⁴ The assignment of absolute configuration was performed by Dr. Chris Levy and Dr. Cliff Baar.

-
- ²⁵ (a) Schurig, V.; Leyrer, U.; Wistuba, D. *J. Org. Chem.* **1986**, *51*, 242. (b) Lazzaroni, R.; Salvadori, P.; Bertucci, C.; Veracini, C. A. *J. Organomet. Chem.* **1975**, *99*, 475. (c) Lardicci, L.; Caporusso, A. M.; Giacomelli, G. *J. Organomet. Chem.* **1974**, *70*, 333. (d) Lazzaroni, R.; Salvadori, P.; Pino, P. *Tet. Lett.* **1968**, 2507. (e) Pino, P.; Lardicci, L.; Centoni, L. *Gazz. Chem. Ital.* **1961**, *91*, 428.
- ²⁶ (a) Lazzaroni, R.; Salvadori, P.; Pino, P. *Tet. Lett.* **1968**, *21*, 2507-2510. (b) Lardicci, L.; Menicagli, R.; Caporusso, A. M.; Giacomelli, G. *Chem. Ind.* **1973**, *4*, 184-5.
- ²⁷ (a) Caporusso, A. M.; Giacomelli, G. P.; Lardicci, L. *Atti Soc. Tosc. Sci. Nat., Mem.* **1973**, *80*, 40-58. (b) Lardicci, L.; Caporusso, A. M.; Giacomelli, G. *J. Organomet. Chem.* **1974**, *70*, 333-338. (c) Lazzaroni, R.; Salvadori, P.; Bertucci, C. *J. Organomet. Chem.* **1975**, *99*, 475-486.
- ²⁸ (a) Sakai, K.; Tsuda, K. *Chem. Pharm. Bull.* **1963**, *11*, 650-3. (b) Tarzia, G.; Tortorella, V.; Romeo, A. *Gazz. Chim. Ital.* **1967**, *97*, 102-8. (c) di Maio, G.; Romeo, A. *Gazz. Chim. Ital.* **1959**, *89*, 1627-31.
- ²⁹ (a) Zambelli, A.; Proto, A.; Pasquale, L. *Ziegler Catalysis*; Springer-Verlag: Berlin, **1995**, 218-235. (b) Oliva, L.; Longo, P.; Zambelli, A. *Macromolecules* **1996**, *29*, 6383.
- ³⁰ (a) Boor, J. *Ziegler-Natta Catalysts and Polymerization*; Academic Press: New York, **1979**. (b) Pino, P.; Mulhaupt, R. *Angew. Chem. Intl. Ed. Engl.* **1980**, *19*, 857. (c) Sinn, H.; Kaminsky, W. *Adv. Organomet. Chem.* **1980**, *18*, 99. (d) Tait, P. J. T.; Watkins, N. D. *Comprehensive Polymer Science*; Pergamon Press: Oxford, **1989** ch. 1 and 2. (e) Brintzinger, H. H.; Fischer, D.; Mulhaupt, R.; Rieger, B.; Waymouth, R. M. *Angew. Chem. Intl. Ed. Engl.* **1995**, *34*, 1143, and references therein.
- ³¹ Herzog, T. Design, Synthesis, and Reactivity of a New Class of Highly Syndiotactic Ziegler-Natta Polymerization Catalyst. Ph.D. Thesis, California Institute of Technology, Pasadena, CA, 1997.
- ³² (a) Stone, K. J.; Little, R. D. *J. Org. Chem.* **1984**, *49*, 1849. (b) Clark, T. J.; Killian, C. M.; Luthra, S.; Nile, T. A. *J. Organomet. Chem.* **1993**, *462*, 247.

-
- ³³ (a) Mengele, W.; Diebold, J.; Troll, C.; Roll, W.; Brintzinger, H. H. *Organometallics* **1993**, *12*, 1931. (b) Bulls, A. R. The Synthesis of Metallization Resistant Bis(Cyclopentadienyl) Ligand Systems. Ph.D. Thesis, California Institute of Technology, Pasadena, CA, 1988.
- ³⁴ Herrmann, W. A.; Morawietz, M. J. A. *J. Organomet. Chem.* **1994**, *482*, 169. (b) Chandra, G.; Lappert, M. F. *J. Chem. Soc. (A)* **1968**, 1940. (c) Diamond, G. M.; Rodewald, S.; Jordan, R. F. *Organometallics* **1995**, *14*, 5.
- ³⁵ Fu, S. C. J.; Birnbaum, S. M.; Greenstein, J. P. *J. Am. Chem. Soc.* **1954**, *76*, 6054-6058.
- ³⁶ Wiley, G. A.; Hershkowitz, R. L.; Rein, B. M.; Chung, B. C. *J. of Chem. Soc.* **1964**, *86*, 964-965.
- ³⁷ Singh, A. K.; Bakshi, R. K.; Corey, E. J. *J. Am. Chem. Soc.* **1987**, *109*, 6187.
- ³⁸ Wood, N. F.; Chang, F. C. *J. Org. Chem.* **1965**, *30*, 2054.
- ³⁹ Miyake, S.; Bercaw, J. E. *J. Mol. Catal. A*, **1998**, *128*, 29.
- ⁴⁰ Desurmont, G.; Li, Y.; Yasuda, H.; Tatsuya, M.; Kanehisa, N.; Kai, Y. *Organometallics* **2000**, *19*, 1811.
- ⁴¹ Beachley, O. T.; Lees, J. F.; Glassman, T. E.; Churchhill, M. R.; Buttrey, L. A. *Organometallics* **1990**, *9*, 2488.
- ⁴² Sinn, H.; Kaminsky, W.; Vollmer, H. J. *Angew Chem Int. Engl.* **1980**, *19*, 390.
- ⁴³ Albemarle Corporation website, www.albemarle.com.
- ⁴⁴ Quast, H.; Frank, R.; Heublein, A.; Schmitt, E. *Liebigs Ann. Chem.* **1980**, 1814.
- ⁴⁵ For a general procedure see: Brown, H. C. *Borane Reagents*, Pelter, A., Smith, K. eds.; Academic Press: London, 1988; 213, 246.
- ⁴⁶ Mancuso, A. J.; Huang, S-L.; Swern, D. *J. Org. Chem.* **1978**, *43*, 2480.
- ⁴⁷ Boden, R. M. *Synthesis*, **1975**, 784.
- ⁴⁸ Oliva, L.; Longo, P.; Zambelli, A. *Macromolecules* **1996**, *29*, 6383.
- ⁴⁹ Manuscript in preparation by Jeff Byers.
- ⁵⁰ Burger, B. J.; Bercaw, J. E. *Experimental Organometallic Chemistry*; ACS symposium Series No. 357; Wayda, A. L., Darensbourg, M. Y. eds.; American Chemical Society: Washington, D.C. 1987, ch.4.

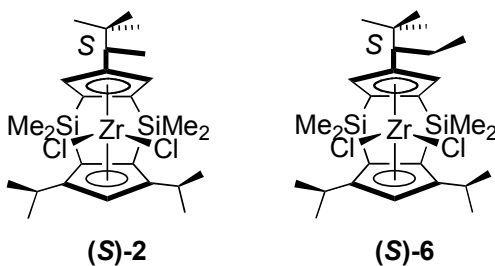
-
- ⁵¹ Marvich, R. H.; Brintzinger, H. H. *J. Am. Chem. Soc.* **1971**, 93, 203.
- ⁵² Vasi, I. G.; Desai, K. R. *J. Indian Chem. Soc.* **1975**, 52, 837.
- ⁵³ Frykman, H.; Öhrner, N.; Norin, T.; Hult, K. *Tetrahedron Lett.* **1993**, 34, 1367.
- ⁵⁴ The ratio of the lithium salt to DME was calculated based on ¹H NMR integration. A second crop was obtained, and the ratios for the salt to DME are different for the first and second crops. The reported product mass is a combination of both crops, and the yield is based moles obtained from both crops based on the respective molecular weights.
- ⁵⁵ The starting material is from two different sources; hence, the ratios of lithium salt to DME are different, and subsequently, the molecular weights differ.
- ⁵⁶ Typically, this reaction is quenched by adding excess water to obtain an amorphous solid, which proves to be difficult to handle on a 500 g scale. Moreover, a significant amount of product is trapped in the amorphous solid. Alternatively, the reaction is quenched by a method prescribed in Fieser, with vigorous stirring, to yield a free-flowing powder. For x g of LAH added, first add x mL of water, then x mL of 15% NaOH, and finally 3x mL of water.
- ⁵⁷ Thanks to Jeff Byers for this idea.
- ⁵⁸ Incomplete oxidation will result in a mixture of aldehyde and carboxylic acid. For the cleanest enantioassay, it is best to have no aldehyde present for the methyl ester formation step. If aldehydes are present, try reducing the amount of olefin/toluene solution or increasing the amount of NaIO₄ and Ru catalyst added. The presence of aldehyde, however, do not appear to affect the ee very much, compared to enantioassay with complete oxidation.

2 CHAPTER TWO

EFFECTS OF SITE EPIMERIZATION ON THE KINETIC RESOLUTION OF CHIRAL α -OLEFINS USING C_1 -SYMMETRIC ZIRCONOCENE POLYMERIZATION CATALYSTS

2.1 ABSTRACT

An enantiopure C_1 -symmetric metallocene, (*S*)-**6**, that has an enantiopure ethylneopentyl substituent on the top cyclopentadienyl ligand was prepared. Activated with MAO, (*S*)-**6** polymerized 3-methyl-1-pentene, 3,4-dimethyl-1-pentene, and 3,5,5-trimethyl-1-hexene with good activity.

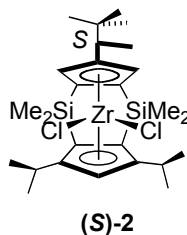


Compared to the selectivity of the parent precatalyst (*S*)-**2**, the selectivity of (*S*)-**6** for 3-methyl-1-pentene improved slightly ($s = 2.4$ to 3.2). The improvement in selectivity for 3,5,5-trimethyl-1-hexene was greater ($s = 2.1$ to 8.5). From (*S*)-**2** to (*S*)-**6**, there was no significant difference in selectivity for 3,4-dimethyl-1-pentene.

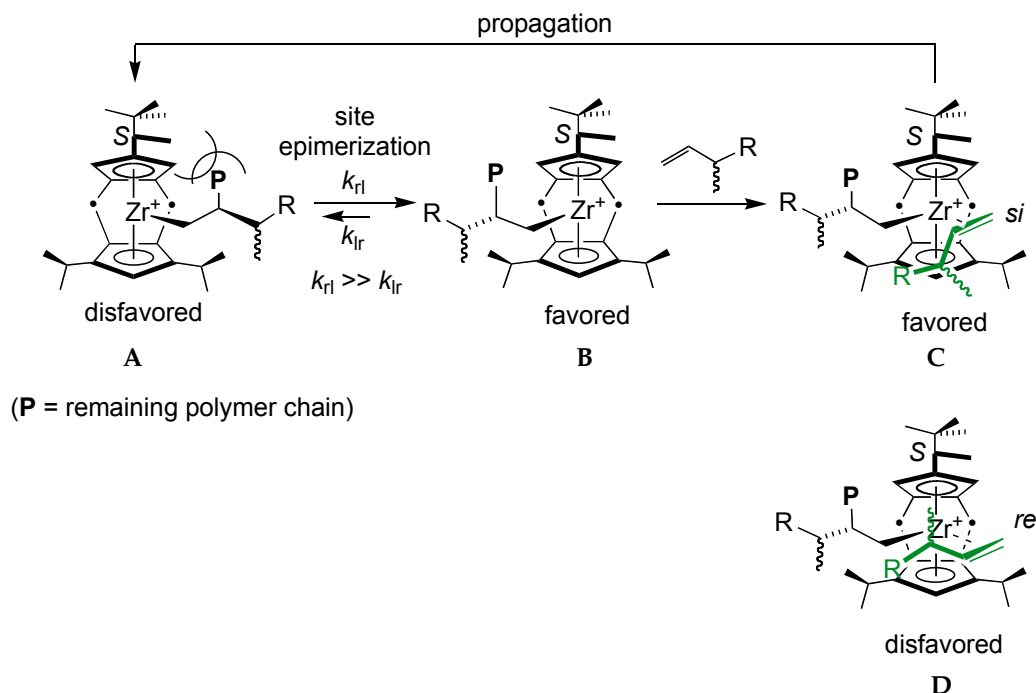
The preparations of (*S*)-methylneopentyl cyclopentadiene and (*S*)-ethylneopentyl cyclopentadiene were optimized. The yields improved from 20% to ~40% for (*S*)-methylneopentyl cyclopentadiene and from 11% to 23% for (*S*)-ethylneopentyl cyclopentadiene.

2.2 INTRODUCTION

In previous works, the mechanism for the polymerization of α -olefins with (*S*)-**2** has been proposed.^{1,2,3}



The *tert*-butyl group of the methylneopentyl (MN) substituent lies above the top cyclopentadienyl (Cp) plane and forces the methyl group to point down and to the right side of the metallocene wedge (Scheme 2.1A). To minimize steric interactions with this methyl group, the growing polymer chain swings to the more open (left) side of the catalyst (Scheme 2.1B). Site epimerization is this process of polymer chain swinging from one side of the metallocene wedge to the other side. With the equilibrium lying farther to the right, the incoming olefin mostly encounters the right side of the wedge (Scheme 2.1C). The olefin prefers to coordinate in an anti fashion to the polymer chain, which leads to *si* insertion.⁴ Coordination of the *re* face is disfavored (Scheme 2.1D). After the olefin insertion, the polymer chain swings to the other side of the catalyst, and the catalyst is ready for another olefin coordination or site epimerization (Scheme 2.1A).



Scheme 2.1. Site epimerization mechanism.

Studies have shown that the relative rates of site epimerization and monomer insertion are important to the control of the tacticity. In one study, Tim Herzog reported that isotactic polypropylene was obtained (*rac*)-**2**/MAO⁵ under dilute monomer conditions.^{1,6} He proposed that the rate of insertion is slower than the rate of site epimerization, which allows the chain to swing away from the methyl side before an insertion can occur. Hence, insertions occur mostly on the right side (*si* insertions), leading to an isotactic polymer. Under concentrated propylene conditions, olefin insertion is faster than the rate of site epimerization. Hence, propylene insertion alternates between both sides of the catalyst (alternating *si/re* insertions), and syndiotactic polymer is formed. Chiral olefins, such as 3-methyl-1-pentene (3M1P), may be bulky enough that the rate of insertion is slower than the rate of site epimerization, similar to

dilute propylene conditions. Consistent with this conjecture, the polymerization of 3M1P using (*S*)-**2**/MAO produced isotactic poly-(3M1P) (Section 1.3.6).

In a related experiment, Chris Levy used (*S*)-**2** to polymerize 3,4,4-trimethyl-1-pentene at two different temperatures, 25 °C and 60 °C.⁷ He found that the selectivity dropped from 12 to 6.1 when the temperature was increased from 25 °C to 60 °C (Table 2.1). The increase in temperature most likely led to an increase in the rates of site epimerization and monomer insertion. The increase in temperature may affect the insertion rates of the two enantiomers differently. Since temperature affects both the insertion and the site epimerization rates, it is difficult to assert which component diminished the selectivity. However, this result demonstrates that the relative rates of insertion and site epimerization has an affect on enantiomer selectivity.

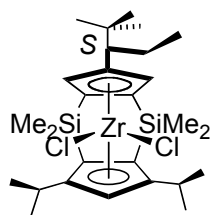
Table 2.1. Temperature affect on the polymerization of 344TM1P using (*S*)-2**.**

Temp (°C)	% Conv	% ee	<i>s</i>
25	21.5	22.2	12
60	36.5	35.9	6.1

Studies have also suggested a relationship between enantiofacial selectivity, (controlling for polymer tacticity) and diastereomeric selectivity (controlling for *S* versus *R* enantiomer selection). For all 3- and/or 4-methyl olefins surveyed, the *S* enantiomer of the monomer was preferentially inserted. As discussed in Section 1.3.6, a *si* insertion on the right side of the metallocene wedge directs for a preferential insertion of the *S* monomer. Insertion on the left side of the wedge, however, is a possibility. In such cases, *re* insertions of the *R* monomer is preferred. Hence, poor control of tacticity can lead to poor diastereoselectivity.

The control of tacticity appears to be an important factor in improving the kinetic resolution of chiral olefins using (*S*)-**2**. Perhaps diastereomeric selectivity may be enhanced by improving the isospecificity of the catalyst, which in turn may be achieved by increasing the rate of site epimerization. There is some evidence to suggest that the rate of site epimerization of (*S*)-**2** has not reached the maximum point. Using ^1H NMR, Tim Herzog analyzed the microstructure of a sample of polypropylene polymerized with (*rac*)-**2**/MAO.⁶ He reported the *m* pentad content to be 61.2% and the *m* diad content to be 85.4%. Although, these figures suggest isotacticity, they also indicate that the isotacticity of the polymer can be further improved.

It was proposed that if the site epimerization rate increased, the incoming monomer would encounter the right side of the metallocene wedge more frequently, and hence the selectivity would increase. Toward this end, (*S*)-ethylneopentyl-ThpZrCl₂, (*S*)-**6**, was prepared. The steric interaction between the ethyl group and the polymer chain is expected to be larger than the interaction between a methyl group of MN and polymer chain. The increased steric interaction should speed up the site epimerization rate.



(S)-6

"S-ethylneopentyl-ThpZrCl₂"

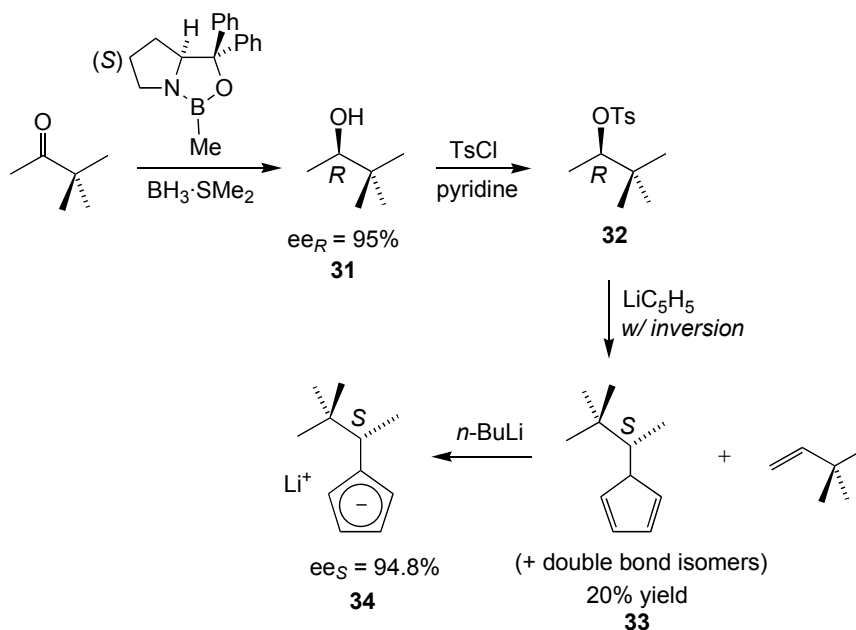
(*S*)-ENThpZrCl₂

In addition, studies were conducted to optimize the yield of the enantiopure top Cp rings, (*S*)-methylnopentyl cyclopentadiene “(*S*)-MNCpH” and (*S*)-ethylnopentyl cyclopentadiene “(*S*)-ENCpH.”

2.3 RESULTS AND DISCUSSION

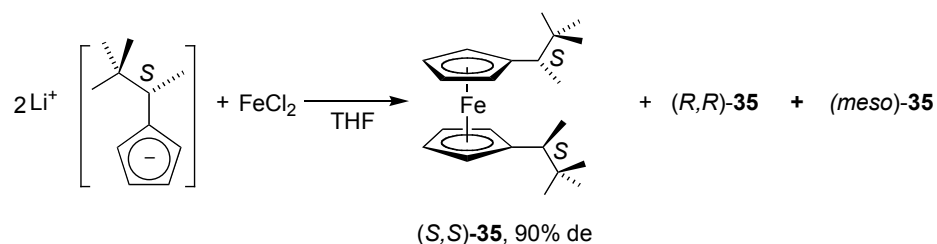
2.3.1 Preparation and Optimization of (*S*)-MNCpH

The preparation of the key feature of (*S*)-**2**, the enantiopure (*S*)-methylnopentyl group on the top Cp ring, was first developed by Chris Levy. The preparation begins with the synthesis of (*R*)-3,3-dimethyl-2-ol ($ee_R > 95\%$), obtained from the asymmetric borane reduction of pinacolone with (*S*)-2-methyl-CBS-oxazaborolidine catalyst, “(*S*)-CBS” (Scheme 2.2).⁸ To determine the enantiomeric excess of the alcohol, the alcohol was converted to the trifluoroacetyl (TFA) derivative and injected onto a chiral GC.



Scheme 2.2. Synthesis of (S)-LiMNCp.

The alcohol (**31**) was subsequently converted to the tosylate (**32**), which was then treated with a cyclopentadienide nucleophile to yield the addition product, (S)-methylneopentyl cyclopentadiene, (S)-MNCpH (**33**). The addition reaction occurs with perfect inversion at the carbon stereocenter. Along with **33**, which is the product of the addition pathway, the elimination product 3,3-dimethyl-1-butene, was also obtained. Although the success of this S_N2 reaction may be surprising, nucleophilic attack of cyclopentadienide anion on some hindered secondary tosylates has been shown to occur with inversion of configuration.⁹ The product **33** is a mixture of double bond isomers, which resolves to one isomer after deprotonation with *n*-BuLi. The enantiomeric excess of **34** was determined by preparation and NMR analysis of the ferrocene derivative (Scheme 2.3).



Scheme 2.3. Synthesis of ferrocene of (S)-LiMNCp.

The ferrocene prepared from (*rac*)-LiMNCp gave equimolar amounts of the racemic (*R, R*/ *S, S*) and meso (*R, S*) products, while the reaction with enantio-enriched (*S*)-LiMNCp produced only a small amount of the meso isomer (5.1% by ^1H NMR spectroscopy). This observed diastereomeric excess (de) corresponds to a 94.8% ee for (*S*)-LiMNCp, similar to the ee of the starting alcohol.

The original preparation of (*S*)-**33** that Chris Levy developed, involved treating **32** with LiCp and tetramethylethylenediamine (TMEDA) in refluxing THF for one week. By this method, a 20% yield of (*S*)-**33** was obtained. It was desired for none of the starting tosylate to remain because the separation of the product from the starting material by Kugelrohr was difficult. A more facile and higher preparation method that favors the addition pathway and proceeds to completion in less time was desired.

Towards this goal, **31** was converted to the mesylate rather than the tosylate because the mesylate is generally considered to be more reactive to nucleophilic attack. Another advantage of the mesylate is that its preparation is easier and faster than that of the tosylate.¹⁰ The required reaction time of the tosylate was found to be inconsistent, varying from a few hours to many days for the reaction to proceed to completion. On the other hand, the mesylate can be prepared in quantitative yield in less than 1 h. The best

results were obtained if the reaction was worked up immediately after completion, and the product was stored cold.

The reaction of LiCp, the starting mesylate, and TMEDA in THF was monitored using ^1H NMR to determine the mole percentage of the addition and elimination products and the starting material over time (Figure 2.1). Figure 2.1 shows that the addition pathway is favored over the elimination pathway. It also shows that the reaction was not complete after 3 d.

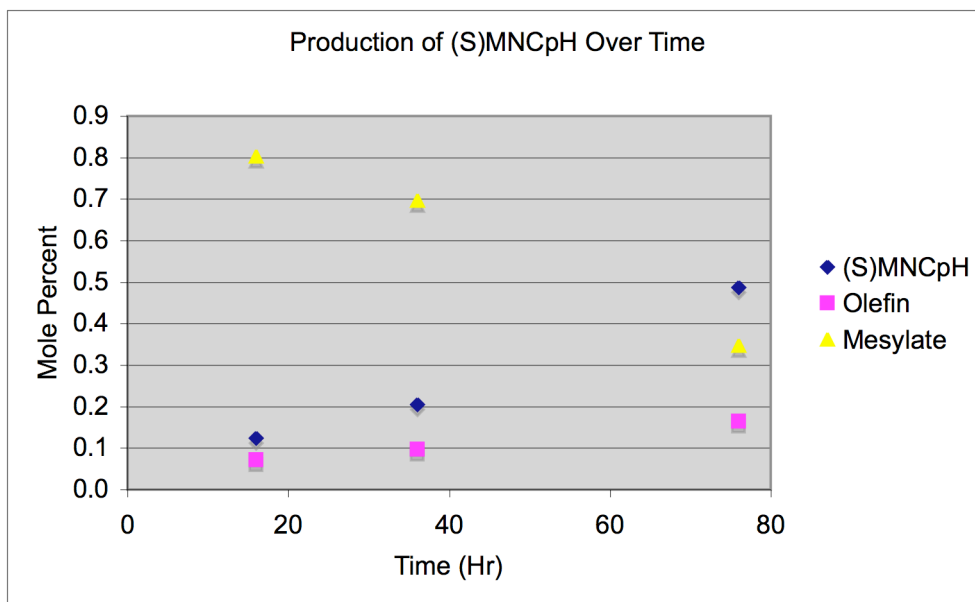


Figure 2.1. NMR Scale Reaction of LiCp + (S)-MNOMs + TMEDA in THF.

In addition to changing the leaving group from tosylate to mesylate, the nucleophile was also changed from LiCp to KCp. Again, an NMR scale reaction of KCp, TMEDA, and mesylate in THF was monitored over 10 d (Figure 2.2). Although the addition pathway was favored over the elimination pathway, the reaction did not go to completion after 10 d. In fact, the reaction appeared to be slower with KCp. After 10 d,

the reaction using KCp was at the same conversion point as the reaction using LiCp at day 3. The slower reactivity was most likely due to the lower solubility of KCp in THF.

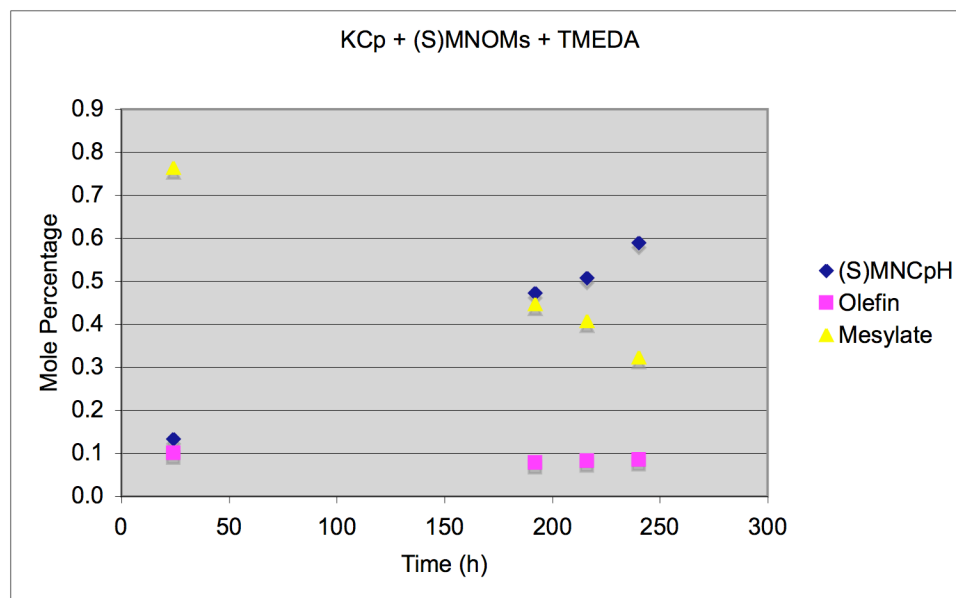


Figure 2.2. NMR Scale Reaction of KCp + (S)-MNOMs + TMEDA in THF.

In order to improve the solvation of KCp and to drive the reaction to completion, the mesylate was reacted with 2 equiv of KCp and 0.1 equiv of 18-crown-6 ether in benzene, toluene, and THF. KCp in the presence of crown ether proved to be quite active. Also, a concentrated reaction solution was prepared since the addition pathway is second order. Unfortunately, the conditions that favors S_N2 pathway also favor the E2 pathway. The reactions were monitored using GC (Table 2.2). Although, the elimination product was observed, the reaction went to completion within 1–2 d. The rate of the reaction appears to correlate to the reaction temperature. The reaction was fastest in toluene, then benzene, then THF. In general, the yields were in the 30% range, with 38% being the highest.

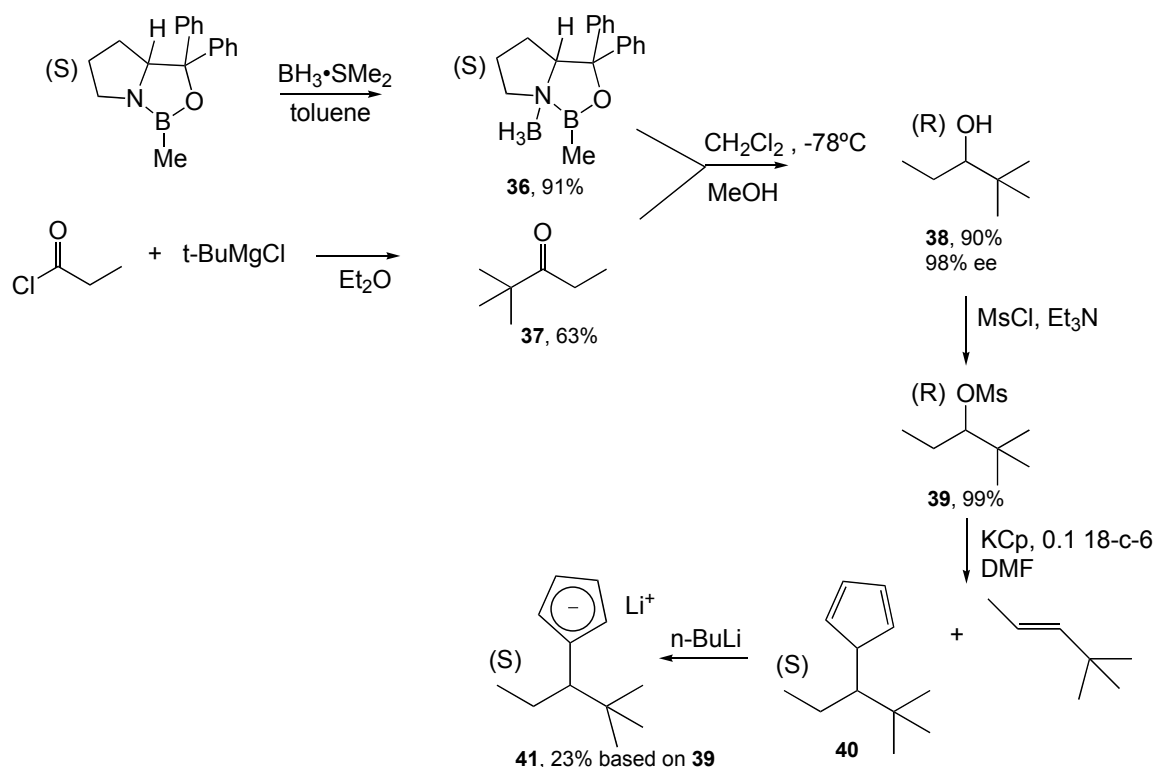
Table 2.2. Dependence of reaction conversion on solvent

Solvent	Time (h)	(S)-MNCpH %	Mesylate %
THF	56	73	27
Benzene	24	58	42
Toluene	24	80	20
Toluene	48	100	0

During the aqueous work-up, Cp dimer is formed, which is very difficult to separate from the product. ^1H NMR of the material after aqueous work-up and Kugelrohr distillation indicate that the crude product material contains 10%–20% Cp dimer. Fortunately, the Cp dimer can be carried over with the product into the subsequent deprotonation step because *n*-BuLi does not react with Cp dimer, and the Cp dimer can be washed away from (S)-LiMNCp.

2.3.2 Preparation of (*R*)-Ethylneopentyl Alcohol (ENOH)

(*R*)-ENOH (**38**) was prepared in a similar manner to (*R*)-MNOH (**31**) from the corresponding ketone (Scheme 2.4). The corresponding ketone, 2,2-dimethyl-3-pentanone (**37**), was prepared by treating propionyl chloride with *tert*-butyl magnesium chloride, followed by an aqueous work-up. The ketone was then treated with (S)-2-methyl-CBS-oxazaborolidine borane adduct (**36**).



Scheme 2.4. Synthesis of (S)-ethylneopentyl alcohol.

To prepare (R)-MNOH of greater than 95% ee, a catalyst loading of 5–10 mol% of (S)-CBS was sufficient. When **39** was treated with this amount of catalyst, the ee was only 80–85%. To increase the ee, a stoichiometric amount of (S)-CBS catalyst was used. For the preparation of (S)-MNOH, the (S)-CBS borane adduct was made in situ. In the case of (S)-ENOH, the borane adduct was first prepared and isolated as a solid. A stoichiometric amount of the solid borane adduct was then used in the reduction step. Also, the addition temperature was lowered from -20°C to -78°C , and the addition time was increased from 2 to 4 h. These conditions increased the ee of (S)-ENOH to 98%. When the (S)-CBS•borane loading was decreased to 0.75 equiv, the ee also dropped to 96%. The ee of the alcohol was determined by treating the alcohol with trifluoroacetyl imidazole (TFAI) to obtain the corresponding ester, which was resolved on a chiral GC.

39 was found to be significantly more moisture and heat sensitive than the methylnepentyl mesylate. **39** will decompose rapidly above 35 °C. Attempts to purify the material by passage through a bed of silica gel resulted in decomposition of the material.

2.3.3 Optimization of (*S*)-ENCpH

Not surprisingly, the yield of (*S*)-ENCpH (**40**, 11%) was lower than that of (*S*)-MNCpH (**33**, 38%) under the same reaction conditions (0.1 equiv 18-crown-6, refluxing benzene). In order to optimize the addition product yield and reduce the elimination yield, NMR scale experiments varying the solvent, temperature, and amount of crown ether were performed. The different solvents used were THF-*d*₈, benzene-*d*₆, toluene-*d*₈, xylenes-*d*₁₀, DMF-*d*₇, and DMSO-*d*₆. The equivalence of crown ether based on **39** was varied from 0 to 0.5. Furthermore, temperatures were varied from room temperature to 160 °C (Table 2.3).

Table 2.3. Composition of products and starting materials in various solvents

	Solvent (equiv 18-c-6)	Temp (°C)	Time (day)	(S)MNCpH mol %	Olefin mol %	Mesylate mol %	<u>(S)MNCpH</u> Olefin
1	THF (.2)	65	20	trace	trace	major	0
2a	Benzene (.1)	90	2	38.8	50.1	11.0	0.8
2b	Benzene (.5)	90	2	43.1	51.3	5.6	0.8
3a	Toluene (.25)	120	2	28.1	68.6	3.2	0.4
3b	Toluene (.5)	120	2	38.1	61.9	0.0	0.6
3c	Toluene (1)	120	2	48.6	50.1	1.3	1.0
4a	DMSO (.25)	180	1	trace	1.0	0.0	0
4b	DMSO (.1)	90	1	31.7	68.3	0.0	0.5
5a	DMF (0)	90	1	40.0	60.0	0.0	0.7
5b	DMF (.1)	90	1	35.8	64.2	0.0	0.6
6	Xylenes (.25)	190	1	trace	1	0	0

The results show that in cases where both the addition and elimination products formed, the elimination product was the major product. Also, of the two possible elimination products, *trans*- or *cis*-3,3-dimethyl-2-pentene, only the more stable *trans* isomer was observed.

As the reaction in refluxing THF shows (entry 1), 65 °C was not a high enough temperature for the reaction to proceed to completion within a reasonable amount of time. In refluxing benzene (entry 2), about 11% of the starting material remained after 2 d. Hence, it seems that the threshold temperature lies somewhere between 65 °C and 90 °C, and most likely closer to 90 °C. As the temperature increases above the threshold temperature, the preference for the elimination pathway also increases. In refluxing DMSO and xylenes (entries 4a and b), only the olefin is produced. Also, the ratio of olefin to (S)-MNCpH was slightly higher in refluxing toluene (entry 3) than in benzene (entry 2). Hence, the temperature for optimizing the yield of (S)-MNCpH, as well as driving the reaction completion within a few days, was a temperature near 90 °C.

Between the nonpolar solvents (benzene and toluene) and polar solvents (DMF and DMSO), the polar solvents helped the reaction to proceed more quickly, but there was not a large difference in the olefin to (*S*)-MNCpH ratio. Similarly, the equivalence of crown ether added does not make a large impact on the product ratio. The experiments in toluene indicate that a greater amount of crown ether slightly improves the ratio toward the addition pathway.

For a preparative scale reaction, DMF was used rather than benzene or toluene. Although the product ratios are similar for all three solvents, benzene and toluene are more difficult to distill away from (*S*)-MNCpH, whereas DMF can be removed with aqueous washings. Hence, DMF was used with a 90 °C oil bath.

2.3.4 Ferrocene of (*S*)-LiENCp

To determine the ee of (*S*)-LiENCp (**41**), the corresponding ferrocene was analyzed by NMR. The ferrocenes of (*rac*)-LiENCp and (*S*)-LiENCp were prepared by treating 2 equiv of LiENCp with FeCl₂ in THF.

Unlike (MNCp)₂Fe (**35**), the ¹H NMR did not result in peaks with baseline separation that are appropriate for integration. However, ¹³C NMR showed peaks with baseline separation that could be used to determine the ee. The ferrocene of (*rac*)-LiENCp produced essentially equimolar amounts of the racemic (*R,R/S,S*) and meso (*R,S*) products as seen by peaks with almost identical integrations (Figure 2.3). The ferrocene derived from (*S*)-LiENCp produced only a small amount of the meso isomer (3.0% by ¹³C NMR spectroscopy). This observed diastereomeric excess (de) corresponds to a 98.5% ee for (*S*)-LiENCp, similar to the ee of the starting alcohol.

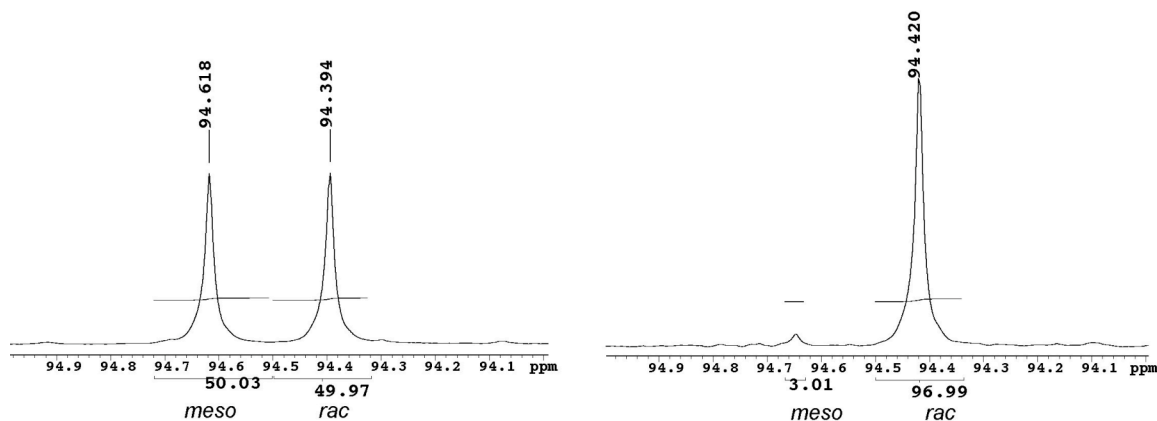
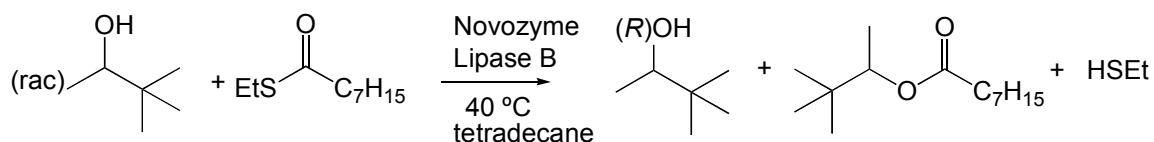


Figure 2.3. ^{13}C NMR of $[(rac)\text{-ENCp}]_2\text{Fe}$ and $[(S)\text{-ENCp}]_2\text{Fe}$.

2.3.5 Enzymatic Kinetic Resolution of (S)-MNOH and (S)-ENOH

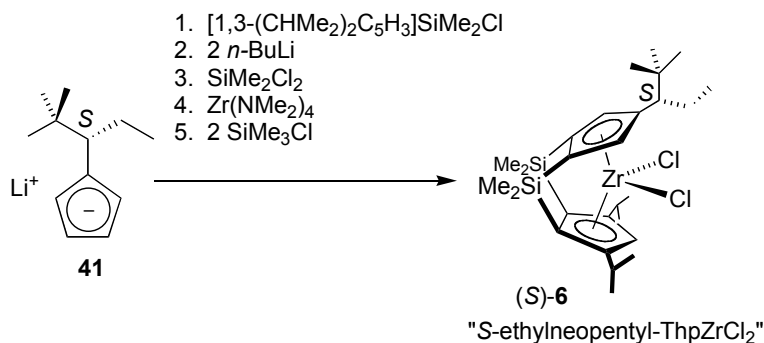
As an alternative method of preparing enantiopure alcohol, racemic methylneopentyl alcohol was treated with an enzymatic yeast that preferentially esterifies the *S* enantiomer of the alcohol (Scheme 2.5).¹¹ The reaction reached 50% conversion under 48 h, and the ee of the unreacted alcohol was >95%. On the other hand, the same treatment on racemic ethylneopentyl alcohol produced low conversion (7.5%) after 5 d, and the resin beads disintegrated into powder. The enzymatic treatment on a 85% ee mixture of ENOH¹² improved the ee by only 1% after 5 d.



Scheme 2.5. Enzymatic kinetic resolution of methylneopentyl alcohol.

2.3.6 Preparation of (S)-6 and Polymerizations of Chiral Olefins Using (S)-6

(S)-6 was prepared in an analogous manner to (S)-2, (S)-3, and (S)-4 (Scheme 2.6). The (S)-LiENCp was treated with $i\text{Pr}_2\text{CpSiMe}_2\text{Cl}$ to produce the singly bridged ligand. This product was then deprotonated with 2 equiv of base and doubly linked with SiMe_2Cl_2 . The ligand was refluxed in xylenes with $\text{Zr}(\text{NMe}_2)_4$ to obtain (S)-ENThpZr(NMe₂)₂. The zirconium amide was treated with TMSCl to obtain the final dichloride precatalyst, (S)-ENThpZrCl₂.

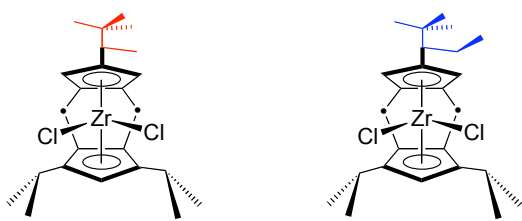


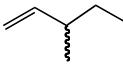
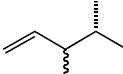
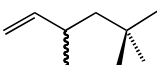
Scheme 2.6. Preparation of (S)-6.

When activated with MAO, (S)-6 catalyzes the polymerization of 3-methyl-1-pentene (3M1P), 3,4-dimethyl-1-pentene (34DM1P), and 3,5,5-trimethyl-1-hexene (355TM1H) with moderate to good kinetic resolution. The polymerization set-up and method were similar to those using (S)-2.¹³ The polymerizations were carried out in tetradecane. The reaction conversion was determined using GC. Once the polymerizations reached 30–60% conversion, all volatiles were vacuum transferred out of the reaction flask. The recovered unreacted olefin was oxidized to the acid, and then to the methyl ester.¹³ The ee was determined from injection of the methyl ester onto a chiral

GC. The selectivity factor (s) was calculated from the experimentally measured conversion and ee. A discussion of selectivity error as a result of experimental errors can be found in Section 1.3.3. One modification to the procedure is the relative amount of toluene and tetradecane used. For polymerizations using (*S*)-**2**, 1.5 mL of tetradecane and 0.5 mL of toluene were used for each polymerization reaction. Subsequent to these experiments, it was observed that a greater amount of toluene increased the reaction rate. Henceforth, the relative amount of toluene used was increased. For polymerizations using (*S*)-**6**, 1.5 mL of toluene and 0.5 mL of tetradecane were used.

In Table 2.4, the polymerization results of (*S*)-**6** are compared to the results of (*S*)-**2**. An increase in activity was observed with all olefins tested, most likely due to the increase in relative amount of toluene. Although $s = 20.5$ for 34DM1P is the highest s value obtained for this monomer with any catalyst, the value is still within the margin of experimental error. In the region of high s value, small changes in conversion and ee make significant changes in s values. Using the values obtained with (*S*)-**2** (%c = 42.4, %ee = 58.6), a one percent drop in conversion would raise the s value from 15.9 to 20.5. One percent error in conversion is experimentally feasible. Hence, it is difficult to conclude if the increase in s value for 34DM1P is a real increase or not. Although the increase in s value for 3M1P (2.4 to 3.2) does not appear to be a significant increase, it can be considered experimentally significant. In order for the s value to increase from 2.4 to 3.2, the conversion has to drop 7% or the ee has to increase 7%. It is unlikely that an experimental error that great was made. The most significant increase in selectivity was observed with 355TM1H (2.1 to 8.5).

Table 2.4. Kinetic resolution of chiral 3-methyl substituted olefins using (S)-6.


	TOF (h ⁻¹)	<i>S</i>	TOF (h ⁻¹)	<i>S</i>
	47	2.4	280	3.2
	34	15.9	75	20.5
	37	2.1	988	8.5

The insignificant increase in *s* of 34DM1P suggests that the monomer insertion rate is on the same order as the rate of site epimerization, meaning that most of the insertions were already taking place on the right side of the wedge. Hence, a further increase in site epimerization rate does not significantly change the insertion pattern of 34DM1P.

On the other hand, the increase in *s* for 3M1P and 355TM1H suggests that the rate of insertion for these monomers is faster than the rate of site epimerization and that the rate of site epimerization of (S)-6 is faster than that of (S)-2. Hence, the monomer encounters the right side of the catalyst more often with (S)-6 than it does with (S)-2. Enchainment on the right side of the catalyst favors the *S* monomer, while enchainment on the left side of the catalyst favors the *R* monomer. One can envision the polymerization of 3M1P and 355TM1H to entail consecutive insertions of the *S* monomer on the right side of the catalyst with occasional misinsertions of the *R* monomer on the

left side of the catalyst. The increase in s value suggests that increase in site epimerization rate has reduced the opportunity for misinsertion on the left side of the catalyst.

The relative sizes of 3M1P and 355TM1H may be a factor as to why 355TM1H experienced a greater increase in s value than 3M1P. It is proposed that the discriminating interaction between the chiral wedge of the catalyst and the larger 355TM1H monomer is greater than that between 3M1P and the chiral metallocene wedge. Also, frequent misinsertions on the left side of the wedge acts as a counteracting force that reduce the s value. Once the counteracting effect is mitigated as a result of increasing the site epimerization rate and reducing the frequency of misinsertions, the discriminating interaction between the catalyst and 355TM1H is realized to a greater extent, as seen by an increase in s . 3M1P, due to its smaller size, does not interact with the catalyst to the degree of 355TM1H. Hence, even when the counteracting effect of misinsertions is reduced, the s value does not increase to the level of 355TM1H.

2.4 EXPERIMENTAL SECTION

General Procedure

All air and/or moisture sensitive materials were handled using high-vacuum line, swivel frit assembly, glovebox, Schlenk and cannula techniques under a nitrogen or argon atmosphere.¹⁴ Argon was purified by passage through MnO on vermiculite and activated 4 Å molecular sieves. All glassware was oven dried before use. Solvents were dried and

degassed over sodium benzophenone ketyl or over titanocene.¹⁵ 1,2-Dimethoxyethane (DME) was dried and degassed over sodium benzophenone ketyl. Methylene chloride, triethylamine, Me_2SiCl_2 , and Me_3SiCl were stored over and distilled from CaH_2 immediately before use. *n*-BuLi (hexane) was stored under Ar at 10 °C.

Unless otherwise mentioned, all starting materials were purchased from Aldrich and used as received. Pinacolone and propionyl chloride were dried over sieves for at least 2 d before use. *t*-BuMgBr (2.0 M/ Et_2O), mesyl chloride, and BH_3SMe_2 (10–10.2 M) were used from freshly opened bottles. ZrCl_4 and FeCl_2 were dried on the vacuum line overnight and handled in the drybox. $\text{Zr}(\text{NMe}_2)_4$ was sublimed before handling in the drybox. (*S*)-**2** was synthesized using the route previously reported for the racemic counterpart, except that (*S*)-LiMNCp was used in place of the racemate.² (*S*)-Ethylthiooctanoate was made according to the literature procedure.¹⁶ Dicyclopentadiene was thermally cracked, and the distilled cyclopentadiene was stored at –80 °C. Novozyme SP435 enzyme was purchased from Aldrich. (*S*)-2-Methyl-CBS-oxazaborolidine was purchased from Aldrich as both powder and toluene solution. 1-(Trifluoroacetyl)imidazole (TFAI) was obtained from Alltech in 0.5 mL ampule form.

All olefins surveyed were purchased from Chemsampco. They were dried and degassed over LAH for 2 d, then vacuum transferred and stored in Schlenk flasks over CaH_2 . In some cases, olefins stored over LAH formed into an unusable gel. Methylaluminoxane (MAO) was purchased from Albemarle as 10% or 30% toluene solution. All volatiles were removed *in vacuo* to give a white powder. The white MAO solid was dried at 150 °C for 12 h at high vacuum. Tetradecane was stirred over pieces of Na metal for 24 h at room temperature. Tetradecane was vacuum distilled using a

Vigoreaux column into a dry Schlenk flask and stored in the drybox. Toluene used for polymerization was vacuum transferred into a small Schlenk flask from sodium benzophenone ketyl and stored over sieves in the drybox. Polymerization and enantioassay procedures are described in chapter 1.

Instrumentation. NMR spectra were recorded on the Varian Mercury VX300 (^1H , 300 MHz, ^{13}C , 75.5 MHz) spectrometer. Gas chromatographs were obtained on an Agilent 6890 Series gas chromatography using a 30 m x 0.25 mm, γ -cyclodextrin trifluoroacetyl “Chiraldex-TA” column from Advanced Separations Technology.

(*R*)-3,3-Dimethyl-2-butanol, 31. CH_2Cl_2 (10 mL) was vacuum transferred onto (*S*)-CBS catalyst¹⁷ (2.90 g, 10 mmol) in a Schlenk flask, and $\text{BH}_3\cdot\text{SMe}_2$ (20 mL, 200 mmol) was syringed onto the (*S*)-CBS solution. While the flask was cooled to $-20\text{ }^\circ\text{C}$, pinacolone (20 g, 200 mmol) was syringed into the solution over 5 h. After stirring the solution for 3 h more at $-20\text{ }^\circ\text{C}$, the solution was transferred to a 250-mL round bottom flask. MeOH (100 mL) was added slowly to control the rate of H_2 emission and to maintain the temperature below $25\text{ }^\circ\text{C}$. The solvent was distilled at $70\text{ }^\circ\text{C}$ until about 30 mL of solution remained. An additional 100 mL of MeOH was added, and the solvent was distilled. When 30 mL of solution remained, a Vigreux column was attached, and the product was collected at $119\text{ }^\circ\text{C}$ to give 15.53 g (76%) of product. ^1H NMR (300 MHz, C_6D_6 , δ): 3.23 (qd, $J = 6.3, 4.8$, 1H, CH), 1.14 (d, $J = 4.8$ Hz, 1H, OH), 0.94 (d, $J = 6.3$ Hz, 3H, CH_3), 0.82 (s, 9H, *t*-Bu).

TFA derivative of alcohols 31 and 38. One drop of alcohol was pipetted into a freshly opened ampule of 0.5 mL of TFAI. The solution was pipetted into a GC vial, capped, and allowed to stand at room temperature for 1 h. The solution was diluted with 1.5 mL of methylene chloride and injected onto a chiral GC column.

(*R*)-3,3-Dimethyl-2-buten-1-yl methanesulfonate, 32Ms. Into a 100-mL round bottom flask, **31** (1.0 g, 9.79 mmol) was weighed and CH₂Cl₂ (50 mL) was vacuum transferred. NEt₃ (2.05 mL, 14.69 mmol) and mesyl chloride (1.23 g, 10.77 mmol) were syringed into the round bottom flask while cooling to 0 °C. After stirring at room temperature for 1 h under Ar, the reaction solution was washed with cold water (25 mL), cold 10% HCl (25 mL), saturated NaHCO₃ (25 mL), and brine (25 mL). The organic layer was dried over MgSO₄, filtered, and concentrated. A clear, orange oil was obtained, 1.82 g (100%). ¹H NMR (300 MHz, C₆D₆, δ): 4.33 (q, *J* = 6.3 Hz, 1H, CH), 2.22 (s, 3H, SO₃CH₃), 1.06 (d, *J* = 6.3 Hz, 3H, CH₃), 0.71 (s, 9H, *t*-Bu).

(*S*)-LiMNCp, 34. 33 (10.76 g, 71.6 mmol) was weighed into an oven-dried 250-mL round bottom flask under ambient atmosphere. The round bottom flask was equipped with an oven-hot swivel frit assembly. While the apparatus was hot and the flask containing **33** was cooled in a –78 °C bath, the apparatus was evacuated on the vacuum line. Diethyl ether (120 mL) was vacuum transferred onto **33**. While cooling in –78 °C bath, *n*-BuLi (49.2 mL, 78.8 mmol, 1.6M hexanes) was syringed quickly onto the clear yellow solution via the side arm under strong Ar purge. After the addition, the –78 °C bath was removed, and the solution was allowed to warm to room temperature and stir for

2 h. A copious amount of white precipitate formed. All volatiles were removed in vacuo, and petroleum ether (100 mL) was vacuum transferred onto the white paste. The white precipitate was filtered from the yellow solution. The solid was washed 3 times. After removing volatiles in vacuo, the solid was dried under vacuum for 3 h (8.35 g, 75%). ^1H NMR (300 MHz, THF- d_8 , δ): 0.83 (s, 9H, C(CH₃)₃), 1.17 (d, J = 7.2 Hz, 3H, CH₃), 2.01 (q, J = 6.9 Hz, 1H, CH), 5.53 (m, 4H, Cp).

[(*S*)-MNCp]₂Fe, (*S*)-35. In a drybox, **34** (200 mg, 1.28 mmol) and FeCl₂ (134 mg, 1.06 mmol) were weighed into a 20-mL vial. THF (10 mL) was added at room temperature. The vial was capped, and the solution was allowed to stir at room temperature for 4 h. Outside of the drybox, the greenish brown solution was transferred to a separatory funnel. Water (20 mL) and petroleum ether (10 mL) were added. After the layers were separated, the yellow organic layer was dried over MgSO₄ and filtered. All volatiles were removed using rotary evaporator while the vial heated in a 40 °C water bath. A dark orange oil remained. ^1H NMR (300 MHz, C₆D₆, δ): 0.84 (s, 18H, C(CH₃)₃), 1.30 (d, J = 7.2 Hz, 6H, CH₃), 2.20 (q, J = 7.2 Hz, 2H, CH), 3.96 (m, 8H, Cp H).

[(*rac*)-MNCp]₂Fe, (*rac*)-35. The same procedure for preparing [(*S*)-MNCp]₂Fe was used. A dark orange oil was obtained. ^1H NMR (300 MHz, C₆D₆, δ): 0.83 (s, 9H, C(CH₃)₃), 0.84 (s, 9H, C(CH₃)₃), 1.30 (d, J = 7.2 Hz, 6H, CH₃), 1.32 (d, J = 7.2 Hz, 6H, CH₃), 2.20 (q, J = 7.2 Hz, 2H, CH), 2.22 (q, J = 7.2 Hz, 2H, CH), 3.96 (m, 16H, Cp).

(S)-2-Methyl-CBS-oxazaborolidine borane, 36. (S)-2-methyl-CBS-

oxazaborolidine powder (25.0 g, 90.2 mmol) was weighed into a 250-mL round bottom flask under ambient conditions. The flask was equipped with a swivel frit assembly. Toluene (30 mL) was vacuum transferred onto the white solid. While cooling the white slurry in a $-78\text{ }^{\circ}\text{C}$ bath, $\text{BH}_3\cdot\text{SMe}_2$ (10.3 mL, 108.2 mmol) was syringe added. The solution was stirred at room temperature, under a closed system for 2 h, then stirred at $-10\text{ }^{\circ}\text{C}$ for 5 h. Pentane (180 mL) was vacuum transferred to precipitate out the product. The white slurry was filtered and washed three times. All volatiles were removed in vacuo, and the solid was dried overnight to yield 23.8 g of white powder (91%). ^1H NMR (300 MHz, C_6D_6 , δ): 0.60 (s, 3H, BCH_3), 0.82 (m, 2H, C4-H_2), 1.24 (m, 2H, C5-H_2), 1.45–2.6 (very br, 3H, BH_3), 2.80(m, 1H, C6-H), 2.90 (m, 1H, C6-H), 4.38 (t, 1H, C3-H), 6.98 (m, 4H, Ar-H), 7.12 (m, 4H, Ar-H), 7.52 (m, 2H, Ar-H).

2,2-Dimethyl-3-pentanone, 37. A 2-necked, 2-L round bottom flask was charged with CuCl (~1.5 g). The flask was equipped with a dry ice condenser and 250-mL addition funnel. The apparatus was purged with argon. Propionyl chloride (previously dried over sieves for 2 d) (148.05 g, 1.6 mol) was cannula transferred. The flask was cooled in a $-78\text{ }^{\circ}\text{C}$ bath. $t\text{-BuMgCl}$ (2.0 M/ Et_2O , 800 mL, 1.6 mol) was added via addition funnel over 2-3 h. The slurry (color can vary from yellow to purple) was allowed to warm to room temperature and to stir for 5 h more. Water (500 mL) was added slowly while cooling in $0\text{ }^{\circ}\text{C}$ bath. 2 N HCl (200 mL) was added to dissolve the slurry. The layers were separated. The organic layer was washed with 2 N NaOH (200 mL), NaHCO_3 (200 mL), and brine (200 mL). The organic layer was dried over MgSO_4

and filtered. The solvent was removed using a rotary evaporator while cooling in an ice bath. The yellow oil was distilled at ambient pressure (118 °C–120 °C). A clear and colorless liquid was obtained (115.31 g, 63%). ¹H NMR (300 MHz, C₆D₆, δ): 0.90 (s, 9H, C(CH₃)₃), 0.95 (t, *J* = 7.2 Hz, 3H, CH₃), 2.01 (q, *J* = 7.2 Hz, 2H, CH₂).

(*R*)-2,2-Dimethyl-3-pentanol, 38. In the drybox, **36** was weighed into a 1-L round bottom flask and equipped with a 180° valve joint. Dry dichloromethane (300 mL) was vacuum transferred. The pale yellow slurry was cooled in a –78 °C bath. The assembly was connected to a Schlenk line. Under a strong Ar purge, the Teflon stopcock was replaced with a septum. While the solution was cooled to –78 °C, **37** (dried for 2 d over sieves) (16.53 g, 143.7 mmol) was syringe added over 4 h. The solution was allowed to stir in the –78 °C bath overnight and to gradually warm to room temperature. While cooling at –78 °C, methanol (250 mL) was added to the slightly yellow, clear solution slowly to control bubbling. The solution was distilled through a short path until the volume was reduced by half. The short path distillation apparatus was replaced with a Vigreux column. The product was vacuum distilled (30 °C, 1 mmHg). A clear and colorless liquid was obtained (15.08 g, 90%). ¹H NMR (300 MHz, C₆D₆, δ): 0.82 (s, 9H, C(CH₃)₃), 0.95 (t, *J* = 7.5 Hz, 3H, CH₃), 1.08 (m, 1H, CH₂), 1.25 (d, 1H, OH), 1.34 (m, 1H, CH₂), 2.82 (m, 1H, CH). (OH peak moves depending on concentration.)

(*R*)-2,2-Dimethyl-3-pent-1-yl methanesulfonate, 39. Into a 500-mL round bottom flask, CH₂Cl₂ (250 mL) and triethylamine (16.0 mL, 0.12 mol) were vacuum transferred. **38** (9.3 g, 0.08 mol) (previously dried over sieves for 24 h) was syringe

added. While cooling in $-78\text{ }^{\circ}\text{C}$ and stirring, mesyl chloride (10.1 g, 0.088 mol) was syringe added over 2 min. The reaction was opened to the Hg bubbler and stirred at $-78\text{ }^{\circ}\text{C}$ for 1 h. After removing the $-78\text{ }^{\circ}\text{C}$ bath, the white slurry was stirred at room temperature for 1 h, upon which the slurry became yellow. The solution was added to a separatory funnel containing 200 mL of water. The layers were separated. The organic layer was washed with 1 M HCl (200 mL), sat. NaHCO_3 (200 mL), and brine (200 mL). The organic layer was dried over MgSO_4 and filtered. All volatiles were removed by rotary evaporator (warming the flask in warm water decomposes the product). A dark, yellow oil was obtained (15.43 g, 99%). The product was used as is in the next step. ^1H NMR (300 MHz, C_6D_6 , δ): 0.78 (s, 9H, $\text{C}(\text{CH}_3)_3$), 0.98 (t, $J = 7.5\text{ Hz}$, 3H, CH_3), 1.37 (m, 2H, CH_2), 2.34 (s, 3H, SO_2CH_3), 4.35 (dd, $J = 7.8, 4.8\text{ Hz}$, 1H, CH).

(S)-ENCpH, 40. In the drybox, KCp (33.2 g, 170 mmol) and 18-crown-6 ether (2.04 g, 8.5 mmol) were weighed into a 250-mL round bottom flask. The flask was equipped with a condenser and 180° valve joint. 40 mL of DMF (dried over sieves) was syringed into the flask. **30** (16.6 g, 85.4 mmol) was dissolved in DMF (20 mL) and syringed onto the KCp solution. The brown solution was heated to $90\text{ }^{\circ}\text{C}$ and allowed to stir overnight. After cooling the brown slurry to room temperature, it was dissolved with 100 mL of water. The solution was diluted with hexanes (50 mL), and the layers were separated. The water layer was extracted with hexanes (50 mL). The combined organic layer was washed with 1 M KHSO_4 (50 mL), sat. NaHCO_3 (50 mL), and brine (50 mL). The organic layer was dried over MgSO_4 and filtered. The solvent was removed by rotary evaporator. The brown oil was Kugelrohr distilled (10^{-3} mmHg , $30\text{ }^{\circ}\text{C}$) to obtain a

dark, yellow oil composed of **40** and Cp dimer (5.34 g, crude yield). The crude product was used in next step without further purification. ^1H NMR (300 MHz, C_6D_6 , δ): 0.85 (t, $J = 7.5$ Hz, 3H, CH_3), 0.92 (s, 9H, $\text{C}(\text{CH}_3)_3$), 1.44 (m, 1H, CH_2), 1.6 (m, 1H, CH_2), 2.07 (dd, $J = 11.7, 2.7$, 1H, CH), 2.78 (br s, 1H, sp^3 Cp), 5.95, 6.14, 6.22, 6.30, 6.47 (m's, 4H, sp^2 Cp).

(S)-LiENCp, 41. The round bottom flask containing the crude **40** was equipped with an oven-hot swivel frit assembly. After evacuating the apparatus, ethyl ether (15 mL) was vacuum transferred. While cooling in -78 °C bath, *n*-BuLi (10.7 mL, 17 mmol) was syringe added, and the solution was allowed to stir for 30 min. The solution was stirred at room temperature for 2 h. If no precipitate forms, add DME. All volatiles were removed *in vacuo*, and petroleum ether (15 mL) was vacuum transferred onto the white paste. The white slurry was filtered and washed 3 times. After removing volatiles *in vacuo*, the white solid was dried overnight to yield 1.72 g (23.4% based on **39**). ^1H NMR (300 MHz, $\text{THF}-d_8$, δ): 0.80 (t, 3H, $J = 7.5$ Hz, CH_3), 0.82 (s, 9H, $\text{C}(\text{CH}_3)_3$), 1.52 (m, 1H, CH_2), 1.75 (m, 1H, CH_2), 2.10 (dd, $J = 11.7, 2.7$ Hz, 1H, CH), 3.27 (s, 5.2H, OCH_3), 3.43 (s, 3.9H, OCH_2), 5.51, 5.59 (m, 4H, Cp H).

$[(rac)\text{-ENCp}]_2\text{Fe}$, (rac)-42. In the drybox, **41** (100 mg, 0.59 mmol) and FeCl_2 (70 mg, 0.55 mmol) were weighed into a vial containing 10 mL of THF. The vial was capped and allowed to stir at room temperature in the drybox for 5 h. Outside the drybox, the greenish brown solution was transferred to a separatory funnel. The solution was diluted with petroleum ether (20 mL) and then washed with water (30 mL). The

aqueous layer was extracted with petroleum ether (2 x 10 mL). The combined organic layer was washed with brine, dried over MgSO_4 , and filtered. The solvent was removed by rotary evaporation while warming in a water bath. A thick, dark orange oil was obtained (100 mg, 89%). ^1H NMR (300 MHz, C_6D_6 , δ): 0.83 (s, 36H, $\text{C}(\text{CH}_3)_3$), 1.17 (t, $J = 7.5$ Hz, 6H, CH_3), 1.18 (t, $J = 7.5$ Hz, 6H, CH_3), 1.66 (m, 4H, CH_2), 1.79 (dd, $J = 5.7$, 2.7, 2H, CH), 1.80 (dd, $J = 5.7$, 2.7, 2H, CH), 2.04 (m, 4H, CH_2), 3.84, 3.96, 3.98, 4.00, 4.04 (m's, 16H, Cp). ^{13}C NMR (300 MHz, C_6D_6 , δ): 17.75 (4C), 25.73, 25.89 (4C), 28.73 (12C), 35.30, 33.34 (4C), 52.12, 52.18 (4C), 67.12, 67.33 (4C), 68.34, 68.40 (4C), 68.54, 68.66 (4C), 71.77, 71.87 (4C), 94.43, 94.65 (4C).

[(*S*)-ENCp] $_2$ Fe, (*S*)-42. The product was prepared using the same procedure for [(*rac*)-ENCp] $_2$ Fe. ^1H NMR (300 MHz, C_6D_6 , δ): 0.82 (s, 18H, $\text{C}(\text{CH}_3)_3$), 1.18 (t, $J = 7.5$ Hz, 6H, CH_3), 1.66 (quint, $J = 7.5$ Hz, 2H, CH_2), 1.81 (dd, $J = 5.7$, 2.7 Hz, 2H, CH), 2.02 (quint of d, $J = 7.5$, 2.4 Hz, 2H, CH_2), 3.84, 3.99, 4.01, 4.05 (m's, 8H, Cp). ^{13}C NMR (300 MHz, C_6D_6 , δ): 17.24 (2C), 25.22 (2C), 28.20 (6C), 34.82 (2C), 51.65 (2C), 66.83 (2C), 68.05 (2C), 68.16 (2C), 71.27 (2C), 93.92 (2C).

Kinetic resolution of 31 using Novozyme SP435. Into a 50-mL round bottom flask, 2,2-dimethyl-3-pentanol (2.0 g, 17.2 mmol), (*S*)-ethylthiooctanoate (3.2 g, 17.2 mmol), tetradecane (250 mg), and Novozyme SP 435 (300 mg) were weighed. The flask was equipped with a reflux condenser and connected to an oil bubbler. The mixture was stirred and heated in a 40 °C oil bath. The reaction was monitored using GC.

[(S)-ENCp](SiMe₂)[(i-Pr)₂Cp] + isomers. The product was prepared in the same manner as **13** using **41** (1.16 g, 6.82 mmol) and ⁱPr₂CpSiMe₂Cl (1.66 g, 6.82 mmol) in THF (40 mL). Clear, yellow oil was obtained (2.31 g, 91%).

Li₂{[(S)-ENCp](SiMe₂)[(i-Pr)₂Cp]}•DME, (S)-44. The product was prepared in the same manner as **14** using **43** (4.14 g, 11.2 mmol) and *n*-BuLi (14.7 mL, 23.5 mmol, 1.6 M/hexanes) in 50 mL of ethyl ether. The ethyl ether was removed *in vacuo*, and petroleum ether (40 mL) and DME (4 mL) were vacuum transferred. The solution was stirred at room temperature overnight. The white slurry was filtered and washed 3 times. All volatiles were removed *in vacuo*, and the solid was dried to obtain an off-white powder (4.7 g, 91%). ¹H NMR (300 MHz, THF-*d*₈, δ): 0.30 (s, 12H, SiMe₂), 0.82 (t, 3H, CH₃), 0.82 (s, 9H, C(CH₃)₃), 1.13 (d, 6H, CH(CH₃)₂), 1.14 (d, 6H, CH(CH₃)₂), 1.54 (m, 1H, CH₂), 1.75 (m, 1H, CH₂), 2.10 (dd, 1H, CH(CH₃)₂), 2.78 (h, 1H, CH(CH₃)₂), 3.18 (h, 1H, CH), 3.27 (s, 5.2H, OCH₃) 3.43 (s, 3.9H, OCH₂), 5.66 (m, 3H, C₅H₂), 5.85 (m, 2H, C₅H₃).

Li₂{[(rac)-ENCp](SiMe₂)[(i-Pr)₂Cp]}•DME, (rac)-44. The product was prepared in the same manner as **(S)-44**. ¹H NMR (300MHz, THF-*d*₈, δ): 0.32 (s, 12H, SiMe₂), 0.71 (t, 3H, CH₃), 0.84 (s, 9H, C(CH₃)₃), 1.00 (quint, 2H, CH₂), 1.12 (d, 6H, CH(CH₃)₂), 1.15 (d, 6H, CH(CH₃)₂), 2.31 (br s, 1H, CH), 2.72 (h, 1H, CH(CH₃)₂), 3.22 (h, 1H, CH(CH₃)₂), 5.60 (m, 3H, C₅H₂), 5.78 (m, 2H, C₅H₃).

[(S)-ENCp](SiMe₂)₂[(i-Pr)₂Cp], 45. The product was prepared using the same procedure for **15**. ¹H NMR (300 MHz, C₆D₆, δ): 0.40 (s, 3H, SiMe₂), 0.48 (s, 3H, SiMe₂), 1.20 (s, 3H, SiMe₂), 1.28 (s, 3H, SiMe₂), 1.70 (s, 9H, C(CH₃)₃), (d, 6H, CH(CH₃)₂), (d, 6H, CH(CH₃)₂), 1.95 (t, 3H, CH₃), 2.28 (m, 1H, CH₂), 2.48 (m, 1H, CH₂), 2.92 (m, 1H, CH), 3.32 (h, 1H, CH(CH₃)₂), 3.88 (h, 1H, CH(CH₃)₂), 4.16 (br s, 1H, sp³ Cp H), 4.18 (br s, 1H, sp³ Cp H), 7.10 (br s, 1H, sp² Cp H), 7.68 (br s, 1H, sp² Cp H), 7.85 (br s, 1H, sp² Cp H).

Li₂[(S)-ENCp](SiMe₂)₂[(i-Pr)₂Cp]•DME, 46. The product was prepared in the same manner as **16** using **45** (4.35 g, 10.2 mmol) and *n*-BuLi (19.0 mL, 22.44 mmol, 1.18 M/hexanes) in ethyl ether (75 mL). The solution was stirred at room temperature for 3 h. All volatiles were removed *in vacuo*, and petroleum ether (75 mL) and DME (5 mL) were vacuum transferred. The slurry was filtered and washed 4 times. A pinkish, beige solid was collected (1.89 g, 3.4 mmol, 33.6%). ¹H NMR (300 MHz, THF-*d*₈, δ): 0.25 (br s, 12H, SiMe₂), 0.83 (s, 9H, C(CH₃)₃), 0.89 (t, 3H, CH₃), 1.19 (d, 12H, *J* = 6.9 Hz, CH(CH₃)₂), 1.58 (m, 1H, CH₂), 1.76 (m, 1H, CH₂), 2.16 (dd, 1H, *J* = 10.5, 2.4 Hz, CH), 3.32 (h, 1H, *J* = 6.9 Hz, CH(CH₃)₂), 3.12 (h, 1H, CH(CH₃)₂), 3.26 (s, 5.4H, OCH₃), 3.42 (s, 3.9H, OCH₂), 5.94 (s, 1H, C₅H₁), 6.00 (s, 2H, C₅H₂).

{[(S)-ENCp](SiMe₂)₂[(i-Pr)₂Cp]}Zr(NMe₂)₂, 47. The product was prepared in the same manner as **17** with **45** (2.07 g, 4.85 mmol) and Zr(NMe₂)₄ (1.30 g, 4.85 mmol) in xylenes (40 mL).

$\{[(S)\text{-ENCp}](\text{SiMe}_2)_2[(i\text{-Pr})_2\text{Cp}]\}\text{ZrCl}_2$, 48. The product was prepared in the same manner as (*S*)-**3** and (*S*)-**4** using **47** (2.9 g, 4.85 mmol) and TMSCl (10 equiv) in toluene (40 mL). White powder was collected from petroleum ether. ^1H NMR (300 MHz, C_6D_6 , δ): 0.50 (s, 6H, SiMe_2), 0.57, 0.58 (s's, 6H, SiMe_2), 0.79 (s, 9H, $\text{C}(\text{CH}_3)_3$), 0.97(d, 6H, $\text{CH}(\text{CH}_3)_2$), 1.37 (d, 6H, $\text{CH}(\text{CH}_3)_2$), 1.41 (m, 3H, EN CH_3), 1.76 (m, 1H, CH_2), 2.47 (coincident m's, 2H, EN CH and CH_2), 3.32 (m, 2H, $\text{CH}(\text{CH}_3)_2$), 6.49 (s, 1H, C_5H_1), 6.61 (d, 1H, C_5H_2), 6.77 (d, 1H, C_5H_2).

REFERENCES AND NOTES

- ¹ Veghini, D.; Henling, L. M.; Terry J. Burkhardt, T. J.; Bercaw, J. E. *J. Am. Chem. Soc.*, **1999**, *121*, 564.
- ² Herzog, T. A.; Zubris, D. L.; Bercaw, J. E. *J. Am. Chem. Soc.* **1996**, *118*, 11988.
- ³ Baar, C. R.; Levy, C. J.; Min, E. Y.; Henling, L. M.; Day, M. W.; Bercaw, J. E. *J. Am. Chem. Soc.* **2004**, *126*, 8216.
- ⁴ (a) Boor, J. *Ziegler-Natta Catalysts and Polymerization*; Academic Press: New York, 1979. (b) Pino, P.; Mulhaupt, R. *Angew. Chem. Intl. Ed. Engl.* **1980**, *19*, 857. (c) Sinn, H.; Kaminsky, W. *Adv. Organomet. Chem.* **1980**, *18*, 99. (d) Tait, P. J. T.; Watkins, N. D. *Comprehensive Polymer Science*; Pergamon Press: Oxford, 1989 ch. 1 and 2. (e) Brintzinger, H. H.; Fischer, D.; Mulhaupt, R.; Rieger, B.; Waymouth, R. M. *Angew. Chem. Intl. Ed. Engl.* **1995**, *34*, 1143, and references therein.
- ⁵ MAO is methylaluminoxane, (MeAlO)_n.
- ⁶ Herzog, T. Design, Synthesis, and Reactivity of a New Class of Highly Syndiotactic Ziegler-Natta Polymerization Catalyst. Ph.D. Thesis, California Institute of Technology, Pasadena, CA, 1997.
- ⁷ Unpublished data, Chris Levy.
- ⁸ Corey, E. J.; Helal, C. J. *Chem. Rev.* **1998**, *37*, 1986.
- ⁹ Giardello, M. A.; Conticello, V. P.; Sabat, M.; Rheingold, A. L.; Stern, C. L.; Marks, T. J. *J. Am. Chem. Soc.* **1994**, *116*, 10212.
- ¹⁰ Crossland, R. K.; Servis, K. L. *J. of Org. Chem.* **1970**, *35*, 3195.
- ¹¹ Orrenius, C.; Haeffner, F.; Rotticci, D.; Ohrner, N.; Norin, T.; Hult, K. *Biocat. and Biotransf.* **1998**, *16*, 1.
- ¹² The 85% ee mixture of ethylneopentyl alcohol was obtained from an asymmetric reduction of the corresponding ketone with 10 mol % of (*S*)-CBS catalyst.
- ¹³ See experimental section of chapter 1.

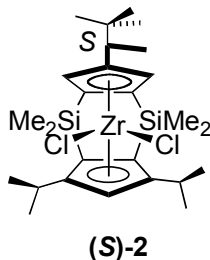
-
- ¹⁴ Burger, B. J.; Bercaw, J. E. *Experimental Organometallic Chemistry*; ACS symposium Series No. 357; Wayda, A. L., Darensbourg, M. Y. eds.; American Chemical Society: Washington, D.C. 1987; ch. 4.
- ¹⁵ Marvich, R. H.; Brintzinger, H. H. *J. Am. Chem. Soc.* **1971**, *93*, 203.
- ¹⁶ Frykman, H.; Öhrner, N.; Norin, T.; Hult, K. *Tetrahedron Lett.* **1993**, *34*, 1367.
- ¹⁷ The CBS catalyst was prepared by Chris Levy following published methods. (a) Mathoure, D. J.; Jones, T. K.; Xavier, L. C.; Blacklock, T. J.; Reamer, R. A.; Mohan, J. J.; Turner Jones, E. T.; Hoogsteen, K.; Baum, M. W.; Grabowski, E. J. J. *J. of Org. Chem.* **1991**, *56*, 751-762. (b) Mathoure, D. J.; Thompson, A. S.; Douglas, A. W.; Hoogsteen, K.; Carroll, J. D.; Corely, E. G.; Grabowski, E. J. J. *J. of Org. Chem.* **1993**, *58*, 2880-2888.

3 CHAPTER THREE

PROGRESS TOWARD THE KINETIC RESOLUTION OF CHIRAL POLAR OLEFINS USING C_1 -SYMMETRIC ZIRCONOCENE POLYMERIZATION CATALYST

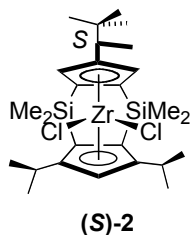
3.1 ABSTRACT

The strategy of selective polymerization to achieve kinetic resolution was applied to chiral functionalized olefins. Towards this goal, 3-buten-2-ol and 4-penten-2-ol were protected with bulky triethyl silyl (TES) and *tert*-butyl dimethyl silyl (TBS) groups. Upon activation with MAO, (*S*)-**2** demonstrated moderate activity for the TBS protected 4-penten-2-ol monomer. The monomers derived from 3-buten-2-ol decomposed slowly in the presence of MAO, precluding determination of accurate conversions for 3-buten-2-ol derived monomers. The protected alcohols can be deprotected with TBAF and derivatized to the Mosher ester cleanly. The enantiomeric excess can be determined by ^1H and ^{19}F NMR. However, a clean enantioassay of unreacted monomer after a polymerization reaction was not achieved.



3.2 INTRODUCTION

The strategy of kinetic resolution of chiral olefins using (*S*)-**2** has been extended to chiral olefins containing oxygen and nitrogen functionalities. One of the challenges with using group IV Ziegler-Natta catalysts is their highly oxophilic nature.^{1,2} Despite this potential hindrance to polymerization, zirconocene/MAO catalysts have been used successfully to copolymerize ethylene with 10-undecen-1-ol and other monomers containing a long methylene spacer between the polar functionality and the vinyl group.^{3,4,5} Although numerous examples of the polymerization of polar olefins with long spacers are present, only a few examples with olefins containing one methylene spacer (allyl monomer) can be found.^{6,7,8} For the purpose of kinetic resolution of chiral polar olefins, olefins containing functionalities on the allyl position are of greater interest.



Hagihara demonstrated good allylamine incorporation (0.65 mol% in polymer) using (*rac*)-SiMe₂-bis(1-indenyl)ZrCl₂/MAO catalyst to copolymerize propylene and allylamine.⁸ Furthermore, Imuta reported the copolymerization of ethylene and allyl alcohol using a bulky zirconocene/MAO/trialkylaluminum catalyst system.⁷ The reported incorporation mol% ranged from 0.33 mol% to 1.2 mol%, depending on the nature of the alkyl group of trialkylaluminum catalyst system. Based on these

precedents, the polymerization of chiral polar olefins, containing short methylene spacers, using (*S*)-**2** seemed promising. The progress toward this goal is reported herein.

3.3 RESULTS AND DISCUSSION

3.3.1 Protection and Polymerization of Olefinic Alcohols with Trialkyl Silyl Groups

In order to impede the metal center from coordinating to the oxygen atom of the monomer, it was necessary to place protecting groups on the hydroxyl moiety. The appropriate protecting group would provide enough steric bulk to impede metal coordination and yet not so much bulk that monomer insertion was not possible (Figure 3.1).

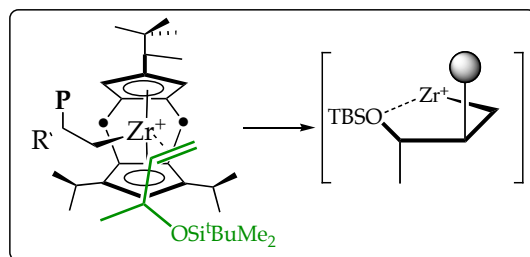
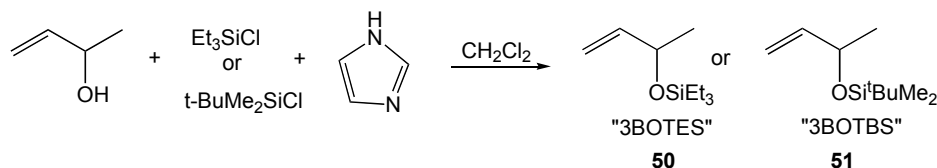


Figure 3.1. Possible coordination of oxygen atom to transition metal center.

For these reasons, *tert*-butyl dimethyl silyl (TBS) and triethyl silyl (TES) groups were chosen to protect two commercially available alcohols, 3-buten-2-ol and 4-penten-2-ol. 3-Buten-2-ol was protected with TBSCl and TESCl, and 4-penten-2-ol was protected with TBSCl. The alcohols were reacted with the corresponding protecting agent and imidazole in methylene chloride (Scheme 3.1).⁹ In addition to the desired protected alcohols, *tert*-butyl dimethyl silanol or triethyl silanol, and the corresponding silyl ethers (TBS_2O or TES_2O) also formed as by-products. The boiling points of the

silanols and the protected alcohols being similar, the separation of the compounds by distillation was difficult. Purification by column chromatography was equally difficult. In order to obtain the purity of material required for polymerization, significant portions of the product were sacrificed in the first and last cuts of the distillation.



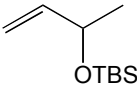
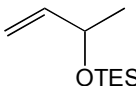
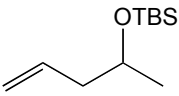
Scheme 3.1. Protection of 3-buten-2-ol with TESC and TBSCl.

For the polymerization of simple olefins, such as 3-methyl-1-pentene, the olefin was vacuum transferred in and out of the polymerization flask (chapter 1). The boiling points of the protected alcohols, however, were too high, and it was not possible to vacuum transfer the olefins. Hence, the usual polymerization procedure and apparatus, as discussed in chapter 1, could not be used. Instead, the polymerization reaction was set up in the drybox. The protected olefins were dried over LAH, filtered, and then stored over sieves before use. After a week of storage over sieves, the integrity of the olefin was checked using NMR and GC. No signs of decomposition were observed. Into a 20-mL vial, MAO, tetradecane, and olefin were weighed. The catalyst was dissolved in toluene and was syringe added to the vial. The vial was then capped and allowed to stir in the drybox at room temperature. GC was used to monitor the reaction conversion.

3.3.2 Degradation of Polar Monomers by MAO

Preliminary polymerization experiments were conducted with (*S*)-MNThpZrCl₂, (*S*)-2. Because the catalyst begins to decompose after a week in solution, it was desired to drive the reaction to 30-60% conversion within one week. In order to reach this conversion range, a catalyst loading 10 times higher than that used to polymerize simple olefins was necessary (Table 3.1).

Table 3.1. Polymerization of Trialkyl Silyl Protected Alcohols

			
	conv % (time hr)	conv % (time hr)	conv % (time hr)
MAO/Zr = 250	4 (51)	2.8 (51)	8 (51)
Olefin/Zr = 1000			
olefin 1g	5 (338)	2.8 (51)	16 (338)
tetradecane 1g			
MAO/Zr = 760	10 (27)	8 (27)	57 (27)
Olefin/Zr = 150			
Olefin 250 mg	13 (168)	10 (168)	67 (168)
tetradecane 1g			

Because the reaction was monitored by the disappearance of the monomer, it was necessary to confirm that the decrease in monomer concentration was indeed due to polymerization and not to decomposition. To test if the protected olefins would remain protected under the polymerization conditions, NMR samples of MAO and monomer were analyzed using ¹H NMR over a period of one week. Furthermore, a vial sample of MAO, monomer, and tetradecane was analyzed over one week by GC. It was found that both the TBS- and TES-protected olefins of 3-butene-2-ol degraded at a rate of 5% per

day over the week-long period. Hence, what initially appeared as polymerization of monomer was actually degradation of protected olefin by the MAO. In the case of TBS-protected 4-penten-2-ol (4POTBS, **52**), the degradation of monomer was not observed. The difference in durability among the monomers may be due to the presence of an acidic allylic proton on **50** and **51**, and absence of it on **52**.

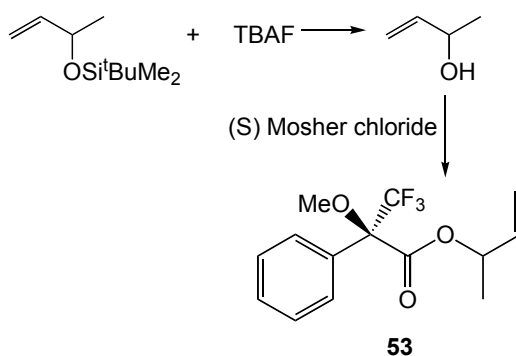
3.3.3 Polymerization of *N, N'*-Bis(Trimethyl Silyl) Allyl Amine

Nitrogen coordinates to zirconium metal less tightly than oxygen. For this reason and also for the value of having enantiopure olefinic amines, preliminary polymerization of protected allyl amine was attempted. The commercially available *N, N'*-bis(trimethylsilyl) allyl amine was dried over sieves before use. To see if bis(TMS) allyl amine degraded in the presence of MAO or sieves, an NMR sample of the olefin and MAO was monitored over one week. A sample of the olefin, MAO, and tetradecane was monitored by GC over one week. Neither NMR nor GC indicated any change to the olefin.

In the drybox, MAO, tetradecane, and olefin were weighed into a 20-mL vial. The catalyst was dissolved in toluene and added to the vial. The catalyst loading was on the same scale as that for the protected alcohols. After one week of stirring at room temperature, the GC trace indicated that no conversion had taken place.

3.3.4 Enantioassay of Polar Monomers

50, **51**, and **52** did not resolve on numerous chiral columns including, β -DM, β -PH, γ -TA, DB-1701, and hydrodex- β . As such, it was necessary to develop an enantioassay method. The monomer was deprotected using 4 equiv of tetrabutyl ammonium fluoride (TBAF).⁹ Injections of trifluoroacetyl and heptafluoropentyl derivatives of the alcohols on chiral γ -TA column also failed to give resolution. Treatment of the olefinic alcohol with NaIO₄/RuCl₃, followed by BF₃/MeOH, also did not yield products that would resolve on the chiral column. 3-Buten-2-ol and 4-penten-2-ol were reacted with enantiopure (*S*)-Mosher chloride to produce the corresponding esters (Scheme 3.2).



Scheme 3.2. Derivatization of polar monomer for enantioassay.

The ¹H NMR of (*S*)-Mosher esters of 3-buten-2-ol (**53**) and 4-penten-2-ol (**54**) showed diagnostic methyl peaks with baseline separation that could be used for integration to determine the ee (Figure 3.2). The ¹⁹F NMR of **54** also showed diagnostic peaks that could be used for determining ee (Figure 3.3). The ¹⁹F NMR of **53**, however, did not produce peaks with baseline separation.

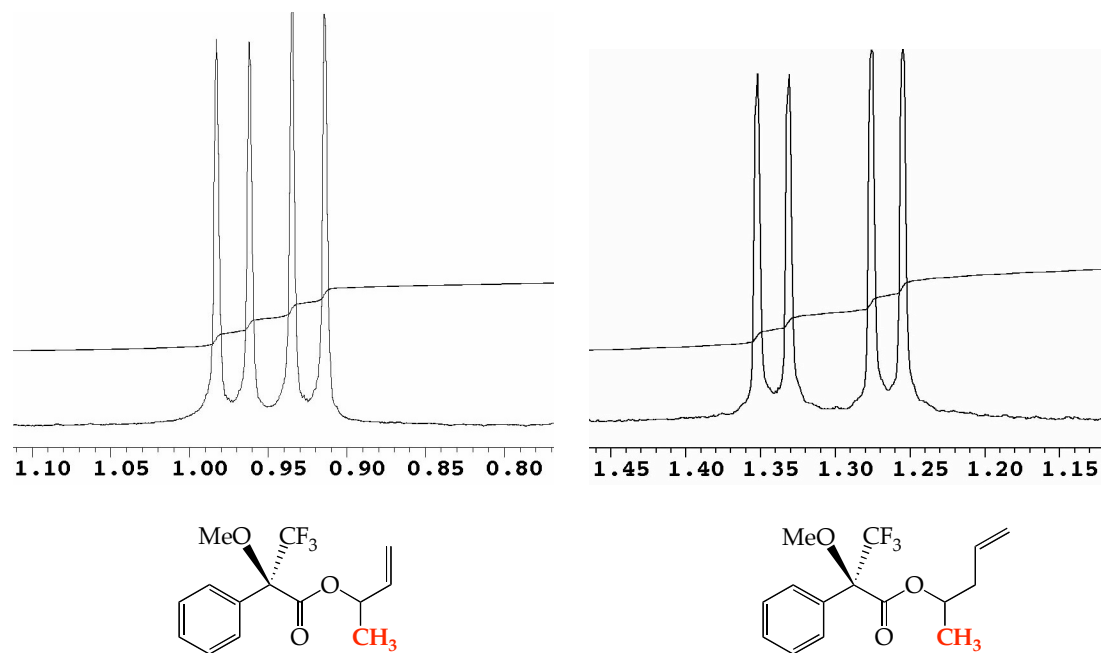


Figure 3.2. ^1H NMR of Mosher esters: 3-buten-2-ol (CDCl_3), 4-penten-2-ol (C_6D_6).

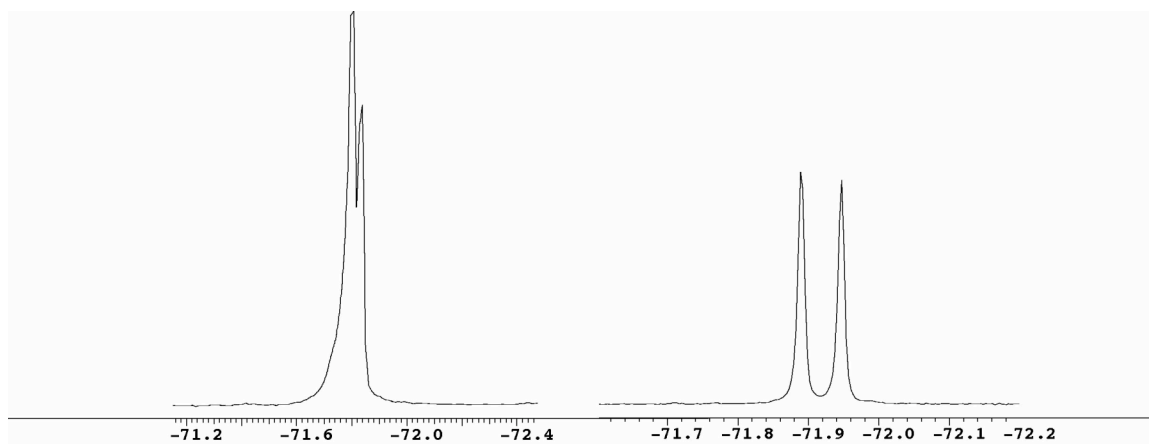


Figure 3.3. ^{19}F NMR (500 MHz) of Mosher esters of 3-buten-2-ol and 4-penten-2-ol.

The procedures to deprotect and analyze the Mosher ester using NMR to determine the ee have been developed. Because the monomer cannot be vacuum transferred out of the polymerization reaction solution, the challenging step was to apply



3.4 CONCLUSIONS

Commercially available 3-buten-2-ol and 4-penten-2-ol were protected with trialkyl silyl groups. The protected olefins of 3-buten-2-ol were found to decompose in the presence of MAO in solution. The derivative of 4-penten-2-ol, however, did not decompose in the presence of MAO. For this monomer, the optimal polymerization condition to reach ~50% conversion within one week was developed. A pure sample of all three protected monomers can be deprotected cleanly with TBAF/THF and derivatized to the (*S*)-Mosher ester. Peaks appropriate for integration to determine ee were found with ^1H and ^{19}F NMR spectra of the (*S*)-Mosher esters. Unfortunately, a procedure to deprotect and derivatize the monomers in situ could not be found. The NMR spectra displayed many overlapping peaks due to impurities.

For future studies, it may be fruitful to protect 3-buten-2-ol with triphenyl protecting groups. This protecting group may prove to withstand degradation by MAO. Also, the challenge of enantioassaying the unreacted monomers may be overcome by converting the monomer to ester in one step by treatment with ZnCl_2 and acetyl chloride.¹⁰

3.5 EXPERIMENTAL SECTION

General Procedure

All air and/or moisture sensitive materials were handled using high-vacuum line, swivel frit assembly, glovebox, Schlenk and cannula techniques under a nitrogen or argon atmosphere.¹¹ Argon was purified by passage through MnO on vermiculite and activated 4 Å molecular sieves. All glassware was oven dried before use. Solvents were dried and degassed over sodium benzophenone ketyl or over titanocene¹².

Unless otherwise mentioned, all starting materials were purchased from Aldrich and used as received. Trifluoroacetyl imidazole and heptafluoropentyl imidazole were purchased from Alltech in 0.5 mL ampules. (*S*)-**2** was synthesized by the route previously reported for the racemic counterpart,^{13,14} except that (*S*)-LiMNCp¹⁵ was used in place of the racemate. Methylaluminoxane (MAO) was purchased from Albemarle. All volatiles were removed *in vacuo* to give a white powder. The white MAO solid was dried at 150 °C for 12 h at high vacuum. Tetradecane was stirred over pieces of Na metal for 24 h at room temperature. Tetradecane was vacuum distilled using a Vigoreaux column into a dry Schlenk flask and stored in the drybox. Toluene used for polymerization was vacuum transferred into a small Schlenk flask from sodium benzophenone ketyl and stored over sieves in the drybox. The trialkyl silyl protected olefins were dried over LAH for 2 d, filtered in the drybox, and stored over sieves in the drybox.

Instrumentation. NMR spectra were recorded on the Varian Mercury VX300 (^1H , 300 MHz, ^{13}C , 75.5 MHz) spectrometer. Gas chromatographs were obtained on an Agilent 6890 Series gas chromatography using a 30 m x 0.25 mm, γ -cyclodextrin trifluoroacetyl “ChiralDEX-TA” column from Advanced Separations Technology.

[2-(3-Buten)](triethyl silyl) ether, “3BOTES” 50. In a 100-mL round bottom flask, 3-buten-2-ol (5.0 g, 69.3 mmol) and imidazole (10.4 g, 152.5 mmol) were weighed and dissolved with 50 mL of methylene chloride. The flask was sealed with a septum. While cooling in an ice bath, chlorotriethyl silane (12.5 g, 83.2 mmol) was syringe added to the solution. The reaction was slightly exothermic. The thick white slurry was vigorously stirred at room temperature overnight. The slurry was transferred to a separatory funnel and washed with saturated aqueous solution of NH_4Cl (50 mL), NaHCO_3 (50 mL), and brine (50 mL). The organic layer was dried over MgSO_4 and filtered. About half of the solvent was removed by rotary evaporator. The solution distilled at ambient pressure to remove methylene chloride and low boiling impurities. The product was vacuum distilled (20 mmHg, 54 °C). ^1H NMR (300 MHz, toluene- d_8 , δ): 0.05 (s, 6H, SiCH_3), 0.97 (s, 9H, *t*-Bu), 1.15 (d, J = 6.0 Hz, 3H, CH_3), 4.14 (quint, J = 6.0 Hz, 1H, CH), 4.92 (dd, J = 10.2, 1.2 Hz, 1H, *trans* (H)(H)C=), 5.16 (dd, J = 17.1, 1.2, 1H, *cis* (H)(H)C=), 5.76 (m, 1H, =C(H)(C)).

[2-(3-Buten)](*tert*-butyl dimethyl silyl) ether, “3BOTBS” 51. The product was prepared in the same manner as **50** with 3-buten-2-ol (5.0 g, 69.3 mmol), imidazole (10.4 g, 152.5 mmol), 50 mL of methylene chloride, and *tert*-butyl chlorodimethyl silane (12.5

g, 83.2 mmol). The product was distilled under vacuum (20 mm Hg, 66-68°C) to collect 22.82 g (82%) of clear and colorless liquid. ^1H NMR (300 MHz, toluene- d_8 , δ): 0.575 (q, $J = 8.1$ Hz, 6H, CH_2), 1.00 (t, $J = 8.1$ Hz, 9H, SiCH_2CH_3), 1.175 (d, $J = 6.3$ Hz, 3H, CH_3), 4.164 (quint, $J = 6.0$ Hz, 1H, CH), 4.915 (dd, $J = 10.2, 1.2$ Hz, 1H, *trans* (H)(H)C=), 5.222 (dd, $J = 17.1, 1.2$, 1H, *cis* (H)(H)C=), 5.801 (m, 1H, =C(H)(C)).

[2-(4-Penten)](*tert*-butyl dimethyl silyl) ether, “4POTBS” 52. The product was prepared in the same manner as **50** with 4-pentene-2-ol (5.0 g, 58.1 mmol), imidazole (8.7 g, 127.8 mmol), 50 mL of methylene chloride, and chlorodimethyl *tert*-butyl silane (9.6 g, 63.9 mmol). The product was distilled under vacuum (20 mm Hg, 63°C) to collect clear and colorless liquid. ^1H NMR (300 MHz, toluene- d_8 , δ): 0.04 (s, 6H, SiCH_3), 0.96 (s, 9H, *t*-Bu), 1.06 (d, $J = 6.0$ Hz, 3H, CH_3), 2.09 (m, 1H, CH_2), 2.15 (m, 1H, CH_2), 3.70 (sextet, $J = 6.3$ Hz, 1H, CH), 4.99 (m, 1H, *trans* (H)(H)C=), 5.04 (m, 1H, *cis* (H)(H)C=), 5.80 (m, 1H, =C(H)(C)).

(*S*)-Mosher ester derivatives of 3-buten-2-ol. ^1H NMR (300 MHz, C_6D_6 , δ): 0.99 (d, $J = 6.3$ Hz, 3H, CHCH_3), 1.03 (d, $J = 6.3$ Hz, 3H, CHCH_3), 3.20 (s, 6H, OCH_3), 4.82 (dd, 2H, vinyl H), 5.05 (dd, 2H, vinyl H), 5.42 (m, 2H, vinyl H), 5.50 (m, 2H, CHCH_3), 7.10, 7.70 (m's, 10 H, Ar H). ^{19}F NMR (500 MHz, CDCl_3 , δ): -71.81 (s, 3F, CF_3); -71.84 (s, 3F, CF_3).

(*S*)-Mosher ester derivatives of 4-penten-2-ol. ^1H NMR (300 MHz, C_6D_6 , δ): 0.92 (d, $J = 6.3$ Hz, 3H, CHCH_3), 0.97 (d, $J = 6.3$ Hz, 3H, CHCH_3), 1.95 (m, 2H, CH_2),

2.10 (m, 2H, CH₂), 3.20 (s, 3H, OCH₃), 3.22 (s, 3H, OCH₃), 4.78, 4.85, 4.95, 5.05 (m's, 6H, vinyl H), 5.50 (m's, 2H, CHCH₃), 7.10, 7.70 (m's, 10 H, Ar H). ¹⁹F NMR (500 MHz, CDCl₃, δ): -71.95 (s, 3F, CF₃), -71.89 (s, 3F, CF₃).

Polymerization procedure. The typical polymerization procedure was carried out as follows. In the drybox, MAO (~600 mg), tetradecane (~1 g, distilled from Na), and olefin were weighed into a 20-mL vial. The vial was capped, and the mixture was allowed to stir at room temperature for 1 h to ensure removal of all traces of moisture. Prior to catalyst injection, an aliquot was transferred to a vial. The vial was capped, and out of the drybox, the aliquot was quenched with *n*-butanol. The catalyst solution was added via syringe (0.50 mL of a 30×10^{-3} M solution in toluene is typical). The solution usually changed from colorless to yellow upon catalyst addition. When the desired conversion was reached, a final aliquot was taken. The reaction vial was removed from the drybox and placed in a -10 °C bath. While cooling in a cold bath, methanol (~18 mL) was added dropwise to the vial, to quench the reaction. The aliquots were used for the GC determination of conversion, with tetradecane acting as the internal standard for integration.

REFERENCES AND NOTES

- ¹ Giannini, U.; Brückner, G.; Pellino, E.; Cassata, A. *Polym. Lett.* **1967**, *5*, 527.
- ² Giannini, U.; Brückner, G.; Pellino, E.; Cassata, A. *J. Polym. Sci., Part C* **1968**, *22*, 157.
- ³ (a) Aaltonen, P.; Löfgren, B. *Macromolecules* **1995**, *28*, 5353. (b) Aaltonen, P.; Fink, G.; Löfgren, B.; Seppala, J. *Macromolecules* **1996**, *29*, 5255.
- ⁴ Hakala, K.; Helaja, T.; Löfgren, B. *J. Polym. Sci., Part A: Polym. Chem.* **2000**, *38*, 1966.
- ⁵ Marques, M. M.; Correia, S. G.; Asceso, J. R.; Ribeiro, A. F. G.; Gomes, P. T.; Dias, A. R.; Foster, P.; Rausch, M. D.; Chien, J. C.W. *J. Polym. Sci., Part A: Polym. Chem.* **1999**, *37*, 2457.
- ⁶ (a) Arit, K. P.; Binsack, R.; Grogo, U.; Neuray, D. U. S. Patent 4423196, 1983; *Chem. Abstr.* **1984**, *100*, 139804.
- ⁷ Imuta, J.; Kashiwa, N. *J. Am. Chem. Soc.* **2002**, *124*, 1176.
- ⁸ Hagihara, H.; Tsuchihara, K.; Sugiyama, J.; Takeuchi, K.; Shiono, T. *Macromolecules* **2004**, *37*, 5145.
- ⁹ Corey, E. J.; Venkateswarlu, A. *J. Am. Chem. Soc.* **1972**, *94*, 6190.
- ¹⁰ Almqvist, F.; Frejd, T. *J. Org. Chem.* **1996**, *61*, 6947.
- ¹¹ Burger, B. J.; Bercaw, J. E. *Experimental Organometallic Chemistry*; ACS symposium Series No. 357; Wayda, A. L., Darensbourg, M. Y. eds.; American Chemical Society: Washington, D.C. 1987; ch. 4.
- ¹² Marvich, R. H.; Brintzinger, H. H. *J. Am. Chem. Soc.* **1971**, *93*, 203.
- ¹³ Veghini, D.; Henling, L. M.; Terry J. Burkhardt, T. J.; Bercaw, J. E. *J. Am. Chem. Soc.*, **1999**, *121*, 564.
- ¹⁴ Herzog, T. A.; Zubris, D. L.; Bercaw, J. E. *J. Am. Chem. Soc.* **1996**, *118*, 11988.
- ¹⁵ Baar, C. R.; Levy, C. J.; Min, E. Y.; Henling, L. M.; Day, M. W.; Bercaw, J. E. *J. Am. Chem. Soc.* **2004**, *126*, 8216.

A. Appendix A

X-Ray Crystallographic Data for

(*S*)-MⁿThp_(3-pentyl)ZrCl₂ [(*S*)-**3**, Chapter 1]

Table A.1. Crystal data and structure refinement for (S)-3: (CCDC_211885)

Empirical formula	$\text{C}_{30}\text{H}_{50}\text{Cl}_2\text{Si}_2\text{Zr} \cdot \frac{1}{2}(\text{C}_7\text{H}_8)$
Formula weight	675.07
Crystallization solvent	Toluene
Crystal habit	Plates
Crystal size	0.24 x 0.22 x 0.15 mm ³
Crystal color	Colorless

Data Collection

Preliminary Photos	Rotation
Type of diffractometer	Bruker SMART 1000
Wavelength	0.71073 Å MoK α
Data Collection Temperature	100(2) K
θ range for 24577 reflections used in lattice determination	2.19 to 28.17°
Unit cell dimensions	$a = 10.3602(5) \text{ Å}$ $\alpha = 97.1990(10)^\circ$ $b = 13.1543(7) \text{ Å}$ $\beta = 104.0680(10)^\circ$ $c = 14.0843(7) \text{ Å}$ $\gamma = 106.2750(10)^\circ$
Volume	1748.26(15) Å ³
Z	2
Crystal system	Triclinic
Space group	P-1

Density (calculated)	1.282 Mg/m ³
F(000)	714
Data collection program	Bruker SMART v5.054
θ range for data collection	1.65 to 28.18°
Completeness to $\theta = 28.18^\circ$	91.9%
Index ranges	$-13 \leq h \leq 13, -17 \leq k \leq 17, -17 \leq l \leq 18$
Data collection scan type	ω scans at 7 ϕ settings
Data reduction program	Bruker SAINT v6.022
Reflections collected	39,577
Independent reflections	7898 [$R_{\text{int}} = 0.0467$]
Absorption coefficient	0.557 mm ⁻¹
Absorption correction	None
Max. and min. transmission	0.9212 and 0.8780

Structure Solution and Refinement

Structure solution program	SHELXS-97 (Sheldrick, 1990)
Primary solution method	Patterson method
Secondary solution method	Difference Fourier map
Hydrogen placement	Geometric positions
Structure refinement program	SHELXL-97 (Sheldrick, 1997)
Refinement method	Full matrix least-squares on F^2
Data/restraints/parameters	7898/0/398

Treatment of hydrogen atoms	Riding
Goodness-of-fit on F^2	2.923
Final R indices [$I > 2\sigma(I)$, 7088 reflections]	$R1 = 0.0407$, $wR2 = 0.0909$
R indices (all data)	$R1 = 0.0459$, $wR2 = 0.0913$
Type of weighting scheme used	Sigma
Weighting scheme used	$w = 1 / \sigma^2(Fo^2)$
Max shift/error	0.002
Average shift/error	0.000
Largest diff. peak and hole	0.569 and $-0.461 \text{ e.}\text{\AA}^{-3}$

Special Refinement Details

The neohexane ligand is disordered, modeled with two equal half-occupancy methyl carbons (C12A and C12B). The crystals also contain toluene as a solvent of crystallization. The solvent sits near an inversion center and was refined at half-occupancy.

Refinement of F^2 against all reflections. The weighted R-factor (wR) and goodness of fit (S) are based on F^2 , conventional R-factors (R) are based on F , with F set to zero for negative F^2 . The threshold expression of $F^2 > 2\sigma(F^2)$ is used only for calculating R-factors(gt) etc. and is not relevant to the choice of reflections for refinement. R-factors based on F^2 are statistically about twice as large as those based on F , and R-factors based on all data will be even larger.

All esds (except the esd in the dihedral angle between two l.s. planes) are estimated using the full covariance matrix. The cell esds are taken into account individually in the estimation of esds in distances, angles and torsion angles; correlations between esds in cell parameters are only used when they are defined by crystal symmetry. An approximate (isotropic) treatment of cell esds is used for estimating esds involving l.s. planes.

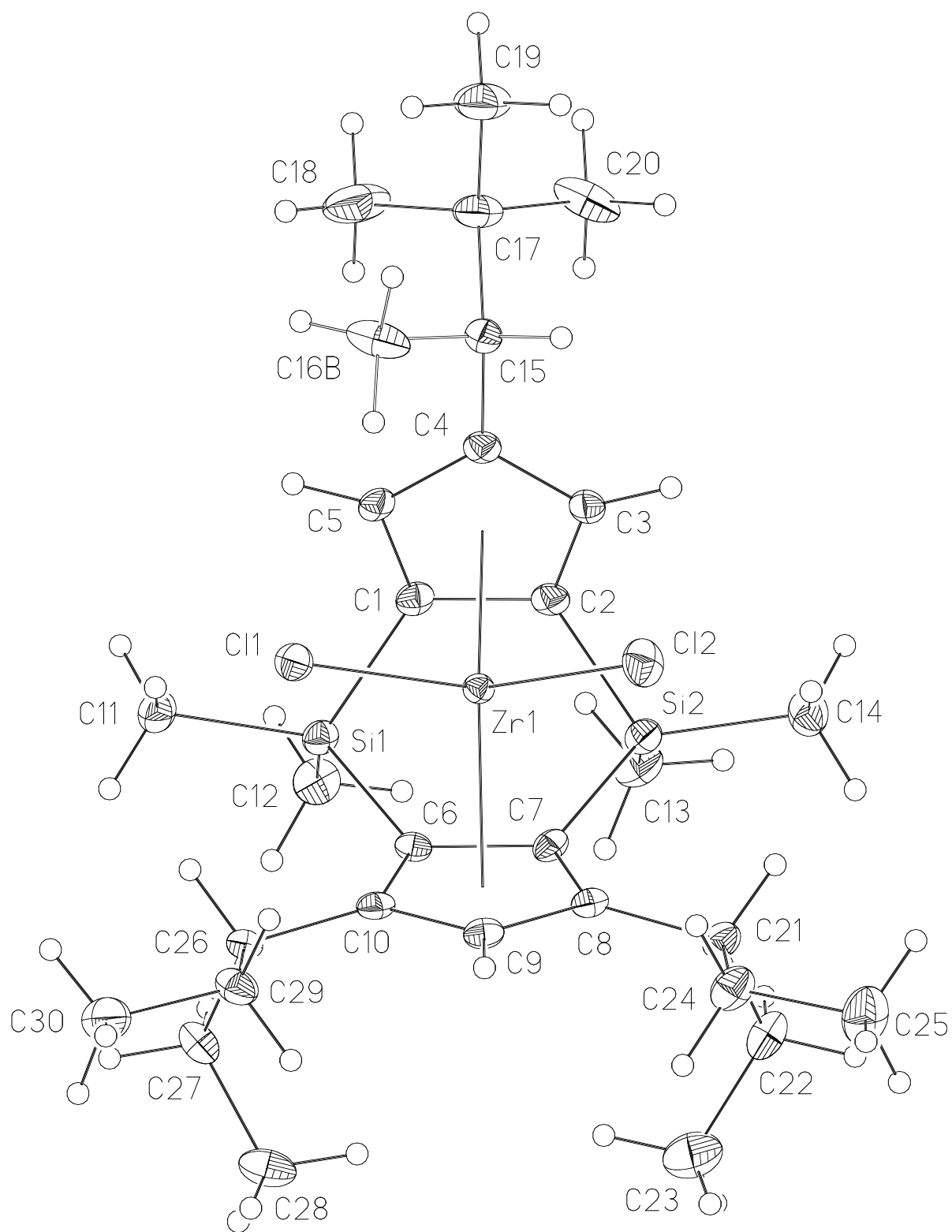


Figure A.1. ORTEP view of (S)-3.

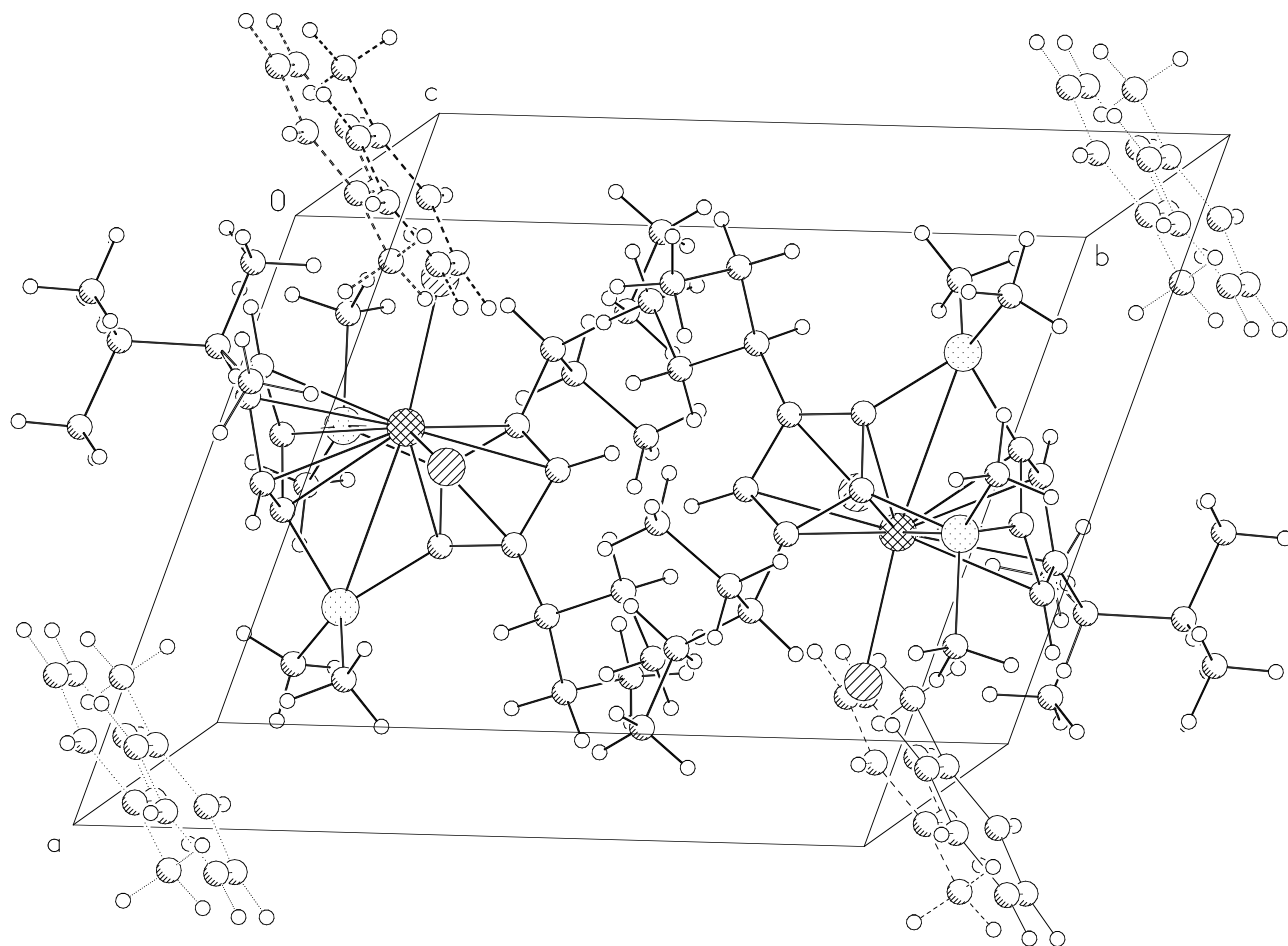


Figure A.2. Unit cell of X-ray structure of (S)-3.

Table A.2. Atomic coordinates and U_{eq} for (S)-3**Atomic coordinates ($\times 10^4$) and equivalent isotropic displacement parameters, U_{eq} ($\text{\AA}^2 \times 10^3$):
CCDC_211885** U_{eq} the trace of the orthogonalized U_{ij} tensor.

	x	y	z	U_{eq}
Zr(1)	6160(1)	7996(1)	7419(1)	11(1)
Cl(1)	8646(1)	8221(1)	7636(1)	18(1)
Cl(2)	5223(1)	7549(1)	5612(1)	23(1)
Si(1)	6565(1)	8472(1)	9768(1)	15(1)
Si(2)	3314(1)	7915(1)	8018(1)	16(1)
C(1)	6232(3)	9323(2)	8820(2)	15(1)
C(2)	4877(3)	9075(2)	8070(2)	15(1)
C(3)	5154(3)	9557(2)	7256(2)	16(1)
C(4)	6601(3)	10104(2)	7467(2)	15(1)
C(5)	7263(3)	9952(2)	8420(2)	15(1)
C(6)	5732(3)	7169(2)	8794(2)	13(1)
C(7)	4353(3)	6941(2)	8051(2)	14(1)
C(8)	4264(3)	6127(2)	7240(2)	14(1)
C(9)	5536(3)	5894(2)	7446(2)	15(1)
C(10)	6412(3)	6479(2)	8407(2)	15(1)
C(11)	8494(3)	8849(2)	10339(2)	21(1)
C(12)	5764(3)	8525(2)	10815(2)	24(1)
C(13)	2552(3)	8102(2)	9074(2)	24(1)
C(14)	1932(3)	7702(2)	6814(2)	25(1)
C(15)	7289(3)	10800(2)	6826(2)	18(1)

C(16A)	6540(3)	10379(2)	5692(2)	24(1)
C(16B)	8719(6)	10736(5)	6874(5)	28(2)
C(17)	7401(3)	12011(2)	7156(2)	23(1)
C(18)	8335(4)	12467(2)	8239(2)	45(1)
C(19)	8071(3)	12677(2)	6473(2)	31(1)
C(20)	5963(4)	12128(3)	7065(2)	34(1)
C(21)	2971(3)	5507(2)	6368(2)	17(1)
C(22)	1818(3)	4884(2)	6792(2)	23(1)
C(23)	2196(4)	4046(3)	7351(3)	39(1)
C(24)	3283(3)	4769(2)	5581(2)	22(1)
C(25)	2035(3)	4216(3)	4657(2)	32(1)
C(26)	7767(3)	6306(2)	8954(2)	16(1)
C(27)	7531(3)	5809(2)	9860(2)	21(1)
C(28)	6493(3)	4654(2)	9597(2)	27(1)
C(29)	8292(3)	5644(2)	8252(2)	20(1)
C(30)	9680(3)	5507(2)	8759(2)	28(1)
C(41)	-1747(8)	-594(8)	3929(6)	44(2)
C(42)	-506(6)	24(5)	4822(5)	29(1)
C(43)	465(7)	949(5)	4767(5)	31(2)
C(44)	1658(7)	1495(5)	5560(5)	31(2)
C(45)	1842(8)	1151(6)	6437(6)	33(2)
C(46)	869(8)	217(5)	6529(5)	36(2)
C(47)	-308(7)	-329(6)	5703(5)	31(2)

Table A.3. Selected bond lengths [\AA] and angles [$^\circ$] for (S)-3: (CCDC_211885)

Zr(1)-Cl(1)	2.4461(7)	Zr(1)-Cl(2)	2.4221(7)
Zr(1)-C(1)	2.437(2)	Zr(1)-C(6)	2.410(2)
Zr(1)-C(2)	2.438(3)	Zr(1)-C(7)	2.426(2)
Zr(1)-C(3)	2.562(3)	Zr(1)-C(8)	2.620(2)
Zr(1)-C(4)	2.671(2)	Zr(1)-C(9)	2.665(2)
Zr(1)-C(5)	2.564(2)	Zr(1)-C(10)	2.606(2)
Cl(2)-Zr(1)-Cl(1)	101.32(2)		

Table A.4. Bond lengths [Å] and angles [°] for (*S*)-3: (CCDC_211885)

Zr(1)-C(6)	2.410(2)	C(2)-C(3)	1.428(4)
Zr(1)-Cl(2)	2.4221(7)	C(3)-C(4)	1.407(4)
Zr(1)-C(7)	2.426(2)	C(4)-C(5)	1.417(4)
Zr(1)-C(1)	2.437(2)	C(4)-C(15)	1.521(3)
Zr(1)-C(2)	2.438(3)	C(6)-C(10)	1.427(4)
Zr(1)-Cl(1)	2.4461(7)	C(6)-C(7)	1.477(3)
Zr(1)-C(3)	2.562(3)	C(7)-C(8)	1.430(3)
Zr(1)-C(5)	2.564(2)	C(8)-C(9)	1.406(4)
Zr(1)-C(10)	2.606(2)	C(8)-C(21)	1.519(4)
Zr(1)-C(8)	2.620(2)	C(9)-C(10)	1.413(4)
Zr(1)-C(9)	2.665(2)	C(10)-C(26)	1.521(4)
Zr(1)-C(4)	2.671(2)	C(15)-C(16B)	1.493(6)
Si(1)-C(11)	1.857(3)	C(15)-C(16A)	1.5476
Si(1)-C(12)	1.862(3)	C(15)-C(17)	1.566(4)
Si(1)-C(1)	1.877(3)	C(17)-C(20)	1.517(4)
Si(1)-C(6)	1.889(3)	C(17)-C(19)	1.539(4)
Si(2)-C(14)	1.865(3)	C(17)-C(18)	1.533(4)
Si(2)-C(2)	1.867(3)	C(21)-C(24)	1.536(4)
Si(2)-C(13)	1.867(3)	C(21)-C(22)	1.541(4)
Si(2)-C(7)	1.889(3)	C(22)-C(23)	1.516(4)
C(1)-C(5)	1.434(4)	C(24)-C(25)	1.520(4)
C(1)-C(2)	1.459(4)	C(26)-C(29)	1.531(4)

C(26)-C(27)	1.545(4)	C(46)-C(47)	1.402(9)
C(27)-C(28)	1.533(4)	C(46)-C(42)#1	1.816(9)
C(29)-C(30)	1.513(4)	C(47)-C(43)#1	0.931(8)
C(41)-C(45)#1	0.808(8)	C(47)-C(42)#1	1.267(9)
C(41)-C(46)#1	1.266(10)	C(6)-Zr(1)-Cl(2)	136.72(6)
C(41)-C(44)#1	1.474(11)	C(6)-Zr(1)-C(7)	35.56(8)
C(41)-C(42)	1.506(9)	Cl(2)-Zr(1)-C(7)	106.23(6)
C(42)-C(42)#1	1.068(11)	C(6)-Zr(1)-C(1)	68.51(8)
C(42)-C(47)#1	1.267(9)	Cl(2)-Zr(1)-C(1)	138.46(6)
C(42)-C(47)	1.366(9)	C(7)-Zr(1)-C(1)	78.60(9)
C(42)-C(43)	1.369(9)	C(6)-Zr(1)-C(2)	79.25(9)
C(42)-C(43)#1	1.475(9)	Cl(2)-Zr(1)-C(2)	107.69(6)
C(42)-C(46)#1	1.816(9)	C(7)-Zr(1)-C(2)	67.46(9)
C(42)-C(44)#1	1.946(9)	C(1)-Zr(1)-C(2)	34.83(8)
C(43)-C(47)#1	0.931(8)	C(6)-Zr(1)-Cl(1)	102.35(6)
C(43)-C(44)	1.387(9)	Cl(2)-Zr(1)-Cl(1)	101.32(2)
C(43)-C(42)#1	1.475(9)	C(7)-Zr(1)-Cl(1)	135.08(6)
C(44)-C(45)	1.357(9)	C(1)-Zr(1)-Cl(1)	102.97(6)
C(44)-C(41)#1	1.474(11)	C(2)-Zr(1)-Cl(1)	134.81(6)
C(44)-C(42)#1	1.946(9)	C(6)-Zr(1)-C(3)	112.32(9)
C(45)-C(41)#1	0.808(8)	Cl(2)-Zr(1)-C(3)	83.38(6)
C(45)-C(46)	1.397(10)	C(7)-Zr(1)-C(3)	95.35(9)
C(46)-C(41)#1	1.266(10)	C(1)-Zr(1)-C(3)	55.13(8)

C(2)-Zr(1)-C(3)	33.07(8)	C(3)-Zr(1)-C(8)	113.82(8)
Cl(1)-Zr(1)-C(3)	122.80(6)	C(5)-Zr(1)-C(8)	144.42(8)
C(6)-Zr(1)-C(5)	96.75(8)	C(10)-Zr(1)-C(8)	52.37(8)
Cl(2)-Zr(1)-C(5)	122.72(6)	C(6)-Zr(1)-C(9)	53.56(8)
C(7)-Zr(1)-C(5)	111.79(8)	Cl(2)-Zr(1)-C(9)	89.77(6)
C(1)-Zr(1)-C(5)	33.21(8)	C(7)-Zr(1)-C(9)	53.41(8)
C(2)-Zr(1)-C(5)	55.02(8)	C(1)-Zr(1)-C(9)	121.99(8)
Cl(1)-Zr(1)-C(5)	80.24(6)	C(2)-Zr(1)-C(9)	120.87(8)
C(3)-Zr(1)-C(5)	52.52(8)	Cl(1)-Zr(1)-C(9)	92.59(6)
C(6)-Zr(1)-C(10)	32.77(8)	C(3)-Zr(1)-C(9)	144.61(8)
Cl(2)-Zr(1)-C(10)	120.07(6)	C(5)-Zr(1)-C(9)	147.47(8)
C(7)-Zr(1)-C(10)	55.14(8)	C(10)-Zr(1)-C(9)	31.07(8)
C(1)-Zr(1)-C(10)	96.93(8)	C(8)-Zr(1)-C(9)	30.84(8)
C(2)-Zr(1)-C(10)	111.97(8)	C(6)-Zr(1)-C(4)	122.70(8)
Cl(1)-Zr(1)-C(10)	80.43(6)	Cl(2)-Zr(1)-C(4)	92.03(6)
C(3)-Zr(1)-C(10)	145.03(8)	C(7)-Zr(1)-C(4)	121.42(8)
C(5)-Zr(1)-C(10)	116.63(8)	C(1)-Zr(1)-C(4)	54.20(8)
C(6)-Zr(1)-C(8)	55.08(8)	C(2)-Zr(1)-C(4)	53.96(8)
Cl(2)-Zr(1)-C(8)	81.64(6)	Cl(1)-Zr(1)-C(4)	91.82(6)
C(7)-Zr(1)-C(8)	32.64(8)	C(3)-Zr(1)-C(4)	31.11(8)
C(1)-Zr(1)-C(8)	111.24(8)	C(5)-Zr(1)-C(4)	31.33(8)
C(2)-Zr(1)-C(8)	95.02(8)	C(10)-Zr(1)-C(4)	147.82(8)
Cl(1)-Zr(1)-C(8)	123.31(6)	C(8)-Zr(1)-C(4)	144.87(8)

C(9)-Zr(1)-C(4)	174.83(8)	C(2)-C(1)-Si(1)	122.91(19)
C(11)-Si(1)-C(12)	107.04(13)	C(5)-C(1)-Zr(1)	78.27(14)
C(11)-Si(1)-C(1)	108.43(12)	C(2)-C(1)-Zr(1)	72.64(14)
C(12)-Si(1)-C(1)	118.68(13)	Si(1)-C(1)-Zr(1)	94.46(10)
C(11)-Si(1)-C(6)	115.40(12)	C(3)-C(2)-C(1)	106.6(2)
C(12)-Si(1)-C(6)	114.27(12)	C(3)-C(2)-Si(2)	126.8(2)
C(1)-Si(1)-C(6)	92.81(11)	C(1)-C(2)-Si(2)	122.29(19)
C(11)-Si(1)-Zr(1)	104.11(9)	C(3)-C(2)-Zr(1)	78.22(15)
C(12)-Si(1)-Zr(1)	148.84(10)	C(1)-C(2)-Zr(1)	72.53(14)
C(1)-Si(1)-Zr(1)	49.61(8)	Si(2)-C(2)-Zr(1)	96.59(10)
C(6)-Si(1)-Zr(1)	48.82(7)	C(4)-C(3)-C(2)	110.3(2)
C(14)-Si(2)-C(2)	108.65(13)	C(4)-C(3)-Zr(1)	78.73(15)
C(14)-Si(2)-C(13)	108.87(14)	C(2)-C(3)-Zr(1)	68.70(14)
C(2)-Si(2)-C(13)	114.15(12)	C(3)-C(4)-C(5)	106.8(2)
C(14)-Si(2)-C(7)	115.25(12)	C(3)-C(4)-C(15)	125.9(2)
C(2)-Si(2)-C(7)	91.97(11)	C(5)-C(4)-C(15)	127.1(2)
C(13)-Si(2)-C(7)	116.92(13)	C(3)-C(4)-Zr(1)	70.15(14)
C(14)-Si(2)-Zr(1)	105.72(10)	C(5)-C(4)-Zr(1)	70.15(14)
C(2)-Si(2)-Zr(1)	48.45(8)	C(15)-C(4)-Zr(1)	128.44(16)
C(13)-Si(2)-Zr(1)	145.15(10)	C(4)-C(5)-C(1)	110.0(2)
C(7)-Si(2)-Zr(1)	48.17(8)	C(4)-C(5)-Zr(1)	78.52(14)
C(5)-C(1)-C(2)	106.2(2)	C(1)-C(5)-Zr(1)	68.53(13)
C(5)-C(1)-Si(1)	125.7(2)	C(10)-C(6)-C(7)	107.0(2)

C(10)-C(6)-Si(1)	128.03(19)	C(9)-C(10)-Zr(1)	76.75(14)
C(7)-C(6)-Si(1)	121.35(18)	C(6)-C(10)-Zr(1)	66.02(13)
C(10)-C(6)-Zr(1)	81.21(14)	C(26)-C(10)-Zr(1)	127.33(16)
C(7)-C(6)-Zr(1)	72.83(14)	C(16B)-C(15)-C(4)	112.0(3)
Si(1)-C(6)-Zr(1)	95.01(10)	C(16B)-C(15)-C(16A)	100.6(3)
C(8)-C(7)-C(6)	106.7(2)	C(4)-C(15)-C(16A)	112.99(13)
C(8)-C(7)-Si(2)	127.15(19)	C(16B)-C(15)-C(17)	109.1(3)
C(6)-C(7)-Si(2)	122.58(18)	C(4)-C(15)-C(17)	110.8(2)
C(8)-C(7)-Zr(1)	81.15(15)	C(16A)-C(15)-C(17)	110.92(14)
C(6)-C(7)-Zr(1)	71.61(13)	C(20)-C(17)-C(19)	108.3(2)
Si(2)-C(7)-Zr(1)	96.37(10)	C(20)-C(17)-C(18)	109.4(3)
C(9)-C(8)-C(7)	108.2(2)	C(19)-C(17)-C(18)	108.5(2)
C(9)-C(8)-C(21)	124.7(2)	C(20)-C(17)-C(15)	111.3(2)
C(7)-C(8)-C(21)	126.6(2)	C(19)-C(17)-C(15)	108.9(2)
C(9)-C(8)-Zr(1)	76.34(14)	C(18)-C(17)-C(15)	110.3(2)
C(7)-C(8)-Zr(1)	66.21(13)	C(8)-C(21)-C(24)	112.8(2)
C(21)-C(8)-Zr(1)	128.98(17)	C(8)-C(21)-C(22)	108.1(2)
C(8)-C(9)-C(10)	109.8(2)	C(24)-C(21)-C(22)	112.8(2)
C(8)-C(9)-Zr(1)	72.82(14)	C(23)-C(22)-C(21)	114.3(2)
C(10)-C(9)-Zr(1)	72.18(14)	C(25)-C(24)-C(21)	113.7(2)
C(9)-C(10)-C(6)	108.0(2)	C(10)-C(26)-C(29)	111.9(2)
C(9)-C(10)-C(26)	124.9(2)	C(10)-C(26)-C(27)	108.4(2)
C(6)-C(10)-C(26)	126.8(2)	C(29)-C(26)-C(27)	113.8(2)

C(28)-C(27)-C(26)	115.1(2)	C(42)#1-C(42)-C(46)#1	111.3(8)
C(30)-C(29)-C(26)	113.4(2)	C(47)#1-C(42)-C(46)#1	50.3(4)
C(45)#1-C(41)-C(46)#1	81.5(9)	C(47)-C(42)-C(46)#1	151.1(6)
C(45)#1-C(41)-C(44)#1	65.6(10)	C(43)-C(42)-C(46)#1	82.0(5)
C(46)#1-C(41)-C(44)#1	121.1(7)	C(43)#1-C(42)-C(46)#1	113.1(5)
C(45)#1-C(41)-C(42)	126.6(11)	C(41)-C(42)-C(46)#1	43.5(4)
C(46)#1-C(41)-C(42)	81.4(6)	C(42)#1-C(42)-C(44)#1	101.9(8)
C(44)#1-C(41)-C(42)	81.5(5)	C(47)#1-C(42)-C(44)#1	115.6(6)
C(42)#1-C(42)-C(47)#1	71.0(7)	C(47)-C(42)-C(44)#1	76.1(5)
C(42)#1-C(42)-C(47)	61.3(7)	C(43)-C(42)-C(44)#1	156.7(6)
C(47)#1-C(42)-C(47)	132.3(5)	C(43)#1-C(42)-C(44)#1	45.3(4)
C(42)#1-C(42)-C(43)	73.3(7)	C(41)-C(42)-C(44)#1	48.5(4)
C(47)#1-C(42)-C(43)	41.1(4)	C(46)#1-C(42)-C(44)#1	78.7(4)
C(47)-C(42)-C(43)	118.3(6)	C(47)#1-C(43)-C(42)	63.6(6)
C(42)#1-C(42)-C(43)#1	62.8(7)	C(47)#1-C(43)-C(44)	128.0(8)
C(47)#1-C(42)-C(43)#1	117.6(6)	C(42)-C(43)-C(44)	121.5(6)
C(47)-C(42)-C(43)#1	38.0(4)	C(47)#1-C(43)-C(42)#1	64.7(6)
C(43)-C(42)-C(43)#1	136.1(5)	C(42)-C(43)-C(42)#1	43.9(5)
C(42)#1-C(42)-C(41)	137.8(9)	C(44)-C(43)-C(42)#1	85.6(5)
C(47)#1-C(42)-C(41)	93.8(6)	C(45)-C(44)-C(43)	119.9(6)
C(47)-C(42)-C(41)	121.1(7)	C(45)-C(44)-C(41)#1	32.8(4)
C(43)-C(42)-C(41)	120.6(7)	C(43)-C(44)-C(41)#1	98.9(5)
C(43)#1-C(42)-C(41)	93.7(6)	C(45)-C(44)-C(42)#1	76.3(5)

C(43)-C(44)-C(42)#1	49.1(4)	C(45)-C(46)-C(42)#1	80.1(5)
C(41)#1-C(44)-C(42)#1	50.0(4)	C(47)-C(46)-C(42)#1	44.1(4)
C(41)#1-C(45)-C(44)	81.6(10)	C(43)#1-C(47)-C(42)#1	75.3(7)
C(41)#1-C(45)-C(46)	63.6(9)	C(43)#1-C(47)-C(42)	77.3(7)
C(44)-C(45)-C(46)	120.2(7)	C(42)#1-C(47)-C(42)	47.7(5)
C(41)#1-C(46)-C(45)	34.9(4)	C(43)#1-C(47)-C(46)	129.0(8)
C(41)#1-C(46)-C(47)	99.1(6)	C(42)#1-C(47)-C(46)	85.6(6)
C(45)-C(46)-C(47)	118.2(6)	C(42)-C(47)-C(46)	121.7(6)
C(41)#1-C(46)-C(42)#1	55.1(5)		

Symmetry transformations used to generate equivalent atoms:

#1 $-x, -y, -z + 1$

Table A.5. Anisotropic displacement parameters ($\text{\AA}^2 \times 10^4$) for (S)-3

The anisotropic displacement factor exponent takes the form: $-2\pi^2 [h^2 a^{*2} U^{11} + \dots + 2 h k a^* b^* U^{12}]$

	U^{11}	U^{22}	U^{33}	U^{23}	U^{13}	U^{12}
Zr(1)	127(1)	106(1)	111(1)	19(1)	34(1)	40(1)
Cl(1)	156(3)	183(3)	213(3)	59(3)	70(3)	60(3)
Cl(2)	264(4)	282(4)	133(3)	28(3)	32(3)	80(3)
Si(1)	173(4)	136(4)	122(4)	8(3)	38(3)	33(3)
Si(2)	141(4)	137(4)	190(4)	14(3)	59(3)	46(3)
C(1)	185(15)	113(13)	134(13)	−9(10)	47(11)	36(11)
C(2)	167(14)	107(12)	192(14)	18(10)	70(11)	70(11)
C(3)	182(15)	114(13)	172(14)	6(10)	26(11)	71(11)
C(4)	171(14)	108(13)	175(14)	14(10)	56(11)	63(11)
C(5)	164(14)	94(12)	158(13)	−22(10)	35(11)	36(11)
C(6)	157(14)	122(13)	134(13)	51(10)	67(11)	47(11)
C(7)	126(14)	134(13)	152(13)	30(10)	57(11)	8(11)
C(8)	159(14)	105(12)	141(13)	26(10)	59(11)	24(11)
C(9)	187(14)	108(12)	162(14)	20(10)	77(11)	44(11)
C(10)	171(14)	109(12)	160(13)	53(10)	67(11)	24(11)
C(11)	208(16)	202(14)	168(14)	14(11)	13(12)	26(12)
C(12)	275(17)	259(16)	181(15)	33(12)	100(13)	75(13)
C(13)	219(16)	204(15)	297(17)	21(12)	116(13)	38(12)
C(14)	195(16)	239(16)	302(17)	32(13)	38(13)	106(13)
C(15)	184(15)	164(14)	172(14)	59(11)	38(12)	41(11)

C(16A)	350(40)	190(30)	170(30)	60(20)	100(30)	60(30)
C(16B)	370(40)	270(30)	440(40)	220(30)	330(30)	220(30)
C(17)	341(18)	145(14)	201(15)	58(11)	86(13)	51(13)
C(18)	720(30)	174(16)	260(18)	25(14)	37(18)	-54(17)
C(19)	420(20)	198(15)	287(17)	104(13)	118(15)	50(14)
C(20)	550(20)	329(18)	356(19)	209(15)	265(17)	304(17)
C(21)	157(14)	136(13)	197(14)	1(11)	51(12)	33(11)
C(22)	169(15)	246(15)	212(15)	-17(12)	45(12)	-1(12)
C(23)	360(20)	321(18)	470(20)	162(16)	157(17)	12(15)
C(24)	222(16)	179(14)	224(15)	-41(12)	65(13)	45(12)
C(25)	320(19)	326(18)	226(16)	-85(13)	18(14)	102(15)
C(26)	167(14)	119(13)	185(14)	54(11)	40(11)	48(11)
C(27)	230(16)	244(15)	189(15)	89(12)	62(12)	131(13)
C(28)	387(19)	231(16)	287(17)	139(13)	186(15)	131(14)
C(29)	205(15)	211(15)	232(15)	114(12)	104(12)	98(12)
C(30)	208(16)	245(16)	436(19)	102(14)	128(15)	91(13)
C(41)	270(40)	670(60)	330(50)	-90(40)	50(40)	210(40)
C(42)	230(40)	330(30)	300(40)	-20(30)	90(30)	100(30)
C(43)	550(50)	280(40)	230(40)	80(30)	160(30)	270(40)
C(44)	340(40)	180(30)	390(40)	50(30)	100(30)	70(30)
C(45)	280(40)	390(50)	230(40)	20(30)	20(30)	40(40)
C(46)	530(50)	260(30)	330(40)	90(30)	140(40)	160(30)
C(47)	230(40)	370(40)	370(40)	100(30)	120(30)	120(30)

B. Appendix B

X-Ray Crystallographic Data for
(*S*)-MNThp_{Cy}ZrCl₂ [(*S*)-**4**, Chapter 1]

Table B.1. Crystal data and structure refinement for (S)-4: (CCDC_213422)

Empirical formula	$\text{C}_{32}\text{H}_{50}\text{Cl}_2\text{Si}_2\text{Zr} \cdot 1\frac{1}{2}(\text{CH}_2\text{Cl}_2)$
Formula weight	776.90
Crystallization Solvent	Dichloromethane
Crystal Habit	Plate
Crystal size	0.26 x 0.20 x 0.09 mm ³
Crystal color	Colorless

Data Collection

Preliminary Photos	Rotation
Type of diffractometer	Bruker SMART 1000
Wavelength	0.71073 Å MoK α
Data Collection Temperature	100(2) K
θ range for 20,102 reflections used in lattice determination	2.54 to 28.33°
Unit cell dimensions	$a = 13.2833(7)$ Å $b = 19.3805(10)$ Å $\beta = 107.1950(10)^\circ$ $c = 14.7651(8)$ Å
Volume	3631.2(3) Å ³
Z	4
Crystal system	Monoclinic
Space group	P2 ₁

Density (calculated)	1.428 Mg/m ³
F(000)	1628
Data collection program	Bruker SMART v5.054
θ range for data collection	1.44 to 28.37°
Completeness to $\theta = 28.37^\circ$	94.5%
Index ranges	$-17 \leq h \leq 16$, $-25 \leq k \leq 25$, $-19 \leq l \leq 19$
Data collection scan type	ω scans at 5 ϕ settings
Data reduction program	Bruker SAINT v6.022
Reflections collected	54,234
Independent reflections	16,726 [$R_{\text{int}} = 0.0645$]
Absorption coefficient	0.760 mm ⁻¹
Absorption correction	None
Max. and min. transmission (predicted)	0.9348 and 0.8269

Structure Solution and Refinement

Structure solution program	SHELXS-97 (Sheldrick, 1990)
Primary solution method	Direct methods
Secondary solution method	Difference Fourier map
Hydrogen placement	Geometric positions
Structure refinement program	SHELXL-97 (Sheldrick, 1997)
Refinement method	Full matrix least-squares on F^2
Data/restraints/parameters	16,726/1/765

Treatment of hydrogen atoms	Riding
Goodness-of-fit on F^2	1.130
Final R indices [$I > 2s(I)$, 12,842 reflections]	$R1 = 0.0374$, $wR2 = 0.0604$
R indices (all data)	$R1 = 0.0589$, $wR2 = 0.0643$
Type of weighting scheme used	Sigma
Weighting scheme used	$w = 1 / \sigma^2(Fo^2)$
Max shift/error	0.002
Average shift/error	0.000
Absolute structure parameter	-0.08(3)
Largest diff. peak and hole	1.171 and -0.758 e.Å ⁻³

Special Refinement Details

The crystals contain dichloromethane as a solvent of crystallization. There are three molecules of solvent per asymmetric unit with one site being disordered over at least two orientations. The carbon and hydrogen atoms of the alternate orientation(s) were not included in least squares refinement because they were not discernable in the electron density map.

Refinement of F^2 against all reflections. The weighted R-factor (wR) and goodness of fit (S) are based on F^2 , conventional R-factors (R) are based on F , with F set to zero for negative F^2 . The threshold expression of $F^2 > 2\sigma(F^2)$ is used only for calculating R-factors(gt) etc. and is not relevant to the choice of reflections for

refinement. R-factors based on F^2 are statistically about twice as large as those based on F , and R-factors based on all data will be even larger.

All esds (except the esd in the dihedral angle between two l.s. planes) are estimated using the full covariance matrix. The cell esds are taken into account individually in the estimation of esds in distances, angles and torsion angles; correlations between esds in cell parameters are only used when they are defined by crystal symmetry. An approximate (isotropic) treatment of cell esds is used for estimating esds involving l.s. planes.

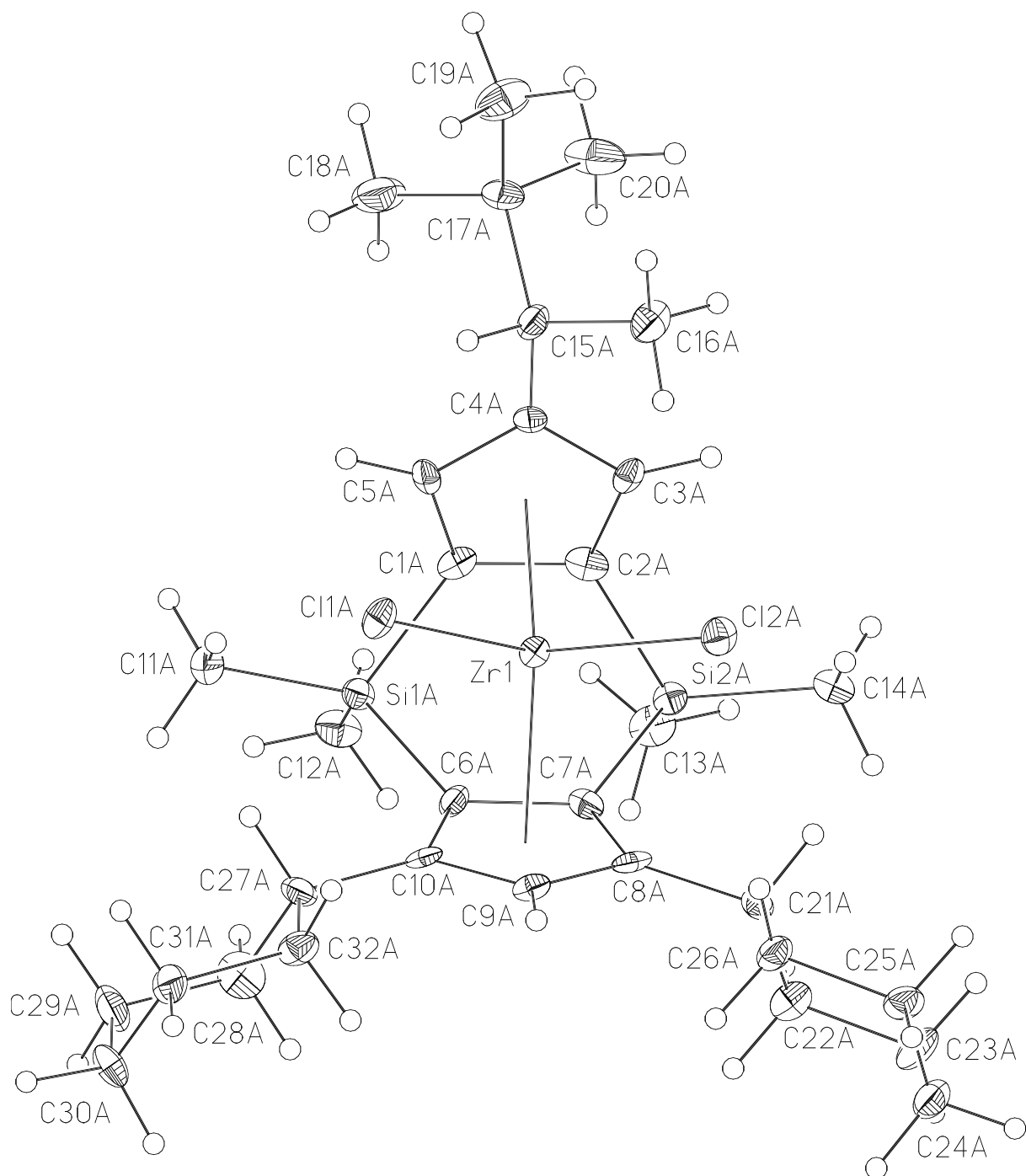


Figure B.1. ORTEP view of (S)-4.

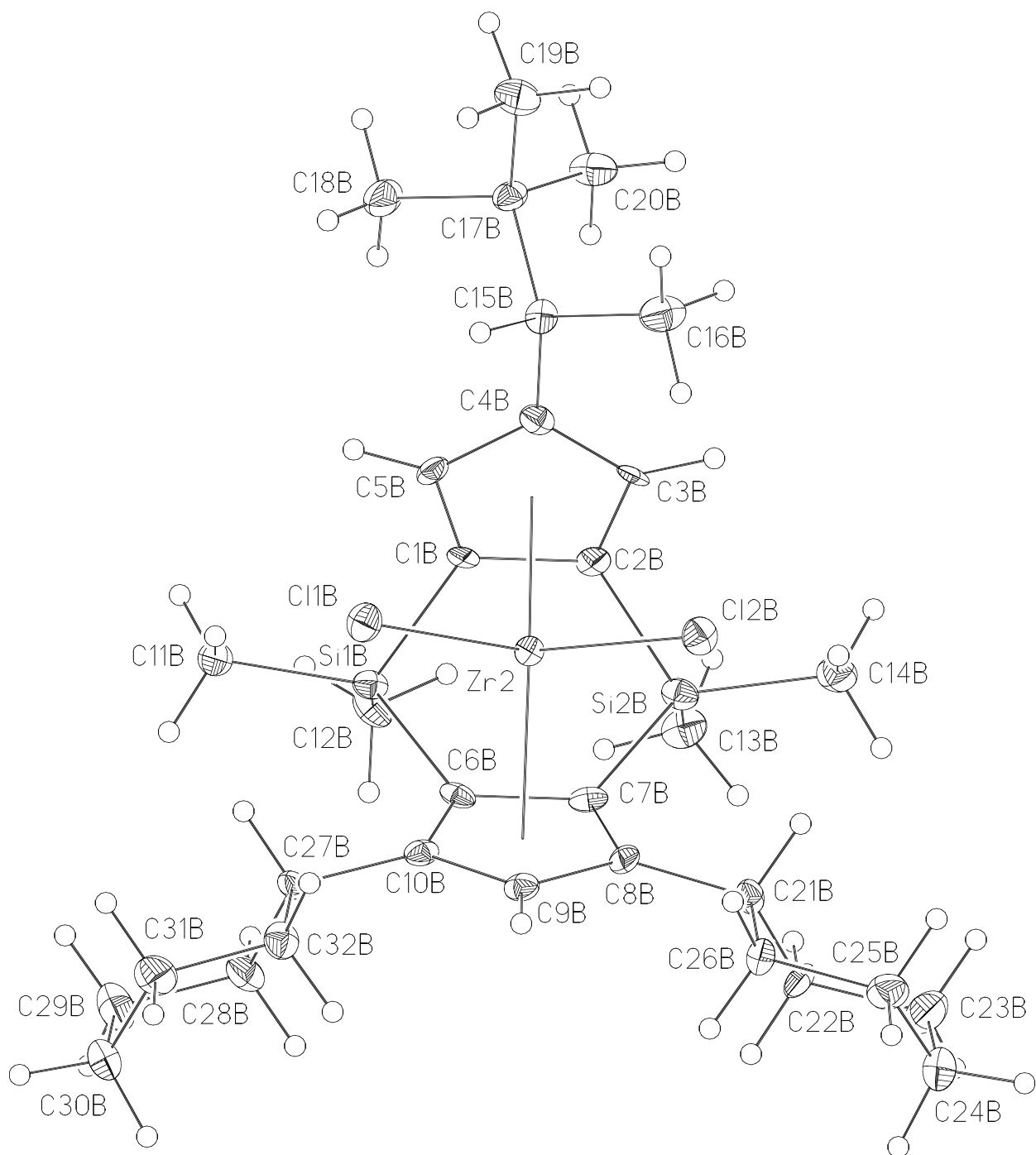


Figure B.2. ORTEP view for (S)-4.

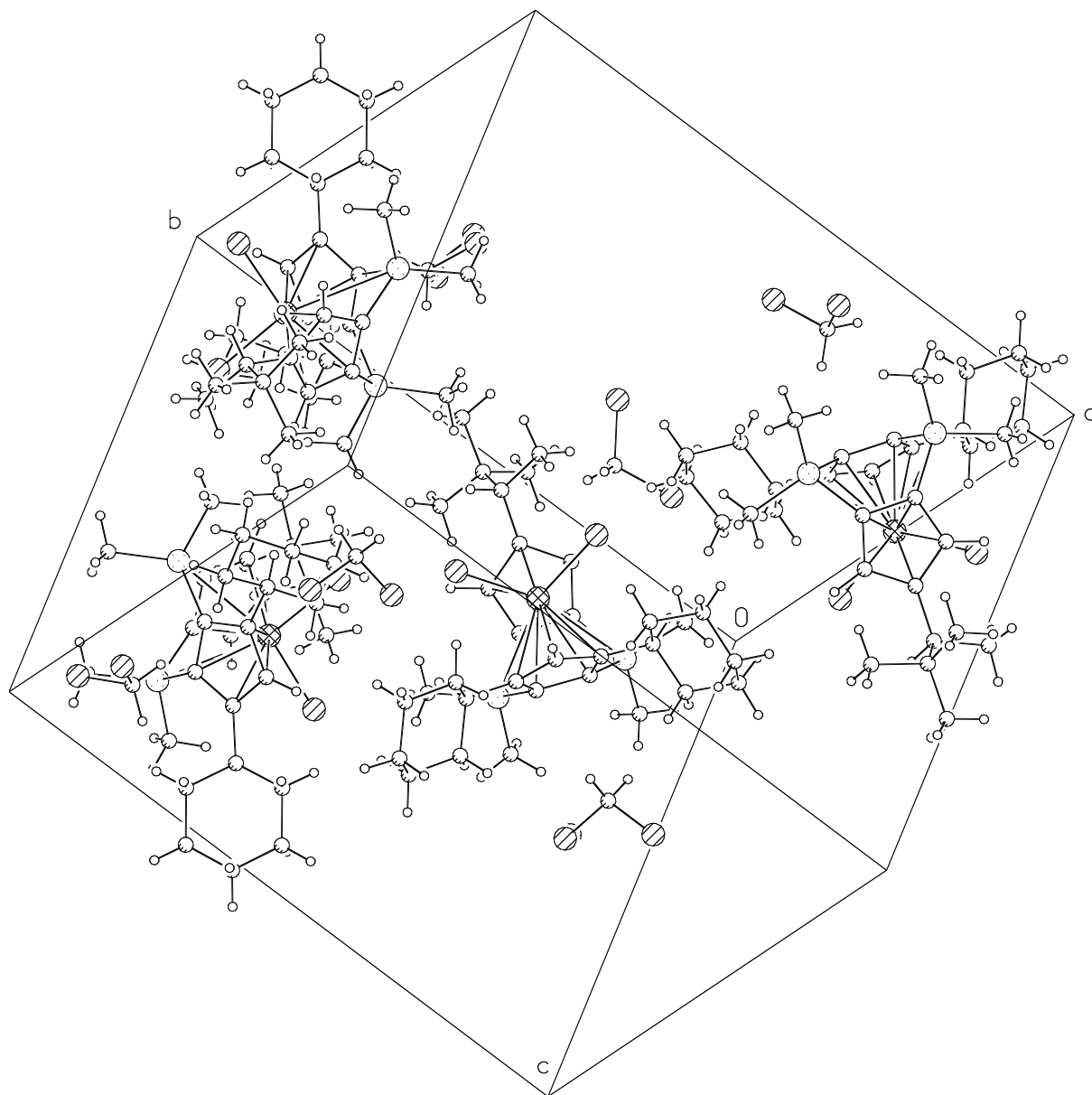


Figure B.3. Unit cell of X-ray structure of (S)-4.

Table B.2. Atomic coordinates and U_{eq} for (S)-4**Atomic coordinates ($\times 10^4$) and equivalent isotropic displacement parameters, U_{eq} ($\text{\AA}^2 \times 10^3$): (CCDC_213422).**

U_{eq} the trace of the orthogonalized U_{ij} tensor.

	x	y	z	U_{eq}
Zr(1)	4648(1)	9913(1)	3917(1)	11(1)
Cl(1A)	5002(1)	11108(1)	3624(1)	17(1)
Cl(2A)	3090(1)	9994(1)	4456(1)	17(1)
Si(1A)	6558(1)	9243(1)	3288(1)	13(1)
Si(2A)	4824(1)	8270(1)	4134(1)	14(1)
C(1A)	6376(3)	9368(2)	4492(3)	13(1)
C(2A)	5647(4)	8978(3)	4850(3)	16(1)
C(3A)	5406(3)	9398(2)	5554(3)	14(1)
C(4A)	5956(3)	10036(3)	5651(3)	13(1)
C(5A)	6534(3)	10001(3)	4981(3)	14(1)
C(6A)	5090(3)	9254(2)	2698(3)	14(1)
C(7A)	4356(4)	8834(2)	3050(3)	14(1)
C(8A)	3322(3)	9139(3)	2670(3)	14(1)
C(9A)	3447(4)	9729(2)	2153(3)	13(1)
C(10A)	4485(3)	9788(2)	2118(3)	13(1)
C(11A)	7265(4)	10012(3)	3038(3)	21(1)
C(12A)	7277(4)	8472(3)	3097(3)	20(1)
C(13A)	5582(4)	7484(3)	4006(3)	22(1)
C(14A)	3759(3)	8005(2)	4648(3)	18(1)

C(15A)	5947(3)	10615(3)	6308(3)	17(1)
C(16A)	4927(3)	10636(2)	6583(3)	22(1)
C(17A)	6957(3)	10624(2)	7201(3)	19(1)
C(18A)	7953(3)	10687(2)	6899(3)	35(1)
C(19A)	6898(3)	11263(2)	7824(3)	28(1)
C(20A)	7021(3)	9989(2)	7805(3)	33(1)
C(21A)	2283(4)	8847(2)	2690(3)	14(1)
C(22A)	2090(3)	8162(2)	2139(3)	18(1)
C(23A)	1050(3)	7833(2)	2125(3)	22(1)
C(24A)	141(3)	8327(2)	1699(3)	24(1)
C(25A)	300(3)	8993(2)	2262(3)	19(1)
C(26A)	1362(3)	9336(2)	2282(3)	17(1)
C(27A)	4860(4)	10281(3)	1492(3)	17(1)
C(28A)	5258(4)	9870(3)	787(3)	24(1)
C(29A)	5685(4)	10353(3)	159(3)	26(1)
C(30A)	4855(4)	10864(3)	−360(3)	24(1)
C(31A)	4440(4)	11269(3)	335(3)	22(1)
C(32A)	4026(4)	10794(2)	982(3)	18(1)
Zr(2)	9687(1)	1753(1)	3963(1)	11(1)
Cl(1B)	8186(1)	1615(1)	4572(1)	18(1)
Cl(2B)	9994(1)	579(1)	3541(1)	17(1)
Si(1B)	9910(1)	3393(1)	4259(1)	13(1)

Si(2B)	11576(1)	2417(1)	3330(1)	15(1)
C(1B)	10711(3)	2661(2)	4928(3)	9(1)
C(2B)	11429(3)	2267(2)	4538(3)	13(1)
C(3B)	11595(3)	1627(2)	5033(3)	11(1)
C(4B)	11032(3)	1607(3)	5692(3)	14(1)
C(5B)	10488(3)	2244(2)	5622(3)	13(1)
C(6B)	9398(3)	2850(2)	3149(3)	12(1)
C(7B)	10102(3)	2441(2)	2757(3)	13(1)
C(8B)	9468(4)	1929(2)	2160(3)	13(1)
C(9B)	8427(4)	1996(3)	2208(3)	13(1)
C(10B)	8370(4)	2562(2)	2773(3)	13(1)
C(11B)	8912(3)	3627(2)	4861(3)	17(1)
C(12B)	10698(3)	4175(3)	4162(3)	20(1)
C(13B)	12311(4)	3206(3)	3137(3)	22(1)
C(14B)	12262(3)	1655(3)	3019(3)	20(1)
C(15B)	11048(4)	1030(2)	6407(3)	13(1)
C(16B)	11396(3)	350(2)	6063(2)	23(1)
C(17B)	11739(3)	1228(2)	7423(3)	15(1)
C(18B)	11292(3)	1865(2)	7783(2)	24(1)
C(19B)	11735(3)	632(2)	8098(3)	25(1)
C(20B)	12866(3)	1392(2)	7437(3)	23(1)
C(21B)	9819(4)	1432(2)	1518(3)	14(1)
C(22B)	10225(4)	1842(3)	799(3)	19(1)

C(23B)	10653(4)	1371(3)	199(3)	27(1)
C(24B)	9819(4)	853(3)	−317(3)	27(1)
C(25B)	9371(4)	459(3)	360(3)	21(1)
C(26B)	8962(4)	929(3)	984(3)	18(1)
C(27B)	7349(3)	2875(2)	2874(3)	13(1)
C(28B)	7185(4)	3589(2)	2390(3)	19(1)
C(29B)	6186(3)	3936(2)	2487(3)	27(1)
C(30B)	5219(3)	3476(2)	2067(3)	25(1)
C(31B)	5384(4)	2755(3)	2512(3)	24(1)
C(32B)	6376(4)	2426(2)	2435(3)	17(1)
C(51)	4060(5)	7942(4)	937(4)	52(2)
Cl(5)	5289(1)	7888(1)	781(1)	48(1)
Cl(6)	3092(1)	7442(1)	149(1)	29(1)
C(52)	7669(6)	8551(4)	−427(5)	57(2)
Cl(7)	7516(2)	8942(1)	560(2)	59(1)
Cl(8)	7307(2)	7688(1)	−545(2)	45(1)
C(53)	1013(4)	8648(3)	9161(4)	35(1)
Cl(9)	2000(1)	9239(1)	9758(1)	28(1)
Cl(10)	−203(1)	9047(1)	8703(1)	44(1)

Table B.3. Selected bond lengths [Å] and angles [°] for (*S*)-4: (CCDC_213422)

Zr(1)-Cl(1A)	2.4267(12)	Zr(1)-Cl(2A)	2.4322(12)
Zr(1)-C(1A)	2.439(4)	Zr(1)-C(6A)	2.417(4)
Zr(1)-C(2A)	2.420(5)	Zr(1)-C(7A)	2.423(4)
Zr(1)-C(3A)	2.532(4)	Zr(1)-C(8A)	2.612(4)
Zr(1)-C(4A)	2.646(4)	Zr(1)-C(9A)	2.645(4)
Zr(1)-C(5A)	2.539(4)	Zr(1)-C(10A)	2.612(4)
Zr(2)-Cl(1B)	2.4321(12)	Zr(2)-Cl(2B)	2.4253(12)
Zr(2)-C(1B)	2.414(4)	Zr(2)-C(6B)	2.417(4)
Zr(2)-C(2B)	2.430(4)	Zr(2)-C(7B)	2.415(4)
Zr(2)-C(3B)	2.571(4)	Zr(2)-C(8B)	2.613(4)
Zr(2)-C(4B)	2.663(4)	Zr(2)-C(9B)	2.678(4)
Zr(2)-C(5B)	2.549(4)	Zr(2)-C(10B)	2.605(4)
Cl(1A)-Zr(1)-Cl(2A)	103.01(4)		
Cl(2B)-Zr(2)-Cl(1B)	102.09(4)		

Table B.4. Bond lengths [Å] and angles [°] for (S)-4: (CCDC_213422)

Zr(1)-C(6A)	2.417(4)	C(2A)-C(3A)	1.429(6)
Zr(1)-C(2A)	2.420(5)	C(3A)-C(4A)	1.422(6)
Zr(1)-C(7A)	2.423(4)	C(4A)-C(5A)	1.422(6)
Zr(1)-Cl(1A)	2.4267(12)	C(4A)-C(15A)	1.485(6)
Zr(1)-Cl(2A)	2.4322(12)	C(6A)-C(10A)	1.429(6)
Zr(1)-C(1A)	2.439(4)	C(6A)-C(7A)	1.479(6)
Zr(1)-C(3A)	2.532(4)	C(7A)-C(8A)	1.448(6)
Zr(1)-C(5A)	2.539(4)	C(8A)-C(9A)	1.410(6)
Zr(1)-C(10A)	2.612(4)	C(8A)-C(21A)	1.500(6)
Zr(1)-C(8A)	2.612(4)	C(9A)-C(10A)	1.400(6)
Zr(1)-C(9A)	2.645(4)	C(10A)-C(27A)	1.512(6)
Zr(1)-C(4A)	2.646(4)	C(15A)-C(16A)	1.527(5)
Si(1A)-C(12A)	1.840(5)	C(15A)-C(17A)	1.579(5)
Si(1A)-C(11A)	1.855(5)	C(17A)-C(20A)	1.508(5)
Si(1A)-C(1A)	1.880(5)	C(17A)-C(18A)	1.522(5)
Si(1A)-C(6A)	1.885(4)	C(17A)-C(19A)	1.558(5)
Si(2A)-C(14A)	1.865(5)	C(21A)-C(26A)	1.523(6)
Si(2A)-C(13A)	1.866(5)	C(21A)-C(22A)	1.538(6)
Si(2A)-C(2A)	1.875(5)	C(22A)-C(23A)	1.515(6)
Si(2A)-C(7A)	1.885(4)	C(23A)-C(24A)	1.524(6)
C(1A)-C(5A)	1.408(6)	C(24A)-C(25A)	1.516(6)
C(1A)-C(2A)	1.445(6)	C(25A)-C(26A)	1.552(6)

C(27A)-C(32A)	1.513(6)	Si(2B)-C(2B)	1.874(4)
C(27A)-C(28A)	1.524(6)	Si(2B)-C(13B)	1.880(5)
C(28A)-C(29A)	1.538(6)	Si(2B)-C(7B)	1.891(5)
C(29A)-C(30A)	1.512(7)	C(1B)-C(5B)	1.404(6)
C(30A)-C(31A)	1.518(6)	C(1B)-C(2B)	1.466(6)
C(31A)-C(32A)	1.540(6)	C(2B)-C(3B)	1.422(6)
Zr(2)-C(1B)	2.414(4)	C(3B)-C(4B)	1.392(6)
Zr(2)-C(7B)	2.415(4)	C(4B)-C(5B)	1.418(6)
Zr(2)-C(6B)	2.417(4)	C(4B)-C(15B)	1.534(6)
Zr(2)-Cl(2B)	2.4253(12)	C(6B)-C(10B)	1.427(6)
Zr(2)-C(2B)	2.430(4)	C(6B)-C(7B)	1.469(6)
Zr(2)-Cl(1B)	2.4321(12)	C(7B)-C(8B)	1.424(6)
Zr(2)-C(5B)	2.549(4)	C(8B)-C(9B)	1.412(6)
Zr(2)-C(3B)	2.571(4)	C(8B)-C(21B)	1.519(6)
Zr(2)-C(10B)	2.605(4)	C(9B)-C(10B)	1.392(6)
Zr(2)-C(8B)	2.613(4)	C(10B)-C(27B)	1.533(6)
Zr(2)-C(4B)	2.663(4)	C(15B)-C(16B)	1.532(5)
Zr(2)-C(9B)	2.678(4)	C(15B)-C(17B)	1.557(5)
Si(1B)-C(11B)	1.858(5)	C(17B)-C(20B)	1.524(5)
Si(1B)-C(12B)	1.870(5)	C(17B)-C(19B)	1.526(5)
Si(1B)-C(1B)	1.872(5)	C(17B)-C(18B)	1.532(5)
Si(1B)-C(6B)	1.897(5)	C(21B)-C(26B)	1.529(6)
Si(2B)-C(14B)	1.864(5)	C(21B)-C(22B)	1.545(6)

C(22B)-C(23B)	1.496(6)	C(2A)-Zr(1)-Cl(2A)	103.79(11)
C(23B)-C(24B)	1.522(7)	C(7A)-Zr(1)-Cl(2A)	102.09(11)
C(24B)-C(25B)	1.513(6)	Cl(1A)-Zr(1)-Cl(2A)	103.01(4)
C(25B)-C(26B)	1.507(6)	C(6A)-Zr(1)-C(1A)	67.66(14)
C(27B)-C(32B)	1.534(6)	C(2A)-Zr(1)-C(1A)	34.59(15)
C(27B)-C(28B)	1.544(6)	C(7A)-Zr(1)-C(1A)	78.31(15)
C(28B)-C(29B)	1.532(6)	Cl(1A)-Zr(1)-C(1A)	105.28(11)
C(29B)-C(30B)	1.535(6)	Cl(2A)-Zr(1)-C(1A)	135.89(11)
C(30B)-C(31B)	1.533(6)	C(6A)-Zr(1)-C(3A)	112.81(15)
C(31B)-C(32B)	1.498(6)	C(2A)-Zr(1)-C(3A)	33.45(13)
C(51)-Cl(5)	1.718(6)	C(7A)-Zr(1)-C(3A)	96.94(14)
C(51)-Cl(6)	1.750(6)	Cl(1A)-Zr(1)-C(3A)	120.18(11)
C(52)-Cl(7)	1.708(8)	Cl(2A)-Zr(1)-C(3A)	81.35(11)
C(52)-Cl(8)	1.734(7)	C(1A)-Zr(1)-C(3A)	55.23(14)
C(53)-Cl(10)	1.737(5)	C(6A)-Zr(1)-C(5A)	94.81(14)
C(53)-Cl(9)	1.768(5)	C(2A)-Zr(1)-C(5A)	54.80(16)
C(6A)-Zr(1)-C(2A)	79.39(15)	C(7A)-Zr(1)-C(5A)	111.09(16)
C(6A)-Zr(1)-C(7A)	35.58(14)	Cl(1A)-Zr(1)-C(5A)	80.70(12)
C(2A)-Zr(1)-C(7A)	68.29(15)	Cl(2A)-Zr(1)-C(5A)	124.96(10)
C(6A)-Zr(1)-Cl(1A)	105.59(11)	C(1A)-Zr(1)-C(5A)	32.78(14)
C(2A)-Zr(1)-Cl(1A)	135.48(12)	C(3A)-Zr(1)-C(5A)	52.77(14)
C(7A)-Zr(1)-Cl(1A)	137.62(11)	C(6A)-Zr(1)-C(10A)	32.73(14)
C(6A)-Zr(1)-Cl(2A)	134.05(11)	C(2A)-Zr(1)-C(10A)	112.11(15)

C(7A)-Zr(1)-C(10A)	55.28(14)	C(10A)-Zr(1)-C(9A)	30.88(13)
Cl(1A)-Zr(1)-C(10A)	82.49(11)	C(8A)-Zr(1)-C(9A)	31.10(14)
Cl(2A)-Zr(1)-C(10A)	121.05(10)	C(6A)-Zr(1)-C(4A)	122.26(14)
C(1A)-Zr(1)-C(10A)	95.78(14)	C(2A)-Zr(1)-C(4A)	54.83(15)
C(3A)-Zr(1)-C(10A)	145.54(15)	C(7A)-Zr(1)-C(4A)	123.09(15)
C(5A)-Zr(1)-C(10A)	113.92(14)	Cl(1A)-Zr(1)-C(4A)	88.86(11)
C(6A)-Zr(1)-C(8A)	55.49(14)	Cl(2A)-Zr(1)-C(4A)	93.25(10)
C(2A)-Zr(1)-C(8A)	96.54(15)	C(1A)-Zr(1)-C(4A)	54.63(14)
C(7A)-Zr(1)-C(8A)	33.15(14)	C(3A)-Zr(1)-C(4A)	31.77(14)
Cl(1A)-Zr(1)-C(8A)	123.20(11)	C(5A)-Zr(1)-C(4A)	31.75(13)
Cl(2A)-Zr(1)-C(8A)	78.79(10)	C(10A)-Zr(1)-C(4A)	145.67(14)
C(1A)-Zr(1)-C(8A)	111.46(15)	C(8A)-Zr(1)-C(4A)	147.88(15)
C(3A)-Zr(1)-C(8A)	116.21(15)	C(9A)-Zr(1)-C(4A)	175.67(14)
C(5A)-Zr(1)-C(8A)	144.22(15)	C(12A)-Si(1A)-C(11A)	107.8(2)
C(10A)-Zr(1)-C(8A)	52.70(14)	C(12A)-Si(1A)-C(1A)	117.8(2)
C(6A)-Zr(1)-C(9A)	53.41(14)	C(11A)-Si(1A)-C(1A)	107.4(2)
C(2A)-Zr(1)-C(9A)	121.93(15)	C(12A)-Si(1A)-C(6A)	116.8(2)
C(7A)-Zr(1)-C(9A)	53.66(14)	C(11A)-Si(1A)-C(6A)	114.5(2)
Cl(1A)-Zr(1)-C(9A)	92.62(10)	C(1A)-Si(1A)-C(6A)	91.79(19)
Cl(2A)-Zr(1)-C(9A)	90.38(11)	C(12A)-Si(1A)-Zr(1)	149.35(17)
C(1A)-Zr(1)-C(9A)	121.04(15)	C(11A)-Si(1A)-Zr(1)	102.85(17)
C(3A)-Zr(1)-C(9A)	147.17(14)	C(1A)-Si(1A)-Zr(1)	48.91(13)
C(5A)-Zr(1)-C(9A)	144.66(14)	C(6A)-Si(1A)-Zr(1)	48.24(13)

C(14A)-Si(2A)-C(13A)	108.3(2)	C(4A)-C(3A)-Zr(1)	78.5(3)
C(14A)-Si(2A)-C(2A)	111.0(2)	C(2A)-C(3A)-Zr(1)	69.0(2)
C(13A)-Si(2A)-C(2A)	114.3(2)	C(3A)-C(4A)-C(5A)	104.8(4)
C(14A)-Si(2A)-C(7A)	114.0(2)	C(3A)-C(4A)-C(15A)	128.3(4)
C(13A)-Si(2A)-C(7A)	116.1(2)	C(5A)-C(4A)-C(15A)	126.9(4)
C(2A)-Si(2A)-C(7A)	92.6(2)	C(3A)-C(4A)-Zr(1)	69.7(2)
C(14A)-Si(2A)-Zr(1)	105.86(15)	C(5A)-C(4A)-Zr(1)	70.0(2)
C(13A)-Si(2A)-Zr(1)	145.81(17)	C(15A)-C(4A)-Zr(1)	124.8(3)
C(2A)-Si(2A)-Zr(1)	48.80(14)	C(1A)-C(5A)-C(4A)	111.6(4)
C(7A)-Si(2A)-Zr(1)	48.89(14)	C(1A)-C(5A)-Zr(1)	69.7(2)
C(5A)-C(1A)-C(2A)	106.4(4)	C(4A)-C(5A)-Zr(1)	78.3(2)
C(5A)-C(1A)-Si(1A)	123.8(4)	C(10A)-C(6A)-C(7A)	107.3(4)
C(2A)-C(1A)-Si(1A)	124.5(3)	C(10A)-C(6A)-Si(1A)	127.4(3)
C(5A)-C(1A)-Zr(1)	77.5(3)	C(7A)-C(6A)-Si(1A)	122.0(3)
C(2A)-C(1A)-Zr(1)	72.0(3)	C(10A)-C(6A)-Zr(1)	81.2(3)
Si(1A)-C(1A)-Zr(1)	95.58(17)	C(7A)-C(6A)-Zr(1)	72.4(2)
C(3A)-C(2A)-C(1A)	106.7(4)	Si(1A)-C(6A)-Zr(1)	96.17(17)
C(3A)-C(2A)-Si(2A)	127.5(4)	C(8A)-C(7A)-C(6A)	106.7(4)
C(1A)-C(2A)-Si(2A)	121.2(3)	C(8A)-C(7A)-Si(2A)	127.1(3)
C(3A)-C(2A)-Zr(1)	77.6(3)	C(6A)-C(7A)-Si(2A)	122.1(3)
C(1A)-C(2A)-Zr(1)	73.4(2)	C(8A)-C(7A)-Zr(1)	80.6(3)
Si(2A)-C(2A)-Zr(1)	95.54(18)	C(6A)-C(7A)-Zr(1)	72.0(2)
C(4A)-C(3A)-C(2A)	110.4(4)	Si(2A)-C(7A)-Zr(1)	95.21(17)

C(9A)-C(8A)-C(7A)	106.9(4)	C(19A)-C(17A)-C(15A)	108.9(3)
C(9A)-C(8A)-C(21A)	124.9(4)	C(8A)-C(21A)-C(26A)	113.2(4)
C(7A)-C(8A)-C(21A)	127.7(4)	C(8A)-C(21A)-C(22A)	109.1(4)
C(9A)-C(8A)-Zr(1)	75.7(3)	C(26A)-C(21A)-C(22A)	109.8(4)
C(7A)-C(8A)-Zr(1)	66.2(2)	C(23A)-C(22A)-C(21A)	112.4(4)
C(21A)-C(8A)-Zr(1)	129.5(3)	C(22A)-C(23A)-C(24A)	110.4(3)
C(10A)-C(9A)-C(8A)	111.2(4)	C(25A)-C(24A)-C(23A)	110.1(3)
C(10A)-C(9A)-Zr(1)	73.3(2)	C(24A)-C(25A)-C(26A)	110.7(4)
C(8A)-C(9A)-Zr(1)	73.2(2)	C(21A)-C(26A)-C(25A)	111.2(4)
C(9A)-C(10A)-C(6A)	107.7(4)	C(10A)-C(27A)-C(32A)	113.2(4)
C(9A)-C(10A)-C(27A)	125.5(4)	C(10A)-C(27A)-C(28A)	109.3(4)
C(6A)-C(10A)-C(27A)	126.5(4)	C(32A)-C(27A)-C(28A)	110.7(4)
C(9A)-C(10A)-Zr(1)	75.9(2)	C(27A)-C(28A)-C(29A)	111.0(4)
C(6A)-C(10A)-Zr(1)	66.1(2)	C(30A)-C(29A)-C(28A)	111.1(4)
C(27A)-C(10A)-Zr(1)	128.3(3)	C(29A)-C(30A)-C(31A)	110.5(4)
C(4A)-C(15A)-C(16A)	111.9(4)	C(30A)-C(31A)-C(32A)	112.2(4)
C(4A)-C(15A)-C(17A)	112.7(4)	C(27A)-C(32A)-C(31A)	111.0(4)
C(16A)-C(15A)-C(17A)	112.2(3)	C(1B)-Zr(2)-C(7B)	79.73(14)
C(20A)-C(17A)-C(18A)	109.6(4)	C(1B)-Zr(2)-C(6B)	68.39(14)
C(20A)-C(17A)-C(19A)	107.8(3)	C(7B)-Zr(2)-C(6B)	35.40(14)
C(18A)-C(17A)-C(19A)	108.0(3)	C(1B)-Zr(2)-Cl(2B)	136.64(11)
C(20A)-C(17A)-C(15A)	111.7(3)	C(7B)-Zr(2)-Cl(2B)	103.68(12)
C(18A)-C(17A)-C(15A)	110.7(3)	C(6B)-Zr(2)-Cl(2B)	135.39(11)

C(1B)-Zr(2)-C(2B)	35.24(14)	C(7B)-Zr(2)-C(10B)	54.87(15)
C(7B)-Zr(2)-C(2B)	68.32(15)	C(6B)-Zr(2)-C(10B)	32.74(14)
C(6B)-Zr(2)-C(2B)	78.97(15)	Cl(2B)-Zr(2)-C(10B)	121.44(10)
Cl(2B)-Zr(2)-C(2B)	105.01(12)	C(2B)-Zr(2)-C(10B)	111.70(15)
C(1B)-Zr(2)-Cl(1B)	104.03(11)	Cl(1B)-Zr(2)-C(10B)	81.68(10)
C(7B)-Zr(2)-Cl(1B)	136.39(11)	C(5B)-Zr(2)-C(10B)	115.46(14)
C(6B)-Zr(2)-Cl(1B)	104.70(11)	C(3B)-Zr(2)-C(10B)	144.59(15)
Cl(2B)-Zr(2)-Cl(1B)	102.09(4)	C(1B)-Zr(2)-C(8B)	112.32(14)
C(2B)-Zr(2)-Cl(1B)	135.73(11)	C(7B)-Zr(2)-C(8B)	32.61(14)
C(1B)-Zr(2)-C(5B)	32.72(13)	C(6B)-Zr(2)-C(8B)	54.90(14)
C(7B)-Zr(2)-C(5B)	112.43(15)	Cl(2B)-Zr(2)-C(8B)	80.66(11)
C(6B)-Zr(2)-C(5B)	96.30(14)	C(2B)-Zr(2)-C(8B)	96.33(14)
Cl(2B)-Zr(2)-C(5B)	122.88(11)	Cl(1B)-Zr(2)-C(8B)	122.31(10)
C(2B)-Zr(2)-C(5B)	55.09(14)	C(5B)-Zr(2)-C(8B)	145.04(15)
Cl(1B)-Zr(2)-C(5B)	80.81(11)	C(3B)-Zr(2)-C(8B)	115.52(14)
C(1B)-Zr(2)-C(3B)	54.93(15)	C(10B)-Zr(2)-C(8B)	51.99(14)
C(7B)-Zr(2)-C(3B)	96.17(14)	C(1B)-Zr(2)-C(4B)	53.87(14)
C(6B)-Zr(2)-C(3B)	111.85(15)	C(7B)-Zr(2)-C(4B)	122.09(15)
Cl(2B)-Zr(2)-C(3B)	81.88(11)	C(6B)-Zr(2)-C(4B)	122.23(15)
C(2B)-Zr(2)-C(3B)	32.89(14)	Cl(2B)-Zr(2)-C(4B)	91.74(11)
Cl(1B)-Zr(2)-C(3B)	121.95(10)	C(2B)-Zr(2)-C(4B)	53.77(14)
C(5B)-Zr(2)-C(3B)	52.38(14)	Cl(1B)-Zr(2)-C(4B)	91.41(10)
C(1B)-Zr(2)-C(10B)	96.24(15)	C(5B)-Zr(2)-C(4B)	31.49(14)

C(3B)-Zr(2)-C(4B)	30.79(13)	C(6B)-Si(1B)-Zr(2)	48.54(13)
C(10B)-Zr(2)-C(4B)	146.81(14)	C(14B)-Si(2B)-C(2B)	107.9(2)
C(8B)-Zr(2)-C(4B)	146.25(14)	C(14B)-Si(2B)-C(13B)	107.1(2)
C(1B)-Zr(2)-C(9B)	121.65(15)	C(2B)-Si(2B)-C(13B)	118.4(2)
C(7B)-Zr(2)-C(9B)	53.33(14)	C(14B)-Si(2B)-C(7B)	115.2(2)
C(6B)-Zr(2)-C(9B)	53.26(14)	C(2B)-Si(2B)-C(7B)	92.54(19)
Cl(2B)-Zr(2)-C(9B)	91.22(11)	C(13B)-Si(2B)-C(7B)	115.3(2)
C(2B)-Zr(2)-C(9B)	121.62(15)	C(14B)-Si(2B)-Zr(2)	103.65(16)
Cl(1B)-Zr(2)-C(9B)	91.78(10)	C(2B)-Si(2B)-Zr(2)	49.24(13)
C(5B)-Zr(2)-C(9B)	145.89(15)	C(13B)-Si(2B)-Zr(2)	149.26(17)
C(3B)-Zr(2)-C(9B)	146.28(14)	C(7B)-Si(2B)-Zr(2)	48.83(13)
C(10B)-Zr(2)-C(9B)	30.52(13)	C(5B)-C(1B)-C(2B)	106.8(4)
C(8B)-Zr(2)-C(9B)	30.92(13)	C(5B)-C(1B)-Si(1B)	127.7(3)
C(4B)-Zr(2)-C(9B)	175.11(14)	C(2B)-C(1B)-Si(1B)	121.5(3)
C(11B)-Si(1B)-C(12B)	109.5(2)	C(5B)-C(1B)-Zr(2)	78.9(3)
C(11B)-Si(1B)-C(1B)	107.9(2)	C(2B)-C(1B)-Zr(2)	73.0(2)
C(12B)-Si(1B)-C(1B)	114.3(2)	Si(1B)-C(1B)-Zr(2)	96.18(17)
C(11B)-Si(1B)-C(6B)	115.1(2)	C(3B)-C(2B)-C(1B)	105.8(4)
C(12B)-Si(1B)-C(6B)	116.7(2)	C(3B)-C(2B)-Si(2B)	125.5(4)
C(1B)-Si(1B)-C(6B)	92.18(19)	C(1B)-C(2B)-Si(2B)	123.7(3)
C(11B)-Si(1B)-Zr(2)	104.84(15)	C(3B)-C(2B)-Zr(2)	79.0(3)
C(12B)-Si(1B)-Zr(2)	145.33(16)	C(1B)-C(2B)-Zr(2)	71.8(2)
C(1B)-Si(1B)-Zr(2)	48.38(13)	Si(2B)-C(2B)-Zr(2)	95.01(17)

C(4B)-C(3B)-C(2B)	110.5(4)	Si(2B)-C(7B)-Zr(2)	95.07(17)
C(4B)-C(3B)-Zr(2)	78.3(3)	C(9B)-C(8B)-C(7B)	108.2(4)
C(2B)-C(3B)-Zr(2)	68.1(2)	C(9B)-C(8B)-C(21B)	125.2(4)
C(3B)-C(4B)-C(5B)	107.0(4)	C(7B)-C(8B)-C(21B)	126.4(4)
C(3B)-C(4B)-C(15B)	126.9(4)	C(9B)-C(8B)-Zr(2)	77.1(2)
C(5B)-C(4B)-C(15B)	126.0(4)	C(7B)-C(8B)-Zr(2)	66.0(2)
C(3B)-C(4B)-Zr(2)	70.9(2)	C(21B)-C(8B)-Zr(2)	126.2(3)
C(5B)-C(4B)-Zr(2)	69.8(2)	C(10B)-C(9B)-C(8B)	109.3(4)
C(15B)-C(4B)-Zr(2)	127.3(3)	C(10B)-C(9B)-Zr(2)	71.8(2)
C(1B)-C(5B)-C(4B)	109.9(4)	C(8B)-C(9B)-Zr(2)	72.0(2)
C(1B)-C(5B)-Zr(2)	68.4(2)	C(9B)-C(10B)-C(6B)	109.0(4)
C(4B)-C(5B)-Zr(2)	78.7(3)	C(9B)-C(10B)-C(27B)	125.2(4)
C(10B)-C(6B)-C(7B)	106.4(4)	C(6B)-C(10B)-C(27B)	125.4(4)
C(10B)-C(6B)-Si(1B)	127.7(3)	C(9B)-C(10B)-Zr(2)	77.7(3)
C(7B)-C(6B)-Si(1B)	122.2(3)	C(6B)-C(10B)-Zr(2)	66.4(2)
C(10B)-C(6B)-Zr(2)	80.9(3)	C(27B)-C(10B)-Zr(2)	127.6(3)
C(7B)-C(6B)-Zr(2)	72.2(2)	C(16B)-C(15B)-C(4B)	110.0(3)
Si(1B)-C(6B)-Zr(2)	95.44(16)	C(16B)-C(15B)-C(17B)	112.4(3)
C(8B)-C(7B)-C(6B)	106.9(4)	C(4B)-C(15B)-C(17B)	111.6(3)
C(8B)-C(7B)-Si(2B)	127.2(4)	C(20B)-C(17B)-C(19B)	110.0(3)
C(6B)-C(7B)-Si(2B)	122.2(3)	C(20B)-C(17B)-C(18B)	107.9(3)
C(8B)-C(7B)-Zr(2)	81.4(3)	C(19B)-C(17B)-C(18B)	107.8(3)
C(6B)-C(7B)-Zr(2)	72.4(2)	C(20B)-C(17B)-C(15B)	111.2(3)

C(19B)-C(17B)-C(15B)	109.1(3)	C(10B)-C(27B)-C(28B)	108.5(4)
C(18B)-C(17B)-C(15B)	110.7(3)	C(32B)-C(27B)-C(28B)	109.1(3)
C(8B)-C(21B)-C(26B)	114.0(4)	C(29B)-C(28B)-C(27B)	111.0(4)
C(8B)-C(21B)-C(22B)	109.7(4)	C(28B)-C(29B)-C(30B)	110.6(4)
C(26B)-C(21B)-C(22B)	109.4(4)	C(31B)-C(30B)-C(29B)	111.1(4)
C(23B)-C(22B)-C(21B)	111.3(4)	C(32B)-C(31B)-C(30B)	111.9(4)
C(22B)-C(23B)-C(24B)	110.5(4)	C(31B)-C(32B)-C(27B)	112.1(4)
C(25B)-C(24B)-C(23B)	111.9(4)	Cl(5)-C(51)-Cl(6)	114.7(3)
C(26B)-C(25B)-C(24B)	112.4(4)	Cl(7)-C(52)-Cl(8)	114.5(4)
C(25B)-C(26B)-C(21B)	110.7(4)	Cl(10)-C(53)-Cl(9)	111.9(3)
C(10B)-C(27B)-C(32B)	113.2(4)		

Table B.5. Anisotropic displacement parameters ($\text{\AA}^2 \times 10^4$) for (S)-4

The anisotropic displacement factor exponent takes the form: $-2\pi^2 [h^2 a^{*2} U^{11} + \dots + 2 h k a^* b^* U^{12}]$

	U ¹¹	U ²²	U ³³	U ²³	U ¹³	U ¹²
Zr(1)	106(2)	102(2)	132(2)	3(2)	30(2)	10(2)
Cl(1A)	156(6)	119(6)	241(6)	10(5)	47(5)	−24(5)
Cl(2A)	129(5)	199(6)	200(5)	−14(5)	64(4)	21(5)
Si(1A)	120(7)	156(8)	124(6)	0(6)	37(5)	13(6)
Si(2A)	150(7)	103(6)	150(6)	−10(5)	43(5)	5(5)
C(1A)	110(20)	90(20)	170(20)	−12(19)	−3(19)	35(19)
C(2A)	190(30)	130(30)	140(20)	20(20)	18(19)	80(20)
C(3A)	70(20)	130(30)	170(20)	40(20)	−4(18)	8(19)
C(4A)	100(20)	170(30)	90(20)	30(20)	−17(17)	20(20)
C(5A)	90(20)	200(30)	120(20)	80(20)	21(17)	30(20)
C(6A)	100(20)	150(30)	150(20)	0(20)	14(19)	−40(20)
C(7A)	190(30)	120(20)	110(20)	4(18)	41(19)	10(20)
C(8A)	100(20)	180(30)	110(20)	−73(19)	−17(18)	10(20)
C(9A)	150(20)	70(20)	120(20)	15(17)	−28(18)	4(18)
C(10A)	110(20)	120(20)	100(20)	−29(18)	−38(17)	−18(19)
C(11A)	200(30)	260(30)	200(30)	−20(20)	90(20)	−60(30)
C(12A)	190(30)	230(30)	180(30)	−30(20)	50(20)	80(20)
C(13A)	240(30)	160(30)	240(20)	10(20)	30(20)	30(20)
C(14A)	210(20)	180(20)	140(20)	2(17)	45(18)	33(19)
C(15A)	120(20)	180(30)	180(20)	30(20)	11(18)	−40(20)

C(16A)	170(20)	220(20)	290(20)	−102(17)	106(17)	−18(16)
C(17A)	230(20)	190(20)	130(20)	−55(17)	43(17)	−6(18)
C(18A)	180(20)	610(30)	230(20)	−130(20)	13(18)	−50(20)
C(19A)	220(20)	250(20)	330(30)	−118(19)	18(19)	24(19)
C(20A)	470(30)	270(20)	190(20)	−46(19)	3(19)	20(20)
C(21A)	180(20)	130(20)	100(20)	14(16)	46(17)	−9(18)
C(22A)	150(20)	150(20)	230(20)	1(18)	16(18)	26(17)
C(23A)	200(20)	130(20)	310(30)	−42(19)	20(19)	−68(17)
C(24A)	170(20)	270(20)	220(20)	27(19)	3(18)	−84(18)
C(25A)	130(20)	230(20)	160(20)	3(18)	−3(17)	12(18)
C(26A)	110(20)	190(20)	180(20)	5(18)	6(17)	−16(18)
C(27A)	150(30)	260(30)	90(20)	0(20)	30(20)	0(20)
C(28A)	280(30)	170(30)	270(30)	10(20)	100(20)	90(30)
C(29A)	270(30)	340(30)	200(30)	60(20)	140(20)	−10(30)
C(30A)	330(30)	260(30)	150(20)	120(20)	80(20)	−40(20)
C(31A)	260(30)	190(30)	190(20)	80(20)	30(20)	−90(20)
C(32A)	170(30)	160(30)	180(20)	30(20)	−20(20)	0(20)
Zr(2)	112(2)	103(2)	115(2)	−6(2)	34(2)	−11(2)
Cl(1B)	164(6)	194(6)	192(5)	−2(5)	83(4)	−18(5)
Cl(2B)	179(6)	130(6)	191(6)	−31(5)	45(5)	−16(5)
Si(1B)	154(7)	100(6)	124(6)	2(5)	8(5)	−4(5)
Si(2B)	114(7)	164(8)	154(7)	27(6)	25(5)	−16(6)
C(1B)	70(20)	90(20)	80(20)	−25(18)	−46(17)	−20(18)

C(2B)	60(20)	190(30)	100(20)	-29(19)	-6(18)	-50(20)
C(3B)	90(20)	90(20)	100(20)	21(18)	-35(17)	26(19)
C(4B)	140(20)	100(30)	130(20)	-19(19)	-10(18)	-4(19)
C(5B)	130(20)	170(30)	70(20)	-38(19)	22(18)	-20(20)
C(6B)	90(20)	140(20)	130(20)	73(19)	21(18)	-3(19)
C(7B)	170(30)	120(20)	90(20)	60(19)	38(19)	-30(20)
C(8B)	170(30)	150(30)	100(20)	27(18)	70(19)	20(20)
C(9B)	110(20)	190(30)	100(20)	25(18)	33(18)	-19(19)
C(10B)	200(30)	90(20)	90(20)	17(17)	28(19)	10(20)
C(11B)	200(20)	140(20)	150(20)	-26(17)	24(18)	23(18)
C(12B)	200(30)	130(20)	270(20)	40(20)	50(20)	20(20)
C(13B)	200(30)	260(30)	200(30)	10(20)	70(20)	-70(20)
C(14B)	130(30)	280(30)	180(20)	10(20)	20(20)	0(20)
C(15B)	180(20)	70(20)	160(20)	55(18)	104(18)	-11(19)
C(16B)	320(20)	160(18)	170(20)	2(15)	31(17)	-10(16)
C(17B)	180(20)	150(20)	110(20)	24(16)	53(16)	-1(17)
C(18B)	370(20)	170(20)	164(19)	-7(16)	78(18)	69(18)
C(19B)	300(20)	220(20)	220(20)	95(18)	63(19)	59(19)
C(20B)	200(20)	280(20)	170(20)	46(17)	10(16)	-22(17)
C(21B)	130(20)	120(20)	160(20)	-32(19)	33(19)	10(20)
C(22B)	200(30)	290(30)	110(20)	-40(20)	70(20)	30(20)
C(23B)	310(30)	330(30)	200(30)	-30(20)	100(20)	0(30)
C(24B)	280(30)	300(30)	230(30)	-40(20)	90(20)	100(30)

C(25B)	220(30)	230(30)	160(20)	−30(20)	10(20)	0(20)
C(26B)	200(30)	190(30)	160(20)	−20(20)	80(20)	50(20)
C(27B)	100(20)	140(20)	120(20)	−21(17)	−12(16)	19(18)
C(28B)	180(20)	150(20)	220(20)	24(18)	23(18)	36(18)
C(29B)	240(20)	240(20)	340(30)	20(20)	100(20)	77(19)
C(30B)	200(20)	300(30)	240(20)	10(20)	61(19)	109(19)
C(31B)	110(20)	370(30)	220(20)	0(20)	18(18)	−5(19)
C(32B)	190(20)	130(20)	200(20)	14(18)	74(19)	8(18)
C(51)	370(40)	610(40)	590(40)	−320(40)	170(30)	−80(30)
Cl(5)	314(7)	378(7)	761(9)	−251(7)	181(7)	−42(5)
Cl(6)	316(7)	266(7)	284(7)	−48(6)	63(6)	−34(6)
C(52)	510(50)	620(50)	490(50)	210(40)	10(40)	−260(40)
Cl(7)	491(15)	461(16)	911(19)	−13(14)	363(14)	104(11)
Cl(8)	466(14)	433(14)	461(13)	113(11)	150(10)	137(11)
C(53)	240(30)	260(30)	490(30)	−250(30)	40(20)	−20(20)
Cl(9)	393(8)	207(7)	218(6)	−25(5)	37(5)	−72(6)
Cl(10)	343(7)	344(6)	549(8)	−136(6)	−17(6)	80(5)

C. Appendix C

X-Ray Crystallographic Data for
(*S*)-MNThp_{TMS}ZrCl₂ [(*S*)-**5**, Chapter 1]

Table C.1. Crystal data and structure refinement for (*S*)-5bc: (CCDC 239369)

Empirical formula	C ₂₆ H ₄₆ Cl ₂ Si ₄ Zr
Formula weight	633.11
Crystallization Solvent	Pentane
Crystal Habit	Blade
Crystal size	0.33 x 0.22 x 0.09 mm ³
Crystal color	Colorless

Data Collection

Type of diffractometer	Bruker SMART 1000
Wavelength	0.71073 Å MoK α
Data Collection Temperature	100(2) K
q range for 17,165 reflections used	
in lattice determination	2.28 to 39.17°
Unit cell dimensions	a = 10.0036(8) Å b = 19.7728(16) Å β = 93.8290(10)° c = 16.0402(13) Å
Volume	3165.7(4) Å ³
Z	4
Crystal system	Monoclinic
Space group	P2 ₁
Density (calculated)	1.328 Mg/m ³

F(000)	1328
Data collection program	Bruker SMART v5.054
θ range for data collection	1.64 to 41.14°
Completeness to $\theta = 41.14^\circ$	88.3%
Index ranges	$-15 \leq h \leq 18, -34 \leq k \leq 36, -29 \leq l \leq 29$
Data collection scan type	ω scans at 5 ϕ settings for $2\theta = -28^\circ$ and 2 at $2\theta = -55^\circ$
Data reduction program	Bruker SAINT v6.45
Reflections collected	68,178
Independent reflections	32,043 [$R_{\text{int}} = 0.0823$]
Absorption coefficient	0.682 mm ⁻¹
Absorption correction	None
Max. and min. transmission	0.9412 and 0.8064

Structure Solution and Refinement

Structure solution program	SHELXS-97 (Sheldrick, 1990)
Primary solution method	Direct methods
Secondary solution method	Difference Fourier map
Hydrogen placement	Geometric positions
Structure refinement program	SHELXL-97 (Sheldrick, 1997)
Refinement method	Full matrix least-squares on F^2
Data/restraints/parameters	32,043/1/595

Treatment of hydrogen atoms	Riding
Goodness-of-fit on F^2	1.195
Final R indices [$I > 2s(I)$, 17,431 reflections]	$R1 = 0.0590$, $wR2 = 0.1066$
R indices (all data)	$R1 = 0.1153$, $wR2 = 0.1141$
Type of weighting scheme used	Sigma
Weighting scheme used	$w=1/\sigma^2(Fo^2)$
Max shift/error	0.001
Average shift/error	0.000
Absolute structure parameter	$-0.06(4)$
Largest diff. peak and hole	3.327 and $-1.743 \text{ e.}\text{\AA}^{-3}$

Special Refinement Details

The molecule, excluding the methylneopentyl group on the upper Cp ring, is nearly centrosymmetric. This is reflected by the pattern of systematic absences in the data with the notable exception of several $h0l$ reflections which are systematically weak but are nevertheless observed. If systematic absences were used as the sole criteria for space group assignment it would be tempting to assign space group $P2_1n$. The model using $P2_1n$ would require disorder in the methylneopentyl group, equivalent to a racemic mixture. However, since the stereochemistry of the methylneopentyl group is known to be (*S*) the non-centrosymmetric space group $P2_1$ was chosen.

Peaks in the final difference Fourier map greater than $1\text{e}/\text{\AA}^3$ are all within 1\AA of zirconium.

Refinement of F^2 against all reflections. The weighted R-factor (wR) and goodness of fit (S) are based on F^2 , conventional R-factors (R) are based on F , with F set to zero for negative F^2 . The threshold expression of $F^2 > 2\sigma(F^2)$ is used only for calculating R-factors(gt) etc. and is not relevant to the choice of reflections for refinement. R-factors based on F^2 are statistically about twice as large as those based on F , and R-factors based on all data will be even larger.

All esds (except the esd in the dihedral angle between two l.s. planes) are estimated using the full covariance matrix. The cell esds are taken into account individually in the estimation of esds in distances, angles and torsion angles; correlations between esds in cell parameters are only used when they are defined by crystal symmetry. An approximate (isotropic) treatment of cell esds is used for estimating esds involving l.s. planes.

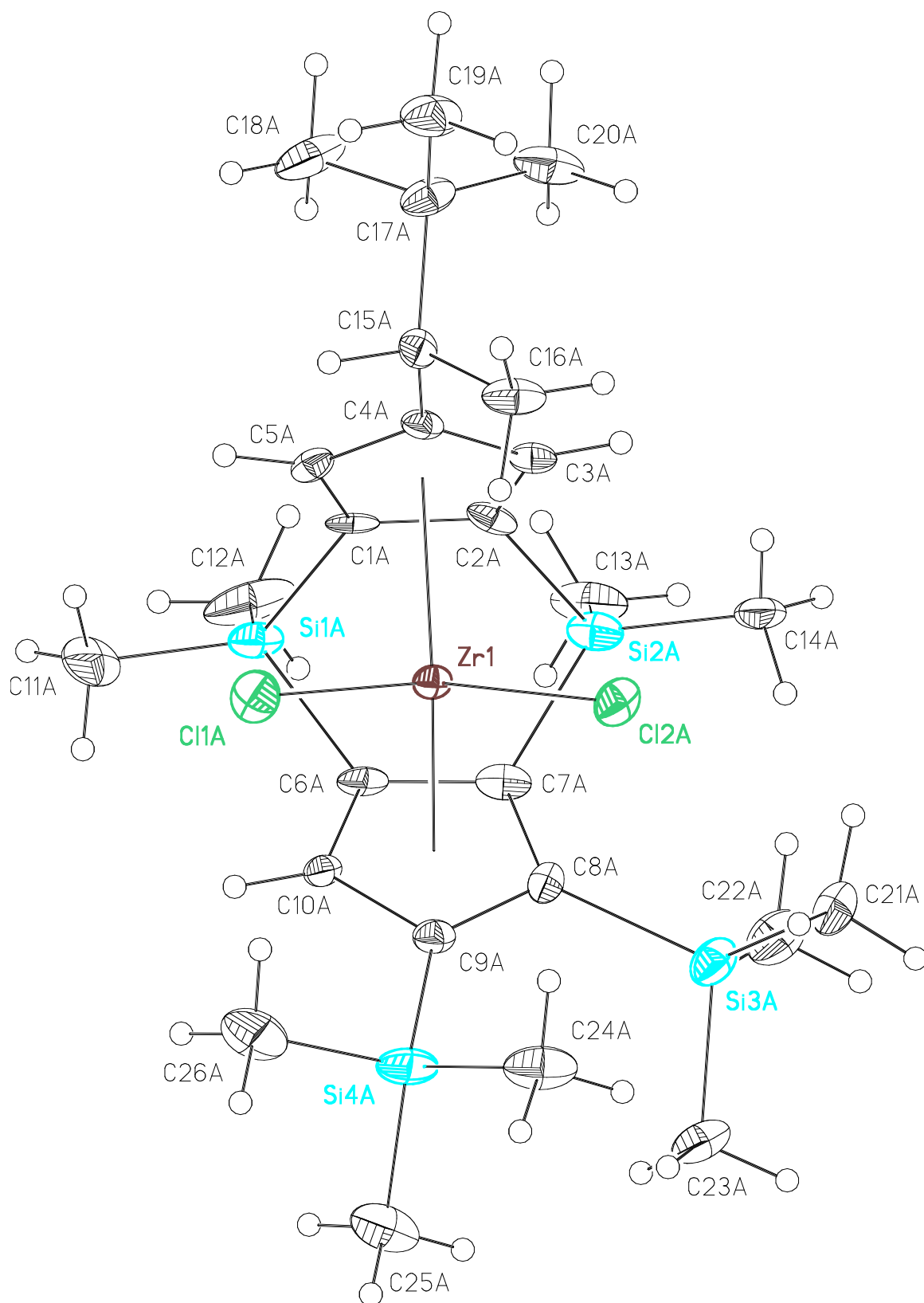


Figure C.1. ORTEP view of (S)-5b.

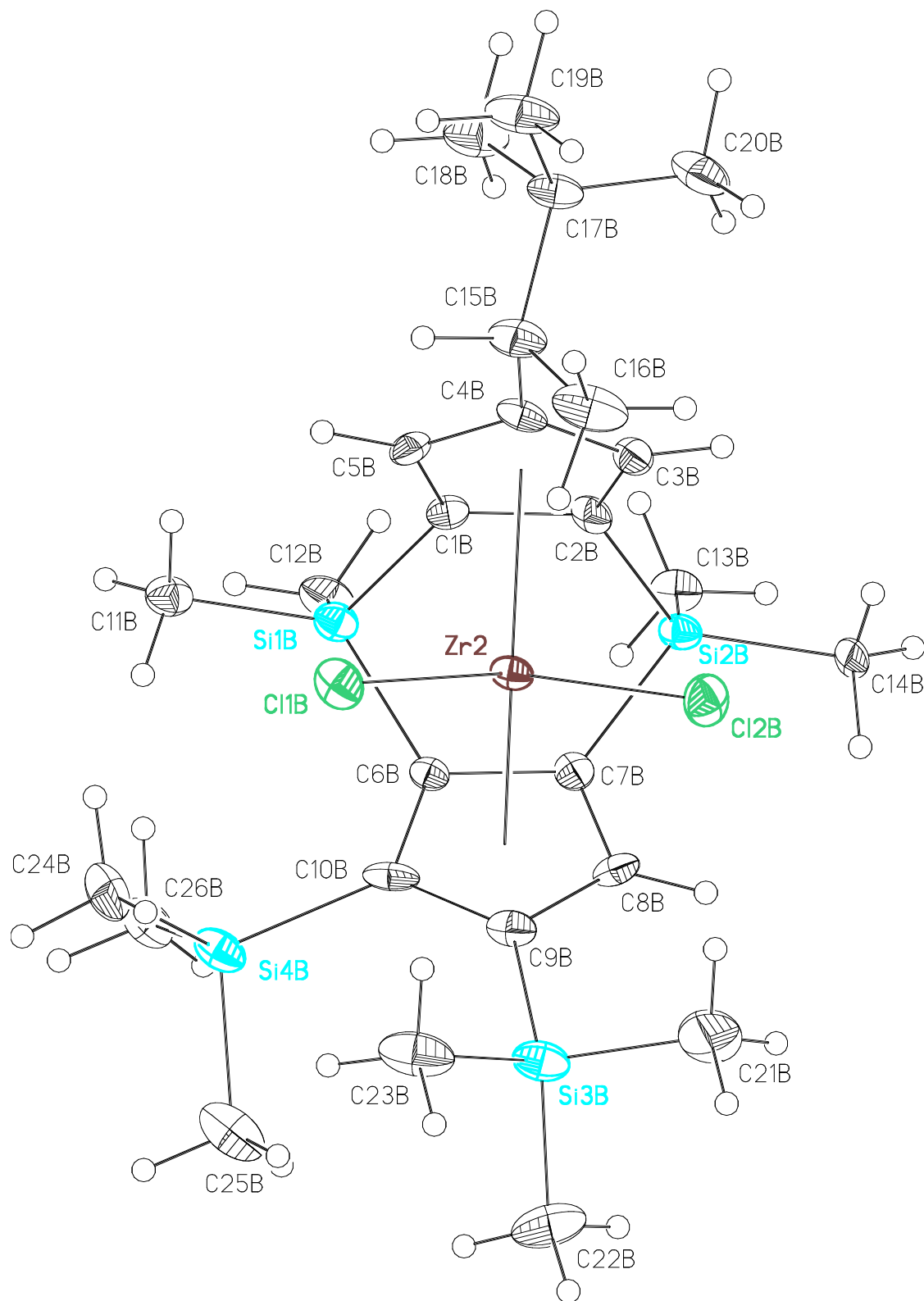


Figure C.2. ORTEP view of (S)-5c.

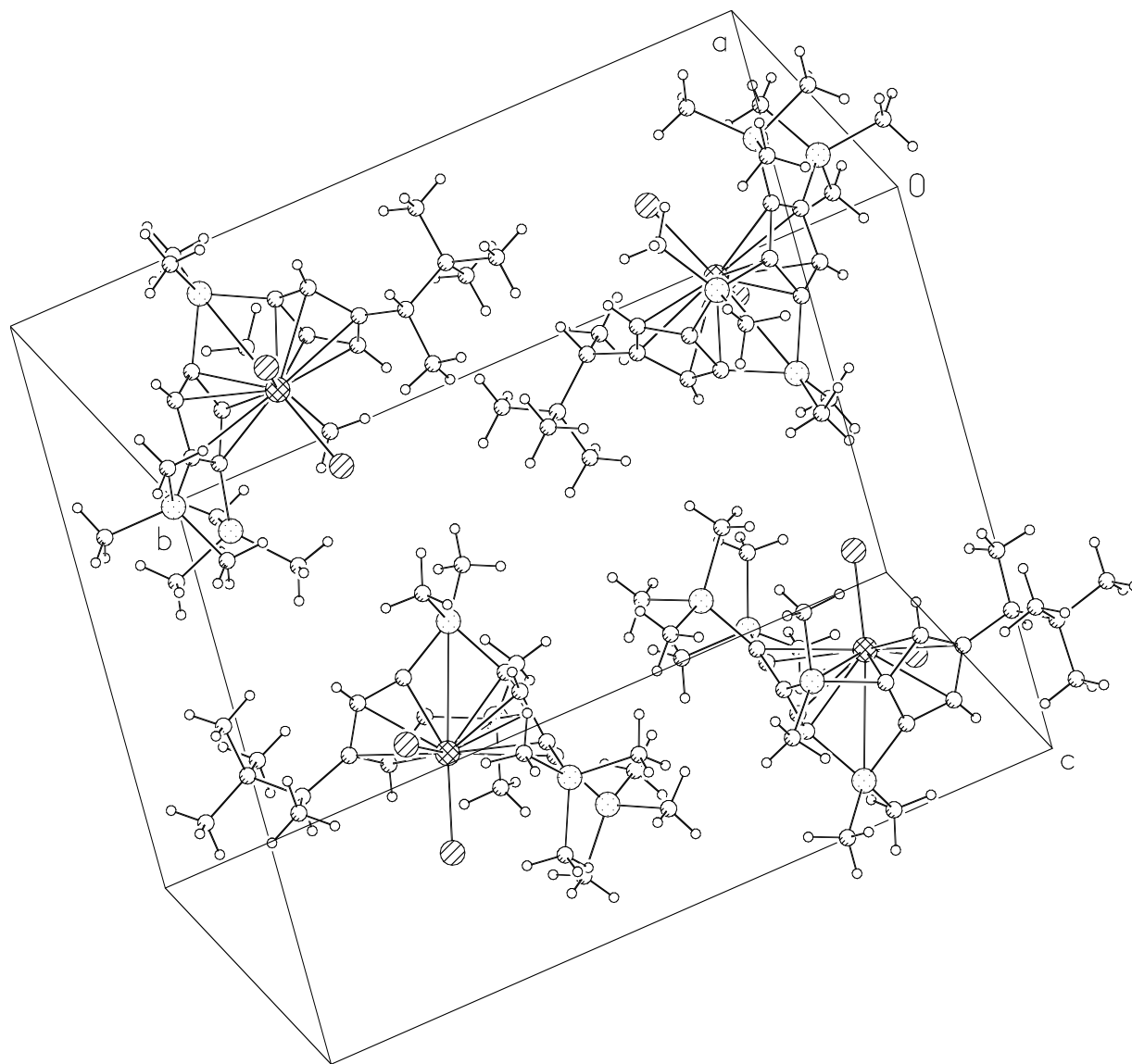


Figure C.3. Unit cell of X-ray structure of (S)-5b and (S)-5c.

Table C.2. Atomic coordinates and U_{eq} for (S)-5bc

Atomic coordinates ($\times 10^4$) and equivalent isotropic displacement parameters, U_{eq} ($\text{\AA}^2 \times 10^3$):
 (S)-5bc: (CCDC 239369).

U_{eq} is defined as the trace of the orthogonalized U^{ij} tensor.

	x	y	z	U_{eq}
Zr(1)	9768(1)	6942(1)	2774(1)	13(1)
Cl(1A)	12064(1)	6674(1)	3253(1)	27(1)
Cl(2A)	8611(1)	6580(1)	3974(1)	22(1)
Si(1A)	10382(2)	7493(1)	947(1)	22(1)
Si(2A)	7153(2)	7327(1)	1610(1)	22(1)
Si(3A)	7010(2)	8406(1)	3603(1)	24(1)
Si(4A)	10822(2)	8477(1)	4329(1)	27(1)
C(1A)	9696(5)	6672(2)	1289(3)	15(1)
C(2A)	8368(5)	6597(3)	1561(3)	17(1)
C(3A)	8355(6)	6005(3)	2063(3)	16(1)
C(4A)	9649(6)	5700(3)	2120(3)	16(1)
C(5A)	10458(5)	6118(3)	1638(3)	17(1)
C(6A)	9773(6)	7945(3)	1892(3)	17(1)
C(7A)	8442(6)	7892(2)	2187(3)	18(1)
C(8A)	8517(5)	8098(3)	3047(3)	16(1)
C(9A)	9891(6)	8221(3)	3306(3)	17(1)
C(10A)	10634(6)	8119(3)	2572(3)	17(1)
C(11A)	12220(6)	7489(3)	1003(4)	36(2)
C(12A)	9696(8)	7792(3)	-114(4)	50(2)
C(13A)	6475(7)	7664(3)	583(4)	38(2)

C(14A)	5828(5)	7005(3)	2243(4)	32(1)
C(15A)	10066(5)	5041(3)	2506(3)	17(1)
C(16A)	9615(5)	4955(2)	3381(2)	26(1)
C(17A)	9630(5)	4448(2)	1868(3)	23(1)
C(18A)	10386(6)	4522(2)	1091(2)	38(1)
C(19A)	9986(6)	3752(3)	2278(4)	32(1)
C(20A)	8151(5)	4455(2)	1631(3)	35(1)
C(21A)	6279(6)	7793(3)	4336(4)	27(1)
C(22A)	5734(6)	8711(3)	2786(4)	35(2)
C(23A)	7409(6)	9193(3)	4195(4)	28(1)
C(24A)	10043(7)	8110(3)	5247(4)	34(2)
C(25A)	10951(7)	9413(3)	4389(4)	37(2)
C(26A)	12565(7)	8165(4)	4363(4)	42(2)
Zr(2)	4813(1)	6799(1)	7773(1)	14(1)
Cl(1B)	3691(2)	7240(1)	8946(1)	23(1)
Cl(2B)	7158(1)	6941(1)	8275(1)	25(1)
Si(1B)	2245(2)	6457(1)	6548(1)	17(1)
Si(2B)	5534(2)	6234(1)	5970(1)	16(1)
Si(3B)	5684(2)	5244(1)	9349(1)	24(1)
Si(4B)	1898(2)	5416(1)	8549(1)	21(1)
C(1B)	3535(5)	7141(3)	6527(3)	16(1)
C(2B)	4931(5)	7072(3)	6314(3)	16(1)

C(3B)	5667(5)	7616(3)	6691(3)	17(1)
C(4B)	4790(6)	8028(3)	7115(3)	17(1)
C(5B)	3514(6)	7751(3)	7028(4)	18(1)
C(6B)	3453(5)	5872(2)	7159(3)	14(1)
C(7B)	4828(6)	5808(3)	6893(4)	17(1)
C(8B)	5613(6)	5577(3)	7610(3)	19(1)
C(9B)	4865(6)	5525(3)	8302(3)	19(1)
C(10B)	3480(6)	5669(3)	8040(3)	19(1)
C(11B)	857(5)	6832(3)	7124(3)	21(1)
C(12B)	1550(6)	6113(3)	5539(3)	24(1)
C(13B)	4878(6)	5966(3)	4905(3)	20(1)
C(14B)	7396(5)	6189(3)	6083(3)	24(1)
C(15B)	5100(6)	8702(3)	7561(4)	24(1)
C(16B)	6223(5)	8639(2)	8247(2)	35(1)
C(17B)	5262(5)	9286(2)	6918(3)	21(1)
C(18B)	4083(5)	9282(2)	6276(3)	31(1)
C(19B)	5281(7)	9959(3)	7384(4)	33(1)
C(20B)	6549(5)	9227(2)	6472(3)	30(1)
C(21B)	7520(7)	5462(4)	9376(5)	57(2)
C(22B)	5657(7)	4314(3)	9458(4)	37(2)
C(23B)	4923(8)	5676(3)	10248(4)	35(2)
C(24B)	1191(6)	6057(3)	9238(4)	31(1)
C(25B)	2214(7)	4629(3)	9164(4)	40(2)

C(26B)	637(6)	5147(3)	7699(4)	28(1)
--------	--------	---------	---------	-------

Table C.3. Selected bond lengths [Å] and angles [°] for (*S*)-5bc: (CCDC 239369)

Zr(1)-Cl(2A)	2.4192(13)	Zr(2)-Cl(1B)	2.4174(14)
Zr(1)-Cl(1A)	2.4324(15)	Zr(2)-Cl(2B)	2.4454(15)
Cl(2A)-Zr(1)-Cl(1A)	100.12(5)	Cl(1B)-Zr(2)-Cl(2B)	100.76(5)

Table C.4. Bond lengths [Å] and angles [°] for (*S*)-5bc: (CCDC 239369)

Zr(1)-C(2A)	2.419(5)	Si(3A)-C(21A)	1.871(6)
Zr(1)-Cl(2A)	2.4192(13)	Si(3A)-C(8A)	1.902(5)
Zr(1)-Cl(1A)	2.4324(15)	Si(4A)-C(26A)	1.847(7)
Zr(1)-C(6A)	2.436(5)	Si(4A)-C(25A)	1.857(6)
Zr(1)-C(1A)	2.437(5)	Si(4A)-C(24A)	1.859(6)
Zr(1)-C(7A)	2.450(5)	Si(4A)-C(9A)	1.901(6)
Zr(1)-C(10A)	2.512(5)	C(1A)-C(5A)	1.428(7)
Zr(1)-C(3A)	2.554(5)	C(1A)-C(2A)	1.433(7)
Zr(1)-C(5A)	2.573(5)	C(2A)-C(3A)	1.423(7)
Zr(1)-C(8A)	2.656(5)	C(3A)-C(4A)	1.426(8)
Zr(1)-C(9A)	2.668(5)	C(4A)-C(5A)	1.421(7)
Zr(1)-C(4A)	2.672(5)	C(4A)-C(15A)	1.490(7)
Si(1A)-C(11A)	1.834(7)	C(6A)-C(10A)	1.388(8)
Si(1A)-C(1A)	1.859(5)	C(6A)-C(7A)	1.446(8)
Si(1A)-C(12A)	1.886(7)	C(7A)-C(8A)	1.436(7)
Si(1A)-C(6A)	1.895(5)	C(8A)-C(9A)	1.429(8)
Si(2A)-C(14A)	1.836(6)	C(9A)-C(10A)	1.448(7)
Si(2A)-C(13A)	1.863(7)	C(15A)-C(16A)	1.512(6)
Si(2A)-C(2A)	1.891(6)	C(15A)-C(17A)	1.598(7)
Si(2A)-C(7A)	1.900(6)	C(17A)-C(20A)	1.503(6)
Si(3A)-C(23A)	1.852(6)	C(17A)-C(18A)	1.506(5)
Si(3A)-C(22A)	1.868(7)	C(17A)-C(19A)	1.556(7)

Zr(2)-C(1B)	2.397(5)	Si(3B)-C(9B)	1.902(6)
Zr(2)-C(2B)	2.413(5)	Si(4B)-C(24B)	1.853(6)
Zr(2)-C(7B)	2.415(5)	Si(4B)-C(25B)	1.859(7)
Zr(2)-Cl(1B)	2.4174(14)	Si(4B)-C(26B)	1.871(6)
Zr(2)-Cl(2B)	2.4454(15)	Si(4B)-C(10B)	1.895(6)
Zr(2)-C(6B)	2.449(5)	C(1B)-C(5B)	1.451(7)
Zr(2)-C(5B)	2.541(5)	C(1B)-C(2B)	1.466(7)
Zr(2)-C(3B)	2.560(5)	C(2B)-C(3B)	1.416(7)
Zr(2)-C(8B)	2.563(5)	C(3B)-C(4B)	1.405(7)
Zr(2)-C(4B)	2.650(5)	C(4B)-C(5B)	1.388(8)
Zr(2)-C(10B)	2.651(5)	C(4B)-C(15B)	1.534(7)
Zr(2)-C(9B)	2.658(5)	C(6B)-C(10B)	1.469(7)
Si(1B)-C(12B)	1.847(5)	C(6B)-C(7B)	1.472(7)
Si(1B)-C(11B)	1.871(5)	C(7B)-C(8B)	1.424(8)
Si(1B)-C(1B)	1.871(5)	C(8B)-C(9B)	1.383(7)
Si(1B)-C(6B)	1.897(6)	C(9B)-C(10B)	1.449(8)
Si(2B)-C(2B)	1.859(5)	C(15B)-C(16B)	1.524(7)
Si(2B)-C(14B)	1.862(5)	C(15B)-C(17B)	1.564(7)
Si(2B)-C(13B)	1.865(6)	C(17B)-C(18B)	1.513(6)
Si(2B)-C(7B)	1.881(6)	C(17B)-C(20B)	1.519(6)
Si(3B)-C(22B)	1.848(6)	C(17B)-C(19B)	1.526(7)
Si(3B)-C(23B)	1.880(6)	C(2A)-Zr(1)-Cl(2A)	105.94(12)
Si(3B)-C(21B)	1.884(7)	C(2A)-Zr(1)-Cl(1A)	132.59(13)

Cl(2A)-Zr(1)-Cl(1A)	100.12(5)	C(1A)-Zr(1)-C(3A)	54.91(17)
C(2A)-Zr(1)-C(6A)	77.62(17)	C(7A)-Zr(1)-C(3A)	96.64(17)
Cl(2A)-Zr(1)-C(6A)	136.28(13)	C(10A)-Zr(1)-C(3A)	143.18(18)
Cl(1A)-Zr(1)-C(6A)	108.84(15)	C(2A)-Zr(1)-C(5A)	54.56(17)
C(2A)-Zr(1)-C(1A)	34.33(17)	Cl(2A)-Zr(1)-C(5A)	122.75(13)
Cl(2A)-Zr(1)-C(1A)	136.73(13)	Cl(1A)-Zr(1)-C(5A)	78.05(12)
Cl(1A)-Zr(1)-C(1A)	103.11(13)	C(6A)-Zr(1)-C(5A)	95.34(17)
C(6A)-Zr(1)-C(1A)	67.14(16)	C(1A)-Zr(1)-C(5A)	32.99(16)
C(2A)-Zr(1)-C(7A)	68.75(18)	C(7A)-Zr(1)-C(5A)	112.17(18)
Cl(2A)-Zr(1)-C(7A)	104.91(14)	C(10A)-Zr(1)-C(5A)	112.61(16)
Cl(1A)-Zr(1)-C(7A)	139.85(14)	C(3A)-Zr(1)-C(5A)	52.46(17)
C(6A)-Zr(1)-C(7A)	34.43(19)	C(2A)-Zr(1)-C(8A)	97.00(18)
C(1A)-Zr(1)-C(7A)	79.19(18)	Cl(2A)-Zr(1)-C(8A)	82.41(11)
C(2A)-Zr(1)-C(10A)	110.10(18)	Cl(1A)-Zr(1)-C(8A)	125.52(13)
Cl(2A)-Zr(1)-C(10A)	124.35(12)	C(6A)-Zr(1)-C(8A)	54.19(16)
Cl(1A)-Zr(1)-C(10A)	85.21(15)	C(1A)-Zr(1)-C(8A)	111.49(17)
C(6A)-Zr(1)-C(10A)	32.53(18)	C(7A)-Zr(1)-C(8A)	32.35(17)
C(1A)-Zr(1)-C(10A)	93.71(16)	C(10A)-Zr(1)-C(8A)	52.71(17)
C(7A)-Zr(1)-C(10A)	54.75(19)	C(3A)-Zr(1)-C(8A)	116.48(17)
C(2A)-Zr(1)-C(3A)	33.11(16)	C(5A)-Zr(1)-C(8A)	144.46(17)
Cl(2A)-Zr(1)-C(3A)	81.98(13)	C(2A)-Zr(1)-C(9A)	122.44(18)
Cl(1A)-Zr(1)-C(3A)	117.75(13)	Cl(2A)-Zr(1)-C(9A)	92.31(12)
C(6A)-Zr(1)-C(3A)	110.73(18)	Cl(1A)-Zr(1)-C(9A)	94.78(13)

C(6A)-Zr(1)-C(9A)	54.06(16)	C(12A)-Si(1A)-C(6A)	117.2(3)
C(1A)-Zr(1)-C(9A)	121.18(16)	C(11A)-Si(1A)-Zr(1)	101.8(2)
C(7A)-Zr(1)-C(9A)	53.78(18)	C(1A)-Si(1A)-Zr(1)	48.71(15)
C(10A)-Zr(1)-C(9A)	32.28(15)	C(12A)-Si(1A)-Zr(1)	147.7(3)
C(3A)-Zr(1)-C(9A)	147.46(17)	C(6A)-Si(1A)-Zr(1)	48.77(16)
C(5A)-Zr(1)-C(9A)	144.86(16)	C(14A)-Si(2A)-C(13A)	112.3(3)
C(8A)-Zr(1)-C(9A)	31.13(16)	C(14A)-Si(2A)-C(2A)	104.4(3)
C(2A)-Zr(1)-C(4A)	54.29(18)	C(13A)-Si(2A)-C(2A)	115.6(3)
Cl(2A)-Zr(1)-C(4A)	91.67(11)	C(14A)-Si(2A)-C(7A)	115.2(3)
Cl(1A)-Zr(1)-C(4A)	86.53(14)	C(13A)-Si(2A)-C(7A)	114.5(3)
C(6A)-Zr(1)-C(4A)	121.47(16)	C(2A)-Si(2A)-C(7A)	93.0(2)
C(1A)-Zr(1)-C(4A)	54.34(16)	C(14A)-Si(2A)-Zr(1)	100.8(2)
C(7A)-Zr(1)-C(4A)	123.04(18)	C(13A)-Si(2A)-Zr(1)	146.7(2)
C(10A)-Zr(1)-C(4A)	143.92(15)	C(2A)-Si(2A)-Zr(1)	48.80(16)
C(3A)-Zr(1)-C(4A)	31.57(18)	C(7A)-Si(2A)-Zr(1)	49.78(16)
C(5A)-Zr(1)-C(4A)	31.37(16)	C(23A)-Si(3A)-C(22A)	101.7(3)
C(8A)-Zr(1)-C(4A)	147.93(18)	C(23A)-Si(3A)-C(21A)	107.6(3)
C(9A)-Zr(1)-C(4A)	175.52(16)	C(22A)-Si(3A)-C(21A)	111.9(3)
C(11A)-Si(1A)-C(1A)	111.7(3)	C(23A)-Si(3A)-C(8A)	111.0(3)
C(11A)-Si(1A)-C(12A)	110.4(3)	C(22A)-Si(3A)-C(8A)	107.5(3)
C(1A)-Si(1A)-C(12A)	114.9(3)	C(21A)-Si(3A)-C(8A)	116.3(2)
C(11A)-Si(1A)-C(6A)	109.7(3)	C(26A)-Si(4A)-C(25A)	105.6(3)
C(1A)-Si(1A)-C(6A)	91.7(2)	C(26A)-Si(4A)-C(24A)	106.9(3)

C(25A)-Si(4A)-C(24A)	112.3(3)	C(3A)-C(4A)-Zr(1)	69.6(3)
C(26A)-Si(4A)-C(9A)	110.1(3)	C(15A)-C(4A)-Zr(1)	129.5(4)
C(25A)-Si(4A)-C(9A)	109.8(3)	C(4A)-C(5A)-C(1A)	110.6(5)
C(24A)-Si(4A)-C(9A)	111.9(3)	C(4A)-C(5A)-Zr(1)	78.2(3)
C(5A)-C(1A)-C(2A)	106.4(4)	C(1A)-C(5A)-Zr(1)	68.3(3)
C(5A)-C(1A)-Si(1A)	126.0(4)	C(10A)-C(6A)-C(7A)	107.3(4)
C(2A)-C(1A)-Si(1A)	123.3(4)	C(10A)-C(6A)-Si(1A)	122.0(5)
C(5A)-C(1A)-Zr(1)	78.7(3)	C(7A)-C(6A)-Si(1A)	125.5(4)
C(2A)-C(1A)-Zr(1)	72.1(3)	C(10A)-C(6A)-Zr(1)	76.8(3)
Si(1A)-C(1A)-Zr(1)	96.3(2)	C(7A)-C(6A)-Zr(1)	73.3(3)
C(3A)-C(2A)-C(1A)	107.5(5)	Si(1A)-C(6A)-Zr(1)	95.4(2)
C(3A)-C(2A)-Si(2A)	125.0(4)	C(8A)-C(7A)-C(6A)	107.7(5)
C(1A)-C(2A)-Si(2A)	123.0(4)	C(8A)-C(7A)-Si(2A)	128.7(4)
C(3A)-C(2A)-Zr(1)	78.7(3)	C(6A)-C(7A)-Si(2A)	119.5(4)
C(1A)-C(2A)-Zr(1)	73.6(3)	C(8A)-C(7A)-Zr(1)	81.7(3)
Si(2A)-C(2A)-Zr(1)	95.2(2)	C(6A)-C(7A)-Zr(1)	72.2(3)
C(2A)-C(3A)-C(4A)	110.0(5)	Si(2A)-C(7A)-Zr(1)	93.9(2)
C(2A)-C(3A)-Zr(1)	68.2(3)	C(9A)-C(8A)-C(7A)	108.4(5)
C(4A)-C(3A)-Zr(1)	78.8(3)	C(9A)-C(8A)-Si(3A)	125.9(4)
C(5A)-C(4A)-C(3A)	105.5(5)	C(7A)-C(8A)-Si(3A)	123.3(4)
C(5A)-C(4A)-C(15A)	125.5(5)	C(9A)-C(8A)-Zr(1)	74.9(3)
C(3A)-C(4A)-C(15A)	128.6(5)	C(7A)-C(8A)-Zr(1)	65.9(3)
C(5A)-C(4A)-Zr(1)	70.5(3)	Si(3A)-C(8A)-Zr(1)	138.5(2)

C(8A)-C(9A)-C(10A)	106.0(5)	C(7B)-Zr(2)-Cl(1B)	140.28(13)
C(8A)-C(9A)-Si(4A)	134.6(4)	C(1B)-Zr(2)-Cl(2B)	133.52(13)
C(10A)-C(9A)-Si(4A)	119.4(4)	C(2B)-Zr(2)-Cl(2B)	100.70(13)
C(8A)-C(9A)-Zr(1)	74.0(3)	C(7B)-Zr(2)-Cl(2B)	104.06(14)
C(10A)-C(9A)-Zr(1)	67.9(3)	Cl(1B)-Zr(2)-Cl(2B)	100.76(5)
Si(4A)-C(9A)-Zr(1)	122.6(3)	C(1B)-Zr(2)-C(6B)	67.95(17)
C(6A)-C(10A)-C(9A)	110.4(5)	C(2B)-Zr(2)-C(6B)	80.74(17)
C(6A)-C(10A)-Zr(1)	70.7(3)	C(7B)-Zr(2)-C(6B)	35.23(18)
C(9A)-C(10A)-Zr(1)	79.8(3)	Cl(1B)-Zr(2)-C(6B)	108.01(13)
C(4A)-C(15A)-C(16A)	113.1(4)	Cl(2B)-Zr(2)-C(6B)	135.54(13)
C(4A)-C(15A)-C(17A)	108.5(4)	C(1B)-Zr(2)-C(5B)	34.02(17)
C(16A)-C(15A)-C(17A)	115.3(4)	C(2B)-Zr(2)-C(5B)	55.55(17)
C(20A)-C(17A)-C(18A)	109.3(4)	C(7B)-Zr(2)-C(5B)	110.4(2)
C(20A)-C(17A)-C(19A)	108.0(4)	Cl(1B)-Zr(2)-C(5B)	81.34(13)
C(18A)-C(17A)-C(19A)	108.8(4)	Cl(2B)-Zr(2)-C(5B)	121.24(14)
C(20A)-C(17A)-C(15A)	112.1(4)	C(6B)-Zr(2)-C(5B)	96.45(17)
C(18A)-C(17A)-C(15A)	109.1(4)	C(1B)-Zr(2)-C(3B)	55.94(17)
C(19A)-C(17A)-C(15A)	109.5(4)	C(2B)-Zr(2)-C(3B)	32.93(17)
C(1B)-Zr(2)-C(2B)	35.49(17)	C(7B)-Zr(2)-C(3B)	95.76(17)
C(1B)-Zr(2)-C(7B)	76.42(19)	Cl(1B)-Zr(2)-C(3B)	119.55(12)
C(2B)-Zr(2)-C(7B)	67.17(18)	Cl(2B)-Zr(2)-C(3B)	78.13(13)
C(1B)-Zr(2)-Cl(1B)	107.34(13)	C(6B)-Zr(2)-C(3B)	113.64(17)
C(2B)-Zr(2)-Cl(1B)	136.87(13)	C(5B)-Zr(2)-C(3B)	52.86(18)

C(1B)-Zr(2)-C(8B)	109.50(18)	C(5B)-Zr(2)-C(10B)	117.00(18)
C(2B)-Zr(2)-C(8B)	94.38(17)	C(3B)-Zr(2)-C(10B)	146.71(17)
C(7B)-Zr(2)-C(8B)	33.09(19)	C(8B)-Zr(2)-C(10B)	52.14(18)
Cl(1B)-Zr(2)-C(8B)	125.71(13)	C(4B)-Zr(2)-C(10B)	147.84(19)
Cl(2B)-Zr(2)-C(8B)	80.96(14)	C(1B)-Zr(2)-C(9B)	122.14(18)
C(6B)-Zr(2)-C(8B)	54.78(18)	C(2B)-Zr(2)-C(9B)	121.39(16)
C(5B)-Zr(2)-C(8B)	143.51(18)	C(7B)-Zr(2)-C(9B)	54.35(18)
C(3B)-Zr(2)-C(8B)	113.91(17)	Cl(1B)-Zr(2)-C(9B)	95.38(12)
C(1B)-Zr(2)-C(4B)	54.48(18)	Cl(2B)-Zr(2)-C(9B)	90.34(14)
C(2B)-Zr(2)-C(4B)	53.68(17)	C(6B)-Zr(2)-C(9B)	54.42(18)
C(7B)-Zr(2)-C(4B)	120.76(18)	C(5B)-Zr(2)-C(9B)	148.37(19)
Cl(1B)-Zr(2)-C(4B)	89.25(12)	C(3B)-Zr(2)-C(9B)	144.55(16)
Cl(2B)-Zr(2)-C(4B)	90.45(14)	C(8B)-Zr(2)-C(9B)	30.66(16)
C(6B)-Zr(2)-C(4B)	122.43(18)	C(4B)-Zr(2)-C(9B)	175.07(16)
C(5B)-Zr(2)-C(4B)	30.92(18)	C(10B)-Zr(2)-C(9B)	31.68(17)
C(3B)-Zr(2)-C(4B)	31.24(16)	C(12B)-Si(1B)-C(11B)	109.3(3)
C(8B)-Zr(2)-C(4B)	144.91(17)	C(12B)-Si(1B)-C(1B)	118.0(2)
C(1B)-Zr(2)-C(10B)	97.29(18)	C(11B)-Si(1B)-C(1B)	105.0(2)
C(2B)-Zr(2)-C(10B)	113.79(17)	C(12B)-Si(1B)-C(6B)	114.7(3)
C(7B)-Zr(2)-C(10B)	55.52(17)	C(11B)-Si(1B)-C(6B)	117.0(2)
Cl(1B)-Zr(2)-C(10B)	85.06(12)	C(1B)-Si(1B)-C(6B)	91.9(2)
Cl(2B)-Zr(2)-C(10B)	121.71(13)	C(12B)-Si(1B)-Zr(2)	148.8(2)
C(6B)-Zr(2)-C(10B)	33.17(16)	C(11B)-Si(1B)-Zr(2)	101.82(17)

C(1B)-Si(1B)-Zr(2)	48.11(17)	C(26B)-Si(4B)-C(10B)	107.6(2)
C(6B)-Si(1B)-Zr(2)	49.76(16)	C(5B)-C(1B)-C(2B)	104.8(5)
C(2B)-Si(2B)-C(14B)	110.9(3)	C(5B)-C(1B)-Si(1B)	123.7(4)
C(2B)-Si(2B)-C(13B)	115.0(3)	C(2B)-C(1B)-Si(1B)	127.3(4)
C(14B)-Si(2B)-C(13B)	111.3(3)	C(5B)-C(1B)-Zr(2)	78.4(3)
C(2B)-Si(2B)-C(7B)	91.1(2)	C(2B)-C(1B)-Zr(2)	72.8(3)
C(14B)-Si(2B)-C(7B)	109.1(2)	Si(1B)-C(1B)-Zr(2)	96.4(2)
C(13B)-Si(2B)-C(7B)	117.8(3)	C(3B)-C(2B)-C(1B)	107.8(4)
C(2B)-Si(2B)-Zr(2)	47.89(15)	C(3B)-C(2B)-Si(2B)	129.4(4)
C(14B)-Si(2B)-Zr(2)	102.21(19)	C(1B)-C(2B)-Si(2B)	119.0(4)
C(13B)-Si(2B)-Zr(2)	146.4(2)	C(3B)-C(2B)-Zr(2)	79.2(3)
C(7B)-Si(2B)-Zr(2)	48.05(16)	C(1B)-C(2B)-Zr(2)	71.7(3)
C(22B)-Si(3B)-C(23B)	111.7(3)	Si(2B)-C(2B)-Zr(2)	97.2(2)
C(22B)-Si(3B)-C(21B)	104.2(4)	C(4B)-C(3B)-C(2B)	108.9(5)
C(23B)-Si(3B)-C(21B)	108.8(4)	C(4B)-C(3B)-Zr(2)	77.9(3)
C(22B)-Si(3B)-C(9B)	111.4(3)	C(2B)-C(3B)-Zr(2)	67.8(3)
C(23B)-Si(3B)-C(9B)	111.9(3)	C(5B)-C(4B)-C(3B)	108.8(5)
C(21B)-Si(3B)-C(9B)	108.4(3)	C(5B)-C(4B)-C(15B)	123.1(5)
C(24B)-Si(4B)-C(25B)	108.4(3)	C(3B)-C(4B)-C(15B)	128.0(5)
C(24B)-Si(4B)-C(26B)	111.3(3)	C(5B)-C(4B)-Zr(2)	70.2(3)
C(25B)-Si(4B)-C(26B)	103.4(3)	C(3B)-C(4B)-Zr(2)	70.8(3)
C(24B)-Si(4B)-C(10B)	116.1(3)	C(15B)-C(4B)-Zr(2)	127.9(4)
C(25B)-Si(4B)-C(10B)	109.4(3)	C(4B)-C(5B)-C(1B)	109.7(5)

C(4B)-C(5B)-Zr(2)	78.9(3)	C(9B)-C(10B)-C(6B)	106.8(5)
C(1B)-C(5B)-Zr(2)	67.6(3)	C(9B)-C(10B)-Si(4B)	129.3(4)
C(10B)-C(6B)-C(7B)	107.3(5)	C(6B)-C(10B)-Si(4B)	121.6(4)
C(10B)-C(6B)-Si(1B)	129.4(4)	C(9B)-C(10B)-Zr(2)	74.4(3)
C(7B)-C(6B)-Si(1B)	118.6(4)	C(6B)-C(10B)-Zr(2)	65.8(3)
C(10B)-C(6B)-Zr(2)	81.0(3)	Si(4B)-C(10B)-Zr(2)	137.3(3)
C(7B)-C(6B)-Zr(2)	71.1(3)	C(16B)-C(15B)-C(4B)	112.5(5)
Si(1B)-C(6B)-Zr(2)	93.99(19)	C(16B)-C(15B)-C(17B)	115.6(4)
C(8B)-C(7B)-C(6B)	105.6(5)	C(4B)-C(15B)-C(17B)	111.1(4)
C(8B)-C(7B)-Si(2B)	124.3(4)	C(18B)-C(17B)-C(20B)	109.0(4)
C(6B)-C(7B)-Si(2B)	126.6(4)	C(18B)-C(17B)-C(19B)	108.8(4)
C(8B)-C(7B)-Zr(2)	79.1(3)	C(20B)-C(17B)-C(19B)	108.3(4)
C(6B)-C(7B)-Zr(2)	73.6(3)	C(18B)-C(17B)-C(15B)	109.6(4)
Si(2B)-C(7B)-Zr(2)	96.6(2)	C(20B)-C(17B)-C(15B)	112.5(4)
C(9B)-C(8B)-C(7B)	112.0(5)	C(19B)-C(17B)-C(15B)	108.6(4)
C(9B)-C(8B)-Zr(2)	78.5(3)		
C(7B)-C(8B)-Zr(2)	67.8(3)		
C(8B)-C(9B)-C(10B)	108.1(5)		
C(8B)-C(9B)-Si(3B)	120.4(4)		
C(10B)-C(9B)-Si(3B)	131.4(4)		
C(8B)-C(9B)-Zr(2)	70.9(3)		
C(10B)-C(9B)-Zr(2)	73.9(3)		
Si(3B)-C(9B)-Zr(2)	123.8(3)		

Table C.5. Anisotropic displacement parameters ($\text{\AA}^2 \times 10^4$) for (S)-5bc

The anisotropic displacement factor exponent takes the form: $-2\pi^2 [h^2 a^{*2} U^{11} + \dots + 2 h k a^* b^* U^{12}]$

	U ¹¹	U ²²	U ³³	U ²³	U ¹³	U ¹²
Zr(1)	185(2)	128(2)	80(2)	6(2)	13(2)	−8(2)
Cl(1A)	218(6)	350(7)	219(5)	−19(5)	−38(5)	28(5)
Cl(2A)	299(7)	218(6)	149(5)	47(4)	82(5)	21(5)
Si(1A)	423(10)	147(7)	110(6)	−2(5)	74(6)	−55(6)
Si(2A)	273(8)	144(7)	214(7)	1(6)	−86(6)	26(6)
Si(3A)	286(8)	193(7)	237(7)	30(6)	91(7)	63(6)
Si(4A)	399(10)	230(8)	159(7)	−74(6)	−48(7)	−34(7)
C(1A)	310(30)	75(18)	64(17)	−28(14)	−59(17)	−2(15)
C(2A)	260(30)	140(20)	96(19)	7(17)	−58(18)	−80(18)
C(3A)	220(30)	130(20)	120(20)	−26(17)	−56(19)	0(17)
C(4A)	250(30)	110(20)	120(20)	−10(17)	40(20)	−56(17)
C(5A)	190(20)	180(20)	120(19)	−48(17)	−10(17)	42(16)
C(6A)	340(30)	120(20)	60(20)	−9(18)	10(20)	−40(20)
C(7A)	300(30)	90(20)	140(30)	48(19)	−70(20)	30(20)
C(8A)	190(30)	100(20)	200(30)	66(19)	70(20)	38(18)
C(9A)	210(30)	120(20)	170(30)	−10(20)	20(20)	−10(20)
C(10A)	250(30)	110(20)	160(20)	−18(17)	110(20)	−39(18)
C(11A)	550(40)	270(30)	290(30)	20(20)	170(30)	−190(30)
C(12A)	1190(70)	190(30)	140(30)	20(20)	210(40)	70(30)
C(13A)	490(40)	210(30)	420(40)	−80(30)	−220(30)	60(30)

C(14A)	230(30)	270(30)	440(30)	−240(20)	−10(20)	−20(20)
C(15A)	190(30)	120(20)	210(20)	30(20)	40(20)	−6(19)
C(16A)	480(30)	140(17)	146(15)	13(13)	−19(18)	−30(17)
C(17A)	390(30)	122(17)	176(18)	20(14)	60(20)	48(18)
C(18A)	750(40)	170(20)	260(20)	−5(16)	220(20)	80(20)
C(19A)	530(40)	170(20)	280(30)	0(20)	110(30)	−60(20)
C(20A)	530(30)	240(20)	270(20)	−78 (17)	−70(20)	−100(20)
C(21A)	280(30)	270(30)	250(20)	40(20)	100(20)	70(20)
C(22A)	400(30)	310(30)	340(30)	10(20)	50(30)	110(20)
C(23A)	440(30)	190(20)	210(20)	−12(19)	80(20)	80(20)
C(24A)	610(40)	240(30)	150(30)	0(20)	−70(30)	−20(30)
C(25A)	550(40)	290(30)	260(30)	0(20)	−30(30)	−160(30)
C(26A)	370(40)	500(40)	350(30)	−150(30)	−160(30)	−110(30)
Zr(2)	205(2)	132(3)	81(2)	−2(2)	11(2)	−13(2)
Cl(1B)	296(7)	254(6)	150(5)	−51(4)	62(5)	−18(5)
Cl(2B)	181(5)	336(6)	236(5)	18(5)	−27(5)	−5(5)
Si(1B)	193(7)	173(7)	151(6)	10(5)	−3(5)	−25(5)
Si(2B)	216(7)	144(6)	117(6)	5(5)	29(6)	4(5)
Si(3B)	339(9)	235(8)	145(7)	50(6)	−16(7)	−27(7)
Si(4B)	305(8)	190(7)	136(6)	−23(5)	53(6)	−70(6)
C(1B)	180(20)	150(20)	130(20)	12(17)	−18(18)	9(16)
C(2B)	220(20)	170(20)	101(18)	−1(16)	61(17)	−5(16)

C(3B)	190(20)	150(20)	170(20)	1(17)	40(19)	-7(16)
C(4B)	280(30)	140(20)	100(20)	14(18)	0(20)	-60(19)
C(5B)	200(20)	120(20)	210(20)	20(18)	20(20)	53(17)
C(6B)	170(30)	100(20)	130(20)	-12(18)	10(20)	-25(18)
C(7B)	210(30)	90(20)	220(30)	-40(20)	70(20)	-5(18)
C(8B)	230(30)	150(20)	180(20)	35(19)	-20(20)	63(19)
C(9B)	300(30)	140(30)	130(20)	0(20)	20(20)	0(20)
C(10B)	370(30)	110(20)	90(20)	21(18)	0(20)	-10(20)
C(11B)	220(20)	170(20)	228(18)	9(18)	-23(17)	-38(17)
C(12B)	290(30)	280(30)	140(20)	40(20)	-50(20)	-80(20)
C(13B)	290(30)	200(20)	110(20)	-26(19)	-30(20)	-19(19)
C(14B)	190(20)	360(30)	176(19)	160(20)	97(18)	80(20)
C(15B)	400(30)	110(20)	200(30)	-30(20)	30(30)	-40(20)
C(16B)	590(30)	200(20)	235(19)	-31(16)	-50(20)	-160(20)
C(17B)	330(30)	119(17)	192(18)	6(14)	-20(20)	-60(18)
C(18B)	400(30)	200(20)	290(20)	33(17)	-70(20)	-85(19)
C(19B)	650(40)	130(20)	210(20)	-7(18)	50(30)	-50(20)
C(20B)	420(30)	200(20)	300(20)	24(16)	120(20)	-94(18)
C(21B)	350(40)	800(50)	540(40)	490(40)	-60(30)	70(30)
C(22B)	540(40)	260(30)	290(30)	50(20)	-150(30)	70(20)
C(23B)	650(50)	250(30)	150(30)	10(20)	0(30)	-50(30)
C(24B)	290(30)	380(30)	290(30)	0(20)	140(20)	-40(20)
C(25B)	500(40)	390(30)	330(30)	20(30)	110(30)	-160(30)

C(26B)	270(30)	280(30)	280(20)	10(20)	30(20)	-100(20)
--------	---------	---------	---------	--------	--------	----------

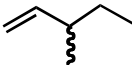
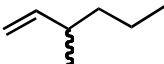
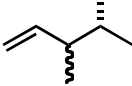
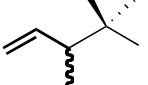
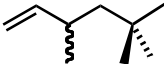
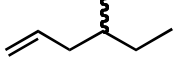
D. Appendix D

Polymerization Data for

(S)-**2**, *(S)*-**3**, and *(S)*-**4**

In the following tables, the data from the polymerization of 3-methyl substituted and 4-methyl-1-hexene olefins using (*S*)-**2**, (*S*)-**3**, and (*S*)-**4** are shown. For more than three runs of the same olefin, a representative polymerization run is listed, and the average *s* values of all runs are shown. The same polymerization condition as described in Table D.1 was also used to generate Table D.2 and Table D.3.

Table D.1. Kinetic resolution of chiral olefins using (*S*)-2****

$\text{olefin} \xrightarrow[\text{MAO (250 mg) + tetradecane (1.5 mL), 25 }^\circ\text{C}]{\text{1 - 2 mg (S)-2}} \text{ isotactic polymer}$					
olefin	t (hr)	TOF (hr ⁻¹)	% conv	% ee	$s^a = \frac{k_S}{k_R}$
	18	72	24	13.3	2.8 ± 0.07
	47	47	38.3	20.3	2.4 ± 0.05
	13.5	551	75	40.0	1.8 ± 0.03
	40.5	45.6	32.5	40.6	17.6 ± 2.6
	69	34	42.4	58.6	15.9 ± 2.0
	12	7.3	26	28	12.1 ± 1.2
	22.7	55.8	37.8	16.2	2.0 ± 0.03
	43	37	56.1	30.3	2.1 ± 0.04
	16.5	77.6	64.4	7.6	1.1 ± 0.005
	16.5	73.7	58.7	4.6	1.1 ± 0.003

a) The value following “±” is the calculated total relative error in *s* when there is a 1% relative error in conversion and 1% relative error in ee.

Table D.2. Kinetic resolution of chiral olefins using (S)-3

Olefin	Time (h)	TOF (h ⁻¹)	% conv	% ee	s^a	avg s^b
3M1P	12.5	415	49	27	2.3 ± 0.05	2.3 (0.25)
3M1H	9.5	360	38	25	2.9 ± 0.08	3 (0.16)
34DM1P	40	107	52	76	12.6 ± 1.3	12.6 (0.55)
344TM1P	24	8.6	20	12	3.3 ± 0.09	2.9 (0.6)
355TM1H	67.8	46	42	47	7.6 ± 0.5	6.4 (0.8)
4M1H	26.3	109	31	2.7	1.2 ± 0.003	1.2 (0.11)

a) The value following “ \pm ” is the calculated total relative error in s when there is a 1% relative error in conversion and 1% relative error in ee.

b) The value in parenthesis is the standard deviation.

Table D.3. Kinetic resolution of chiral olefins using (S)-4

Olefin	Time (h)	TOF (h ⁻¹)	% conv	% ee	s^a	avg s^b
3M1P	18.3	474	47	31	2.7 ± 0.07	2.55 (0.26)
3M1H	6.7	686	48	21	1.9 ± 0.03	1.9 (0.03)
34DM1P	29	127	40	52	13.9 ± 1.5	13.9 (0.28)
344TM1P	7	99	31	36	12.5 ± 1.5	N/A
355TM1H	10.5	349	48	13	1.5 ± 0.014	1.5 (0.23)
4M1H	2.75	1490	44	5	1.17 ± 0.005	1.15 (0.041)

a) The value following “ \pm ” is the calculated total relative error in s when there is a 1% relative error in conversion and 1% relative error in ee.

b) The value in parenthesis is the standard deviation.